Vapour-liquid Equilibrium of Carbon Dioxide in Newly Proposed Blends of Alkanolamines

Thesis submitted in partial fulfillment
of the requirement for the degree of

Doctor of Philosophy

in

Chemical Engineering

by

Gaurav Kumar
(Roll No – 509CH103)

Under the guidance of

Dr. Madhusree Kundu

Department of Chemical Engineering
National Institute of Technology
Rourkela, Odisha – 769008
August 2013

Dedicated to

My Parents and Late Dadajee

Department of Chemical Engineering
National Institute of Technology, Rourkela
Odisha, India – 769008

Certificate

This is to certify that the thesis entitled 'Vapour-liquid Equilibrium of Carbon Dioxide in Newly Proposed Blends of Alkanolamines**'** submitted by ***Gaurav Kumar*** is a record of an original research work carried out by him under my supervision and guidance in partial fulfillment of the requirements for the award of the degree of ***Doctor of Philosophy*** in ***Chemical Engineering*** during the session July'2009 – August' 2013 in the Department of Chemical Engineering, National Institute of Technology, Rourkela. Neither this thesis nor any part of it has been submitted for the degree or academic award elsewhere.

Dr. Madhusree Kundu
Associate Professor
Department of Chemical Engineering
National Institute of Technology, Rourkela

PRELUDE

The thesis entitled 'Vapour-liquid equilibrium of carbon dioxide in newly proposed blends of alkanolamines', is a pursuit of my PhD work; being carried out in the Department of Chemical Engineering at National Institute of Technology Rourkela, India. The motive behind the present work was to propose newer blends of alkanolamines, which could be best used for effective removal of CO_2 from natural gas, power plant flue gas, refinery off gases etc.

Adsorption using MOFs, de-sublimation of CO_2 from natural gas or flue gas stream by cryogenic cooling, and membrane separation are the technologies available for CO_2 removal and are under trial for commercialization. Aqueous amine absorption/stripping is by far the best technology currently available for CO_2 removal. Recently room temperature *ionic liquids* (ILs'); called green solvents are emerging as promising candidates to capture CO_2 due to their wide liquid range, low melting point, negligible vapour pressure, high CO_2 solubility and reasonable thermal stability. However, it is difficult to realize *ionic liquids* industrially owing to its high viscous nature and high cost, which left us with limited options like CO_2 absorption in alkanolamines or in Sodium and Potassium salts of primary or tertiary amino acids promoted with reactive alkanolamines.

The first aqueous alkanolamine used commercially was triethanolamine; way back in 1930. Henceforth, various alkanolamines including some proprietary formulations of alkanolamine solutions were proposed in this regard. Because of the need to exploit poorer quality crude and natural gas twined with the enhanced environmental obligations, energy efficient and selective acid gas treating at a competitive price are of dire need. As a result, there has been a rekindling of interest in new alkanolamine formulations and particularly in aqueous blends of those alkanolamines.

For the rational design of gas treating processes knowledge of vapour liquid equilibrium of the acid gases in alkanolamines are essential, besides the knowledge of mass transfer and kinetics of absorption and regeneration. The experimentation on VLE of CO_2 in the proposed alkanolamine blends corroborated multi-component and multiphase equilibria.

Present thesis is organized into the following chapters:

- **Chapter 1:** Background, origin of the work, objective, and outline of the thesis are being discussed here.
- **Chapter 2:** Chemical reaction equilibria and thermodynamics related to CO_2 gas treating through alkanolamine solutions is presented here. This chapter also presents the recent literature on CO_2 removal using aqueous alkanolamine solvents.
- **Chapter 3:** This chapter includes experimentation set-up, methods, and their validation. Generated VLE data on aqueous, (DEA + MDEA/AMP), *N*-methyl-2-ethanolamine (MAE) and aqueous *N*-ethyl-ethanolamine (EAE) solutions have been reported here. The deprotonation and carbamate reversion constants for EAE are also reported here.
- **Chapter 4:** Experimental VLE data on (EAE + MDEA/AMP) and (MAE + MDEA/AMP) blends for various relative amine compositions over a wide range of temperature and CO_2 pressure are reported with analysis. The CO_2 solubility in the newly proposed blends has been compared with (DEA + MDEA/AMP) blends. Present chapter also includes the correlation of VLE data of (CO_2 + EAE + MDEA + H_2O) system using rigorous thermodynamic model.
- **Chapter 5:** COSMO solvation model, calculation of thermodynamic property using COSMO-RS, computational procedure and applicability of COSMO-RS are included here. This chapter provides the COSMO predicted thermodynamic properties of binary (MAE/EAE + water) and ternary (CO_2+ MAE/EAE + water) systems.
- **Chapter 6:** This chapter is devoted to density data generation of (EAE + MDEA + H_2O), (EAE + AMP + H_2O), (MAE + AMP + H_2O) and (MAE + MDEA + H_2O) systems and their correlation using Redlich-Kister equation and the Nissan type of correlation.
- **Chapter 7:** In an ending note, chapter 7 concludes the thesis with future recommendations.

Based on the dissertation, five numbers of publications in various International journals are already published. Publication number 2 & 3 (as per the vita) is related to chapter 3. Publication number 1 & 5 (as per the vita) is related to chapter 4. Publication number 4 (as per the vita) is related to chapter 6. Another research article (number 6 as per the vita) is related to chapter 5 has been communicated.

Acknowledgement

I would like to express my respect and sincere gratitude to my thesis supervisor, Dr. Madhusree Kundu, for giving me an opportunity to work under her supervision for my doctoral program at the National Institute of Technology, Rourkela. I am indebted to professor Kundu for her invaluable supervision and esteemed guidance. As my supervisor, her insight, observations and suggestions helped me to establish the overall direction of the research and to achieve the objectives of the work. Her continuous encouragement and support have been always a source of inspiration and energy for me.

I express my sincere thanks to Prof. R. K. Singh, Head, Chemical engineering department and members of Doctoral Scrutiny Committee (DSC) Prof. P. Rath, Prof. B. Munshi and Prof. S. Sarkar, and all the faculty members of Chemical Engineering Department for their suggestions and constructive criticism during the preparation of the thesis.

I acknowledge all my seniors like Dr. Achyut Panda, Dr. Nihar Ranjan Biswal, Dr. Ramakrishna Gottipatti, Dr. Nagesh Tripathy, research scholars, and staff of Chemical Engineering Department for their support during my research work.

Thanks are also due to Mr. Rajib Ghosh, Mr. Yogesh, Mr. Akhilesh, Mr. Arun, Mr. & Mrs. Jeevan, Mr. Sachin, Mr. Arvind, Mr. vamsi, Mr. Sambhurisha, Mr. Tripathy, Mr. Sujeevan, Mr. Sheshu, Ms. Shivani, Mr. Deokaran and other friends and family members of mine, whom I could not mention here, for their encouragement and moral support.

I must acknowledge the academic resources provided by N.I.T., Rourkela and the research fellowship granted by Ministry of Human Resource and Development (MHRD),

and project fund given by Department of Science and Technology (DST), New delhi, India, to carry out this work.

Finally, I am forever indebted to my parents, brother, brother-in-law, sister and sister-in-law for their understanding, endless patience and encouragement from the beginning; and heartiest love to adolescent's from my family like my younger brother & sister Nishu, Guddi, Sonali and Sanu. Special love and fondness to Apporva, Mayank, Gunja, Rounak, Dolly and Adhikaar…….

National Institute of Technology ***Gaurav Kumar***

Rourkela, Odisha

August 2013

ABSTRACT

VAPOUR-LIQUID EQUILIBRIUM OF CARBON DIOXIDE IN NEWLY PROPOSED BLENDS OF ALKANOLAMINES

BY

GAURAV KUMAR

In the backdrop of a major climatic change vastly due to the greenhouse gas emission, gas treating has become a significant area of interest as it has never been earlier. Carbon dioxide (CO_2), one of the major greenhouse gases are treated mainly by absorption in alkanolamine solvents, though ionic liquids and Sodium and Potassium salts of primary or tertiary amino acids are given consideration presently for effective and energy efficient CO_2 capture. Gas treating research is actually passing through a transition which has been chronicled in the present work. Among the different technologies available for CO_2 mitigation, capture of CO_2 by chemical absorption is the technology that is closest to get implemented commercially. In the present context, the role of alkanolamine solvents in sour gas treating research should be revered, hence, *N*-methyl-2-ethanolamine (MAE), and 2-(ethylamino) ethanol (EAE) has been prudently explored for CO_2 capture. Apart from the knowledge of mass transfer and kinetics, the equilibrium solubility of acid gases over alkanolamines presumes an instrumental role in gas treating processes. To exploit poorer quality crude and natural gas twined with the enhanced environmental legislations, highly selective and economic acid gas treating processes are in an unprecedented need. In view of this, the present work was taken up to investigate the possibility of (EAE/MAE + MDEA/AMP) solvent as effective blends towards CO_2 absorption.

Measurement of solubility of CO_2 in aqueous single amine, MAE and EAE and aqueous amine blends MAE/AMP, MAE/MDEA, EAE/AMP and EAE/MDEA have been done in this work up to a maximum CO_2 pressure of 600 kPa for various temperatures and amine concentrations using the VLE measurement set-up developed in this work. The deprotonation and carbamate reversion constants were found out. The VLE data generated on (CO_2 + EAE + MDEA + H_2O) system was correlated with rigorous thermodynamic model. The vapour phase non-ideality was taken care off in terms of fugacity coefficient calculated using *Virial* equation of state. Extended *Debye-Hückel* theory of electrolytic solution was used to address the liquid phase non-ideality. The experimental set-up and procedure has been validated with the systematic VLE data generated on CO_2 solubility in

(DEA + AMP/MDEA + H_2O) systems. Some of the VLE data generated on the mentioned blends have been compared with the literature data. The generated data are also correlated with a rigorous; activity based thermodynamic model with minimal correlation deviations, thus indicating the robustness of our set-up and procedure. Moreover the new VLE data generated on (CO_2 + DEA + AMP/MDEA + H_2O) system have enhanced and enriched the data base.

Engineers and scientists usually refer excess Gibbs energy models for vapour- liquid equilibria calculations such as WILSON, NRTL, UNIQUAC, and UNIFAC. In order to describe the thermodynamics for mixtures, these methods compute the activity coefficient of the compounds using the information on binary interaction parameters that are derived from experimental results. Thus, these models have limited applicability in thermodynamics properties and VLE prediction for the new systems that have no experimental data. For solution of this problem, Solvation thermodynamics models based on computational quantum mechanics, such as the Conductor – like Screening Model (COSMO), provide a good alternative to traditional group-contribution and activity coefficient methods for predicting thermodynamic phase behaviour. This thesis provides the COSMO predicted thermodynamic properties of binary (MAE/EAE + H_2O) and (MAE/EAE + CO_2 + H_2O) and systems. The COSMOtherm calculations have been performed the latest version of software that is COSMOtherm C30_1201.

The densities of aqueous blends of (MAE/MDEA), (MAE/AMP), EAE/MDEA, and EAE/AMP for various relative amine compositions have been measured over a wide range of temperature and relative amine composition, and useful correlations developed for prediction of densities of the amine blends. It is expected that the physico-chemical parameters thus generated will also be useful for the database for process design.

CONTENTS

List of Figures **Page No.**

List of Tables **Page No.**

NOMENCLATURE

μ	Chemical potential
f	Fugacity
ΔG , dG	Gibbs free energy
H	Planck' s constant
V	Force functioning on a particle
Ψ	Wave perform
∇^2	Operator describes the behavior of the wave perform with position
E	State energy of the particle or the system
E^T	Electronic energy depends on kinetic energy from electronic motion
E^V	Potential energy of electron nuclear attraction and repulsion of nuclei pairs
E^J	Electronic repulsion
E^{XC}	Exchange correlation terms which will take into consideration the non-counted electronic interaction
ρ	Electronic density
$\emptyset_i$	i-th molecular orbital
$C_{\mu i}$	Molecular expansion coefficient
X_μ	μ-th atomic orbital also known as arbitrary basis function
n	Number of atomic orbitals
ε	Dielectric screening constant for the solute
E	Total electrostatic field from the solute and polarized charges
σ^*	Ideal screening charge density
E_{misfit}	Electrostatic interaction energy
a_{eff}	Effective area of contact between two solute molecules surface segments
$\sigma,\ \sigma'$	Surface screening charge densities for solute molecules
$\mu_{S\,(\sigma)}$	Sigma potential

$P^{Xi}(\sigma)$	Sigma profile of compound X
$n_i\ (\sigma)$	Number of divided segments that has surface charge density (σ)
$A_i\ (\sigma)$	Segments surface area that has charge density σ
A_i	Area of the whole surface cavity that is embedded is the medium
P_s	Sigma profile of the whole mixture
σ_i	Surface charge density
τ_{vdW} , τ'_{vdW}	Van der Waals interaction parameter
E_{HB}	Hydrogen bonding energy
c_{HB}	Adjustable parameter used for hydrogen bond strength
σ_{HB}	Adjustable parameter for hydrogen bonding threshold
σ_{donor}	Screening charge density for hydrogen bond donor surface area
$\sigma_{acceptor}$	Screening charge density for hydrogen bond acceptor surface area
E_{gas}^{Ci}	Total energy of the molecule in the gas phase computed by quantum mechanics
E_{COSMO}^{Ci}	Total COSMO energy of the molecule in solution computed by solvation model using quantum mechanics
E_{vdW}^{Ci}	Van der Waals energy of the molecule
μ_{gas}^{Ci}	Chemical potential of pure component in ideal gas
k	Boltzmann constant
T	Temperature in K
γ_S^{Ci}	Activity coefficients of the component i as predicted by COSMOtherm.
μ_S^{Ci}	Chemical potential in the Solvent S
μ_{Ci}^{Ci}	Chemical potential of the pure component
R	Ideal gas constant
P^{tot}	Total pressure of the mixture
P_{vap}^{Ci}	Vapor pressure of pure component i
x_i	Mole fractions in the liquid phase

y_i	Mole fractions in the gas phase
P_{CO_2}	Equilibrium pressure
P_t	Total pressure of cell
P_v	Vapor pressure
V_{jk}^E	Excess molar volume for a binary solvent system
V^E	Excess molar volume
V_i^0	Molar volume of the pure fluids at the system temperature
V_m	Molar volume of the liquid mixture
M_i	Molar mass of pure component i
ρ_m	Measured liquid Density
V	molar volume of solvent, m^3/kmol
β_{ij}	interaction parameter
ξ	reaction extent
φ	vapour phase fugacity coefficient
α_{ij}	two-body interaction parameter in equation
α_{ijk}	three body interaction in equation
φ_i	volume fraction of solvent i
$\hat{\varphi}_i$	vapour phase fugacity coefficient of i^{th} component in a vapour phase mixture
A	*Debye-Hückel* limiting slope
Z	charge number on the ion
I	ionic strength

ABBREVIATIONS

CO_2	Carbon Dioxide
COS	Carbonyl Sulphide
H_2S	Hydrogen Sulphide
PZ	Piperazine
2-PE	2-Piperidineethanol
AMP	2-Amino-2-methyl-1-propanol
AHPD	2-Amino-2-Hydroxymethyl-1, 3-Propanediol
MEA	Monoethanolamine
DEA	Diethanolamine
MDEA	N-Methyl-Diethanolamine
DIPA	Diisopropanolamine
MAE	N-Methyl-2-Ethanolamine
EAE	N-Ethyl-Ethanolamine
DGA	2-(2-Aminoethoxy) Ethanol
DIPA	Diisopropanolamine
TEA	Triethanolamine
TSP	Trisodium Phosphate
ILs’	Ionic Liquids
COSMO	Conductor – like Screening Model
COSMO-RS	Conductor – like Screening Model for Real Solvent
AM1	Austin Model 1
PBE	Perdew-Burke-Ernzerhof
BP	Becke-Perdew
TZVP	Triple Zeta Polarized Valence
SVP	Split Valence Plus Polarization Function
DFT	Density Functional Theory
MM	Molecular Mechanics
SE	Semi-Empirical
MD	Molecular Dynamics
QM	Quantum Mechanics

LDA	Local Density Approximation
CGTO	Contracted Gaussian Type Orbital
SCRF	Self-Consistent Reaction Field Models
VLE	Vapor liquid equilibrium

Chapter 1

INTRODUCTION TO CARBON DIOXIDE REMOVAL PROCESSES

Chapter 1

INTRODUCTION TO CARBON DIOXIDE REMOVAL PROCESSES

1.1 INTRODUCTION

Carbon dioxide is a natural, fluctuating component of the Earth's atmosphere. It is the most important anthropogenic greenhouse gas and because of its increasing accretion in the atmosphere, world faces the global warming effects and serious environmental problems. CO_2 concentration in the atmosphere has increased from 280 to 370 parts per million (ppm) (an increase of circa 30 %) by the past 200 years, mostly because of the natural gas, coal based fired power plant, steel and aluminum industry and due to transportation that uses burning of coal, natural gas and petroleum oil (Luis, 2007). So, capturing and storing CO_2 instead of releasing it to the atmosphere will help in reducing global CO_2 emission, thus preventing global warming (Eirik, 2005). CO_2 storage involves the injection of supercritical CO_2 into a geologic formation. On geological time scales this CO_2 will partly be fixed in minerals by carbonation reactions. There are three common options for geological CO_2 storage; saline aquifers, oil and gas reservoirs, and estranged coal seams. It is expected that saline aquifer formations provide the largest storage capacities quantities for CO_2, followed by oil and gas reservoirs. A number of projects

involving the injection of CO_2 into oil reservoirs have been conducted, primarily in the USA and Canada for enhanced oil recovery (EOR).

In order to sustain economic growth besides achieving conformity with the Kyoto agreement, we have to rely on fossil fuels, thus, CO_2 capture and sequestration has attracted extensive attentions. The removal of CO_2 from gas streams is an important step in many industrial processes and is required because of process technical, economical or environmental reasons. In the presence of water, CO_2 being an acid gas can cause corrosion to process equipment. Besides this, the presence of CO_2 reduces the heating value of a natural gas stream and also wastes energy for pipeline transportation. In LNG (liquefied natural gas) plants, it should be removed to prevent freezing in the low temperature chillers. Moreover, in the manufacture of ammonia, it would poison the catalyst. Finally, CO_2 is also the most important greenhouse gas and held responsible for the recent climate changes (Derks, 2006).

There are currently three primary methods available for CO_2 capture; post-combustion capture, pre-combustion capture and oxy-fuel processes. Post-combustion capture involves scrubbing CO_2 from the flue gas from a combustion process. Oxyfuel combustion refers to combustion of fuel using pure oxygen, thereby produce a CO_2-rich gas. In a pre-combustion process, gasification is followed by CO_2 separation prior to the use of the produced hydrogen as a fuel gas as per the Figure 1.1 (Thambimuthu and Davidson, 2004; Bolland, 2004). The technologies available for CO_2 mitigation vary in complexity, degree of maturity and cost. Figure 1.2 presents other classifications regarding CO_2 capture technologies.

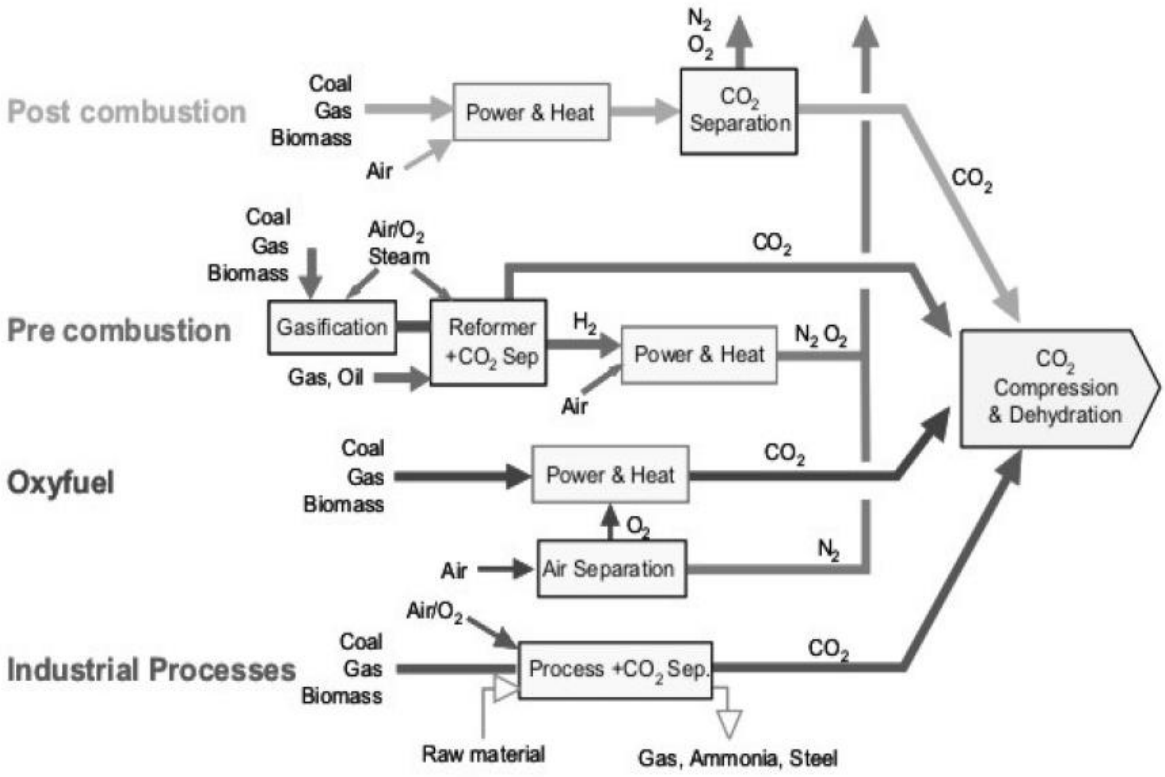

Figure 1.1: Technologies for CO_2 capture (Bolland, 2004).

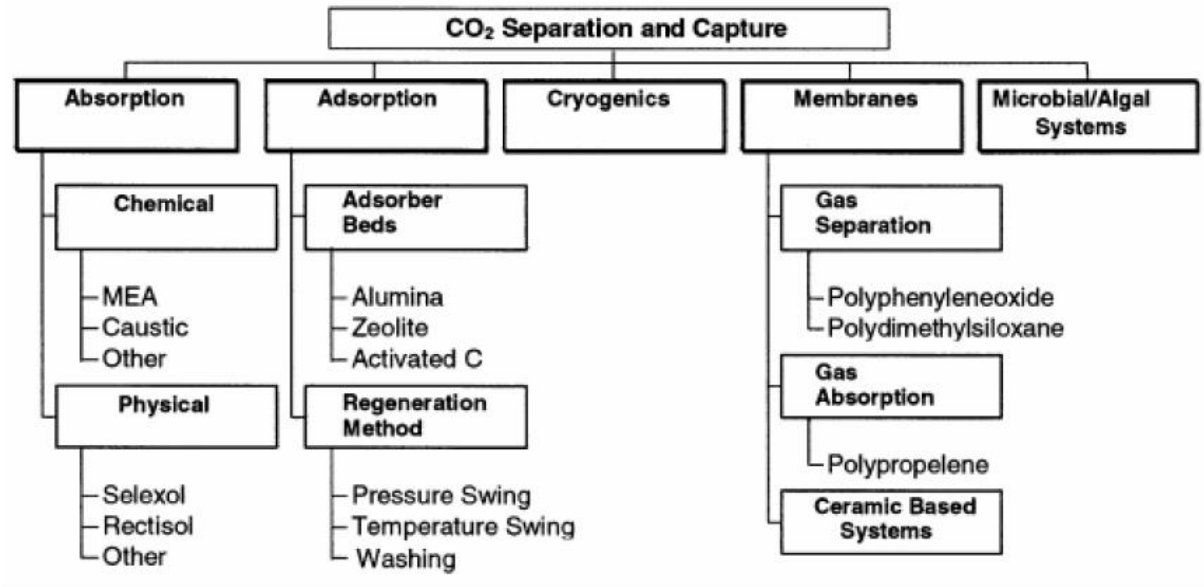

Figure 1.2: Technologies for CO_2 Capture (Rao and Rubin, 2002).

1.2 CARBONDIOXIDE REMOVAL PROCESSES

There are a numbers of ways for CO_2 removal. Varieties of processes and their advancement over the years to treat sour gas with the aim of optimizing capital cost and operating cost, meeting gas specifications, and environmental obligations have enriched the technology of sour gas treating.

The major processes available are grouped as follows (Maddox, 1998):

- Absorption Processes (Chemical and Physical absorption)
- Adsorption Process (Solid Surface)
- Physical Separation (Membrane, Cryogenic Separation)
- Hybrid Solution (Mixed Physical and Chemical Solvent)

1.2.1 Absorption Processes

1.2.1.1 *Physical Absorption Processes*

Physical solvent processes use organic solvents to physically absorb acid gas components rather than react chemically. Transfer of CO_2 through the gas-liquid interface is rate limiting, large concentration of CO_2 is found at the interface in the gas side while reactions between absorbent molecules with acid gases are not enough fast to carry them into the liquid side. The solubility of CO_2 depends on the partial pressure and on the temperature of the feed gas. Higher CO_2 partial pressure and lower temperature favors the solubility of CO_2 in the solvents. At these conditions, complete removal of acid gas from natural gas is possible. Regeneration of the spent solvent is achieved by flashing to lower pressure or by stripping with vapour or inert gas, while some solvent is regenerated by flashing only and require no heat (Dimethyl ether of Polyethylene Glycol). Some of the physical solvents are as follows:

Physical solvents:	**Trade names**
Propylene carbonate	Flour
Dimethylether of polyethylene glycol	Selexol
N-methyl-2-pyrolidone	Purisol
Chilled methanol	Rectisol

1.2.1.2 *Chemical Absorption Process*

Chemical absorption processes are based on exothermic reaction of the solvent with the gas stream to remove the CO_2 present. Most chemical reaction are reversible, in this case, reactive material (solvent) removes CO_2 in the contactor at high pressure and preferably at low temperature. The reaction is then reversed by endothermic stripping process at high temperature and low pressure. Chemical absorption processes are particularly applicable where acid gas (CO_2) partial pressure are low and low level of acid gas are allowable in the residue gas. The water content of the solution minimizes heavy hydrocarbon absorption, thus making the solvent more suitable for feed sour gas rich in heavy hydrocarbon. Presently absorption using alkanolamines is the most efficient natural gas purification and post-combustion CO_2 capture technology. This, in part reflects technological maturity, the technology was patented for natural gas sweetening as early as 1930 by R.R. Bottoms (Kohl and Nielsen, 1997). Triethanolamine (TEA) was the first alkanolamine commercially available and used in early gas-treating plants. Same technology has been in use for small-scale removal of CO_2 from exhaust gas (Reddy *et al*. 2003 and Yagi *et al*. 2004).Absorption is also a technology that can be fairly easily installed and existing power plants and industry can be retrofitted with equipment for absorption (Thambimuthu and Davidson, 2004); whereas many other technologies for CO_2 removal involve new forms of power plant technology. There has been constant endeavor to improve the different technologies, and improvements are likely to change the relative performance of different technologies. Investigations have however; suggested that absorption of CO_2 in alkanolamines and formulation of new alkanolamines is likely to remain a highly competitive technology for CO_2 capture in near future (Kvamsdal *et al*. 2004). A list of chemical solvents and hybrid solvents are as follows:

Chemical solvents:	**Trade names**
Monoethanolamine (MEA)	SNPA
(20-35 wt % in water)	
Diethanolamine (DEA)	SNPA
(30 wt % in water)	
Diglycolamine (DGA)	Econamine
(30 wt % in water)	

Diisopropanolamine (DIPA)	ADIP
Methyldiethanolamine (MDEA)	Ucarsol HS, SIPM
Promoted hot K_2CO_3 solution	Benfield, Catacrab
(25-30 wt % K_2CO_3, 5 % promoter)	
Sterically hindered amine	Flexsorb SE, Flexsorb HP
2-amino-2-methyl-1-propanol (AMP)	Flexsorb

Hybrid systems	**Trade names**
(Chemical and Physical solvents)	
DIPA-sulfolane-water	Sulfinol D
(40-40-20 wt %)	
MDEA-sulfolane-water	Sulfinol M
(40-40-20 wt %)	
MEA or DEA-methanol	Amisol
DIPAM (diisopropyl amine)	ADIP
DETA (diethylamine)-methanol	Improved Amisol
AMP-sulfolane-water	Flexsorb PS

There are three major categories of alkanolamines; primary, secondary and tertiary. The most commonly used alkanolamines are the primary amine monoethanolamine (MEA), the secondary amines diethanolamine (DEA), diglycolamine (DGA) and di-isopropanolamine (DIPA) and the tertiary amine methyldiethanolamine (MDEA). Triethanolamine was found to be less attractive mainly due to its low absorption capacity (resulting from higher equivalent weight), its lower reactivity and its relatively poor stability. Di-isopropanolamine (DIPA) was used to some extent in the Adip process and in the Sulfinol process, as well as in the SCOT process for Claus plant tail gas purification but gradually displaced by Methyldiethanolamine (MDEA) in gas sweetening applications. The advantage of tertiary alkanolamines is that the equilibrium is easily reversed in the stripper. Tertiary alkanolamines are often combined with promoters in order to take advantage of the shuttle-effect (Bishnoi and Rochelle, 2002; Zhang *et al*.

2003). One important class of amines is the sterically hindered amines (SHA), e.g., 2-amino-2-methyl-1-propanol (AMP), 2-piperidineethanol (PE) and 2-amino-2-hydroxymethyl- 1,3-propanediol (AHPD). Sterically hindered amines have been defined as amines, for which either a primary amine group is attached to a tertiary carbon atom or a secondary amine group is attached to a secondary or tertiary carbon atom. N-methyl-2-ethanolamine (MAE) and N-ethyl-ethanolamine (EAE) are the two alkanolamines not exactly following the definition of SHA but ample properties resembling the SHA because of their electronic structure. The carbamate stability is an important parameter determining the CO_2 absorption capacity and the CO_2 regeneration energy requirement. It is long been identified that steric hindrance is an important parameter in reducing the carbamate stability and is affecting the basicity of amine based solvents. It is also noticed that the level of steric hindrance (low to high) depends on the number and type of functional group substituted at α-carbon to the amine group, affecting the solvents characteristics for CO_2 absorption capacity and CO_2 absorption kinetics accordingly.

Some solvents have been proposed with multiple amine functionalities. Of such solvents, piperazine has been extensively used in gas treating. Piperazine is usually used as a promoter (Bishnoi and Rochelle, 2002; Zhang *et al*. 2003 and Jenab *et al*. 2005). A problem with piperazine is that, it has fairly low solvability in water. Recent work (Ma'mun *et al*. 2004 and Bonenfant *et al*. 2005) has suggested that N- (2-hydroxyethyl) ethylenediamine (AEEA) is a promising diamine solvent. Multiple amine functionalities suggest a potential to bind more CO_2 with a single solvent molecule. Further research is probably required to determine if there is a particular benefit in using such solvents.

Hindered amine-based processes (Flexsorb SE, Flexsorb PS, Flexsorb HP) for selective removal of H_2S and for non-selective removal of CO_2 and H_2S have also been commercialized by Exxon Research & Engineering Co. (Goldstein *et al.,* 1986; Gas Process Handbook'92, Hydrocarbon Processing, April, 1992). It is indicated (Goldstein *et al.,* 1986) that hindered amine-based process, Flexsorb SE, is a potentially attractive replacement for selective H_2S removal approaches e.g., MDEA-based and direct conversion processes, which are in commercial use now. In fact, results of a commercial test reported by Goldstein *et al.* (1986) showed 40% energy saving when Flexsorb SE replaced the MDEA-based H_2S selective absorption process. Several proprietary formulations of alkanolamine solutions containing, besides the amine; corrosion inhibitors, foam depressants and activators are being offered under various trade names such as UCARSOL, Amine Guard (Union Carbide Corporation), and GAS/SPEC IT-1 Solvents

(Dow Chemical Company) and Activated MDEA (BASF Aktiengesellschaft), etc. Among the patented solvents, the KS 1-3 (Mimura *et al*. 1999) were developed by Mitsubishi Heavy Industries. Salako (2005) believed KS 1 to be a mixture of AMP with a promoter. A few are known about KS 2 and 3. The researchers at Mitsubishi have however concentrated on amino-amide molecules (Nagao *et al*. 1998) and these could be the possible ingredients of their formulated solvents. The Canadian company Cansolv had filed a patent application of absorbents for CO_2 capture (Hakka and Ouimet, 2004). This appears to be a promoter-based system and here tertiary amines are utilized with promoter as piperazine or a derivative of piperazine. The novel feature of this patent appears to be the use of oxidation inhibitors and molecules with two tertiary amine functionalities. Use of piperazine-promoted MDEA was disclosed through U.S. Patent 4,336,233 issued June 22, 1982 with BASF Aktiengesellschaft as assignee. Since the patent's expiry in 2002, most solvent vendors now offer a piperazine-activated MDEA solvent under a range of trade names. Over the years between 1982 and 2002, BASF's a MDEA® (for activated MDEA) solvent captured the lion's share of the market in ammonia synthesis gas purification and many other areas of application where CO_2 removal was the primary concern.

Chemical absorption processes using alkanolamines for gas treating may be divided into three conceptual categories distinguished by the rate at which the solvent reacts with CO_2. The first group of processes can be termed "bulk" CO_2 treating processes, and are distinguished by their ability to remove CO_2 to very low levels. Bulk removal stresses the faster reacting solvents available, primary and secondary alkanolamines and promoted hot carbonate salts. Promoted hot carbonate processes are widely used for bulk CO_2 removal where clean gas specifications are not stringent and the partial pressure of CO_2 is moderately high (Astarita *et al*. 1983). Aqueous primary or secondary alkanolamines are generally employed for bulk CO_2 removal when the partial pressure of CO_2 in the feed is relatively low and/or the required product purity is high. Though the reaction of CO_2 with these amines is fast, it is accompanied by a highly exothermic heat of reaction (Kohl and Nielsen, 1997), which must be supplied in the regenerator to regenerate the solvent. Consequently, these processes can be energy intensive (Astarita *et al*. 1983).

The second group of processes employing tertiary or hindered alkanolamines to avoid the faster carbamate formation reaction constitutes the second group of "selective" treating processes. These selective processes are capable of passing as much as 90% of the CO_2 in the feed gas while removing H_2S to very low levels (less than 4 ppm) (Kohl and

Nielsen, 1997). In selective gas treating applications (such as for gas processing plants with a sulfur recovery unit (SRU)) CO_2 removal below certain limits is undesirable, since it results in higher than necessary circulation rates and reboiler steam requirements, and lower H_2S partial pressure for the SRU. In order to save energy in these applications, the tertiary alkanolamine MDEA was proposed for use as a selective treating agent. Hence, over the years MDEA has become known as a solvent providing good selectivity for H_2S in the presence of CO_2 (Kohl and Nielsen, 1997).

A third, hybrid category of processes has grown out of the selective treating category. These hybrid processes seek to remove most of the CO_2 and H_2S present in the rich gas stream, and also seek to retain the beneficial energy characteristics of selective solvents. The increase in CO_2 reaction rate has been demonstrated industrially by "promoting" a tertiary alkanolamine solvent with a small amount of faster-reacting primary or secondary amine (Kohl and Nielsen, 1997). These solvents are better known as blended amine solvents. By judiciously adjusting the relative compositions of the constituent amines, the blended amine solvents (with a much larger amount of the tertiary or sterically hindered amine and very small amount of the primary or secondary amine or even without that) can also become very good solvents for selective removal of H_2S in the presence of CO_2 in the gas streams. A blended amine solvent may result in substantial lower solvent circulation rates compared to a single amine solvent due to the higher absorption capacities. It also saves regeneration energy.

A simplified schematic of a typical gas treating operation which employs an aqueous alkanolamine solution is shown in Figure 1.3. The gas stream containing CO_2 and H_2S is contacted counter currently with the amine solution at 40 ^{0}C and 1000 psia. The amine solution selectively absorbs the acidic components from the sour gas to produce a sweet product gas. The amine solution, which now contains the acid gases, called rich amine, is sent to the top of the stripper column through a heat recovery exchanger. A steam-heated reboiler maintains 120 ^{0}C in the stripper to reverse the absorption reactions. The desorbed gases are then either sent to a Claus plant for conversion of the H_2S to elemental sulfur in case of a selective treating process, or to an incinerator depending on the H_2S concentration. The now "lean amine" is recycled back through the heat exchanger to the top of the absorber.

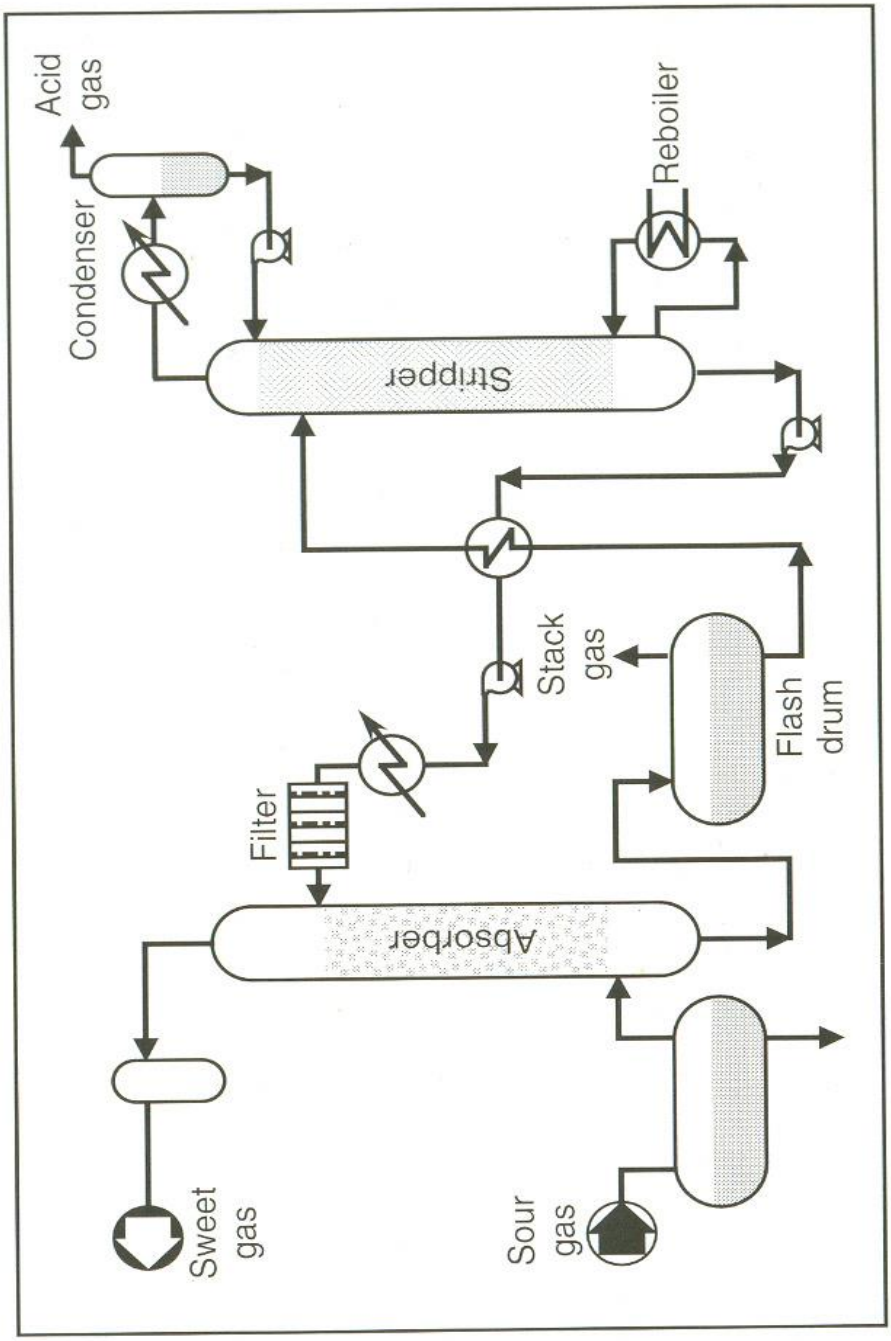

Figure 1.3 Basic flow scheme for alkanolamine acid gas removal processes

1.2.2 Membrane Process

Although the traditional packed bed absorbers have been used in the chemical industry for decades, there are several disadvantages such as flooding at high flow rates, unloading at low flow rates, channeling and foaming, which lead to difficulties in mass transfer between gas and liquid. Phase dispersion and limited mass-transfer area are the major drawbacks of the conventional equipment. In the context of extensive use of alkanolamines for the absorption of acid gases in industry and the substantial energy requirement of acid-gas-treating plants, there has been a considerable incentive for the development of more energy-efficient and more-flexible methods for sour gas separation.

A microporous/porous membrane based non-dispersive gas absorption technique has been introduced by Sirkar, 1992; Reed *et al*. (1995); and Gabelman and Hwang (1999). Several researchers have studied the absorption of CO_2 in different single and blended alkanolamine solvents using conventional gas-liquid membrane contactors. Paul and coworkers (2008) have studied theoretically the absorption of carbon dioxide in different single and blended alkanolamine solvents using flat sheet membrane contactor (FSMC). Wang *et al*. (2006) have studied the absorption of CO_2 into water using parallel-plate gas–liquid membrane contactor. A theoretical analysis to capture CO_2 using different aqueous single and blended alkanolamine solutions in a hollow-fiber membrane contactor (HFMC) have been reported by Paul and coworkers (2007). Zhang *et al*. (2006) reported the absorption of CO_2 in aqueous diethanolamine (DEA) solution using HFMCs. They built models for the absorption of CO_2 with its varying concentration in the gas phase. Gong *et al.* (2006) have presented the experiments and simulation of CO_2 removal using aqueous blends of *N*-methyldiethanolamine (MDEA) and monoethanolamine (MEA) in HFMCs. Yeon *et. al.* (2005) reported a pilot-scale membrane contactor hybrid process to recover CO_2 from the flue gas. Porous polyvinylidene fluoride (PVDF) hollow fiber module was used as membrane contactor and its performance was compared by the group with a conventional packed column. Wang *et al*. (2004) theoretically studied the absorption of CO_2 in HFMCs using three typical alkanolamines solutions of 2-amino-2-methyl-1-propanol (AMP), DEA, and MDEA.

The largest membrane based natural gas processing plant in the world is located at **Qadirpur, Pakistan** (Dortmundt, UOP, 1999).

Other Plants (UOP) using membranes for CO_2 removal:

- Kadanwari, Pakistan - 2 stage unit for treatment of 210 MMSCFD gas at 90 bars (1995 installed)
- Taiwan (1999) - 30 MMSCFD at 42 bar.
- EOR facility, Mexico - processes 120 MMSCFD gas containing 70 % CO_2 (1997 installed)
- Slalm & Tarek, Egypt - 3 two-stage units each treating 100 MMSCFD natural gas at 65 bar (1999 installed).
- Texas, USA - 30 MMSCFD of gas containing 30% CO" at 42 bar (1993 installed).
- Indonesia, A hybrid system operating at 750 psia, processing 245 MMSCFD of 40% CO_2 gas down to 20% in the membrane and then down to 8% in a traditional solvent system. (2006 installed).

Companies with membranes for CO_2 removal:

- NATCO Group (Cyanara membranes)
- Aker Kværner Process Systems
- Air Liquid
- UOP

Process integrated membrane and absorption unit are advantageous because of reduced size of membrane gas liquid contactors and weight (important offshore), wide range of liquid and gas flows (separation of gas/liquid phase), lower capital costs compared with alternative schemes, reduction in energy (if membranes are integrated with the stripping unit), reduction in solvent losses, no entrainment, flooding or channelling. The Santos Gas Plant, Queensland, Australia's largest gas producer uses the gas/liquid contactor and it has novel polyamide membrane facility for CO_2 removal (installed 2003).

The fascinating facts could not be transformed in to a full flagged; commercially viable CO_2 capture technology at large scales. The real issues are:

- ✓ Low selectivity & flux - large scale systems not economically viable (yet)
- ✓ Thermal stability of polymer membranes.

- ✓ Degradation & lifetime of membrane.
- ✓ Immature technology (in *industrial terms*, compared with existing solutions)

1.2.3 Adsorption Process

Adsorption process involves the absorption of acid gas components by solid adsorbent. The removal processes is either by chemical reaction or by ionic bonding of solid particles with the acid gas. Commonly used adsorption processes are; the iron oxide, zinc oxide, MOFs and molecular sieve (zeolite) process. Generally, a micro-porous structure characterizes any adsorbent, which selectively retains the components to separate them. The saturated bed is removed from the system and gets regenerated by flowing hot sweet gas through the bed. MOFs (metal organic frames) and their CO_2 sorption capacity are currently an active area of research in this category. MOFs are hybrid organic/inorganic structures that are essentially scaffolds made up of metal hubs linked together with struts of organic compounds, a structure designed to maximize surface area. MOF sorption properties can be readily tailored by modifying either the organic linker and/or the metal hub. In recent years, there has been considerable research on the use of zeolites, metal organic frameworks (MOFs), and zeolitic imidazolate frameworks (ZIFs) for selective adsorption of CO_2 from CO_2/H_2, CO_2/CH_4 and CO_2/N_2 mixtures (Chowdhury *et al*. 2012; Mishra *et al*. 2012; Mason *et al*. 2011; Krishna and Van Baten, 2007 and 2011; Krishna and Baur, 2003). The adsorptive separation of CO_2 from CO is of particular interest to NASA's MARS in-situ resource utilization program (Krishna and van Baten, 2012).

Hydrogen is mainly produced by steam reforming of natural gas, a process which generates a synthesis gas mixture containing H_2, CO_2, CO, and CH_4. In order to obtain pure H_2, pressure swing adsorption (PSA) is used to remove these impurities from the synthesis gas mixture. In practice, the adsorbed impurities (CO_2, CO, and CH_4) are then recovered from the column by desorption at lower pressures. The CO_2/CH_4/CO purge gas is normally used for combustion purposes in a steam reformer. In view of the current concerns about CO_2 emissions there is an incentive to remove CO_2 from the purge gas mixture. After selective adsorption of CO_2 from the purge gas, the recovered CO and CH_4 are usable as fuel gas in the steam reformer. Rajamani Krishna (2012) compared the performance of three metal–organic frameworks (MOFs): CuBTC, MIL-101, and Zn(bdc)dabco, with that of NaX zeolite for selective adsorption of CO_2 from mixtures containing CH_4 and CO in a pressure swing adsorption (PSA) unit operating at pressures

ranging to 60 bar. He also stated that the working capacity for CO_2 adsorption, is significantly higher for MOFs than for NaX zeolite as the pressures are increased significantly above 2 bar.

UOP LLC, in collaboration with Vanderbilt University, the University of Edinburgh, the University of Michigan, and Northwestern University is working to develop a MOF-based CO_2 removal process and to design a pilot study to evaluate the performance and economics of the process in a commercial power plant.

1.2.4 Cryogenic Process

Low temperature distillation (Cryogenic separation) is a commercial process commonly used to liquefy and purify carbon dioxide from relatively high purity (>90%) sources. It involves cooling the gases to a very low temperature (lower than -73.3 ^{o}C) so that the carbon dioxide can freeze-out / liquefy/ and separate.

Current technologies available in the market for natural gas treating may not be ideally suitable for treating highly contaminated natural gas where CO_2 geo-sequestration is required. Use of physical and chemical absorption solvents have been the most popular method for treating natural gas with high CO_2, and to a lesser extent, membranes and adsorption methods. These technologies remove CO_2 at near ambient pressures thus requiring substantial amount of compression to levels needed for geo-sequestration. Cryogenic CO_2 removal methods can capture CO_2 in a liquid form thus making it relatively easy to pump underground for storage or send for enhanced oil recovery. Hart and Gnanendran (2009) presented field experience and test results from Cool Energy's CryoCell® demonstration plant in Western Australia. The CryoCell® process was developed by Cool Energy Ltd and tested in collaboration with other industrial partners including Shell Global Solutions. Basic economic comparisons between the CryoCell® process and an amine-based process including CO_2 geo-sequestration were also presented.

A new and novel method is removing CO_2 in raw natural gas streams by cooling the natural gas stream to -130 °C at near ambient pressures, causing CO_2 in the natural gas stream to desublimate. Desublimation occurs in a novel desublimating heat exchanger with a low vapor pressure contact liquid and/or liquefied natural gas (LNG). The heat exchanger is staged, with the raw natural gas feed bubbled through contact liquid and/or LNG. The desublimating solid CO_2 is entrained in the contact liquid and/or LNG and

subsequently separated through filtration. The cold purified CO_2 and natural gas products then return through a regenerative heat exchanger to cool the incoming natural gas and melt the purified solid CO_2 stream. The overall energy efficiency of this system exceeds that of competing desublimation technologies by reducing the required pressure of operation and eliminating the significant losses of a distillation tower in reboiling and condensing. This technology is applicable for post combustion CO_2 -laden flue gas.

A promising novel option is to freeze out (desublimate) CO_2 from flue gases using cryogenically cooled surfaces. High cooling costs could be minimized by exploiting the cold duty available at Liquefied Natural Gas (LNG) re-gasification sites. A novel process concept has been developed by Tuinier (2011), based on the periodic operation of cryogenically cooled and dynamically operated packed beds.

In fine, we can conclude as pointed out by Tuinier (2011), 'while compared with other technologies, it is found that the preferred technology depends heavily on the availability of utilities. The cryogenic concept requires a cold source, such as the evaporation of LNG at a re-gasification terminal, while amine scrubbing requires low pressure steam in order to strip the solvent. When both LNG and steam are not available at low costs, membrane technology shows advantages. When steam is available at low costs, especially when using an advanced amine, scrubbing is the preferred technology. The cryogenic concept could be the preferred option, when LNG is available at low costs. Especially when pressure drops can be decreased and the simultaneous removal of impurities can be incorporated in one process, the concept could become a serious candidate for capturing CO_2 from flue gases'.

1.3 VAPOR- LIQUID EQUILIBRIUM

For the rational design of gas treating processes knowledge of vapour liquid equilibrium of the acid gases in alkanolamines are essential, besides the knowledge of mass transfer and kinetics of absorption and regeneration. Moreover, equilibrium solubility of the acid gases in aqueous alkanolamine solutions determines the minimum recirculation rate of the solution to treat a specific sour gas stream and it determines the maximum concentration of acid gases which can be left in the regenerated solution in order to meet the product gas specification. One of the drawbacks of the conventional equilibrium stage approach to the design and simulation of absorption and stripping is that, in practice absorbers and strippers often do not approach equilibrium conditions. A

better approach to design such non-equilibrium processes (mass transfer operation enhanced by chemical reaction) is by the use of mass and heat transfer rate based models (Hermes and Rochelle, 1987; Sivasubramanian *et al.*, 1985; Rinker, 1997). However, phase and chemical equilibria continue to play important roles in a rate-based model by providing boundary conditions to partial differential equations describing mass transfer coupled with chemical reaction. Accurate speciation of the solution is an integral part of the equilibrium calculations required by the rate-based models.

1.4 THERMODYNAMIC PROPERTY

Both, the acid gas in the liquid phase and alkanolamines are weak electrolytes. As such they partially dissociate in the aqueous phase to form a complex mixture of nonvolatile or moderately volatile solvent species, highly volatile acid gas (molecular species), and non-volatile ionic species. The equilibrium distribution of these species between a vapour and liquid phase are governed by the equality of their chemical potential among the contacting phases. Chemical potential or partial molar Gibbs free energy is related to the activity coefficient of the species through partial molar excess Gibbs free energy. An activity coefficient model (or excess Gibbs energy model) is an essential component of VLE models. Excess enthalpy data is useful for modeling because of its link to the temperature dependence of excess Gibbs energy. Therefore, in Gibbs energy model for activity coefficient, excess enthalpy measurements or predicted values will provide more accurate temperature dependence for the model. The main difficulty has been to develop a valid excess Gibbs energy function, taking into consideration of interactions between all species (molecular or ionic) in the system. The derivation of binary/ternary interaction parameters needs experimental data. For newer alkanolamine systems, where there is no experimental data is present, molecular modeling can be a savior by predicting all thermodynamic properties like excess enthalpy, excess Gibbs energy, total pressure, activity coefficients, chemical potential and infinite dilution activity coefficient of binary (alkanolamine + water), ternary (CO_2+ alkanolamine + water) and quaternary (CO_2+alkanolamine blends + water) systems.

1.5 MOLECULAR MODELLING

Molecular modelling encompasses all theoretical methods and computational techniques, which are used to model the behavior of molecules. Molecular simulation based on quantum mechanics calculation is attractive alternative to conventional

engineering modeling techniques. Molecular simulation strategies give an intermediate layer between direct experimental measurements and engineering models (as shown in Figure 1.4). Molecular simulation method can provide results applicable over wider ranges of process conditions because of the fewer approximations that are made during computation.

A priori prediction of the thermodynamic behavior of mixtures is industrially important problem. Engineers and scientists usually refer excess Gibbs energy models for vapor- liquid equilibria calculations such as WILSON, NRTL, UNIQUAC, and UNIFAC. In order to describe the thermodynamics for mixtures, the aforementioned models compute the activity coefficient of the compounds using the information on binary interaction parameters that are derived from experimental results. Thus, these models have limited applicability in thermodynamics properties and VLE prediction for the new systems like (CO_2 + MAE/EAE + MDEA/AMP + H_2O) that have no/limited experimental data. For solution of this problem, Solvation thermodynamics models based on computational quantum mechanics, such as the Conductor – like Screening Model (COSMO), provide a good alternative to traditional group-contribution and activity coefficient methods for predicting thermodynamic phase behavior. The major molecule-specific COSMO model is based on surface charge density sigma profile and using a basis set like DFT/TZVP (density functional theory/triple zeta polarized valence). In this work, molecular modeling software COSMOtherm (COSMOtherm C30_1201) has been used.

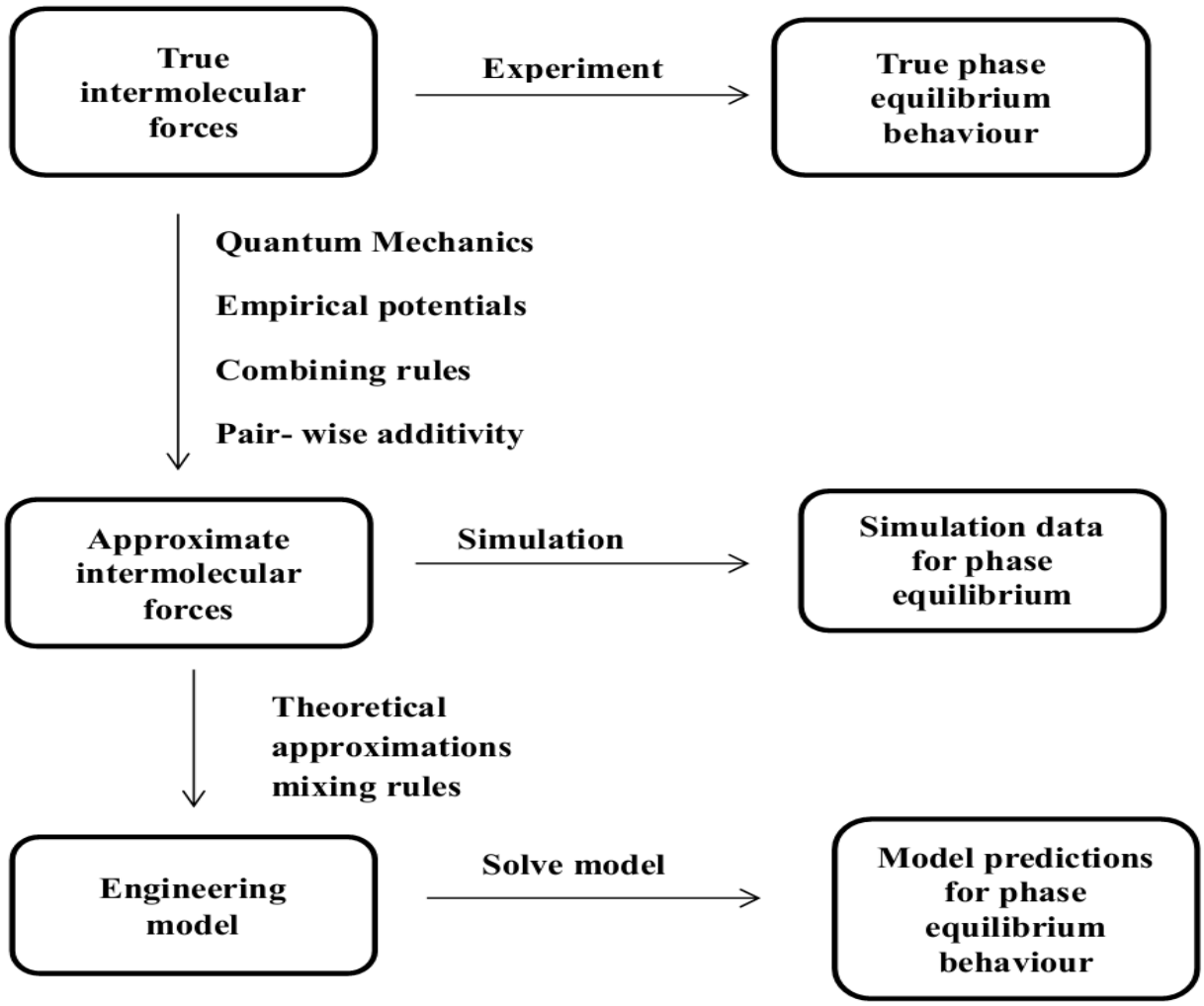

Figure 1.4: Relationships between engineering and molecular simulation-based predictions of phase equilibria.

1.6 ORIGIN OF THE UNDERTAKEN WORK

May it be the CO_2 removal from the flue gas of existing coal fired power plants or from sour natural gas, or the refinery off gases, aqueous alkanolamine absorption/stripping is currently the best technology available; by and large. Because of the need to exploit poorer quality crude and natural gas twined with the enhanced environmental obligations, highly economical and selective acid gas treating processes are of dire need. As a result, there has been a rekindling of interest in new alkanolamine formulations and particularly in aqueous blends of those alkanolamines. Alkanolamine solvents suffer from several common drawbacks; such as energy used for solvent regeneration, solvent volatility, and the oxidative and thermal degradation of solvent. Blended MEA-AMP generally requires

lower heat energy consumption for solvent regeneration than that of blended MEA-MDEA, and DEA-MDEA, which was attested by Sakwattanapong *et al*. (2005). Last decade has witnessed an extensive R&D activity on advanced alkanolamine formulations, ionic liquids, and tertiary amino acid salts dedicated to effective CO_2 capture.

The rate studies conducted by Mimura et al., 1998, led them to establish the fact that MAE followed by EAE possessed higher reaction rate towards CO_2 than even the primary alkanolamine monoethanolamine (MEA). They also stated MAE's good absorption and regeneration characteristics, low corrosion even at a high amine concentration and approximately 20% less regeneration energy as compared with MEA in pilot plant scale. The aforesaid facts have been an impetus in exploring MAE and EAE; the secondary hindered amines, with respect to their CO_2 absorption capacity. The relative comparison of the CO_2 absorption capacity of the proposed alkanolamines with DEA, AMP, MEA and MDEA solvents revealed some encouraging results, which offered the necessary momentum to carry out the work.

The blends of DEA with MDEA and AMP, PZ activated MDEA are currently in use for post combustion CO_2 capture. (MAE/EAE+ AMP/MDEA) blends might be effective for bulk CO_2 removal. As stated earlier in this chapter that aqueous primary or secondary alkanolamines are generally employed for bulk CO_2 removal when the partial pressure of CO_2 in the feed is relatively low and/or the required product purity is high. Though the reaction of CO_2 with these amines is fast, it is accompanied by a highly exothermic heat of reaction (Kohl and Nielsen, 1997), which must be supplied in the regenerator to regenerate the solvent. Consequently, these processes can be energy intensive (Astarita *et al.*, 1983). MAE and EAE in their blends are likely to offer higher reaction rate in comparison to DEA/MEA. Due to their inherent structure, MAE and EAE carbamate in the equilibrated liquid phase are likely to suffer from instability, insisting bicarbonate formation instead and resulting in reduced energy requirement in the regenerator.

In order to establish a solvent to be used in the absorber, a systematic VLE data generation over a wide range of temperature, CO_2 pressure and various relative amine compositions are mandatory. Though various solvents are in use for CO_2 absorption, but a systematic comparison of their performances remained unevaluated so far. Physicochemical properties are of immense significance as far as the design database of gas treating processes is concerned.

The amount of acid gas in equilibrium with slightly loaded solution cannot be measured accurately. Therefore, there is a need for better data or more accurate methods of estimating acid gas solubility at low loading. By improving our knowledge of the thermodynamics in the binary alkanolamine-water system, we can extrapolate the binary model to very low acid gas loading. Activity based models require regression of experimental VLE data on (aqueous alkanolamine + CO_2) systems for estimating binary interaction parameters among various ionic, molecular species present in the equilibrated liquid phase, hence encouraging a little empiricism. Molecular modeling provides an useful alternative to those activity based models; especially where no experimental data are present. The estimated thermodynamic properties like excess Gibbs free energy, excess enthalpy, activity coefficient, activity coefficients of alkanolamines at infinite dilution, and chemical potential using molecular modeling may be used to regress the binary/ternary interaction parameters while developing their activity-based models. One cannot deny the role of correlating the experimental data within a thermodynamic framework to systematically interpolate between and extrapolate (prediction) beyond the range of experimentation. In view of this, the following are the objectives of the present dissertation.

1.7 AIM OF THE THESIS

Proposition of new alkanolamine blends through rigorous experimental and theoretical investigation of vapour-liquid equilibrium (VLE) and thermodynamic properties of CO_2 + aqueous alkanolamines.

1.8 SPECIFIC OBJECTIVES IN REACHING THE GOAL

- ✓ Standardization of developed experimental set-up and methods.
  - ✖ Generation of VLE data on aqueous (diethanolamine (DEA) + *N*-methyl-diethanolamine (MDEA)) solutions.
  - ✖ Generation of VLE data on aqueous (diethanolamine (DEA) + 2-amino-2-methyl-1-propanol (AMP)) solutions.
  - ✖ Correlation of the generated (CO_2 + DEA + AMP + H_2O) and (CO_2 + DEA + MDEA + H_2O) VLE data with rigorous thermodynamic model.
- ✓ Vapour Liquid equilibria of CO_2 over
  - ✖ Aqueous N-methyl-2-ethanolamine (MAE) solutions.
  - ✖ Aqueous N-ethyl-ethanolamine (EAE) solutions

- ✖ Aqueous (N-methyl-2-ethanolamine (MAE) +*N*-methyl-diethanolamine (MDEA)) solutions.
- ✖ Aqueous (N-methyl-2-ethanolamine (MAE) + 2-amino-2-methyl-1-propanol (AMP)) solutions.
- ✖ Aqueous (Ethyl-amino-ethanolamine (EAE) +*N*-methyl-diethanolamine (MDEA)) solutions.
- ✖ Aqueous (Ethyl-amino-ethanolamine (EAE) + 2-amino-2-methyl-1-propanol (AMP)) solutions.

✓ Evaluation of thermodynamic properties of aqueous solutions of MAE and EAE as well as (CO_2 + EAE + H_2O) and (CO_2 + MAE + H_2O) solutions using COSMOtherm.

✓ Generation and correlation of new density data of the following systems

- ✖ $(\mathrm{EAE} + \mathrm{MDEA} + \mathrm{H_2O})$
- ✖ $(\mathrm{EAE} + \mathrm{AMP} + \mathrm{H_2O})$
- ✖ $(\mathrm{MAE} + \mathrm{AMP} + \mathrm{H_2O})$
- ✖ $(\mathrm{MAE} + \mathrm{MDEA} + \mathrm{H_2O})$

REFERNCES

Astarita, G., Savage. D.W. and Bisio, A. (**1983**). Gas treating with chemical solvents. John Wiley and Sons, New York.

Bishnoi, S. and Rochelle, G. T. (**2002**). Absorption of Carbon Dioxide in Aqueous Piperazine / Methyldiethanolamine. *AIChE Journal*, 2788-2799.

Bolland, O. (**2004**). CO_2 Capture Technologies- an Overview. The Second Trondheim Conference on CO_2 Capture, Transport and Storage.

Bonenfant, D., Mimeault, M. and Hausler, R. (**2005**) Comparative analysis of the carbon dioxide absorption and recuperation capacities in aqueous 2-(2-aminoethylamino)ethanol (AEE) and blends of aqueous AEE and N-methyldiethanolamine solutions. *Industrial and Engineering Chemistry Research*, 44, 3720-3725.

Chowdhury, P., Mekala, S., Dreisbach, F. and Gumma, S. (**2012**). Adsorption of CO, CO_2 and CH_4 on Cu-BTC and MIL-101 Metal Organic Frameworks: Effect of Open Metal Sites and Adsorbate Polarity. *Microporous and Mesoporous Materials.* 152, 246-252.

Derks P. W. J. (**2006**). Carbon Dioxide Absorption in Piperazine Activated N-Methyldiethanolamine, PHD Thesis, University of Twente, Netherlands.

Eirik F. S. (**2005**). Computational Chemistry Study of Solvents for Carbon Dioxide Absorption. PHD Thesis at Norwegian University of Science and Technology, Trondheim, 99-111.

Gabelman, A., and Hwang, S. **(1999).** Hollow fiber membrane contactors. *Journal of Membrane Science*, 159, 61.

Gas Process Handbook '92, Hydrocarbon Processing, Vol. 71, No. 4, April 1992.

Goldstein, A.M., Heinzelmann, F.J., and Say, G.R. (**1986**). New FLEXORB gas treating technology for acid gas removal. *Energy Progress*, 6(2), 67-70.

Gong, Y., Wang, Z. and Wang, S. (**2006**). Experiments and simulation of CO_2 removal by mixed amines in a hollow fiber membrane module. *Chemical Engineering Process*, 45, 652.

Hakka, L. and Ouimet, M. A. (**2004**). Method for recovery of CO_2 from gas streams, US patent application.

Hart, A. and Gnanendran, N. (**2009**). Cryogenic CO_2 capture in natural gas. *Energy Procedia I, GHGT-9*, 697-706.

Hermes, J. E., and Rochelle, G. T. (**1987**). A mass transfer based process model of acid gas absorption absorption/stripping using methyldiethanolamine. Presented at the American Chemical Society National Meeting, New Orleans, LA.

Jenab, M.H., Abdi, M.A., Najibi, S.H., Vahidi, M. and Matin, N.S. (**2005**). Solubility of Carbon Dioxide in Aqueous Mixtures of N-Methyldiethanolamine + Piperazine + Sulfolane. *Journal of Chemical and Engineering Data*, 5.

Kohl, A.L, Nielsen, R. B. (**1997**). Gas Purification 5th edition, Gulf Publishing Company, Houston, USA.

Krishna, R. (**2012**). Adsorptive separation of $CO_2/CH_4/CO$ gas mixtures at high pressures. *Microporous and Mesoporous Materials*, 156, 217-223.

Krishna, R. and Baur, R. (**2003**). Modelling issues in zeolite based separation processes, *Separation and Purification Technology*, 33, 213-254.

Krishna, R. and van Baten, J.M. (**2007**). Using molecular simulations for screening of zeolites for separation of CO_2/CH_4 mixtures. *Chemical Engineering Journal*, 133, 121-131.

Krishna, R. and van Baten, J.M. (**2011**). Investigating the potential of MgMOF-74 membranes for CO_2 capture. *Journal of Membrane Science*, 377, 249-260.

Krishna, R. and van Baten, J.M. (**2012**). A comparison of the CO_2 capture characteristics of zeolites and metal-organic frameworks. *Separation and Purification Technology*, 87, 120-126.

Kvamsdal, H.M., Maurstad, O., Jordal, K. and Bolland, O. (**2004**). Benchmark of gas turbine cycles with CO_2 capture. 7th International Conference on Greenhouse Gas Control Technologies, Vancouver, Canada.

Luis M. B. (**2007**). Evaluation of Cosmo-RS for Henry Constants and Selectivity Prediction, Universidade de Aveiro, 27-51.

Ma'mun, S., Svendsen, H.F., Hoff, K.A. and Juliussen, O. (**2004**). Selection of new absorbents for carbon dioxide capture. 7th International Conference on Greenhouse Gas Control Technologies, Vancouver, Canada.

Maddox, R. N. (**1998**). Gas Conditioning and Processing – Advanced Techniques and Applications, Ed.

Mason, J.A., Sumida, K., Herm, Z.R., Krishna, R. and Long, J.R. (**2011**). Evaluating Metal-Organic Frameworks for Post-Combustion Carbon Dioxide Capture via Temperature Swing Adsorption. *Energy and Environmental Science*, 3, 3030-3040.

Mimura, T., Satsumi, S., Iijima, M. and Mitsuoka, S. (**1999**). Development on Energy Saving Technology for Flue Gas CO2 Recovery by the Chemical Absorption Method in Power Plant. *Greenhouse Gas Control Technol*., ProcInt Conf.

Mimura, T., Suda, T., Iwaki, I., Honda, A. and Kumazawa, H. (**1998**). Kinetics of Reaction between Carbon dioxide and Sterically Hindered Amines for Carbon dioxide Recovery from Power Plant Flue Gases. *Chemical Engineering Communication.*170, 245-260.

Mishra, P., Mekala, S., Dreisbach, F., Mandal, B. and Gumma, S. (**2012**). Adsorption of CO2, CO, CH4 and N2 on a zinc based metal organic framework, *Separation and Purification Technology*, 94, 124-130.

Nagao, Y., Hayakawa, A., Suzuki, H., Iwaki, T., Mimura, T. and Suda, T. (**1998**). Comparative study of various amines for the reversible absorption capacity of carbon dioxide Studies. *Surface Science and Catalysis*, 669-672.

Paul, S., Ghoshal, A.K. and Mandal, B. (**2008**). Theoretical studies on separation of CO_2 by single and blended aqueous alkanolamine solvents in flat sheet membrane contactor (FSMC), *Chemical Engineering Journal*, 144 352.

Paul, S., Ghoshal, A.K. and Mandal, B. (**2007**). Removal of CO_2 by single and blended aqueous alkanolamine solvents in hollow-fiber membrane contactor: modeling and simulation. *Industrial Engineering and Chemistry Research*, 46, 2576.

Rao, A. B. and Rubin, E. S. (**2002**). A Technical, Economic, and Environmental Assessment of Amine-Based CO_2 Capture Technology for Power Plant Greenhouse Gas Control. *Environmental Science and Technology.*

Reddy, S., Scherffius, J., Freguia, S. and Roberts, C. (**2003**). Fluor's Econamine FG Plus SM Technology. Second International Conference on Carbon Sequestration.

Reed, B. W., Semmens, M. I. and Cussler, E. L. In *Membrane Separations Technology: Principles and Applications*; R. D. Noble, S. A. Stern, Eds.; Elsevier: Amsterdam, 1995.

Rinker, E.B. (**1997**). Acid gas treating with blended alkanolamines. Ph.D. dissertation. University of California, Santa Barbara, USA.

Sakwattanapong, R., Aroonwilas, A. and Veawab, A. (**2005**). Behavior of reboiler heat duty for CO_2 capture plants using regenerable single and blended alkanolamines. *Industrial and Engineering Chemistry Research,* 44, 4465-4473.

Salako A. E. (**2005**). Removal of Carbon dioxide from Natural Gas for LNG Production, Institute of Petroleum Technology Norwegian University of Science and Technology Trondheim, Norway. Pp 6-19.

Sirkar, K. K. Other New Membrane Processes. In *Membrane Handbook*; W. S. W. Ho; K. K. Sirkar, Eds.; Van Nostrand Reinhold: New York, 1992; Kluwer Academic Publishers: Boston, 2001.

Sivasubramanian, M.S. (**1985**). The heat and mass transfer rate approach for the simulation and design of acid gas treating units. Ph.D. dissertation. Clarkson College, New York.

Thambimuthu, K. and Davidson, J. (**2004**). Overview of CO_2 Capture. 7th International Conference on Greenhouse Gas Control Technologies, Vancouver, Canada.

Tuinier, M.J. (**2011**). Novel process concept for cryogenic CO_2 capture. Ph.D Dissertation. Eindhoven University of Technology, Netherlands.

Wang, R., Li, D.F. and Liang, D.T. (**2004**). Modelling of CO_2 capture by three typical amine solutions in hollow fiber membrane contactors. *Chem. Eng. Process.*, 43, 849.

Wang, W.P., Lin, H.T. and Ho, C.D. (**2006**). An analytical study of laminar co-current flow gas absorption through a parallel-plate gas–liquid membrane contactor. *Industrial and Engineering Chemistry Research*, 278, 181.

Yagi, Y., Mimura, T., Iijima, M., Ishida, K., Yoshiyama, R., Kamijo, T. and Yonekawa,T. (**2004**). Improvements of Carbon Dioxide Capture Technology. 7thInternational Conference on Greenhouse Gas Control Technologies, Vancouver, Canada.

Yeon, S.H., Sea, B., Park, Y.I. and Lee, K.H. (**2005**). Application of pilot-scale membrane contactor hybrid system for removal of carbon dioxide from flue gas. *Journal of Membrane Science*, 257, 156.

Zhang, H.Y., Wang, R., Liang, D.T. and Tay, J.H. (**2006**). Modeling and experimental study of CO_2 absorption in a hollow fiber membrane contactor. *Journal of Membrane Science,* 279, 301.

Zhang, X., Wang, J., Zhang, C. F., Yang, Y. H. and Xu, J. J. (**2003**). Absorption rate intoa MDEA aqueous solution blended with piperazine under a high CO_2 partial pressure. *Industrial and Engineering Chemistry Research,* 42, 118-122.

Chapter 2

BASIC CHEMISTRY AND THERMODYNAMICS OF CO_2-AQUEOUS ALKANOLAMINE SYSTEMS

Chapter 2

BASIC CHEMISTRY AND THERMODYNAMICS OF CO_2 - AQUEOUS ALKANOLAMINE SYSTEMS

2.1 INTRODUCTION

This chapter is an introduction to the basic chemistry of aqueous alkanolamines with CO_2 and thermodynamics of aqueous alkanolamine system. It provides a brief review of the chemical reactions in the (CO_2 + alkanolamine + water) systems and different concentration scales and their conversion, ideal and non-ideal solutions, activity coefficient, different standard state conventions, Chemical and phase equilibria, the relations between chemical potential, fugacity, activity coefficient and excess Gibbs energy functions, especially as they are related to the weak electrolyte systems. Equilibrium thermodynamics is the combination of physical vapor - liquid equilibrium (VLE) of molecular species and chemical reaction equilibrium that typically occur in aqueous alkanolamine systems. To understand and model the acid gas + aqueous alkanolamine systems, one should be aware of the multi-component and multiphase equilibria prevailing here and efficacy of the thermodynamic relations.

A review of research being carried out; especially in the recent past on thermodynamics and vapor-liquid equilibrium of CO_2 in (alkanolamine + water) system are presented in this chapter.

2.2 BASIC CHEMISTRY OF CO_2 + AQUEOUS ALKANOLAMINES

Amines, which have two hydrogen atoms directly attached to a nitrogen atom, such as monoethanolamine (MEA) and 2-(2-aminoethoxy) ethanol (DGA), are called primary amines and are generally the most alkaline. Diethanolamine (DEA),diisopropanolamine (DIPA) *N*-methyl-2-ethanolamine (MAE), and *N*-ethyl-ethanolamine **(**EAE) have one hydrogen atom directly attached to the nitrogen atom and are called secondary amines. Triethanolamine (TEA) and methyldiethanolamine (MDEA) represent completely substituted ammonia molecules with no hydrogen atom directly attached to the nitrogen atoms, and are called tertiary amines. The structural formulas of some important amines and sterically hindered amines like 2-amino 2-methylpropanol (AMP), *N*-methyl-2-ethanolamine (MAE), and *N*-ethyl-ethanolamine (EAE) for gas treating are presented in Figure 2.1. Nitrogen lone pair of electrons renders the basicity, whereas the presence of hydroxyl group increases water solubility for the alkanolamines, hence reduces their vapor pressure. Molecular structure determines the degree of steric hindrance, the hybridization, the possibility to form intra-molecular or intermolecular hydrogen bonding and the presence of functional groups may further affect the electronic structure via their electron donating or withdrawing character (inductive and electrostatic effects, mesomeric effects).

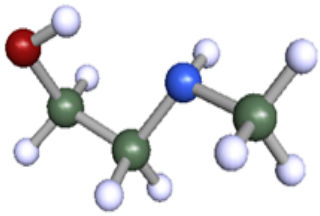

1-(Methylamino)ethanol (MAE)

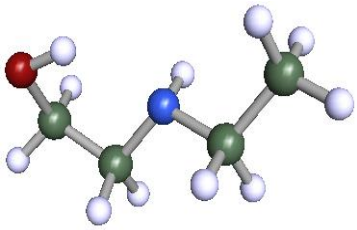

2-(Ethylamino)ethanol (EAE)

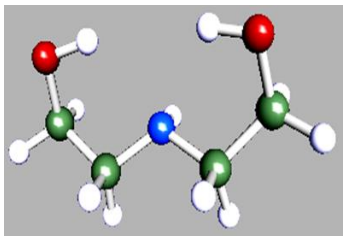

2,2'-Iminodiethanol (DEA)

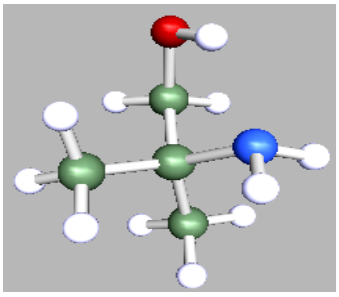

2-amino-2-methyl-1-propanol (AMP)

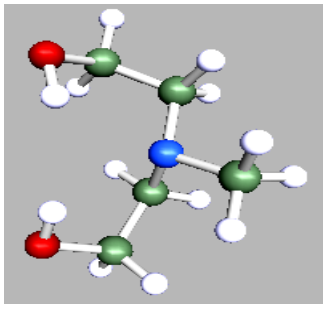

N-Methyldiethanolamine (MDEA)

Figure 2.1: Structure of Alkanolamines.

It is the basicity, which plays an important role in reaction mechanism and the overall reaction enthalpy. The basicity of the alkanolamine solvents and their carbamate stabilities enjoy a non-linear relationship.

Carbamate reactive solvents (e.g. MEA, DEA) have higher capacity to dissolve the CO_2 molecules. They have higher rate of reactions so that they are able to overcome the mass transport limitation through the interface. In principle, quick reactions remove the absorbate molecules readily from interface and give empty space for new molecules to arrive. Since this process is exothermic, the process of regeneration is costly and energy demanding. Hook (1997) studied different type of amines including sterically hindered amines like AMP (two methyl groups at the alpha-carbon to the amine group) and N-methylalanine (one methyl group at the alpha-carbon to the amine group) for CO_2 absorption and regeneration by performing experiments and by doing NMR studies to determine the carbamate, bicarbonate and carbonate concentration in solution. It was found that the presence of two methyl groups at the alpha carbon next to the nitrogen molecule reduces the stability of the carbamate but the effect of one methyl group at alpha carbon next to the amine group is however insufficient to induce full conversion of the carbamate species into bicarbonate (Singh, 2011). McCann *et al*. (2011) studied the carbamate stability for different sterically hindered amines by NMR analysis. It was found that an increase in the level of steric hindrance resulted in a decreased carbamate stability. Chakraborty *et al*. (1988) investigated the changes in the electronic characteristics due to various substituents on the alpha carbon atom adjacent to the amine group in sterically hindered amines, altering their basicity, and carbamate stability. Carbamate stability was studied by da Silva *et al*. (2006) for various amine based solvent including AMP and MEA by using ab initio calculation methods and a free energy of perturbation method.

The development of a reaction mechanism is, of course, a prerequisite to the understanding, equilibrium / rate modelling of CO_2 with amine systems and the next section is devoted to it.

2.2.1 CO_2-Alkanolamine Reactions

In aqueous solutions of primary and secondary alkanolamines, the following reactions with CO_2 occur (Danckwerts and Sharma, 1966; Danckwerts, 1979).

2.2.1.1 Carbamate formation reaction:

$$CO_2 + 2RR'NH \leftrightarrow RR'NCOO^- + RR'NH_2^+ \qquad (2.1)$$

$R' = H$ for primary amines

The zwitterion mechanism originally proposed by Caplow (1968) and reintroduced by Danckwerts (1979) is generally accepted as the reaction mechanism for reaction (2.1).

$$CO_2 + RR'NH \leftrightarrow RR'NH^+COO^- \quad (2.2)$$

$$RR'NH^+COO^- + B \leftrightarrow RR'NCOO^- + BH^+ \quad (2.3)$$

This mechanism comprises two steps: formation of the CO_2-amine zwitterion (reaction (2.2)), followed by base catalyzed deprotonation of this zwitterion (reaction (2.3)). Here B is a base, which could be amine, OH^-, or H_2O (Blauwhoff*et al.*, 1984). However, Versteeg and van Swaaij (1988) argued that, for aqueous amine solutions, the contribution of the hydroxyl ion is minor due to its low concentration, and may be neglected without a substantial loss of accuracy. Laddha and Danckwerts (1981) considered only the amine as the base in Eq. (2.3) for aqueous alkanolamine solutions. Thus, the equilibrium loading capacities of primary and secondary alkanolamines are limited by stoichiometry of reaction (2.1) to 0.5 mole of CO_2/mole of amine. For normal primary and secondary amines e.g. MEA, DEA, etc. the carbamates formed (reaction (2.1)), are quite stable. Although Danckwerts and other investigators after considering that the zwitterion species to be attacked by a base which extracts a proton in their work, they ignore the suggestion that the amine group may be hydrated before forming the zwitterion. More recent da Silva and Svendsen (2004) and Ohno *et al*. (1999) suggested on the basis of quantum mechanical calculations that any zwitterion species is likely to be very unstable. The zwitterion may be an entirely transient state (giving a single-step mechanism), it may be a short-lived species or it may be a transition state (Singh, 2011). Crooks and Donnellan (1989), proposed a single step mechanism:

$$RR'NH + B + CO_2 \leftrightarrow RR'NCOO^- + BH^+ \quad (2.4)$$

2.2.1.2 Carbamate reversion reaction:

If the amine is hindered, the carbamate is unstable and it may undergo carbamate reversion reaction as follows (Sartori and Savage, 1983):

$$RR'NCOO^- + H_2O \leftrightarrow RR'NH + HCO_3^- \quad (2.5)$$

Reaction (2.5) means that for the hindered amines one mole of CO_2 is absorbed per mole of amine. However, a certain amount of carbamate hydrolysis (reaction (2.5)) occurs with all amines so that even with MEA and DEA the CO_2 loading may exceed 0.5, particularly

at high pressures and higher contact times (Sartori and Savage, 1983). The degree of hydrolysis of the carbamate species depends on several factors, such as its chemical stability, which is strongly influenced by the temperature. McCann *et al*. (2011) stated that 'the amines with a lower pKa values (basicity) typically show lower carbamate equilibrium constants'.

2.2.1.3 Other proposed reaction schemes for bicarbonate formation:

Yih and Shen (1988) have presumed that sterically hindered amine; 2-amino-2-methyl-1-propanol (AMP) cannot form carbamate. Hence, the following alternative reaction (2.4) was proposed by them for AMP. This kind of reactions are likely to happen partially for *N*-methyl-2-ethanolamine (MAE), and *N*-ethyl-ethanolamine (EAE).

$$RR'NH^+COO^- + H_2O \leftrightarrow RR'NH_2^+ + HCO_3^- \quad (2.6)$$

Another alternative mechanism for the bicarbonate formation has been proposed by Chakraborty *et al.* (1986).

$$RR'NH + CO_2 + H_2O \leftrightarrow RR'NH_2^+ + HCO_3^- \quad (2.7)$$

However, Eq. (2.7) is similar to reaction of CO_2 with tertiary amines (e.g., MDEA).

It is anticipated that for MAE and EAE, probably the carbamate reversion reaction is much facile than DEA. The role of Eqs. (2.6 and 2.7) can't even be denied fully.

2.2.1.4 Hydration of CO_2

CO_2 can also react directly in aqueous amine systems to form bicarbonate. The formation of bicarbonate from CO_2 and water can be described by the following three (related) reactions.

$$CO_2(aq) + H_2O \leftrightarrow H_2CO_3 \quad (2.8)$$

$$CO_2(aq) + OH^- \leftrightarrow +HCO_3^- \quad (2.9)$$

$$H_2CO_3 + OH^- \leftrightarrow +HCO_3^- + H_2O \quad (2.10)$$

2.2.1.5 Deprotonation of bicarbonate

Bicarbonate can again be deprotonated by a base molecule (B).

$$HCO_3^- + B \leftrightarrow +CO_3^{2-} + BH^+ \quad (2.11)$$

The base molecule is usually an amine moleecule or a hydroxyl ion (OH^-). Bicarbonate formation is, however, a rather slow reaction. It has been observed that this reaction

proceeds more quickly in the presence of amine molecules, an effect to be considered besides the direct roles of the amines as bases (Donaldsen and Nguyen, 1980). This is in accordance with the statement by Sharma and Danckwerts (1963) that 'Brønsted bases can catalyze the formation of bicarbonate'.

2.2.1.6 CO_2 - tertiary amine reaction:

$$RR'R''N + H_2O + CO_2 \leftrightarrow RR'R''NH + HCO_3^- \quad (2.12)$$

Tertiary amines cannot form carbamates and therefore they act as chemical sink for CO_2 in aqueous solutions simply by providing basicity, the final product being bicarbonate. Hence, the stoichiometry of the CO_2 - tertiary amine reactions is one mole of CO_2 per mole of amine.

2.3 CONVERSION IN CONCENTRATION SCALES

One difficulty that is encountered in modeling aqueous alkanolamine-acid gas systems is that experimental data exists in three different concentration units, mole fraction, molality, and molarity. In order to keep a consistent model we must use a single concentration system for all equations and experimental data. Therefore, relationships are needed to convert between the different concentration bases. Mole fraction scale embodies a theoretical significance not possessed by other concentration scales. Such as, the entropy of mixing of an ideal solution is proportional to the sum of the product of the component mole fraction and the logarithm of component mole fraction. Also for ideal solutions obeying Henry's law and Raoult's law, the equilibrium partial pressure of any component above the solution is directly proportional to its mole fraction in the solution, but is not directly proportional to its molality or molarity, except for very dilute solutions.

2.3.1 Molality to Mole Fraction

Molality, m_i, is defined as moles of substance i per kg of solvent. Molality units are typically used for dilute solutions in water where mole fractions would require many decimal places to maintain accuracy. The conversion of molality to mole fraction is performed as follows, where MW_{solv} is the molecular weight of the solvent in grams per gram mole.

$$X_i = \frac{m_i \times MW_{Solv} \times 1\ kg}{1000g} \quad (2.13)$$

Assuming the solvent is water, Eq. (2.13) becomes

$$X_i = \frac{m_i \times 18}{1000} \tag{2.14}$$

2.3.2 Molarity to Mole Fraction

Molarity unit requires more information for conversion to mole fractions than does molality. Molarity is defined as moles of substance of interest per liter of solution. A liter of solution is not well defined since the density of alkanolamine solutions change with concentration and temperature. Therefore the density of the solution (g solution / liter solution) must be known in order to convert to mole fractions. First; the weight fraction; w_i, of the alkanolamine is calculated from Eq.

$$W_i = \frac{M_i \times MW_i}{\rho_{soln} \times 1000} \tag{2.15}$$

Where, W_i is the weight fraction of i, gram i / total gram soln.

M_i is the molarity of component i, mole i / L solution.

MW_i is the molecular weight of component i, gram i / gram mole i.

ρ_{soln} is the density of the solution, gram solution / mL solution.

To convert weight fraction to mole fraction, one has to assume that amine and water are the only important species. This is usually possible since the experimental data is reported as a function of the unloaded amine-water concentration even at very high acid gas loadings. Eq. (2.16) is used to convert weight fraction to mole fraction.

$$X_i = \frac{{}^{W_i}/_{MW_i}}{\left(\left({}^{W_i}/_{MW_i}\right) + \left({}^{(1-W_i)}/_{18}\right)\right)} \tag{2.16}$$

2.4 CONDITIONS OF EQUILIBRIUM

Let us consider a heterogeneous closed system made up of two or more phases. Each phase is treated as an open system within the larger closed system allowing mass and heat transfer between the various phases. Neglecting surface effects and gravitational, electric and magnetic fields, at thermal and mechanical equilibrium we expect the temperature and pressure to be uniform throughout the entire homogeneous closed system. Gibbs showed that at chemical equilibrium each species must have a uniform value of chemical potential in all co-existing phases between which it can pass. These conditions of phase equilibrium for the closed heterogeneous system can be summarized as:

$$\begin{aligned} T^1 &= T^2 = \ldots\ldots\ldots T^n \\ P^1 &= P^2 = \ldots\ldots\ldots P^n \quad i= 1, 2,\ldots,m \\ \mu_i^1 &= \mu_i^2 = \ldots\ldots\ldots \mu_i^n \end{aligned} \tag{2.17}$$

Where n is the number of phases and m is the number of species present in the closed system. μ_i is defined by the Eq. (2.18).

$$\mu_i = \left(\partial G / \partial n_i\right)_{T,\, P,\, n_{j\neq i}} \tag{2.18}$$

G is the Gibbs free energy of the open system (phase) and n_i is the number of moles of component i.

2.5 CHEMICAL EQUILIBRIA AND PHASE EQUILIBRIA

In a closed vapour - liquid system containing both electrolytes and non - electrolytes, the electrolyte species will partially or wholly dissociate in the liquid phase to form ionic species. However, unless the system temperature is very high, vapour phase dissociation of electrolyte components will be negligible. This suggests that, in practice, it is necessary to apply Eq. (2.17) only to neutral molecular species to determine the equilibrium distribution of components between the vapour and liquid phases. Because ions will be present only in the liquid phase for applications of interest in this work, Eq. (2.17) can be neglected for ionic species. This is not to suggest that ionic species do not play an important role in phase equilibrium calculations. Chemical equilibrium governs the distribution of an electrolyte in the liquid phase between its molecular and ionic forms. Since, it is the molecular form of the electrolyte that comes to equilibrium with the same component in the vapour phase, chemical equilibrium significantly affects the phase equilibrium and vice-versa. In addition, the presence of ionic species in the liquid phase results in highly nonideal thermodynamic behaviour that is manifested in activity coefficients, which depart significantly from unity. Aqueous mixtures of weak acid and weak base electrolytes behave drastically different than single solute systems. When a weak acid gas and a weak base, like alkanolamine, are present together in aqueous solution, the extent of the respective dissociation reactions are enhanced. This shift towards the ionic form reduces the concentrations of the molecular or unreacted forms of the weak electrolytes in solution. Since, it is the molecular forms of the weak electrolytes that come into equilibrium with the same species in the vapour phase, the equilibrium partial pressure of the weak electrolytes in the vapour phase can be greatly reduced.

Chemical potential is a difficult thermodynamic variable to use in practice, partly because only relative values of this variable can be computed. Moreover, as the mole fraction of a component approaches infinite dilution, its chemical potential approaches negative infinity. To overcome these difficulties, G.N. Lewis (Lewis and Randal, 1961) defined a new thermodynamic variable called fugacity. $f_{i,}$ which he related to the chemical potential as

$$\mu_i - \mu_i^0 = RT \ln \hat{f}_i / f_i^0 \qquad (2.19)$$

Where μ_i^0 and f_i^0 are arbitrary, but not independent, values of the chemical potential and fugacity of component i for some chosen reference state. $\hat{f}_i$ is the value of the fugacity of component i in the mixture. The difference in chemical potential $\mu_i - \mu_i^0$, is written for an isothermal change between the arbitrary reference state and the actual state for any component in the system. The ratio $\hat{f}_i / f_i^0$ is called the activity of the species i,(a_i). Lewis was able to show from Eqs. (2.17) and (2.19) that an equivalent and more conveniently applicable, expression of phase equilibrium for all species at constant and uniform values of the system temperature and pressure is

$$f_i^1 = f_i^2 = ...f_i^n ; \; i= 1,2,\ldots,m \qquad (2.20)$$

Eq. (2.20) has been widely adopted for phase equilibrium calculations. However the concept of chemical potential continues to be used in chemical literature, specially as it relates to chemically reactive systems including electrolyte systems. Indeed, because of its relation to Gibbs free energy, chemical potential is the thermodynamic variable generally manipulated to determine the equilibrium distribution of species in a chemically reacting system at constant temperature and pressure. Both the phase and chemical equilibrium must be considered. Fugacity coefficient and activity coefficient are the two important variables in vapour phase and liquid phase thermodynamics.

2.6 IDEAL SOLUTIONS, NON-IDEAL SOLUTIONS AND THE ACTIVITY COEFFICIENT

A solution is defined to be ideal if the chemical potential of every species in the solution is a linear function of the logarithm of its mole fraction. That is for every component in an ideal solution the following relation holds:

$$\mu_i = \mu_i^0 + R\,T \ln x_i \tag{2.21}$$

Where μ_i^0 is known as standard state or reference state chemical potential of component i. μ_i^0 depends on the reference state temperature and pressure. Both Raoult's law and Henry's law can be derived from Eqs. (2.19) and (2.21) assuming that the vapour phase behaves as an ideal gas. For a real solution, the chemical potential is not a linear function of the logarithm of the mole fraction. In order to preserve the form of Eq. (2.21) for real solutions, the activity coefficient γ_i, is defined such that

$$\mu_i = \mu_i^0 + R\,T \ln x_i\gamma_i \tag{2.22}$$

Where γ_i is a function of temperature, pressure, and composition of the solution. It is emphasized that Eq. (2.22) should be viewed as a definition of the activity coefficient. Comparing Eqs. (2.19) and (2.22), it can be seen that

$$\gamma_i = \hat{f}_i / x_i f_i^0 = a_i / x_i \tag{2.23}$$

The definition of activity coefficient from Eq. (2.23) is incomplete until a reference state is specified and thus a value of μ_i^0. This can be accomplished by identifying the conditions of temperature pressure and composition at which γ_i becomes unity. μ_i^0 is then the chemical potential of component i at the conditions at which γ_i is taken, by convention, to be unity.

2.7 STANDARD STATE CONVENTION

The process of identifying reference or standard states at which the activity coefficients of all species in a solution becomes unity is referred to as normalization.

2.7.1 Normalization Convention I

By Normalization Convention 1, the activity coefficient of each component approaches unity as its mole fraction approaches unity at the system temperature and system reference pressure. That is for all components

$$\mu_s = \mu_i^0 + RT \ln x_i\ \gamma_s \qquad \gamma_s \to 1 \text{ as } x_s \to 1 \tag{2.24}$$

Since this normalization convention holds for all components of a solution, it is known as the symmetric normalization convention; activity coefficients normalized in this manner, are said to be symmetrically normalized. This convention leads to Raoult's law and applied when all components of the solution are liquid at system temperature and pressure.

2.7.2 Normalization Convention II

The reference state for the solvent is different from the reference state for the solutes adopted under Convention II. For the solvent, the reference state is the same as that adopted under Normalization Convention I. The reference state for a solute is taken to be the hypothetical state of pure solute found by extrapolating its chemical potential from infinite dilution in solvent to the pure solute (Denbigh, 1981) at the solution temperature and reference pressure. It is sometimes referred to as the ideal dilute reference state. For a binary solution, Convention II leads to the following expressions for chemical potentials and activity coefficients.

$$\mu_s = \mu_s^0 + R\,T \ln x_s \gamma_s \qquad \gamma_s \to 1 \quad \text{as} \quad x_s \to 1 \tag{2.25}$$

$$\mu_i = \mu_i^0 + R\,T \ln x_i \gamma_i^* \qquad \gamma_i^* \to 1 \text{ as} \quad x_i \to 0 \tag{2.26}$$

Where, the subscripts i and s refer to solute and solvent respectively. Since solute and solvent activity coefficients are not normalized in the same way, Convention II is known as the unsymmetric normalization convention. The superscript, *, on the activity coefficient of the solute is used to indicate that the activity coefficient of this solute approaches unity as its mole fraction approaches zero. This normalization convention leads to Henry's law and is applicable when some components of the solution are gases or solids at the system temperature and pressure.

2.7.3 Normalization Convention III

The concentration of solutes including salts and gases are often measured on molality scale. Accordingly, activity coefficients of these species are also often defined with reference to the molality scale. According to the Normalization Convention III, the activity coefficient of solute and solvent for a binary solution is defined as

$$\mu_s = \mu_s^0 + RT \ln x_s \gamma_s \qquad \gamma_s \to 1 \text{ as } x_s \to 1 \tag{2.27}$$

$$\mu_i = \mu_i^{\Delta} + RT \ln m_i\, \gamma_i^{\Delta} \qquad \gamma_i^{\Delta} \to 1 \text{ as } m_i \to 0 \tag{2.28}$$

μ_s^0 is the chemical potential of the pure solvent at the system temperature and reference pressure. μ_i^Δ is the chemical potential of the solute in a hypothetical solution of unit molality (Denbigh, 1981). That is, μ_i^Δ is the chemical potential of the solute in a hypothetical ideal solution when m_i and γ_i^Δ are both equal to unity.

2.8 RELATION BETWEEN ACTIVITY COEFFICIENTS BASED ON DIFFERENT STANDARD STATES

Activity coefficients, which are normalized unsymmetrically, are related to the corresponding symmetrically normalized activity coefficients in the binary solution in the following way (Prausnitz *et al.*, 1986; Van Ness and Abbott, 1979):

$$\gamma_i = \frac{\hat{f}_i}{x_i\, f_{purei}} \tag{2.29}$$

$$\gamma_i^* = \frac{\hat{f}_i}{x_i\, H_{i,s}} \tag{2.30}$$

Where $H_{i,s}$ is defined as follows

$$H_{i,s} = \lim_{x_i \to 0} \frac{\hat{f}}{x_i} \tag{2.31}$$

Comparison of Eq. (2.29) with Eq. (2.22) reveals that $H_{i,s}$ is the reference state fugacity of the solute. It is called the Henry's constant of solute i in solvent s. Dividing Eq. (2.29) by Eq. (2.30) gives

$$\frac{\gamma_i}{\gamma_i^*} = \frac{H_{i,s}}{f_{purei}} \tag{2.32}$$

We know that, $\lim_{x_i \to 0} \gamma_i^* = 1$

Hence, $\lim_{x_i \to 0} \gamma_i = \frac{H_{i,s}}{f_{purei}}$ (2.33)

Substituting Eq. (2.33) into Eq. (2.32),

$$\frac{\gamma_i}{\gamma_i^*} = \lim_{x_i \to 0} \gamma_i \tag{2.34}$$

or $$\frac{\gamma_i}{\gamma_i^*} = \gamma_i^\infty \tag{2.35}$$

and $$\ln \gamma_i^* = \ln \gamma_i - \ln \gamma_i^\infty \tag{2.36}$$

Where γ_i^∞ is the symmetrically normalized activity coefficient of solute i at infinite dilution in solvent.

$$\gamma_i^\infty = \lim_{x_i \to 0} \gamma_i \tag{2.37}$$

2.9 CHEMICAL EQUILIBRIUM

2.9.1 The Traditional Approach and Equilibrium Constants

In a chemically reacting system, the mole numbers, n_i, are related to the extents of R independent reactions, ξ_i by

$$n_i = n_i^0 + \sum_{j=1}^{R} \nu_{ij} \xi_j \quad i = 1, 2, \ldots, N \tag{2.38}$$

Where ν_{ij} is the stoichiometric coefficient of species i in reaction j, and n_i^0 is some reference amount of species i. Eq. (2.38) serves as a definition for ξ_i which has units of moles. Therefore, the Gibbs free energy, G, of the system can be transformed from a function of temperature, pressure, and N mole numbers to a function of temperature, pressure, and R extent of reaction.

$$G = G(T, P, \xi_1, \xi_2, \ldots\ldots\ldots \xi_R) \tag{2.39}$$

The condition of chemical equilibria is found by minimizing G at constant temperature and pressure with respect to the R extent of reaction. The first order necessary conditions for a minimum in G are

$$\left(\frac{\partial G}{\partial \xi}\right)_{T, P, \xi_{j \neq k}} = 0 \qquad j = 1, 2, \ldots\ldots\ldots, R \tag{2.40}$$

Using the chain rule for differentiation, $\left(\frac{\partial G}{\partial \xi}\right)_{T, P, \xi_{j \neq k}}$ can be expressed as

$$\left(\frac{\partial G}{\partial \xi}\right)_{T, P, \xi_{j \neq k}} = \sum_{i=1}^{N} \left(\frac{\partial G}{\partial n_i}\right)_{T, P, n_{k \neq i}} \left(\frac{\partial n_i}{\partial \xi_j}\right)_{\xi_{j \neq k}} \quad j = 1, 2, \ldots, R \tag{2.41}$$

From Eq. (2.38)

$$\left(\frac{\partial n}{\partial \xi}\right)_{\xi_{j\neq k}} = \nu_{ij} \tag{2.42}$$

Combining Eqs. (2.38), (2.41), (2.42) and (2.18) finally gives

$$\sum_{i=1}^{N} \nu_{ij}\, \mu_i = 0 \qquad j = 1, 2, \ldots, R \tag{2.43}$$

Eq. (2.43) are the classical forms of the equilibrium conditions (Smith and Missen, 1982). When appropriate expressions are introduced for the chemical potential in terms of mole numbers, the non linear Eq. (2.43) can be solved, together with N minus R independent linear mass balance equations, for the composition of the system at equilibrium. The composition of the system at equilibrium can be determined using Eq. (2.38).

For electrolyte solutions, chemical potentials are often written in terms of mole fractions and unsymmetrically normalized activity coefficients. For a system in which a single chemical reaction takes place, substitution of Eqs. (2.25) and (2.26) for μ_i in Eq. (2.43) for any reaction j yields

$$\sum_{i=1}^{N} \nu_i\, \mu_i^0 + RT \sum_{i=1}^{N} \nu_i \ln \gamma_i x_i = 0 \tag{2.44}$$

Where, the summations are over all N components of the system. The activity coefficients of solvent species are symmetrically normalized in Eq. (2.43) while the solute activity coefficients are unsymmetrically normalized. Rearranging Eq. (2.44) gives

$$\ln \prod \left(\gamma_i\, x_i\right)^{\nu_i} = -\frac{1}{RT}\left(\sum_{i=1}^{N} \nu_i\, \mu_i^0\right) \tag{2.45}$$

The right hand side is a function of temperature only at specified reference state for all components. A thermodynamic equilibrium constant, based on the mole fraction scale; K_x, can be defined in the following way

$$RT \ln K_x = -\sum_{i=1}^{N} \nu_i\, \mu_i^0 = \Delta G_T^0 \tag{2.46}$$

Eq. (2.41) relates equilibrium constants (K) to the N values of the reference state chemical potentials, μ_i^0. ΔG_T^0 is the standard Gibbs free energy change of reaction at the specified

temperature T. Eq. (2.46) indicates that for any reaction K_x is a function of temperature only at the specified standard states for the participating components. Combining Eqs. (2.45) and (2.46) yields

$$K_x = \Pi \left(\gamma_i \, x_i\right)^{\nu_i} \tag{2.47}$$

Using $\gamma_i \, x_i = a_i$, Eq. (2.47) can also be expressed as

$$K_x = \Pi \left(a_i\right)^{\nu_i} \tag{2.48}$$

Concentration and activity coefficients of solute in electrolyte solutions are also often based on molality scale. If the molality based activity coefficient convention is adopted then Eqs. (2.46) and (2.47) can be written in the following way,

$$R \, T \ln K_m = -\sum_{i=1}^{N} \nu_i \, \mu_i^{\Delta} = \Delta \, G_T^{\Delta} \tag{2.49}$$

$$K_m = \Pi (\gamma_i m_i)^{\nu_i} \tag{2.50}$$

Where the superscript to the activity coefficient for solute species denoting unsymmetrically normalized activity coefficients expressed on the molality scale has been omitted for generality. Eqs. (2.47) and (2.48) represent the traditional approach for solving equilibrium composition. The equilibrium constant is the only available thermodynamic data related to the standard states of components in a reaction. The purpose of the above discussion was to establish a definition for the equilibrium constant, K_x, and to show how it is related to other thermodynamic variables, in particular, the mole fraction and activity coefficient.

2.9.2 Relation Between the Equilibrium Constants Based on the Mole Fraction Scale and the Molality Scale.

Considering the dissociation reaction of CO_2 into water, if the concentrations and activity coefficients are expressed in terms of the mole fraction scale in accordance with Convention II, we can write,

$$K_{x,CO_2} = \frac{x_{H_3O^+} \; x_{HCO_3^-} \; \gamma^*_{H_3O^+} \; \gamma^*_{HCO_3^-}}{x_{H_2O} \; x_{CO_2} \gamma_{H_2O} \; \gamma^*_{CO_2}} \tag{2.51}$$

The super script $*$ on the activity coefficients of the solutes indicate that they are based on the mole fraction scale and they approach unity as the corresponding mole fraction of each solute approaches zero. The activity coefficient of water approaches unity as its mole fraction approaches unity. Similarly if the concentrations and activity coefficients are based on the molality scale in accordance with Convention III, we can write,

$$K_{m,CO_2} = \frac{m_{H_3O^+}\ m_{HCO_3^-}\ \gamma^{\Delta}_{H_3O^+}\ \gamma^{\Delta}_{HCO_3^-}}{m_{H_2O}\ m_{CO_2}\ \gamma_{H_2O}\ \gamma^{\Delta}_{CO_2}} \tag{2.52}$$

The super script Δ on the activity coefficients of the solutes indicate that they are based on the molality scale and they approach unity as the corresponding mole fraction of each solute approaches zero.

The relation between K_x and K_m for dissociation reaction of CO_2 reaction can be found most easily at the infinitely dilute state where all the activity coefficients in Eq. (2.51) and (2.52) are defined to be unity. For dilute solution using the relation between molality and mole fraction, it can be shown that

$$K_x = K_m \left(\frac{M_S}{1000}\right) \tag{2.53}$$

$$\ln K_x = \ln K_m - \ln\left(1000/M_s\right) \tag{2.54}$$

While Eqs. (2.53) and (2.54) were derived for an infinitely dilute aqueous solution of CO_2, they hold for all finite CO_2 concentrations. Similar reactions can be derived for all other reactions. In general, to convert the logarithm of an equilibrium constant for the dissociation of an electrolyte in water from the molality scale to mole fraction scale, it is necessary to subtract $\ln(1000/M_s)$ for each non-water component on the right hand side of a stoichiometric expression and to add $\ln(1000/M_s)$ for each non water component on the left hand side of a stoichiometric expression. The temperature dependence of equilibrium constant is often reported as

$$\ln K = C_1 + \frac{C_2}{T} + C_3 \ln T + C_4\ T \tag{2.55}$$

The coefficients C_1 through C_4 for different reactions are taken from different literature sources. To convert a value of K_m reported in the form of Eq. (2.55), to K_x, it is necessary

only to adjust the value of C_1, using an equation equivalent to (2.54). The same is true for reverse process, i.e, converting K_x to K_m.

2.9.3 Relation Between Equilibrium Constants Based on Different Standard States

The dissociation equilibrium constants of weak bases are reported in molality scale in literature. Considering the reaction, protonation of alkanolamine

$$H_2O + R\,R'\,R''N\,H^+ \leftrightarrow H_3O^+ + R\,R'\,R''N \tag{2.56}$$

The dissociation equilibrium constant of protonated alkanolamine (Eq. (2.56)) can be expressed in terms of Eq. (2.52),

$$K_{m,R\,R'\,R''\,N} = \frac{{}^{m}_{H_3O^+}\;{}^{m}_{R\,R'\,R''\,N}\;\overset{\Delta}{\gamma}_{H_3O^+}\;\overset{\Delta}{\gamma}_{R\,R'\,R''\,N}}{{}^{x}_{H_2O}\;\gamma_{H_2O}\;{}^{m}_{R\,R'\,R''\,NH^+}\;\overset{\Delta}{\gamma}_{R\,R'\,R''\,NH^+}} \tag{2.57}$$

The superscript on the activity coefficients of solute indicates that they are based on molality scale, they approach unity as the corresponding mole fraction of each solute approaches zero. The corresponding equilibrium constant based on mole fraction scale can be written in the following way,

$$K_{x,R\,R'\,R''\,N} = \frac{{}^{x}_{H_3O^+}\;{}^{x}_{R\,R'\,R''\,N}\;\overset{*}{\gamma}_{H_3O^+}\;\overset{*}{\gamma}_{R\,R'\,R''\,N}}{{}^{x}_{H_2O}\;\gamma_{H_2O}\;{}^{x}_{R\,R'\,R''\,NH^+}\;\overset{*}{\gamma}_{R\,R'\,R''\,NH^+}} \tag{2.58}$$

where the superscript $*$ on the solute activity coefficients indicates that they are unsymmetrically normalized according to the Convention II. But in the VLE model, where alkanolamines are treated as solvents, it exists as liquid at the concerning temperature and pressure. So activity coefficients of alkanolamines are to be symmetrically normalized like water in accordance with the Convention II.

$$\gamma_{R\,R'\,R''\,N} \rightarrow 1 \text{ as } x_{R\,R'\,R''\,N} \rightarrow 1 \tag{2.59}$$

In view of the adopted normalization convention for the activity coefficients of alkanolamines, a new dissociation equilibrium constant is proposed,

$$K'_{x,R\,R'\,R''\,N} = \frac{{}^{x}_{H_3O^+}\;{}^{x}_{R\,R'\,R''\,N}\;\overset{*}{\gamma}_{H_3O^+}\;\gamma_{R\,R'\,R''\,N}}{{}^{x}_{H_2O}\;\gamma_{H_2O}\;{}^{x}_{R\,R'\,R''\,NH^+}\;\overset{*}{\gamma}_{R\,R'\,R''\,NH^+}} \tag{2.60}$$

The relation between K_x and K'_x can be obtained by dividing Eq. (2.60) by Eq. (2.58).

$$K'_x = K_x \frac{\gamma_{R\,R'\,R''\,N}}{\gamma^{*}_{R\,R'\,R''\,N}} \tag{2.61}$$

By substituting Eq. (2.35) in Eq. (2.61),

$$K'_x = K_x\, \gamma^{\infty}_{R\,R'\,R''\,N} \tag{2.62}$$

where $\gamma^{\infty}_{R\,R'\,R''\,N}$ is the symmetrically normalized activity coefficient of alkanolamine at infinite dilution in water, and can be obtained from the VLE data (TPx, and TPxy) for the binary amine water mixture by extrapolation of the alkanolamine activity coefficient to the infinite dilution or by molecular modelling.

2.10 PHASE EQUILIBRIUM

The condition of phase equilibrium in a multiphase system at constant and uniform values of temperature and pressure is given by Eq. (2.15). This is sometimes referred to as the isofugacity condition. For a two-phase vapour - liquid multicomponent system, Eq. (2.15) may be expressed as

$$\hat{f}_i^{\,v}(T, P, y_i) = \hat{f}_i^{\,l}(T, P, x_i)\ ;\ i = 1, 2, \ldots\ldots, N \tag{2.63}$$

Where $\hat{f}_i^{\,V}$ and $\hat{f}_i^{\,l}$ are the fugacities of component i in the vapour mixtures and liquid mixtures respectively, and y_i and x_i represent the mole fraction of all components in the vapour and liquid phases respectively. Eq. (2.63) is of little value in practice unless the fugacities can be related to experimentally accessible state variables including T, P, x, y. The desired relation between the vapour phase fugacity and the accessible vapour phase state variable is provided by the vapour phase fugacity coefficient, φ. A similar relation for the liquid phase fugacity is provided by the activity coefficient.

2.10.1 Vapour Phase Fugacity

The vapour phase fugacity of each species in a mixture is related to its concentration, y_i, and the system pressure, P, through the fugacity coefficient.

$$\hat{f}_i^{\,V}(T, P, y_i) = \hat{\varphi}_i(T, P, y_i) y_i P\ ;\ i = \text{vapour phase component} \tag{2.64}$$

Where $\hat{\varphi}_i$ is defined as

$$\hat{\varphi}_i = \hat{f}_i^v / y_i P \tag{2.65}$$

The present study is focused on VLE of low to moderate partial pressure range, for which vapour phase has been assumed to be ideal, so vapour phase fugacity of any component can be considered as its partial pressure and fugacity coefficient $\hat{\varphi}_i$ becomes unity. This assumption of vapour phase ideality is valid upto acid gas partial pressure 5500 kPa (Li and Mather, 1997).

2.10.2 Liquid Phase Fugacity

The liquid phase fugacity can also be calculated from equation-of-state. However, equations of state often do not satisfactorily describe the volumetric properties of the condensed phase. In addition, volumetric data are usually not available over the entire density range from zero pressure to the system pressure. Therefore, an alternate method is usually adopted by which deviation from ideality is described in terms of excess functions. Using the activity coefficient, the fugacity of a component of a liquid solution can be expressed as

$$\hat{f}_i^l(T, P, x_i) = \gamma_i(T, P, x_i) x_i f_i^{oL}(T) \tag{2.66}$$

Where, i = components of vapour phase

$f_i^{oL}(T)$ is the arbitrary reference state fugacity. For a solvent $f_i^{oL}(T)$ is usually taken to be the fugacity of the pure liquid at the solution temperature and at the specified reference pressure, often its vapour pressure at the solution temperature, so that

$$f_i^{oL}(T) = \lim_{x_s \to 1} \hat{f}_s(T, x_i) / x_s = f_s(T) \quad s = \text{solvent} \tag{2.67}$$

Where $f_s(T)$ is the pure component fugacity. If the reference pressure is specified to be the saturation pressure of the solvent then $f_i^{oL}(T)$ can be expressed in terms of the fugacity coefficient as

$$f_s^{oL}(T) = p_s^0(T) \varphi_s^0(T) \tag{2.68}$$

Where $p_s^0(T)$ is the saturation is vapour pressure at the system temperature and $\varphi_s^0(T)$ is the fugacity coefficient of pure saturated vapour s (at equilibrium $\varphi_s^l(T) = \varphi_s^v(T)$) at the system temperature and pressure $p_s^0(T)$. For many solvents $\varphi_s^0(T)$ is approximately unity at temperatures of interest. Using Eq. (2.68) for the reference state fugacity, the fugacity of a solvent in a liquid mixture is given by

$$\hat{f}_s^l(T,P,x_i) = \gamma_i(T,P,x_i)x_i p_s^0(T)\varphi_s^0(T) \tag{2.69}$$

Where $\gamma_S(T,P,x_i)$ is symmetrically normalized so that $\gamma_s \to 1$ as $x_s \to 1$ at the system temperature and the reference pressure. A similar reference state fugacity is not convenient for a gaseous solute if the system temperature exceeds the critical temperature for that solute as this requires extrapolating the vapour pressure of the pure liquid component (i) beyond its critical temperature. A more convenient standard state for near critical or supercritical components was suggested earlier by activity coefficient Normalization Convention II. For gaseous solute it is common to adopt a reference state such that

$$f_i^{oL}(T) = \text{Lim}\ \hat{f}_i(T,x_i)\Big/ x_i = H_{i,s}^{pref}(T) \tag{2.70}$$

The reference fugacity defined here is known as the Henry's law constant for component i in the solvent s. $H_{i,s}^{pref}(T)$ can be determined from experimental solubility data. The reference pressure for the molecular solute is chosen to be the vapour pressure of the solvent, p_s^0, at the system temperature. Using Eq. (2.70), the fugacity of a gaseous component in a liquid mixture can be expressed as

$$\hat{f}_i^l(T,P,x_i) = \gamma_i^*(T,P,x_i)x_i H_{i,s}^{pref}(T);\ \text{i = solute,} \tag{2.71}$$

Classical thermodynamics has little to tell about the activity coefficient; as always, thermodynamics does not give us the experimental quantity we desire but only relates it to other experimental quantities. Thus, thermodynamics relates the effect of pressure on the activity coefficient to the partial molar volume, and it relates the effect of temperature on the activity coefficient to the partial molar enthalpy. These relations are of limited use because good data for partial molar volume and for the partial molar enthalpy are rare. However there is one useful tool for correlating and extending the experimental data; the

Gibbs-Duhem equation. For practical purpose, the utility of Gibbs-Duhem equation is best realized through the concept of excess Gibbs energy, and can be used to interpolate or extrapolate experimental data with respect to composition. Applying the Gibbs-Duhem equation, the individual activity coefficients can be related to G^E. Unfortunately, the Gibbs Duhem equation tells nothing about interpolating or extrapolating such data with respect to temperature or pressure. Many expressions relating g^E (G^E per mole of mixture) to composition have been proposed, containing adjustable parameters, which, at least in principle, depend on temperature. All of them have the strong empirical flavour. The primary effect of temperature on vapour-liquid equilibrium is contained in pure component vapour pressures or, more precisely, in the pure component liquid fugacities. While activity coefficients depend on temperature as well as composition, the temperature dependence is usually small when compared with the temperature dependence of the pure liquid vapour pressures. The activity coefficient is a weak function of pressure. At low to moderate pressures, the effect of pressure on the activity coefficient can be usually neglected.

2.11 PREVIOUS WORK

Rapid urbanization as well as industrialization and Carbon dioxide (CO_2) emission; the two events are entwined. Erratic climatic change has instigated the research related to energy efficient CO_2 capture. Among the various avenues available for efficient CO_2 removal, absorption in aqueous alkanolamine solutions is long proven and has been most effective so far. However, solvent loss and high regeneration costs of alkanolamines have driven researchers for new and alternative technologies. Gas treating research is actually passing through it's transition which is needed to be chronicled and that might offer a better perspective of my present work.

Recently room temperature *ionic liquids* (ILs'); called green solvents are emerging as promising candidates to capture CO_2 due to their wide liquid range, low melting point, negligible vapor pressure, high CO_2 solubility and reasonable thermal stability. Off late, the idea of mixing ILs and alkanolamines has been receiving great attention from the industries (Camper *et al*. 2008; Zhao *et al*. 2010; Ahmady *et al*. 2011). It might not be inappropriate to include some of the recent initiatives that have been taken for CO_2 capture using ionic liquids. Xu et al. (2012) reported the solubility of CO_2 in aqueous mixture of a low viscous IL ([C2OHmim][N(CN)2]) and MEA at temperature 313.15 K and 333.15 K, over CO_2 partial pressure ranging from 100 to 1000 kPa and IL concentration varying

from 5% to 30% . Ahmady *et al*. (2010) suggested that presence of a low concentration of 1-butyl-3-methylimidazolium tetrafluoroborate) ([bmim][BF4]) in aqueous 4 mole L^{-1} MDEA has no significant effect on the mixture loading capacity, but increased the initial absorption rate. The amine CO_2 loading capacity showed a significant decrease in the presence of high concentrations of ionic liquid in the mixture. Zhang *et al.* (2009) proposed dual amino-functionalised phosphonium ionic liquids for CO_2 capture. A series of 20 dual amino functionalized phosphonium ionic liquids, (3-aminopropyl) tributyl phosphonium amino acid salts ($[aP_{4443}][AA]$) with varying anions were tested of their CO_2 absorption capacity. ILs almost reached equilibrium within 80 min, ILs approached one mole CO_2 per mole ionic liquid and the ($[aP_{4443}][AA]$) ILs could be repeatedly recycled for CO_2 uptake. Camper *et al*. (2008) found that RTILs (room temperature ionic liquids) and alkanolamines combined in an efficient and effective manner for CO_2 gas capture could be superior to the use of analogous, amine-functionalized TSILs (task specific ionic liquid). Muldoon *et al*. (2007) established that the anion frequently played a key role in determining CO_2 solubility in ionic liquids. ILs that contained a level of fluorination had improved CO_2 solubility. However, fluorinated ILs may be less environmentally benign than some of the possible non-fluorinated ILs. They also stated that the non-fluorinated ILs containing ether linkages and flexible alkyl chains to increase free volume can be designed to have a high affinity for CO_2. The use of such ILs, however, will be dependent on whether their chemical stability and viscosity are suitable for the given application. However, it is difficult to realize industrially owing to its high viscous nature and high cost, which left us with limited options like CO_2 absorption in alkanolamines or in Sodium and Potassium salts of primary or tertiary amino acids promoted with reactive alkanolamines.

Post combustion CO_2capture is coming under the purview of gas treating which has initiated a new dimension of research and development activity in this category. Huge CO_2 gas at high temperature emitting at atmospheric pressure provide very little driving force in the absorbers, hence it requires advanced solvent formulation. Post-combustion CO_2 capture using alkanolamine solvents suffer from several common drawbacks; such as energy used for solvent regeneration, solvent volatility, and the oxidative and thermal degradation of solvent. For efficient CO_2 capture, Wagner *et al*. (2009) in their patent proposed the use of mixture of alkanolamine and tertiary amino acid salts. Weiland and Hatcher (2011) reported the performance of a CO_2 capture plant using Sodium-glycine

(NaGly), MEA-promoted Potassium salt of dimethylglycine (KDiMGly), piperazine-promoted KDiMGly, 30 wt% MEA and Piperazine-promoted MDEA.The results revealed that "the regeneration energy required with piperazine-promoted KDiMGly was about 20% lower that for MEA in an identical plant and with 20 % lower solvent rates".

Alvis *et al.* (2012) presented a review on CO_2 capture from Syngas. Piperazine-activated MDEA and Potassium Dimethylglycinate were the agents for absorption.In order to remove CO_2 from syngas as well as natural gas, Piperazine has been the most commonly used promoter to alkanolamine solvents. Alkazid *DIK*, which has been in use for very long time; is not at all volatile and expected to be less prone towards oxidation in contrast to other alkanolamines. Those findings ameliorate the expectation of amino acid salts to qualify as worthy solvents.

In the present context, the role of alkanolamine solvents in sour gas treating research should be revered. It seems appropriate to present a brief account on acid gas treating using alkanolamine solvents. Triethanolamine (TEA) was the first ethanolamine used commercially for gas treating (Kohl and Reisenfield, 1985). Later, TEA has been largely replaced by other amines. Sartori and Savage (1978, 1983) have developed the concept of using hindered amines for gas sweetening processes. Sharma (1964) has also proposed the use of highly branched amines such as 2-amino-2-methyl-1-propanol (AMP) for CO_2 absorption because he thought these amines, due to steric hindrance, could show considerable advantage over conventional amines with respect to cyclic absorption capacity. Goar (1980) discussed the advantages of using MDEA compared to other amine solvents and described several gas treating schemes employing MDEA.

The use of blended amine solvents in gas treating processes is common today. A mixed amine solvent, which is an aqueous blend of a primary or secondary amine with a tertiary amine or a sterically hindered amine, combines the higher equilibrium capacity of the tertiary amine with the higher reaction rate of the primary or secondary amine and can bring about considerable improvement in gas absorption and great savings in regeneration energy requirements. The blended amines are less corrosive, and require lower circulation rates to achieve a desirable degree of sweetening. Simulation studies with blends of MDEA/MEA and MDEA/DEA have indicated considerable improvements in absorption and substantial savings in energy requirements compared to the single amine systems (Chakravarty *et al.*, 1985; Katti and Wolcott, 1987). Blends of primary and tertiary amines (such as mixtures of MEA and MDEA) or secondary and tertiary amines (such as mixtures

of DEA and MDEA) have been suggested by (Chakravarty *et al.*, 1985; Kohl and Nielsen, 1997) for industrial gas treating processes. Austgen *et. al.* (1991) reported CO_2 solubility in (2.0 M MDEA + 2.0 M DEA) aqueous solutions at 313 and 353 K over the CO_2 partial pressure range of 0.136 – 310 kPa and they extended their earlier model (NRTL) for representing the acid gas solubility in ternary mixture of (H_2O – (MDEA+DEA)). Dawodu and Meisen (1994) reported the equilibrium solubility of CO_2 in the temperature range of 343 – 453 K and in the CO_2 partial pressure range of 65 – 3200 kPa for (3.4 M MDEA + 0.8 M DEA) and (2.1 M MDEA + 2.1 M DEA) aqueous solutions. They observed that the solubility of CO_2 in the blends decreased with the increasing temperature but increased with an increase in CO_2 partial pressure. As reported by Dawodu and Meisen (1994), at low partial pressure of CO_2, the equillibrium CO_2 loading in the amines were in the order MDEA+MEA> MDEA+DEA>MDEA for the same total amine concentration. However, at high partial pressures the equilibrium CO_2 loading in the MDEA solutions were higher than those in (MDEA+MEA) and (MDEA+DEA) blends of equal molar strengths due to stoichiometric loading limitations of MEA and DEA. The non-additivity of the equilibrium loadings for single amine systems highlights the need for independent measurements with amine blends. Guevera *et al.* (1998) measured the solubility of CO_2 in (10 wt % DEA + 15 wt % MDEA), (10 wt % DEA + 20 wt % MDEA), (20 wt % DEA + 10 wt % MDEA), and (10 wt % DEA + 35 wt % MDEA) aqueous solutions at 313.15 and 393.15 K.

The sterically hindered amine, AMP, which has an equilibrium absorption capacity of 1.0 mole of CO_2 per mole of amine, a reaction rate constant for CO_2, comparable to that of DEA, can be a very good alternative to MDEA as a component of the blended amine solvents. From these considerations (H_2O – (AMP+DEA)) and (H_2O – (AMP+MEA)) are expected to be attractive new blended amine solvents for the gas treating processes. Experimental results on the solubility of CO_2 in aqueous blends of MEA/AMP or DEA /AMP are limited. Seo and Hong (1996) reported the solubility of CO_2 in blends of DEA and AMP in the CO_2 partial pressure range of 10-300 kPa and in the temperature range of 313-353 K. The concentrations of the amine mixtures studied were (6 mass% DEA + 24 mass% AMP), (12 mass% DEA + 18 mass% AMP), and (18 mass% DEA + 12 mass% AMP). They observed that as the temperature increased, the solubility of CO_2 decreased. Guevara *et al.* (1998) reported the CO_2 solubility for different relative amine compositions; (25 wt% DEA + 5 wt% AMP) and (20 wt% DEA + 10 wt% AMP) in the

temperature range of 313.15 – 373.15 K and in the CO_2 partial pressure range of 22- 2600 kPa.

A recent range of alkanolamines like Piperazine (PZ), 2-piperidineethanol (2-PE), 2-amino-2-hydroxymethyl-1,3-propanediol (AHPD), *N*-methyl-2-ethanolamine(MAE) and *N*-ethyl-ethanolamine (EAE) have been proposed for CO_2 capture. In order to establish the acceptability of some of the alkanolamines, extensive R&D initiatives were taken; among them a few deserve mentioning. Appl *et al*. (1982) articulated 'Piperazine' as the most effective would be accelerator to conventional alkanolamines. It was confirmed later by Bishnoi that "the rate constant of piperazine is 10 times higher than that of conventional alkanolamines such as MEA". The past decade has witnessed several investigations on acid gas absorption using Piperazine solvent. Bishnoi and Rochelle (2002) presented CO_2 solubility data in activated MDEA solutions (0.6 molar PZ + 4 molar MDEA) at 313 and 343 K. Kamps *et al*. (2003) presented a thermodynamic model to describe VLE of CO_2 in $(PZ + H_2O)$ and in $(PZ + MDEA + H_2O)$ solution. They also reported CO_2 solubility in 2 and 4 molar aqueous piperazine solutions at 313 to 393 K and pressures as high as 9.6 MPa. Aroua and Salleh (2003) correlated the CO_2 solubility in PZ using Kent Eisenberg approach and measured the solubilities of CO_2 aqueous PZ solutions in the temperature range 293-323 K, with CO_2 partial pressures ranging from 0.4-95 kPa. Derks *et al*. (2005) presented new VLE data of CO_2 over aqueous PZ solution of 0.2 and 0.6 molar concentrations at 298-343 K. They also correlated all the available data in the open literature including their own with the electrolyte equation of state. Garry Rochelle and his research group continued to undertake focused R& D activities in CO_2 capture from coal-fired power plants and extensively experimented with newer amine formulations, design and simulation of absorbers and strippers. According to them, aqueous amine absorption/stripping is currently the best technology to remove CO_2 from the flue gas of existing coal fired power plants but it requires advanced alkanolamine solvents. It might not be inappropriate to mention some of their contributions. Cullinane (2005) reported an innovative blend of potassium carbonate (K_2CO_3) and piperazine (PZ) as a solvent for CO_2 removal from combustion flue gas in an absorber/stripper. The equilibrium partial pressure and the rate of absorption of CO_2 were measured in a wetted-wall column in 0.0 to 6.2 m K_2CO_3 and 0.6 to 3.6 m PZ at 298 to 383 K. A rigorous thermodynamic model based on electrolyte non-random two-liquid (eNRTL) theory, was developed to represent equilibrium behavior. A rate model was developed to describe the absorption rate by

integration of eddy diffusivity theory with complex kinetics. Both models were used to explain behavior in terms of equilibrium constants, activity coefficients, and rate constants. Hilliard (2008) used the Electrolyte Nonrandom Two-Liquid Activity Coefficient model in Aspen Plus^{TM} to develop a rigorous and consistent thermodynamic representation for the base sub-component systems associated with aqueous combinations of K_2CO_3, $KHCO_3$, MEA, and piperazine (PZ) in a mixed-solvent electrolyte system for the application of CO_2 absorption/stripping from coal fired power plants. Dugas (2009) presented wetted wall column experiments that measure the CO_2 equilibrium partial pressure and liquid film mass transfer coefficient 7, 9, 11, and 13 m MEA and 2, 5, 8, and 12 m PZ solutions. A 7 m MEA/2 m PZ blend was also examined. Absorption and desorption experiments were performed at 313, 333, 353, and 373 K over a range of CO_2 loading. They concluded that 7m MEA/2m PZ has a 45% greater CO_2 capacity than 7m MEA and 7m MEA/2m PZ shows faster rates than 7m MEA in the most important partial pressure range, 1000 to 5000 Pa. Chen (2011) measured equilibrium CO_2 partial pressure and characterized liquid film mass transfer coefficient for CO_2-loaded and highly concentrated aqueous amines at 313–373 K over a range of CO_2 loading with a Wetted Wall Column (WWC). The acyclic amines tested were ethylenediamine, 1,2-diaminopropane, diglycolamine®, methyldiethanolamine (MDEA)/Piperazine (PZ), 3-(methylamino) propylamine, 2-amino-2-methyl-1-propanol and 2-amino-2-methyl-1-propanol/PZ. The cyclic amines tested were piperazine derivatives including proline, 2-piperidineethanol, N-(2-hydroxyethyl) piperazine, 1-(2-aminoethyl) piperazine, N-methylpiperazine (NMPZ), 2-methylpiperazine (2MPZ), 2,5-trans-dimethylpiperazine, 2MPZ/PZ, and PZ/NMPZ/1,4-dimethylpiperazine (1,4-DMPZ). The cyclic CO_2 capacity and heat of CO_2 absorption were estimated with a semi-empirical vapor-liquid-equilibrium model. 5 m MDEA/5 m PZ, 8 m 2MPZ, 4 m 2MPZ/4 m PZ and 3.75 m PZ/3.75 m NMPZ/0.5 m 1,4-DMPZ were identified as promising solvent candidates for their large CO_2 capacity, fast mass transfer rate and moderately high heat of absorption.

Bandyopadhyay and his research group also undertook focused R&D activities on CO_2 absorption in PZ activated solutions. Dash *et al*. (2012) presented VLE data of CO_2 in piperazine (PZ)-activated concentrated aqueous 2-amino-2-methyl-1-propanol (AMP) for the temperature range of (303 to 328) K and PZ concentration range of (2 to 8) wt%, keeping the total amine concentration in the solution at 40 wt% and 50 wt%. The partial pressures of CO_2 were in the range of (0.2 to 1500) kPa. The electrolyte non-random two-

liquid (ENRTL) theory was used to correlate the experimental data for the quaternary system (CO_2 + AMP + PZ + H_2O) to describe the equilibrium behaviour of the solution. Dash *et al*. (2011) presented rate of CO_2 in piperazine (PZ)-activated concentrated aqueous 2-amino-2-methyl-1-propanol (AMP) in the temperature range of (303 to 323) K and PZ concentration range of (2 to 8) wt%, keeping the total amine concentration in the solution at 40 wt%. The absorption experiments were carried out in a wetted wall contactor over CO_2 partial pressure range of 5–15 kPa. Samanta and Bandyopadhyay (2011) presented absorption of CO_2 into PZ activated aqueous MDEA solution over the temperature range of 298–313 K under atmospheric pressure using a wetted wall model contactor. The CO_2 partial pressure was varied in the range 2–14 kPa, keeping the total amine concentration at 30 wt%.

In view of the aforesaid facts, it can be well concluded that exhaustive R&D activity in the last decade has revolved around PZ. Apart from PZ, following scarce efforts have undertaken with other newer solvent formulations. Rebolledo-Libreros and Trejo (2004) presented the solubility of CO_2 in aqueous solutions of mixtures of three alkanolamines; MDEA, DEA, and AMP under conditions prevailing typically at an absorption tower as well as at a stripping tower. Bougie and Iliuta (2010) measured and reported CO_2 solubility in aqueous mixtures of 2-amino-2-hydroxymethyl-1,3-propanediol (AHPD) and piperazine over a range of temperature from (288.15 to 333.15) K and for amine concentrations up to 3.1 kmole.m^{-3}(0.37 total amine mass fraction). The CO_2 partial pressure was kept within (0.21 to 2 637) kPa using a vapor-liquid equilibrium (VLE) apparatus based on a static-analytic method. Balsora and Mondal (2011) presented experimental results on CO_2 solubility in a new blend of Diethanolamine (DEA) and Trisodium phosphate (TSP) at temperatures ranging from (303.14 to 333.14) K and over the partial pressure range of (10.133 to 20.265) kPa. Total concentrations of aqueous (DEA + TSP) blends were kept as (1.0, 1.5, and 2.0) mole.dm^{-3}. Mole fractions of TSP varied in the range 0.02 to 0.20 in those blends. The results show that CO_2 solubility in a blend increases with increasing mole fraction of TSP at fixed amine concentration, temperature and partial pressure of CO_2. In an effort to establish *N*-methyl-2-ethanolamine (MAE) as a potential solvent for CO_2 capture, Kumar and Kundu, (2012a) reported CO_2 solubility in *N*-methyl-2-ethanolamine aqueous solutions of concentrations (0.968, 1.574, 2.240 and 3.125 mole.$kg^{-1}$of MAE solvent; / 0.0676, 0.1052, 0.1427, and 0.1878 mass fractions of MAE) at temperatures (303.1, 313.1 and 323.1) K in the CO_2 pressure range of

(1 to 350) kPa. Kumar and Kundu, (2012b) also reported CO_2 solubility in various aqueous blends of MAE +MDEA and MAE +AMP at temperatures (303.1, 313.1 and 323.1) K and CO_2 pressure in the range of (1 to 545) kPa.

Classical thermodynamics provides a framework for calculating the equilibrium distribution of species between a vapour and liquid phase in a closed system through the equality of their chemical potential among the contacting phases. In this regard, both apparent and rigorous thermodynamic models have been proposed by various researchers to correlate and predict the vapour-liquid equilibrium of CO_2 in aqueous alkanolamines.

With respect to the models for the acid gas VLE in alkanolamines reported so far, the most significant ones are as follows. Kent and Eisenberg (1976) created the first equilibrium model that received widespread use. Their model was based on pseudo-equilibrium constants and Henry's law. They regressed the pseudo-equilibrium constants for the amine protonation and carbamate reversion reactions for MEA and DEA systems to fit experimental vapour-liquid equilibria (VLE) data. Deshmukh and Mather (1981) produced a more rigorous model based on extended Debye-Hückel theory and the work of Edwards *et al.* (1975, 1978) and Beuiter and Renon (1978).Weiland *et al.* (1993, 1995) used the Deshmukh-Mather model to predict CO_2 and H_2S equilibrium in aqueous MEA, DEA, DGA and MDEA. Austgen *et al.* (1989) utilized the NRTL theory developed by Chen and coworkers in a series of articles (Chen *et al.* 1979, 1982; Chen and Evans, 1986; and Mock *et al.* 1986) to model acid gas VLE. The contribution of Chang *et al.* (1993) to this model lies in correcting the binary amine-water interaction parameters by measuring and regressing binary freezing point depression data. Posey (1996), contributed towards the more accurate temperature dependence of the model by measuring excess enthalpy for MEA, DEA, and MDEA solutions and also improved the prediction ability of the model for very low acid gas loaded solutions, where accurate experimental VLE data is lacking, by performing conductivity and pH measurements of the acid gas loaded solutions up to a temperature limit of 50 and 40 ^{0}C respectively. Li and Mather (1994, 1996, and 1997) simplified the Clegg-Pitzer equations and applied them to predict the solubility of single gas in mixed amine solvent systems and mixed gas in aqueous single amines. The interaction parameters determined from binary and ternary systems (single amine) were used to predict the quaternary mixed amine or mixed gas systems without any additional parameters.

The electrolyte equation of state was first proposed by Furst and Renon (1993). This was applied for CO_2 and H_2S solubility representation in strong electrolyte solution by Furst & Renon, (1993), Zuo & Furst, (1997). The same model was applied for CO_2 and H_2S solubility representation in aqueous MDEA solutions over a wide temperature range, MDEA concentrations and gas loadings by Chunxi and Furst (2000). Huttenhuis et. al., (2005) presented the new solubility data of H_2S and CO_2 in aqueous MDEA solution at temperature range 10 to 25 ^{0}C with pressure varied from 6.9 to 69 bar (methane was used as make-up gas) and correlated the experimental data with an electrolyte Equation of State Model. Even Solbraa (2002) studied the high-pressure effects related to the removal of carbon dioxide from natural gas. Experiments, where carbon dioxide was absorbed into water and MDEA solutions were performed at pressures up to 150 bar and at temperatures 25 and 40°C. According to him 'Compared to electrolyte models based on equations for the Gibbs excess energy, the electrolyte equation of state has the advantage that the extrapolation to higher pressures and solubility calculations of supercritical components is less cumbersome'. The extended UNIQUAC model was proposed by Thomsen and Rasmussen (1999). This was applied to the thermodynamic representation of CO_2 absorption in aqueous monoethanolamine (MEA), methyldiethanolamine (MDEA) and varied strength mixtures of the two alkanolamines (MEA + MDEA) by Faramarzi et al., (2009).

Models based on modified Clegg-Pitzer equations, NRTL, UNIQUAC, UNIFAC are the most popular models currently in use. Those models find out activity coefficients of the compounds using the structural property information of pure components and binary interaction parameters between the components existing in the equilibrated liquid phase. Molecular simulation using conductor like screening model may be an useful alternative to those models. Prediction of any thermodynamic property of solution starts with quantum theory and solvation model. First, the Schrodinger equation is resolved by Density Functional Theory (DFT) using an appropriate basis set, and then the conductor-like screening model (COSMO) model can be applied to predict the sigma profile and finally application of statistical thermodynamics to predict the thermodynamic properties and VLE. A brief review on COSMO-RS (COSMO applied for real solvents) application is documented in *Chapter 5*.

REFERENCES

Ahmady, A., Hashim, M.A. and Aroua, M.K. **(2010).** Experimental investigation on the solubility and initial rate of absorption of CO_2 in aqueous mixtures of methyldiethanolamine with the ionic liquid 1-butyl-3-methlimidazolium tetrafluoroborate. *Journal of Chemical and Engineering Data*, 55, 5733-5738.

Ahmady, A., Hashim, M.A. and Aroua, M.K. **(2011).** Absorption of carbon dioxide in the aqueous mixtures of methyldiethanolamine with three types of imidazolium-based ionic liquids. *Fluid Phase Equilibria*, *309*, 76-82.

Alvis, R.S., Hatcher, N.A. and Weiland, R.H. (**2012**). CO_2 Removal from Syngas using Piperazine-Activated MDEA and Potassium Dimethyl Glycinate. Paper presented at Nitrogen + Syngas **2012**, 20-23 February **2012** Athens, Greece.

Appl, M., Wagner, U., Henrici, H.J., Kuessnet, K., Volkamer, F. and Ernst-Neust, N. (**1982).**Removal of CO_2 and/or H_2S and/or COS from gases containing these constituents. US Patent Nr 4336233.

Aroua, M.K. and Mohd Selleh, R. (2003). Solubility of CO2 in aqueous piperazine and its modeling using Kent-Eisenberg approach. *Chemical Engineering Technology*, 27, 65-70.

Austgen, D. M., and Rochelle, G. T. (**1991**). Model of vapour- liquid equilibria for aqueous acid gas-alkanolamine systems.2 Representation of H_2S and CO_2 solubility in aqueous MDEA and CO_2 solubility in aqueous mixture of MDEA with MEA or DEA. *Industrial and Engineering Chemistry Research*, 30, 543-555.

Austgen, D.M., Rochelle, G.T., Peng, X. and Chen, C.C. (**1989**).Model of vapour liquid equilibria for aqueous acid gas- alkanolamine systems using the Electrolyte - NRTL equation. *Industrial and Engineering Chemistry Research*, 28, 1060 - 1073.

Balsora, H.K. and Mondal, M.K. **(2011).**Solubility of CO_2 in an aqueous blend of diethanolamine and Trisodium Phosphate. *Journal of Chemical and Engineering Data, 56,* 4691-4695

Beutier, D., and Renon, H. (1**978**). Representation of NH_3–H_2S–H_2O, NH_3–CO_2– H_2O, and NH_3–SO_2–H_2O vapour liquid equilibria. *Industrial Engineering Chemistry Processes Design and Development*, 17(3), 220-230.

Bishnoi, S. and Rochelle, G.T. (**2002a).**Absorption of carbon dioxide in aqueous piperazine/ methyldiethanolamine. *A.I.Ch.E. J., 48*, 2788–2799.

Blauwhoff. P.M.M., Versteeg, G.F., and van Swaaij, W.P.M. (**1984**). A study on the reaction between CO_2 and alkanolamines in aqueous solutions. *Chemical Engineering Science*, 39, 207-225.

Bougie, F. and Iliuta, M.C. (**2010).** CO_2 Absorption into mixed aqueous solutions of 2-amino-2-hydroxymethyl-1, 3-propanediol and piperazine. *Industrial and Engineering Chemistry Research*, 49, 1150-1159.

Camper, D., Bara, J.E., Gin, D.L. and Noble, R.D. (**2008**). Room-temperature ionic liquid - amine solutions: Tunable solvents for efficient and reversible capture of CO_2. *Industrial and Engineering Chemistry Research*, 47, 8496-8498.

Caplow, M. (**1968**). Kinetics of carbamate formation and breakdown. *Journal of the American Chemical Society*, 90, 6795-6803.

Chakraborty, A.K., Astarita, G., and Bischoff, K.B. (**1986**). CO_2 absorption in aqueous solutions of hindered amines. *Chemical Engineering Science*, 41, 997-1003.

Chakraborty, A.K., Astarita, G., Bischoff, K.B. and Damewood, J.R. Jr. (**1988**). molecular orbital approach to substituent effects in amine-CO_2 interactions. *Journal of American Chemical Society*, 110, 6947.

Chakravarty, T., Phukan, U.K., and Weiland, R.H. (**1985**). Reaction of acid gases with mixtures of amines. *Chemical Engineering Progress*, 81(4), 32-36.

Chang, H.T., Posey, M., and Rochelle, G.T. (**1993**). Thermodynamics of alkanolamine-water solutions from freezing point measurements. *Industrial and Engineering Chemistry Research*, 32, 2324- 2335.

Chen, C.C., and Evans, L.B. (**1986**). A local composition model for the excess Gibbs energy of aqueous electrolytes systems. *AIChE Journal*, 32(3), 444 - 454.

Chen, C.C., Britt, H. L., Boston, J.F., and Evans, L.B. (**1979**). Extension and application of the Pitzer equation for vapour-liquid equilibrium of aqueous electrolyte systems with moleecular solutes. *AIChE Journal*, 25(5), 820-831.

Chen, C.C., Britt, H.L., Boston, J.F., and Evans, L.B. (**1982**). Local composition model for excess Gibbs energy of electrolytes systems, Part I: Single solvent, single completely dissociated electrolyte systems. *AIChE Journal*, 28(4), 588-596.

Chen, X. (**2011**). Carbon dioxide thermodynamics, kinetics and mass transfer in aqueous piperazine derivatives and other amines. Ph.D. Dissertation, The University of Texas at Austin.

Chunxi, L. and Furst, W. (**2000**). Representation of CO_2 and H_2S absorption by aqueous solutions in aqueous MDEA solutions using an electrolyte equation of state. *Chemical Engineering Science*, 55, 2975-2988.

Crooks, J.E., Donnellan, J.P. (**1989**). Kinetics and mechanism of the reaction between carbon dioxide and amines in aqueous solution. *Journal of Chemical Society*, Perkins Trans., II, 331.

Cullinane, J.T. **(2005).** Thermodynamics and Kinetics of Aqueous Piperazine with Potassium Carbonate for Carbon dioxide Absorption. Ph.D. Dissertation, The University of Texas at Austin.

da Silva, E.F. and Svendsen, H. F. (**2006**). Study of the carbamate stability of amines using Ab Initio methods and free-energy perturbations. *Industrial & Engineering Chemical Research*, 45, 2497-2504.

da Silva, E.F., Svendsen, H.F. (**2004**). Ab initio study of the reaction of carbamate formation from CO_2 and alkanolamine. *Industrial Engineering Chemical Research*, 43, 3413-3418.

Danckwerts, P.V. (**1979**). The reaction of CO_2 with ethanolamines. *Chemical Engineering Science*,34, 443-446.

Danckwerts, P.V., and Sharma, M.M. (**1966**). The absorption of carbon dioxide into aqueous solutions of alkalis and amines (with some notes on hydrogen sulphide and carbonyl sulphide). *Chemical Engineer*, 10, CE244-CE280.

Dash, S.K., Samanta, A.N. and Bandyopadhyay, S.S. (**2012**). Experimental and theoretical investigation of solubility of carbon dioxide in concentrated aqueous solution of 2-amino-2-methyl-1-propanol and piperazine. *The Journal of Chemical Thermodynamics,* 51, 120-125.

Dash, S.K., Samanta, A., Samanta, A.N. and Bandyopadhyay, S.S. (**2011**).Vapor−liquid equilibria of carbon dioxide in dilute and concentrated aqueous solutions of piperazine at low to high pressure. *Fluid Phase Equilibria*, 300, 145−154.

Dawodu, O.F. and Meisen, A. (**1994**). Solubility of carbon dioxide in aqueous mixture of alkanolamines. *Journal of Chemical and Engineering Data*. 39, 548-552.

Denbigh, K. (**1981**). *The principles of chemical equilibrium*. 4th Ed., Cambridge University Press, Cambridge.

Derks, P.W.J., Dijkstra, H.B.S., Hogeniloorn, J.A. and Versteeg, G.F. (**2005).** Solubility of Carbon dioxide in Aqueous Piperazine Solutions. *A.I.Ch.E. J*., 51, 2311-2327.

Deshmukh, R.D. and Mather, A.E. (**1981**). A mathematical model for equilibrium solubility of hydrogen sulfide and carbon dioxide in aqueous alkanolamine solutions. *Chemical Engineering Science*, 36, 355-362.

Donaldsen, T.L. and Nguyen, Y.N. (**1980**). Carbon dioxide reaction kinetics and transport in aqueous amine membranes. *Industrial Engineering Chemical Fundamental*, 19, 260–266.

Dugas, R.E. (**2009).** Carbon dioxide Absorption, Desorption and Diffusion in Aqueous Piperazine and Monoethanolamine. Ph.D. Dissertation, The University of Texas at Austin.

Edwards, T. J., Maurer, G., Newman, J., Prausnitz, J. M. (**1978**). Vapour-liquid equilibria in multicomponent aqueous solutions of volatile electrolytes. *AIChE Journal*, 24, 966-976.

Edwards, T. J., Newman, J., Prausnitz, J. M. (**1975**). Thermodynamics of aqueous solutions containing volatile weak electrolytes. *AIChE Journal*, 21(2), 248-259.

Faramarzi, L., Kontogeorgis, G., Thomsen, K. and Stenby, E. H. (**2009**). Extended UNIQUAC model for thermodynamic modeling of CO_2 absorption in aqueous alkanolamine solutions. *Fluid Phase Equilibria*, 282(2), 121-132.

Furst, W. and Renon, H. (**1993**). Representation of excess properties of electrolyte solutions using a new equation of state. *AIChE Journal*, 39, 335-343.

Goar, B.G. (**1980**). Selective gas treating produces better Claus feeds. *The Oil and Gas Journal*, 78, 239-242.

Guevera, F., Libreros, M. E., Martinez, A., and Trejo, A. (**1998**). Solubility of CO_2 in aqueous mixture of dithanolamine with methyldiethanolamineand 2-amino-2-methyl-1-propanol. *Fluid Phase equilibria*, 150, 721 – 729.

Hilliard, M.D. (**2008).** A Predictive Thermodynamic Model for an aqueous blend of Potassium Carbonate, Piperazine and Monoethanolamine for Carbon dioxide capture from flue gas. Ph.D. Dissertation, The University of Texas at Austin.

Hook, J.R. (**1997**). An investigation of some sterically hindered amines as potential carbon dioxide scrubbing compounds. *Industrial Engineering Chemical Research,* 36, 1779-1790.

Huttenhuis, P.J.G., Agrawal, N.J., Hogendoorn, J.A. and Versteeg., G.F. (**2005**). Experimental determination of H_2S and CO_2 solubility data in aqueous amine solutions and a comparison with an electrolyte equation of state.Proc. 7th World Congress of Chemical Engineering in Glasgow, United Kingdom,.

Katti, L. and Wolcott, R. A. (**1987**). Fundamental aspects of gas treating with formulated amine mixtures. Paper No. 5b, Presented at the AIChE National Meeting, Minneapolis, MN.

Kent, R. L. and Eisenberg, B. (**1976**). Better data for amine treating. *Hydrocarbon Process,* 55, 87-90.

Kohl, A.L. and Nielsen, R.B. (**1997**).*Gas Purification,* 5th ed., Gulf publishing Company, Houston.

Kohl, A.L. and Riesenfeld, F.C. (**1985**). *Gas Purification*, 4th ed., Gulf publishing Company, Houston.

Kumar, G.; Kundu, M. (**2012a**). Vapor-liquid equilibrium of CO_2 in aqueous solutions of *N*-methyl-2-ethanolamine. *Canadian Journal of Chemical Engineering, 90*, 627-630.

Kumar, G.; Kundu, M. (**2012b**). Solubility of CO_2 in aqueous blends of (N-Methyl-2-ethanolamine + N-Methyldiethanolamine) and (N-Methyl-2-ethanolamine + 2-Amino-2-methyl-1-propanol). *Journal of Chemical and Engineering Data,* 58, 3203-3209.

Ladha, S.S. and Danckwerts, P.V. (**1981**). Reaction of CO_2 with ethanolamines: kinetics from gas-absorption. *Chemical Engineering Science*, 36, 479-482.

Lewis, G.N., and Randall, M. (**1961**). *Thermodynamics* (revised by K. S. Pitzer and L. Brewer). MacGraw-Hill Book Company, New York.

Li, Y.G. and Mather, A.E. (**1997**). Correlation and prediction of the solubility of CO_2 and H_2S in aqueous solutions of methyldiethanolamine. *Industrial and Engineering Chemistry Research,* 36, 2760 - 2765.

Li, Y.G., and Mather, A.E. (**1997**). Correlation and prediction of the solubility of CO_2 and H_2S in aqueous solutions of methyldiethanolamine. *Industrial and Engineering Chemistry Research*, 36, 2760-2765.

Li, Y.G., and Mather, A.E. (**1994**). The correlation and prediction of the solubility of carbon dioxide in a mixed alkanolamine solution. *Industrial and Engineering Chemistry Research*,33, 2006-2015.

Li, Y.G., and Mather, A.E. (**1996**). Correlation and prediction of the solubility of CO_2 and H_2S in aqueous solutions of triethanolamine. *Industrial and Engineering Chemistry Research*, 35, 4804 - 4809.

McCann, N., Duong, P., Fernandes, D. and Maeder, M.A. (**2011**). Systematic Investigation of Carbamate Stability Constants by H-1 NMR. *Internation Journal of Greenhouse Gas Control*, 5, 396– 400.

Mock, B., Evans, L.B., and Chen, C.C. (**1986**). Thermodynamic representation of phase equilibria of mixed solvent electrolyte systems. *AIChE Journal*, 32(10), 1655 - 1664.

Muldoon, M.J., Aki, S.N.V.K., Anderson, J.L., Dixon, J.K. and Brennecke, J.F. (**2007**). Improving carbon dioxide solubility in ionic liquids. *Journal of Physical Chemistry B*, 111, 9001-9009.

Ohno, K., Inoue, Y., Yoshida, H. and Matsuura, E. (**1999**). Reaction of aqueous 2-(Nmethylamino) ethanol solutions with carbon dioxide chemical species and their conformations studied by vibrational spectroscopy and ab initio theories. *Journal of Physical Chemistry A*, 103, 4283–4292.

Perez-Salado Kamps, A., Xia, J. and Maurer, G. (**2003).** Solubility of CO_2 in (H_2O + Piperazine) and in (H_2O + MDEA + Piperazine). *A.I.Ch.E. J*., 49, 2662-2670.

Posey, M.L. (**1996**). Thermodynamic model for acid gas loaded aqueous alkanolamine solutions. Ph.D. Thesis, University of Texas, Austin.

Prausnitz, J.M., Lichtenthaler, R.N., and de Azevedo, E.G. (**1986**). *Moleecular thermodynamics of fluid phase equilibria.* Prentice-Hall Inc., Englewood Cliffs, N. J.

Rebolledo-Libreros, M.E. and Trejo, A. (**2004**). Gas Solubility of CO_2 in aqueous solutions of N-methyldiethanolamine and diethanolamine with 2-amino-2-methyl-1-propanol. *Fluid Phase Equilibria*, 218, 261−267.

Samanta, A.K. and Bandyopadhyay, S.S. (**2011**). Absorption of carbon dioxide into piperazine activated aqueous N-methyl-di-ethanolamine. *Chemical Engineering Journal*, 734– 741.

Sartori, G. and Savage D.W. (**1978**). U.S. Patent 4094957, June 13.

Sartori, G. and Savage, D.W. (**1983**). Sterically hindered amines for CO_2 removal from gases. *Industrial and Engineering Chemistry Fundamentals*, 22, 239-249.

Sartori, G., and Savage, D.W. (**1983**). Sterically hindered amines for CO_2 removal from gases. *Industrial and Engineering Chemistry Fundamentals*, 22, 239-249.

Seo, D.J., Hong, W.H. (**1996**). Solubilities of carbon dioxide in aqueous mixtures of diethanolamine and 2-amino-2-methyl-1-propanol. *Journal of Chemical and Engineering Data*, 41, 258-260.

Sharma, M.M. (**1964**). Kinetics of gas absorption.absorption of CO_2 and COS in alkaline and amine solutions. Ph.D. Dissertation. University of Cambridge.

Sharma, M.M. and Danckwerts, P.V. (**1963**). Catalysis by Brønsted bases of the reaction between CO_2 and water. *Transactions of the Faraday Society*, 59, 386–395.

Singh, P., Brilman, D.W.F. and Groeneveld, M.J. (**2011**). Evaluation of CO_2 solubility in potential aqueous amine-based solvents at low CO_2 partial pressure. *International Journal of Greenhouse Gas Control*, 5 (1), 61-68.

Smith, W. R., and Missen, R.W. (**1982**). *Chemical equilibrium analysis: Theory and algorithms*, John Wiley and Sons, New York.

Solbraa, E. (**2002**). Equilibrium and non-equilibrium thermodynamics of natural gas processing. PhD thesis, Norwegian University of Science and Technology.

Thomsen, K. and Rasmussen, P. (**1999**). Modeling of vapor-liquid-solid equilibrium in gas-aqueous electrolyte systems. *Chemical Engineering Science*, 54, 1787-1802.

Van Ness, H.C., and Abbott, M.M. (**1979**). Vapour-liquid equilibrium. *AIChE Journal*, 25 (4), 645.

Versteeg, G.F., and van Swaaij, W.P.M. (**1988b**). On the kinetics between $CO_2$and alkanolamines both in aqueous and nonaqueous solutions-II.Tertiary amines. *Chemical Engineering Science*, 43, 587-591.

Versteeg, G.F., and van Swaaij.W.P.M. (**1988a**). On the kinetics between $CO_2$and alkanolamines both in aqueous and nonaqueous solutions-L Primary and secondary amines. *Chemical Engineering Science*, 43, 573-585.

Wagner, R., Lichtfers, U. and Schuda, V. (**2009).** Removal of Carbon Dioxide from Combustion Exhaust Gases, Patent Application US 2009/0320682 A1, 31December.

Weiland, R.H. and Hatcher, N.A. (**2011**). Post-combustion CO_2 Capture with Amino-Acid Salts. Paper presented at SOGAT **2011**, Abu Dhabi, UAE.

Weiland, R.H., Chakravarty T., and Mather, A.E. **(1993**). Solubility of carbon dioxide and hydrogen sulfide in aqueous alkanolamines. *Industrial and Engineering Chemistry Research*,32**,** 1419 - 1430. Also see corrections **(1995)**. *Industrial and Engineering Chemistry Research*, 34, 3173.

Xu, F., Dong, H., Zhang, X., Gao, H., Wang, Z, Zhang, S. and Ren, B. (**2012**). Solubilities of CO_2 in aqueous solutions of ionic liquid and monoethanolamine. Innovations of Green Process Engineering for sustainable Energy and Environment, in the proceedings of 12th AIChe annual meeting, Pittsburgh, PA, October 28-November 2.

Yih, S.M., and Shen, K.P. (**1988**). Kinetics of carbon dioxide reaction with sterically hindered 2-amino-2-methyl-1-propanol aqueous solutions. *Industrial and Engineering Chemistry Research*, 27, 2237-2241.

Zhang, Y., Zhang, S., Lu, X., Zhou, Q., Fan, W. and Zhang, X.P. (**2009**). Dual Amino-functionalised phosphonium ionic liquids for CO_2 capture. *Chemical European Journal*, 15, 3003-3011.

Zhao, Y., Zhang, X., Zeng, S., Zhou, Q., Dong, H., Tian, X. and Zhang, S. (**2010).** Density, Viscosity, and Performances of Carbon Dioxide Capture in 16 Absorbents of Amine+ Ionic Liquid + H_2O, Ionic Liquid + H_2O, and Amine + H_2O Systems. *Journal of Chemical and Engineering Data*, *55*, 3513-3519.

Zuo, Y. X. and Furst, W. (**1997**). Prediction of Vapor Pressure for Nonaqueous Electrolyte Solutions Using an Electrolyte Equation of State. *Fluid Phase Equilibria*, 138, 87-104.

Chapter 3

VAPOUR – LIQUID EQUILIBRIUM OF CO_2 IN AQUEOUS ALKANOLAMINES: SET-UP VALIDATION AND INTRODUCTION OF NEW SOLVENTS

Chapter 3

VAPOUR – LIQUID EQUILIBRIUM OF CO_2 IN AQUEOUS ALKANOLAMINES: SET-UP VALIDATION AND INTRODUCTION OF NEW SOLVENTS

3.1 INTRODUCTION

For the rational design of gas treating processes through absorption, the equilibrium solubility of acid gases over alkanolamines of recent interest is extremely important besides the knowledge of mass transfer and kinetics. The rate studies conducted by Mimura *et al*., 1998 on the sterically hindered secondary alkanolamines like N-methyl-2-ethanolamine (MAE), ethylaminoethanol (EAE), butylamino ethanolamine (BAE) revealed that MAE > EAE > MEA > BAE is the order of reaction rate towards CO_2. Earlier, they also stated about MAE's good absorption and regeneration characteristics, low corrosion even at a high amine concentration and approximately 20% less regeneration energy as compared to MEA in pilot plant scale. Those encouraging revelations instigated researchers like Abharchaei (2010) to use a stirred tank reactor to measure the absorption rate of carbon dioxide by aqueous solutions of 2-(methyl)-amino ethanol. Kumar and Kundu (2012) reported the CO_2 solubility in MAE over a wide concentration range and at typically absorption temperature. Kumar and Kundu (2013) also reported VLE of (CO_2 + EAE + H_2O) system along with the thermodynamics of binary (EAE + H_2O) and ternary (CO_2 + EAE + H_2O) systems.

MAE and EAE are yet to be established as potential solvents either to the gas treating industry or to the gas treating research community. As a maiden perspective, a comprehensive summary of physical properties like molecular weight; boiling point; viscosity; refractive index etc., of MAE and EAE along with some other potential alkanolamine solvents like MEA, DEA and TEA are presented in Table 3.1. The physicochemical properties, transport properties, corrosion resistance, degradation resistance, and rate studies on MAE and EAE solvent need to be explored. The determination of the CO_2solubility in aqueous MAE and EAE solution deserves immense significance and according to my knowledge, no reference; apart from ours on vapor-liquid equilibrium (VLE) of CO_2 over MAE and EAE is available in the open literature until now. In view of this, the present chapter comprises the vapor-liquid equilibrium (VLE) of CO_2 over aqueous MAE and EAE of different composition at temperature 303.1, 313.1 and 323.1 K. The experimental set-up and procedure has been validated with the systematic VLE data generated on CO_2 solubility in (DEA + AMP/MDEA + H_2O) systems. Some of the VLE data generated on the mentioned blends have been compared with the literature data. The generated data on (CO_2 + DEA + AMP/MDEA + H_2O) systems are also correlated with a rigorous; activity based thermodynamic model with minimal correlation deviations, thus indicating the robustness of my set-up and procedure. Moreover, the new VLE data of CO_2 generated in (DEA + AMP + H_2O) and (DEA + MDEA + H_2O) blends have enhanced and enriched the database.

Table 3.1 Significant physical properties of [#]MAE and EAE along with ** MEA, DEA, and TEA.

	MEA	***DEA***	***TEA***	***MAE***	***EAE***
Chemical Name	Monoethanolamine	Diethanolamine	Triethanolamine	N-methyl-2-ethanolamine	2-(Ethylamino) ethanol
Molecular formula	C_2H_7NO	$C_4H_{11}NO_2$	$C_6H_{15}NO_3$	C_3H_9NO	$C_4H_{11}NO$
Molecular weight	61.08	105.14	149.19	75.11	89.14
Specific gravity	1.017	1.092	1.126	0.94	0.914
Boiling Point (^{0}C)	170.4	268	335	152-162	169-170
Vap. Pressure (mm Hg)	<1	<0.01	<0.001	<0.5	<1
Abs. Viscosity at 20 ^{0}C	24.1	380 at 30 ^{0}C	921	13	
Refractive Index	1.4539	1.4747	1.4852	1.44	1.439
Solubility in water	complete	complete	complete	complete	complete

[#] (ARKEMA inc. datasheet)

[**](DOW datasheet)

3.2 EXPERIMENTAL SECTION

3.2.1 Materials

N-methyl-diethanolamine (MDEA), *N*-methy-2-ethanolamine (MAE), *N*-ethyl ethanolamine (EAE) and 2-amino-2-methyl-1-propanol (AMP) were supplied by E. Merck, Germany, and had a mole % purity of > 98, > 98, > 97, and > 95 respectively. Double distilled water, degassed by boiling was used for making the alkanolamine solutions. Alkanolamines may be distilled under vacuum in order to remove any possible traces of moisture and other impurities like CO_2 before they are used to prepare the solutions. In the present study, the prepared aqueous alkanolamine solutions were kept

under vacuum for more than 10-20 minutes before commencement of reaction in the VLE cell, so that the solutions exist under their own vapor pressure only. The mole L^{-1} (strengths) equivalent of requisite mass fraction of single alkanolamine solutions were determined by titration with standard HCl using methyl orange indicator. Following the standard acid-base titration procedure, the normality of aqueous alkanolamine solutions were determined. The uncertainty in determining the composition sneaked in at transfers from pipette and burette. The estimated uncertainty in molarity was ±1 % assuming the precise and perfect determination of endpoints of titrations. Methyl orange indicator used to determine endpoints undergo color change over a narrow range of pH (3.1- 4.4) in comparison to other indicators like Bromophenol blue (3.0 – 4.6) and Bromocresol green (3.8 – 5.4). Pure carbon dioxide, obtained from Vadilal Gases Limited, India, had mole % purity of 99.99.

3.2.2 Apparatus

The solubility of CO_2 in aqueous alkanolamine was measured in a stainless steel equilibrium cell. VLE measurements were done at pressures ranging from (1 to 500) kPa and at temperatures (303.1, 313.1 and 323.1) K. The VLE apparatus consists of two stainless steel cylindrical tanks namely buffer vessel and vapor-liquid equilibrium cell of volumes 1505 ml and 785 ml, respectively, submerged in a water bath. The temperature of the water bath, hence, equilibrium cell and gas buffer is controlled within ±0.2 K of the desired level with the help of a circulator temperature controller (Polyscience, USA model No: 9712) operated on an external mode and the uncertainty in temperature measurement is ±0.1 K. Pre-calibrated platinum sensors (Pt-100, Julabo) with temperature indicator (Julabo TD300) are additionally used for measurement of temperatures in the equilibrium cell and gas buffer and the uncertainty in temperature measurement is ±0.1 K. A vacuum pump (INDVAC, Model-IV-50), capable of creating 2 kPa pressure is attached to the buffer vessel through VLE cell, and is used to evacuate both the vessels before the commencement of the experiment. Pressure transducers in the range of (0 to 1724), and (0 to 689) kPa (PMP450, FUTEK, Germany) are attached to the buffer vessel and the equilibrium cell, respectively. The accuracy and non-repeatability of each of the pressure transducers are ±0.25 % and ±0.1 % of the rated output, respectively. In the event of attainment of pressures equal to the maximum pressure limits measurable by the pressure transducers, the maximum combined uncertainty (k=2) in the pressure measurements can reach up to ± 0.36 % (≅ ±0.4 %) and ± 0.46 % (≅ ±0.5 %) of the transducers' readings

attached to the buffer vessel and the equilibrium cell, respectively (Appendix). The VLE cell is equipped with a liquid phase stirrer (SPINOT - Magnetic Stirrer, TARSON).There are ball valves (Swagelok, Germany) controlling the transfer of gas from CO_2 cylinder to buffer vessel, and from buffer vessel to VLE cell. Figures 3.1 and 3.2 show the schematic and photograph for VLE experimental set up, respectively.

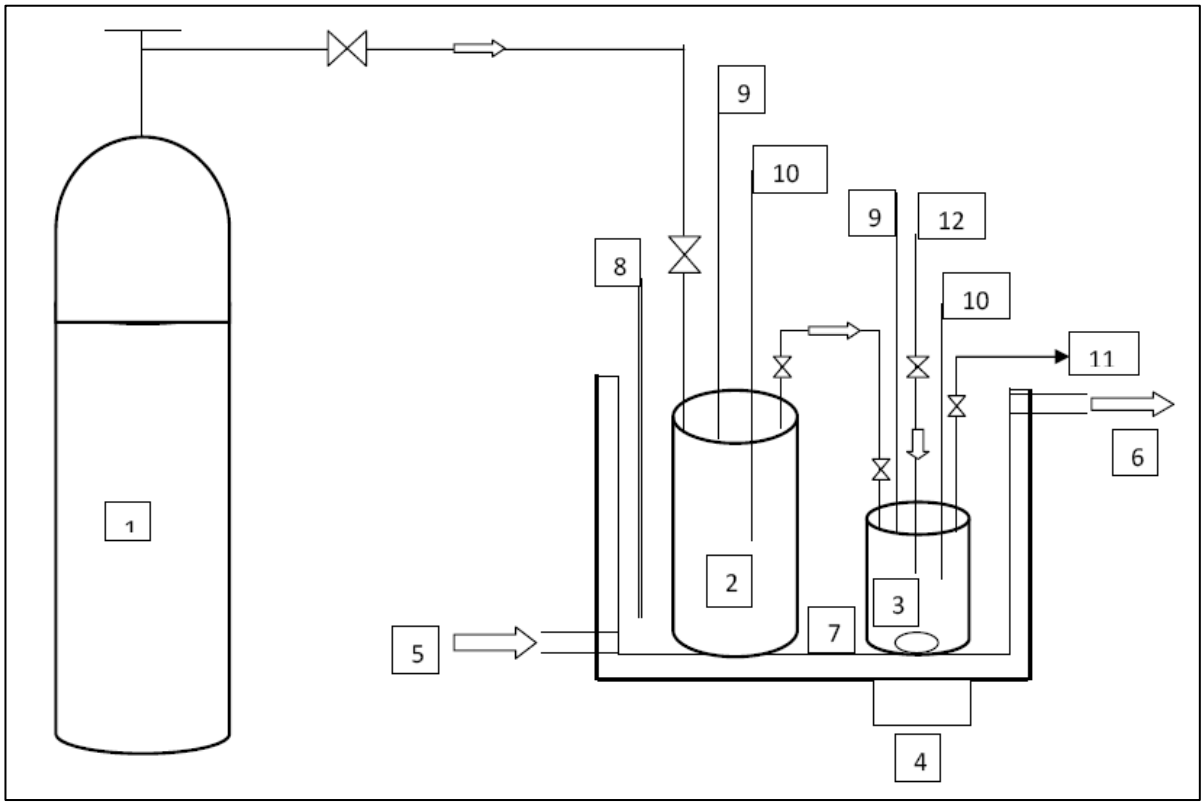

Figure 3.1: Schematic of Experimental Set-up. 1, CO_2 cylinder; 2, Buffer vessel; 3, VLE cell; 4, Magnetic Stirrer; 5, Water from circulator; 6, Water to circulator; 7, Water bath; 8, Pt. 100 temperature sensor; 9, Pressure transducer; 10, Temperature sensor; 11, Vacuum pump; 12, Burette, (Kumar *et al*., 2012).

Figure 3.2: Photograph of the experimental VLE set-up.

3.2.3 Procedure

For each set of run, the buffer vessel and the VLE cell were allowed to reach in temperature equilibration with water bath undergoing constant water recirculation with the help of the circulator temperature controller. Air was evacuated by vacuum pump from both the vessels at a time by opening the valve connecting both the vessel. After evacuation, the buffer vessel was made isolated from VLE cell by closing the valve between them and was allowed to receive 1.5 to 2.5 times of the desired maximum CO_2 partial pressure (total pressure here) from pure CO_2 gas cylinder. 25 ml of freshly prepared aqueous alkanolamines solution of the desired concentration was sucked into the VLE cell with the help of attached burette, and the cell was fully sealed. The maximum error in the transferred volume was estimated to be 0.05 ml. A vacuum was initially present in the VLE cell and it was again evacuated for the second time. The VLE cell was kept under this condition over ten to twenty minutes duration so that the liquid existed under its own vapor pressure. This solution vapor pressure (p_v) was noted. The CO_2 gas from the buffer was then allowed to enter to the equilibrium cell and after the transfer the buffer vessel was temporarily isolated from the VLE cell with the help of the valve.

Amount of CO_2, hence, moles of CO_2 being transferred from the buffer vessel was calculated using the difference in pressure transducer reading attached to it. At the commencement of absorption in VLE cell, the liquid phase stirrer was kept on. The attainment of equilibrium in the VLE cell was ensured when there was no change in total pressure of the VLE cell for at least one hour while the temperature was maintained constant at its desired level. It took about 1 hour to reach equilibrium for each run (one equilibrium point). The pressure transducer attached to the VLE cell was an indication of the total cell pressure (P_t). The equilibrium pressure (P_{CO_2}) was calculated taking the difference of total pressure of cell, P_t and vapor pressure p_v,$\left(\mathrm{P_{CO_2}} = \mathrm{P_t}\text{- }\mathrm{p_v}\right)$. Moles of CO_2 absorbed by the aqueous alkanolamine blends in the VLE cell was calculated by the difference in moles of CO_2 being transferred from the buffer vessel and moles of CO_2 present in the gas phase of the VLE cell at equilibrium pressure by taking in to account the compressibility factor of the gas. The method of calculation adopted regarding the number of moles of CO_2 absorbed in the liquid phase; was that of described by (Park and Sandall, 2001). At that total equilibrium pressure, the CO_2 loading has been expressed as moles of CO_2 absorbed per moles of alkanolamine. Liquid phase mole fraction of CO_2 at equilibrium was also calculated at each equilibrium point. The maximum combined

uncertainty (k=2) in CO_2 loading was found to be ±3.0 % of the estimated loading. After the completion of one run, once again the valve between the buffer vessel and the VLE cell was re-opened and gas was transferred from buffer vessel to VLE cell and the whole procedure was repeated for the second run in order to generate solubility data at higher CO_2 pressure than the previous one.

To validate the present experimental set-up, several VLE measurements were done in aqueous solutions of DEA as well as in (DEA + AMP) blend at 313.1 K and checked with the experimental results available in the open literature (Seo and Hong, 1996; Kundu, 2004). Table 3.2 presents some representative results of validation with an average absolute deviation percentage (AAD %) of 6.2 & 12.8 in predicting equilibrium CO_2 partial pressure over aqueous DEA, and (DEA + AMP) blend, respectively. In Table 3.2, the CO_2 loading (α) has been expressed as moles of CO_2/mole of alkanolamine.

Table 3.2: Comparison among CO_2 solubility in aqueous solutions of DEA & (DEA + AMP) generated in this work and literature value at 313.1 K.

DEA = 30 wt %				**DEA + AMP = 6 wt % + 24 wt %**			
Loading (α_{CO_2})	P_{CO_2} / kPa	P_{CO_2} / kPa[ref a]	[c]AAD %	Loading (α_{CO_2})	P_{CO_2} / kPa	P_{CO_2} / kPa[ref b]	[c]AAD %
0.39	2.2	1.8	6.2	0.372	2.0	1.61	12.8
0.51	14.5	15.0		0.614	12.7	15.3	
0.59	56.0	56.4		0.686	30.1	32.0	
0.64	85.3	87.5		0.774	85.2	89.5	

[ref a] = (Kundu, 2004)

[ref b] = (Seo and Hong, 1996)

[c]AAD% = $\left[\sum_n \left(p_{cal} - p_{exp}\right)/p_{exp}\right]/n \times 100$

3.3 VLE OF (CO_2 + DEA + AMP/MDEA + H_2O) SYSTEM

The aqueous alkanolamine blends of (DEA+AMP/MDEA) were used to generate the systematic CO_2 solubility data at temperatures (303.1, 313.1 and 323.1) K and in the CO_2 pressure range of (1 to 350) kPa. Aqueous ternary mixtures of (DEA + AMP) and (DEA + MDEA) with the following compositions (0.06 mass fraction/0.571 mol.L^{-1} DEA + 0.24 mass fraction/ 2.692 mol.L^{-1} AMP), (0.09 mass fraction/0.856 mol.L^{-1} DEA + 0.21 mass fraction/2.356 mol.L^{-1} AMP), (0.12 mass fraction/1.141 mol.L^{-1}DEA+ 0.18 mass fraction/2.019 mol. L^{-1} AMP), and (0.15 mass fraction/1.427 mol.L^{-1} DEA + 0.15 mass fraction/1.683 mol.L^{-1} AMP) and (0.06 mass fraction/0.571 mol.L^{-1} DEA + 0.24 mass fraction/2.014 mol.L^{-1} MDEA), (0.09 mass fraction/0.856 mol.L^{-1} DEA + 0.21 mass fraction/1.762 mol.L^{-1} MDEA), (0.12 mass fraction/1.141 mol.L^{-1} DEA + 0.18 mass fraction/1.511 mol.L^{-1} MDEA), and (0.15 mass fraction/1.427 mol.L^{-1}DEA + 0.15 mass fraction/1.259 mol.L^{-1} MDEA) were considered. The total alkanolamine mass fraction was held constant at 0.3. The rigorous thermodynamic model developed in this work used two types of equilibria; phase equilibria and chemical reaction equilibria. The vapor phase non-ideality was taken care off in terms of fugacity coefficient calculated using *Virial* equation of state. Extended *Debye-Hückel* theory of electrolytic solution was used to address the liquid phase non-ideality. The rigorous model developed in this work was a model with less computational rigor than any other rigorous thermodynamic model which is being used presently for predicting VLE of acid gases over alkanolamine blends. For (CO_2 + DEA + AMP + H_2O) and (CO_2 + DEA + MDEA + H_2O) systems, the correlated and experimental CO_2 pressures were in good agreement (Kumar *et al.* (2012))

3.3.1 Chemical Equilibria

The following chemical equilibria are involved in the aqueous phase for the (CO_2 + DEA/MAE/EAE + AMP + H_2O) and (CO_2 + DEA/MAE/EAE + MDEA + H_2O) systems.

Ionization of water

$$H_2O \overset{K_1}{\leftrightarrow} H^+ + OH^- \tag{3.1}$$

Hydration of carbon dioxide

$$CO_2 + H_2O \overset{K_2}{\leftrightarrow} H^+ + HCO_3^- \tag{3.2}$$

Dissociation of bicarbonate

$$HCO_3^- \overset{K_3'}{\leftrightarrow} H^+ + CO_3^{-2} \tag{3.3}$$

Dissociation of protonated secondary amine (DEA/MAE/EAE)

$$RR'R^{"}NH^+ \overset{K_4'}{\leftrightarrow} H^+ + RR'R^{"}N \tag{3.4}$$

Dissociation of protonated tertiary amine (MDEA)

$$RR'R'NH^+ \overset{K_5}{\leftrightarrow} H^+ + RR'R'N \tag{3.5}$$

Dissociation of Carbamate

$$RR'R^{"}NCOO^- + H_2O \overset{K_6'}{\leftrightarrow} HCO_3^- + RR'R^{"}N \tag{3.6}$$

Hydration of AMP

$$H_2O + (C_2H_2(CH_3)_2OH)NH_2 \overset{K_7^{"}}{\leftrightarrow} OH^- + (C_2H_2(CH_3)_2OH)NH_3^+ \tag{3.7}$$

$$AMPH^+ \overset{K_8}{\rightarrow} AMP + H^+ = RR'R'NH^+ \overset{K_8}{\leftrightarrow} H^+ + RR'R'N \tag{3.8}$$

$$K_8 = \frac{K_1}{K_7^{"}} \tag{3.9}$$

For DEA, R , R' and R'' represent H, C_2H_4OH and C_2H_4OH respectively; for MAE R , R' and R'' represent H, CH_3 and C_2H_4OH respectively ; for EAE R , R' and R'' represent H, C_2H_5 and C_2H_4OH respectively; for MDEA, R , R' and R' are $CH_3$and C_2H_4OH , and C_2H_4OH respectively and for AMP R , R' and $R'$are H, H, and $C_2H_2(CH_3)_2OH$, respectively. The equilibrium constant for deprotonation of AMP was obtained by mathematical manipulation of reactions (3.1) and (3.7), which resulted in reaction (3.8). $K_i'$is the mol fraction based equilibrium constants, $K_i^{"}$ is the equilibrium constant in molalrity scale ($kmol.m^{-3}$), K_i is the equilibrium constant in molality scale ($mol\ of\ solute\ alkanolamine\ per\ kg\ water$). The equilibrium constant for reaction (3.7) is in molarity ($kmol.m^{-3}$) scale, equilibrium constants for reaction (3.4) and (3.6) are mol fraction based which were converted to molality scale in order to adapt in the proposed model. The temperature dependent equilibrium constants along with their literature sources are presented in Table 3.3.

3.3.2. Thermodynamic Framework

For the (CO_2 + DEA +AMP+ H_2O) and (CO_2 + DEA +MDEA+ H_2O) systems, the equilibrated liquid phase is assumed to contain three molecular species (H_2O, DEA, and AMP/MDEA) and five ionic species ($AMPH^+$/ $MDEAH^+$, HCO_3^-,$DEAH^+$, $DEACOO^-$, and H_3O^+). Species like free molecular CO_2, OH^-, and CO_3^{2-} will have a little effect on the observed equilibria. Several previous workers (Haji-Sulaiman *et al.*; Posey) have observed that neglecting the concentrations of free molecular CO_2, and OH^- and CO_3^{-2} ions in the liquid phase in this system for CO_2 loading (moles of CO_2 per moles of alkanolamine) below 1.0 does not result in significant error in the VLE predictions. In our calculation of activity coefficients of the components in the aqueous phase, the activity coefficients of DEA, AMP/MDEA, H_2O, $DEAH^+$, $AMPH^+$/$MDEAH^+$, $DEACOO^-$and HCO_3^- are included to account for the non-ideality of the liquid phase. As the free molecular CO_2 concentration in the liquid phase is negligible below the loading of 1.0, the value of γ_{CO_2} will be close to unity following the un-symmetric normalization of activity coefficient. We can calculate molal concentrations (mole/kg solvent water) of species in liquid phase based on true molecular or ionic species.

3.3.3 Standard States

For developing the model, both AMP/MDEA and DEA are treated as solutes and only solvent considered is water. The standard state associated with solvent water is the pure liquid at the system temperature and pressure. The adopted standard state for ionic solutes is the ideal, infinitely dilute aqueous solution at the system temperature and pressure. The reference state chosen for molecular solute CO_2 is the ideal, infinitely dilute aqueous solution at the system temperature and pressure.

3.3.4 Vapour-Liquid Equilibria

We have assumed that the amine is nonvolatile (relative to the other molecular species), an assumption that can be easily relaxed if necessary. It is assumed a physical solubility (Henry's law) relation for the (non-condensable) acid gases. Thus, the following iso-fugacity relation is applicable:

$$\varphi_{CO_2} P_{CO_2} = \gamma_{CO_2} m_{CO_2} H_{CO_2} \qquad (3.10)$$

Where, φ_{CO_2} is the fugacity coefficient of CO_2, H_{CO_2} is a Henry's constant for CO_2 in pure water, $P_{CO_2}$is the equilibrium partial pressure of CO_2. The Henry's constant was taken

from literature and presented in Table 3.3. The vapor phase fugacity coefficient was calculated using the *Virial* equation of state.

3.3.5 Thermodynamic Expression of Equilibrium Partial Pressure

From the aforesaid chemical reaction equilibria, mathematically, the corresponding equilibrium constants (converted in molality scale) are defined in terms of activity coefficients, γ, and molalities; m $(mol.kg^{-1}\ solvent\ water)$ of the species present in the equilibriated liquid phase.

$$K_1 = \gamma_{H^+} m_{H^+} \gamma_{OH^-} m_{OH^-} \tag{3.11}$$

$$K_2 = \frac{\gamma_{H^+} m_{H^+} \gamma_{HCO_3^-}\, m_{HCO_3^-}}{\gamma_{CO_2}\, m_{CO_2}} \tag{3.12}$$

$$K_3 = \frac{\gamma_{H^+} m_{H^+} \gamma_{CO_3^{2-}} m_{CO_3^{2-}}}{\gamma_{HCO_3^-}\, m_{HCO_3^-}} \tag{3.13}$$

$$K_4 = \frac{\gamma_{H^+} m_{H^+} \gamma_{RR'R"N} m_{RR'R"N}}{\gamma_{RR'R"H^+} m_{RR'R"H^+}} \tag{3.14}$$

$$K_5 = K_8 = \frac{\gamma_{H^+} m_{H^+} \gamma_{RR'R'N} m_{RR'R'N}}{\gamma_{RR'R'NH^+}\, m_{RR'R'NH^+}} \tag{3.15}$$

$$K_6 = \frac{\gamma_{HCO_3^-} m_{HCO_3^-} \gamma_{RR'R"N} m_{RR'R"N}}{\gamma_{RR'R"NCOO^-}\, m_{RR'R"NCOO^-}} \tag{3.16}$$

The following balance equations for the reacting species can be formed:

Total amine balance:

$$m_1 = \left[RR'R"N\right] + \left[RR'R"NH^+\right] + \left[RR'R"NCOO^-\right] \tag{3.17}$$

$$m_2 = [RR'R'N] + [RR'R'NH^+] \tag{3.18}$$

Carbon dioxide balance:

$$(m_1 + m_2)\alpha = [CO_2] + [HCO_3^-] + [CO_3^{2-}] + \left[RR'R"NCOO^-\right] \tag{3.19}$$

Equation of electro neutrality:

$$[H^+] + \left[RR'R"NH^+\right] + [RR'R'NH^+] = [OH^-] + [HCO_3^-] + 2[CO_3^{2-}] + \left[RR'R"NCOO^-\right] \tag{3.20}$$

Where α has been expressed as mole CO_2 per mole of alkanolamine. Putting the value of $\gamma_{CO_2} m_{CO_2}$ from Eq. (3.12) into Eq. (3.10) and the equation will be

$$\varphi_{CO_2} P_{CO_2} = \frac{\gamma_{H^+} m_{H^+} \gamma_{HCO_3^-} m_{HCO_3^-}}{K_2'} H_{CO_2} \tag{3.21}$$

Taking the value of $\gamma_{H^+} m_{H^+}$ from Eqs. (3.14 and 3.15) and ($\gamma_{HCO_3^-} m_{HCO_3^-}$) from Eq. (3.16) and substituting them into Eq. (3.21), the following relation results,

$$P_{CO_2} = \frac{H_{CO_2}}{\varphi_{CO_2}} \left(K_4 \frac{\gamma_{RR'R"H^+} m_{RR'R"H^+}}{\gamma_{RR'R"N} m_{RR'R"N}} + K_5 \frac{\gamma_{RR'R'H^+} m_{RR'R'H^+}}{\gamma_{RR'R'N} m_{RR'R'N}} \right) \left(\frac{K_6}{K_2} \frac{\gamma_{RR'R"NCOO^-} m_{RR'R"NCOO^-}}{\gamma_{RR'R"N} m_{RR'R"N}} \right) \tag{3.22}$$

The equilibrium concentrations of $m_{RR'R"H^+}$, $m_{RR'R"N}$, $m_{RR'R'NH^+}$, $m_{RR'R'N}$ $m_{RR'R"NCOO^-}$ and $m_{HCO_3^-}$ $(mol.kg^{-1}\ solvent\ water)$ can be calculated rearranging the Eqs. (3.16 to 3.20) mathematically, which are as follows:

$$m_{RR'R"N} = m_1 - m_1\alpha - z \tag{3.23}$$

$$m_{RR'R'N} = m_2 - m_2\alpha \tag{3.24}$$

$$m_{RR'R"H^+} = m_1\alpha \tag{3.25}$$

$$m_{RR'R'H^+} = m_2\alpha \tag{3.26}$$

$$m_{RR'R"NCOO^-} = z \tag{3.27}$$

$$m_{HCO_3^-} = (m_1 + m_2)\alpha - z \tag{3.28}$$

Where

$$z = \frac{(K_6' + m_1) - \left[(K_6' + m_1)^2 - 4m_1^2\alpha(1-\alpha)\right]^{\frac{1}{2}}}{2} \tag{3.29}$$

Where α has been expressed as mole CO_2 per mole of alkanolamine in Eqs. (3.23-3.29).

3.3.6 Activity Coefficient Model

The activity coefficient model consists of Debye-Hückel term, which is one of the dominant terms in the expression for the activity coefficients in dilute solution, accounts

for electrostatic, non-specific long-range interactions. At higher concentrations, short range; non-electrostatic interactions have to be taken into account. This is usually done by adding ionic strength dependent terms to the *Debye-Hückel* expression. The mathematical description of the two basic assumptions in the specific ion interaction theory is as follows:

$$ln\,\gamma_i = -\frac{AZ_i^2 I^{0.5}}{1+I^{0.5}} + 2\sum_j \beta_{ij} m_j \qquad (3.30)$$

Here, A, is the *Debye-Hückel* limiting slope (0.509 at 25 ^{0}C in water), and $I$is the ionic strength, defined as

$$I = {}^1\!/_2 \sum_i m_i Z_i^2 \qquad (3.31)$$

Here, Z is the charge number on the ion, $\beta_{ij}(kg.mol^{-1})$ represent the net effect of various short-range two-body forces between different molecular and ionic solutes. The summation in the second term of Eq. (3.30) is taken over all solute pairs but excludes interactions between solutes and the solvent, water. Physically, the first term on the right represents the contribution of electrostatic forces; the second term represents short-range Van-der Waals forces.

3.3.7 Calculation of Fugacity Coefficient

The fugacity coefficients were calculated using the *Virial* Equation of State. The fugacity coefficient of an acid gas in the gaseous mixture was approximated by the value of the fugacity coefficient of the acid gas (total CO_2 pressure here) at its partial pressure.

$$ln\,\varphi_{CO_2} = \frac{B_{ii}}{RT}\int_0^P dP \qquad (3.32)$$

or, $$ln\,\varphi_{CO_2} = \frac{B_{ii}P}{RT} \qquad (3.33)$$

B_{ii} Corresponds to interactions between pairs of molecules and can be calculated from *Virial* equation of state.

$$ln\,\varphi_{CO_2} = \frac{B_{ii}P_C P_R}{RT_C T_R} \qquad (3.34)$$

$$ln\,\varphi_{CO_2} = (B_1 + \omega B_2)\frac{P_R}{T_R} \qquad (3.35)$$

Where,

$$B_1 = 0.083 - \frac{0.422}{{T_R}^{1.6}} \qquad (3.36)$$

$$B_2 = 0.139 - \frac{0.172}{T_R{}^{4.2}} \tag{3.37}$$

Here, P_R and P_C are reduced and critical pressure; T_R and T_C are reduced and critical temperature and ω is the acentric factor it has been taken to be 0.239 for CO_2. The values considered for P_C and T_C are 73.87 bar and 304.2 K, respectively. φ_{CO_2}, thus calculated was used in Eq. (3.22). Some of the representative fugacity coefficients calculated is included in the appendix.

3.3.8 Method of Solution

In this work the solubility data of CO_2 in aqueous blended alkanolamine solutions of various compositions, in a wide range of CO_2pressure and temperatures below a CO_2 loading of 1.0 mol CO_2 /mol amine, have been used to estimate the interaction parameters by regression analysis.

. The objective function used for optimization is presented by Eq. (3.38)

$$F = \sum \left| \frac{\left\{ (P_{CO_2})_{cal} - (P_{CO_2})_{rxp} \right\}}{\left\{ (P_{CO_2})_{cal} (P_{CO_2})_{rxp} \right\}} \right| \tag{3.38}$$

Owing to the presence of multiple solutions some approaches were unable to obtain the global solution for the parameter estimation problem because they could not jump over the local minima. A constrained optimization function using quasi-Newton and Sequential Quadratic Programming (SQP) method from MATLAB was used for minimization of the proposed objective function with variable bounds.

3.4 RESULTS AND DISCUSSION

The solubility of CO_2 in (DEA + MDEA+ H_2O) and (DEA + AMP + H_2O) systems are presented in Tables 3.4 to 3.11. It is evident from the Tables, that at a fixed temperature, an increase in mass fraction of DEA in the alkanolamine blends, there is a decrease in solution CO_2 loading capacity. For any constant relative compositions in (DEA + AMP + H_2O) and (DEA + MDEA + H_2O) blends and CO_2 pressure, there is a decrease in solution CO_2 loading capacity with increasing temperature. The interaction parameters of the activity coefficient model for (CO_2 + DEA + AMP + H_2O) and (CO_2+ DEA + MDEA + H_2O) systems were obtained by regression analysis using the quaternary solubility data generated in this work. Twelve numbers of interaction parameters

$\left(\beta_{ij}(kg.mol^{-1})\right)$for each system were regressed with overall average correlation deviations in CO_2 partial pressure (with respect to the experimentally generated CO_2 pressure) by 5.3 % and 8.0 %, respectively for (CO_2 + DEA + AMP + H_2O) and (CO_2 + DEA + MDEA + H_2O) systems. The resulted interaction parameters for the aforesaid systems are listed in Tables 3.12 and 3.13, respectively.

Figures (3.4 to 3.7) and (3.8 to 3.11) show the comparison between the correlated and the experimental solubility data of CO_2 in aqueous ternary mixtures of (DEA (2) + AMP (3)) and (DEA (2) + MDEA (3)), respectively, with various relative amine compositions. The figures reveal an acquiescent resemblance between the experimental and correlated solubility, especially for aqueous (DEA (2) + MDEA (3)) blends.

The successful correlation and close agreement with literature data facilitated an affirmative conclusion about the robustness of set-up and procedure for experimentation.

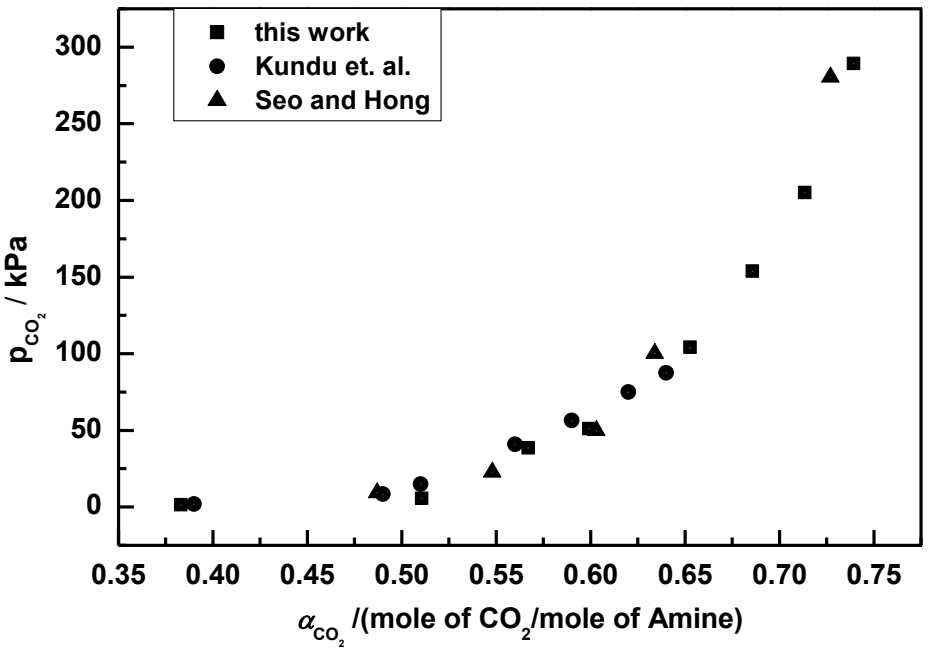

Figure 3.3: Comparison of solubility data for CO_2 (1) in aqueous solution of 0.30 mass fraction DEA (2) at T = 313.1 K.

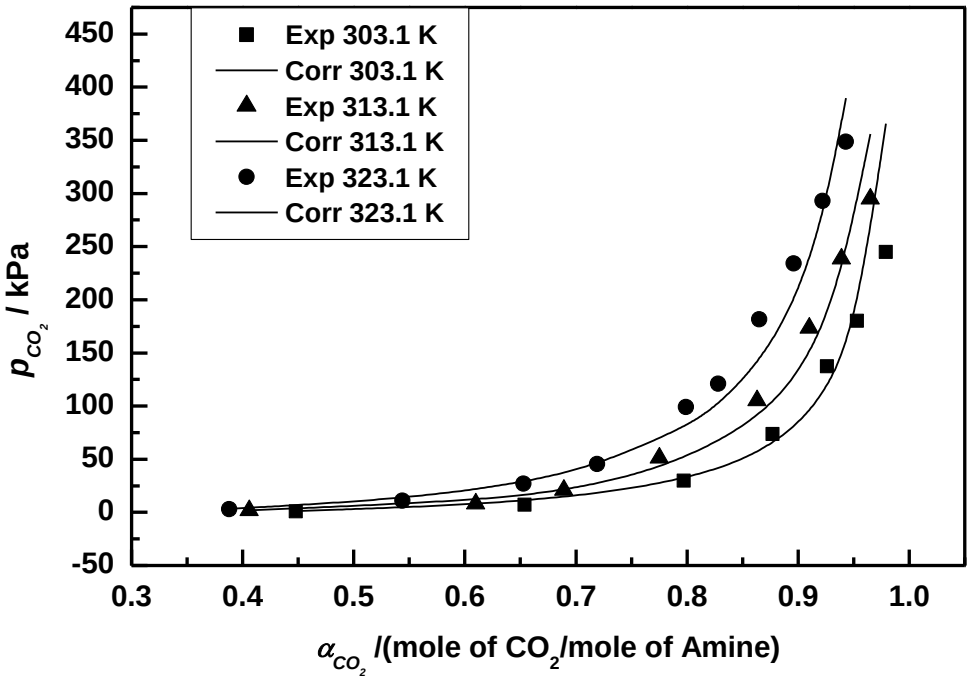

Figure 3.4: Solubility of CO_2 (1) in aqueous alkanolamine solution of mass fraction (0.06 DEA (2) + 0.24 AMP (3)) at T = (303.1 to 323.1) K.

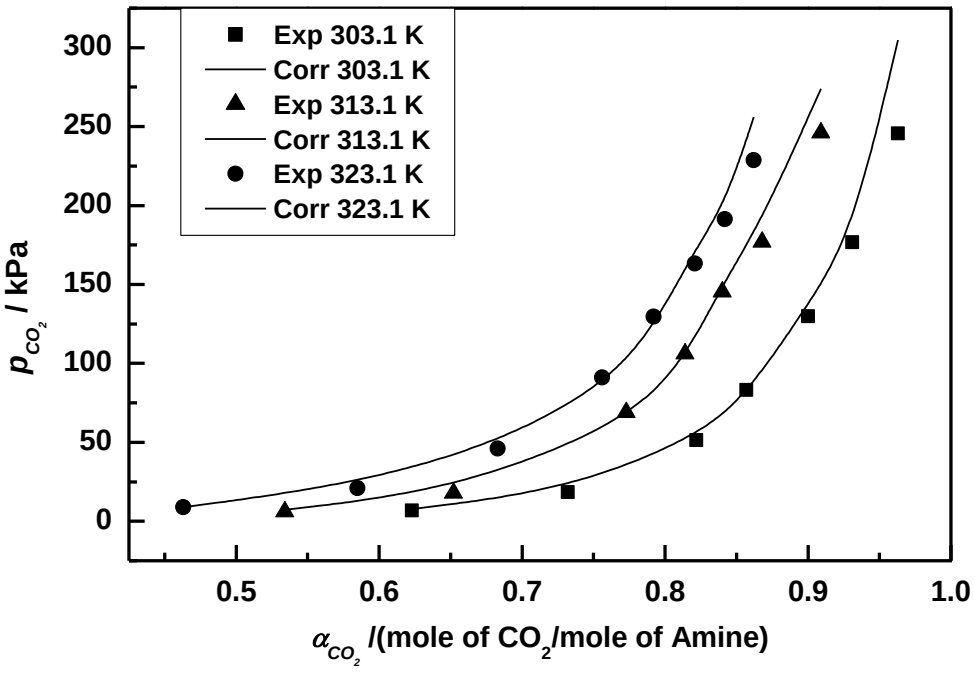

Figure 3.5: Solubility of CO_2 (1) in aqueous alkanolamine solution of mass fraction (0.09 DEA (2) + 0.21 AMP (3)) at T = (303.1 to 323.1) K.

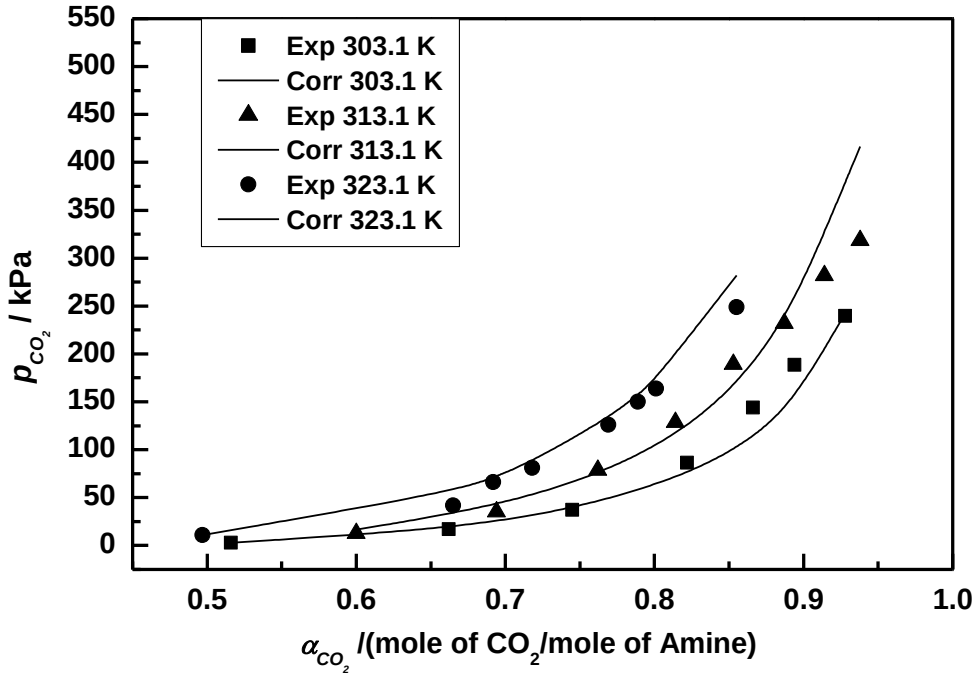

Figure 3.6: Solubility of CO_2 (1) in aqueous alkanolamine solution of mass fraction (0.12 DEA (2) + 0.18 AMP (3)) at T = (303.1 to 323.1) K.

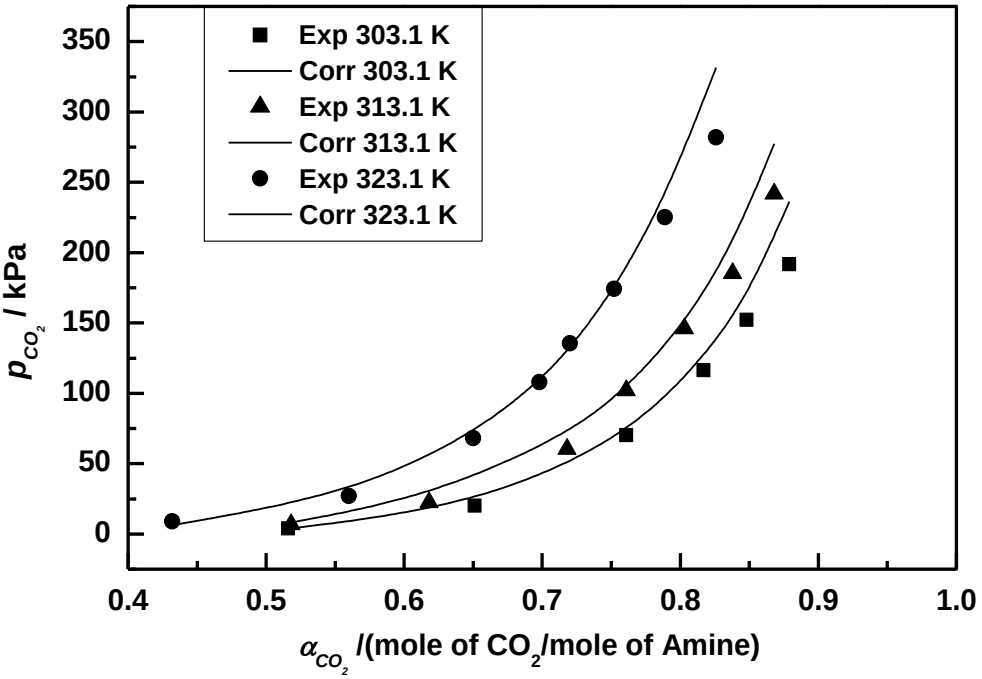

Figure 3.7: Solubility of CO_2 (1) in aqueous alkanolamine solution of mass fraction (0.15 DEA (2) + 0.15 AMP (3)) at T = (303.1 to 323.1) K.

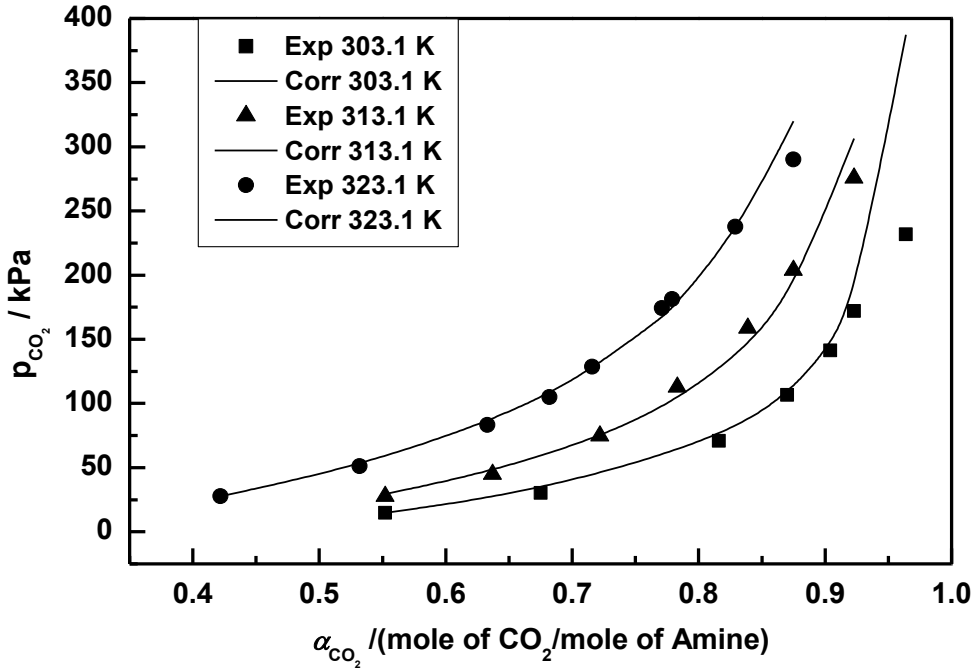

Figure 3.8: Solubility of CO_2 (1) in aqueous alkanolamine solution of mass fraction (0.06 DEA (2) + 0.24 MDEA (3)) at T = (303.1 to 323.1) K.

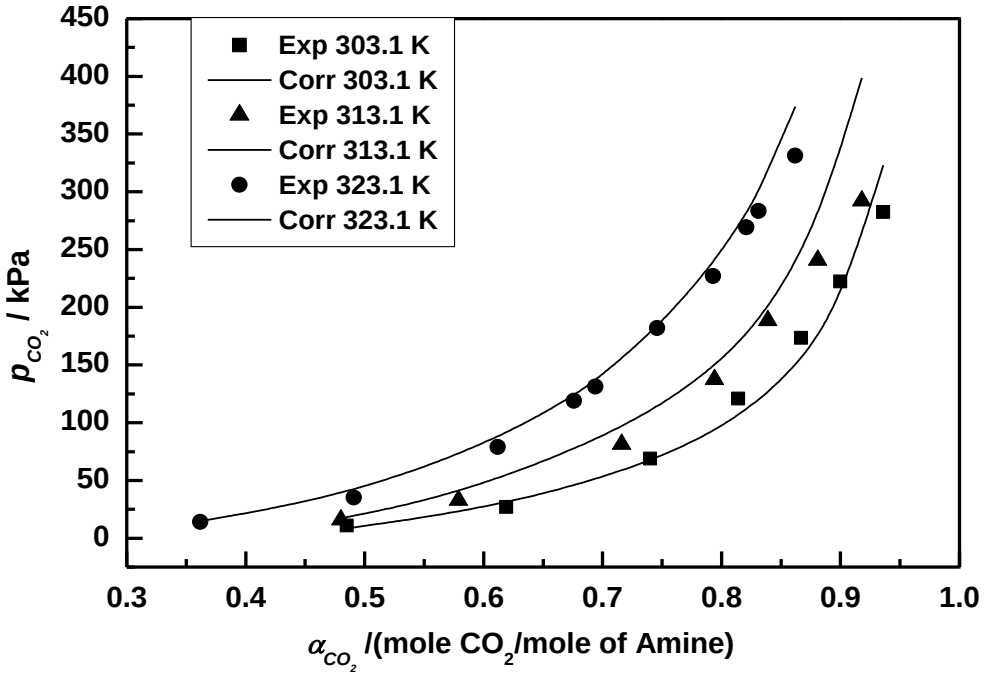

Figure 3.9: Solubility of CO_2 (1) in aqueous alkanolamine solution of mass fraction (0.09 DEA (2) + 0.21 MDEA (3)) at T = (303.1 to 323.1) K.

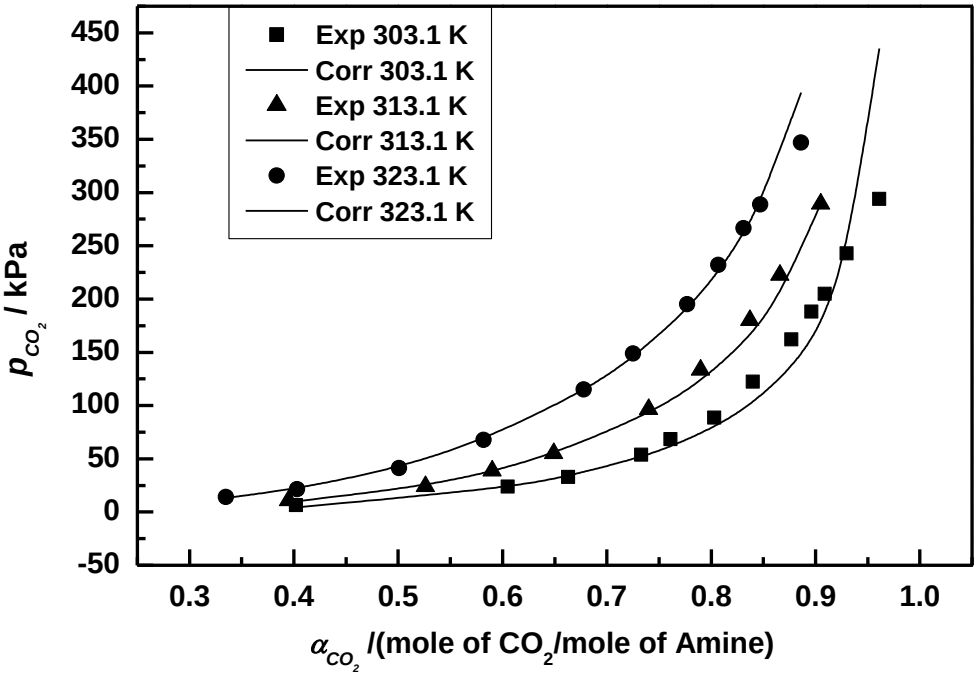

Figure 3.10: Solubility of CO_2 (1) in aqueous alkanolamine solution of mass fraction (0.12 DEA (2) + 0.18 MDEA (3)) at T = (303.1 to 323.1) K.

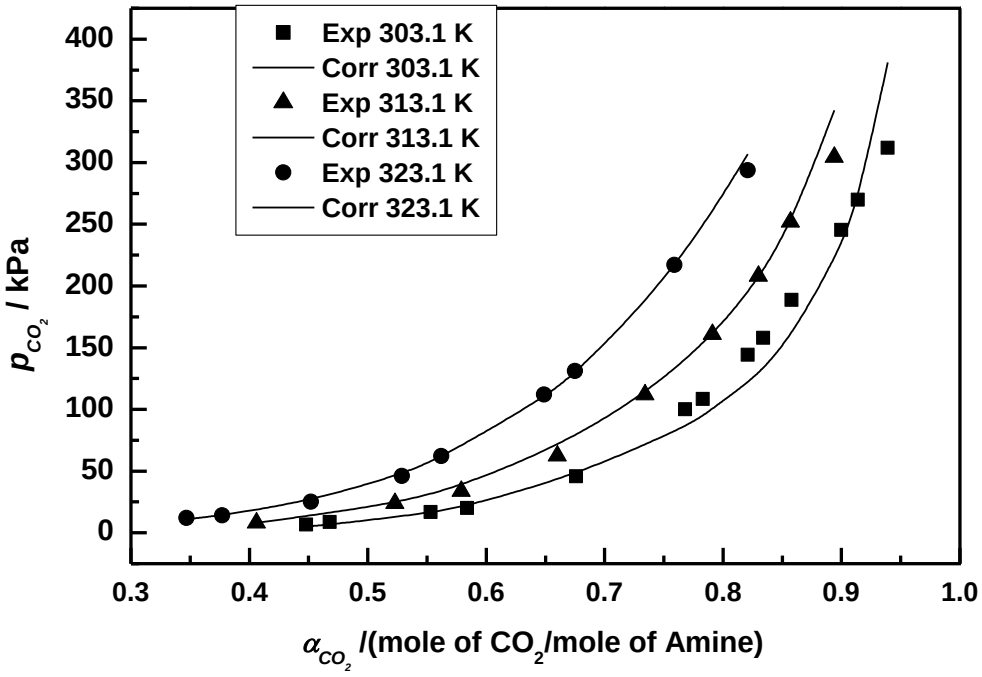

Figure 3.11: Solubility of CO_2 (1) in aqueous alkanolamine solution of mass fraction (0.15 DEA (2) + 0.15 MDEA (3)) at T = (303.1 to 323.1) K..

(α_{CO_2} / (moles of CO_2/moles of alkanolamine))

Table 3.3: Temperature dependence of the equilibrium constants and Henry's constant.

$$ln\ {K_i}/{mol.kg^{-1}} = C_1 + {C_2}/{T}_K + C_3 ln\ {T}/{K} + C_4\ {T}/{K} \quad \text{where, i = 1, 2, 5}$$

$$ln\ K_i' = C_1 + {C_2}/{T}_K + C_3 ln\ {T}/{K} + C_4\ {T}/{K} \quad \text{where, i = 4, 6}$$

$$ln\ {K_i^{"}}/{kmol.m^{-3}} = {C_1}/{T}_K + C_2 ln\ {T}/{K} + C_4 \quad \text{where, i = 7}$$

$$ln\ {H_{CO_2}}/{kg.atm.mol^{-1}} = C_1 + {C_2}/{T}_K + C_3 ln\ {T}/{K} + C_4\ {T}/{K}$$

Reaction	C_1	C_2	C_3	C_4	Ref
2	235.482	-12092.1	-36.7816	0	[c]
4	-6.7936	5927.65	0	0	[a]
6	4.5416	-3417.34	0	0	[a]
5	-59.55	1709	8.01	0	[b]
7	-7261.78	-22.4773	0	142.586	[d]
1	-13445.9	-22.4773	0	140.932	[d]
H_{CO_2}	94.4914	-6789.04	-11.4519	-0.010454	[c]

[a]Austgen *et al.*, 1989; [b]Posey, 1996; [c]Edwards *et al.*, 1978; [d]Silkenbäumer *et al.*, 1998.

Table 3.4: Solubility of CO_2 in aqueous (0.06 mass fraction DEA + 0.24 mass fraction MDEA) solutions in the temperature range of 303.1 – 323.1 K.

303.1 K			***313.1 K***			***323.1 K***		
CO_2 Partial pressure (kPa)	Loading (α_{CO_2})	x_{CO_2}	CO_2 Partial pressure (kPa)	Loading (α_{CO_2})	x_{CO_2}	CO_2 Partial pressure (kPa)	Loading (α_{CO_2})	x_{CO_2}
14.79	0.552	0.038	27.58	0.552	0.033	27.56	0.422	0.025
30.12	0.675	0.041	44.94	0.637	0.038	51.11	0.532	0.032
70.89	0.816	0.049	74.70	0.722	0.043	83.30	0.633	0.037
106.7	0.870	0.052	112.9	0.783	0.046	104.9	0.682	0.040
141.2	0.904	0.054	158.7	0.839	0.049	128.7	0.716	0.041
171.9	0.923	0.056	203.9	0.875	0.051	174.3	0.771	0.045
231.8	0.964	0.057	275.8	0.923	0.053	181.2	0.779	0.046
						237.6	0.829	0.048
						290.1	0.875	0.052

Table 3.5: Solubility of CO_2 in aqueous (0.09 mass fraction DEA + 0.21 mass fraction MDEA) solutions in the temperature range of 303.1 – 323.1 K.

303.1 K			***313.1 K***			***323.1 K***		
CO_2 Partial pressure (kPa)	Loading (α_{CO_2})	x_{CO_2}	CO_2 Partial pressure (kPa)	Loading (α_{CO_2})	x_{CO_2}	CO_2 Partial pressure (kPa)	Loading (α_{CO_2})	x_{CO_2}
6.496	0.402	0.025	10.89	0.395	0.024	14.03	0.335	0.021
23.86	0.605	0.037	24.05	0.526	0.032	21.30	0.403	0.025
32.83	0.663	0.040	38.92	0.590	0.036	41.08	0.501	0.030
53.91	0.733	0.044	55.11	0.649	0.039	67.47	0.582	0.035
68.54	0.761	0.045	96.64	0.740	0.044	114.9	0.678	0.040
88.38	0.803	0.048	133.4	0.790	0.047	148.8	0.725	0.043
122.2	0.840	0.050	180.2	0.837	0.050	195.0	0.777	0.046
162.1	0.877	0.052	222.7	0.866	0.051	232.0	0.807	0.048
188.2	0.896	0.053	289.5	0.905	0.054	266.3	0.831	0.049
204.7	0.909	0.055				288.9	0.847	0.050
242.8	0.930	0.056				346.9	0.886	0.053
294.0	0.961	0.058						

Table 3.6: Solubility of CO_2 in aqueous (0.12 mass fraction DEA + 0.18 mass fraction MDEA) solutions in the temperature range of 303.1 – 323.1 K.

303.1 K			***313.1 K***			***323.1 K***		
CO_2 Partial pressure (kPa)	Loading (α_{CO_2})	x_{CO_2}	CO_2 Partial pressure (kPa)	Loading (α_{CO_2})	x_{CO_2}	CO_2 Partial pressure (kPa)	Loading (α_{CO_2})	x_{CO_2}
10.81	0.485	0.030	15.89	0.480	0.029	14.07	0.362	0.023
26.89	0.619	0.038	32.88	0.579	0.035	35.29	0.491	0.030
68.80	0.740	0.045	81.51	0.716	0.043	79.12	0.612	0.038
120.7	0.814	0.049	137.4	0.794	0.048	119.0	0.676	0.040
173.5	0.867	0.052	188.7	0.839	0.050	131.1	0.694	0.042
222.4	0.900	0.054	241.0	0.881	0.053	181.8	0.746	0.045
282.3	0.936	0.056	292.1	0.918	0.055	227.1	0.793	0.048
						269.1	0.821	0.049
						283.3	0.831	0.050
						331.1	0.862	0.052

Table 3.7: Solubility of CO_2 in aqueous (0.15 mass fraction DEA + 0.15 mass fraction MDEA) solutions in the temperature range of 303.1 – 323.1 K.

303.1 K			***313.1 K***			***323.1 K***		
CO_2 Partial pressure (kPa)	Loading (α_{CO_2})	x_{CO_2}	CO_2 Partial pressure (kPa)	Loading (α_{CO_2})	x_{CO_2}	CO_2 Partial pressure (kPa)	Loading (α_{CO_2})	x_{CO_2}
6.489	0.448	0.028	8.014	0.406	0.024	11.98	0.347	0.022
8.632	0.468	0.029	23.79	0.523	0.032	14.21	0.377	0.024
16.91	0.553	0.034	33.91	0.579	0.036	25.09	0.452	0.028
20.20	0.584	0.036	62.49	0.660	0.041	45.92	0.529	0.033
45.82	0.676	0.042	112.0	0.734	0.045	62.02	0.562	0.035
100.0	0.768	0.047	161.0	0.791	0.047	112.0	0.649	0.040
108.4	0.783	0.048	208.0	0.830	0.051	131.2	0.675	0.042
144.3	0.821	0.050	251.9	0.857	0.052	217.0	0.759	0.046
157.8	0.834	0.051	304.5	0.894	0.054	293.8	0.821	0.050
188.7	0.858	0.052						
245.3	0.900	0.054						
269.8	0.914	0.055						
312.0	0.939	0.057						

Table 3.8: Solubility of CO_2 in aqueous (0.06 mass fraction DEA + 0.24 mass fraction AMP) solutions in the temperature range of 303.1 – 323.1 K.

303.1 K			***313.1 K***			***323.1 K***		
CO_2 Partial pressure (kPa)	Loading (α_{CO_2})	x_{CO_2}	CO_2 Partial pressure (kPa)	Loading (α_{CO_2})	x_{CO_2}	CO_2 Partial pressure (kPa)	Loading (α_{CO_2})	x_{CO_2}
1.021	0.448	0.035	1.987	0.406	0.031	3.007	0.388	0.030
6.996	0.654	0.050	8.298	0.610	0.047	11.01	0.544	0.042
29.78	0.797	0.060	20.91	0.689	0.053	26.79	0.653	0.050
73.48	0.877	0.066	51.20	0.775	0.061	45.32	0.719	0.055
137.4	0.926	0.070	105.1	0.863	0.064	99.11	0.799	0.061
180.0	0.953	0.071	173.6	0.910	0.068	121.1	0.828	0.063
244.9	0.979	0.073	238.7	0.939	0.070	181.5	0.865	0.065
			295.0	0.965	0.072	234.1	0.896	0.067
			354.8	0.989	0.074	293.0	0.922	0.069
						348.6	0.943	0.071

Table 3.9: Solubility of CO_2 in aqueous (0.09 mass fraction DEA + 0.21 mass fraction AMP) solutions in the temperature range of 303.1 – 323.1 K.

303.1 K			***313.1 K***			***323.1 K***		
CO_2 Partial pressure (kPa)	Loading (α_{CO_2})	x_{CO_2}	CO_2 Partial pressure (kPa)	Loading (α_{CO_2})	x_{CO_2}	CO_2 Partial pressure (kPa)	Loading (α_{CO_2})	x_{CO_2}
6.695	0.623	0.047	6.038	0.534	0.040	8.987	0.463	0.035
18.41	0.732	0.055	18.01	0.562	0.049	21.01	0.585	0.044
51.31	0.822	0.061	69.11	0.773	0.057	46.02	0.683	0.051
83.08	0.857	0.063	106.1	0.814	0.060	91.08	0.756	0.056
129.8	0.900	0.066	145.4	0.840	0.062	129.5	0.792	0.059
176.8	0.931	0.068	176.9	0.868	0.064	163.2	0.821	0.061
245.6	0.963	0.071	246.1	0.909	0.067	191.3	0.842	0.062
						228.7	0.862	0.064

Table 3.10: Solubility of CO_2 in aqueous (0.12 mass fraction DEA + 0.18 mass fraction AMP) solutions in the temperature range of 303.1 – 323.1 K.

303.1 K			***313.1 K***			***323.1 K***		
CO_2 Partial pressure (kPa)	Loading (α_{CO_2})	x_{CO_2}	CO_2 Partial pressure (kPa)	Loading (α_{CO_2})	x_{CO_2}	CO_2 Partial pressure (kPa)	Loading (α_{CO_2})	x_{CO_2}
3.013	0.516	0.039	12.56	0.600	0.045	11.01	0.497	0.047
17.01	0.662	0.049	35.31	0.694	0.052	41.63	0.665	0.050
37.02	0.745	0.056	78.58	0.762	0.056	66.01	0.692	0.052
86.51	0.822	0.061	128.6	0.814	0.060	81.00	0.718	0.055
144.1	0.866	0.064	189.2	0.853	0.063	125.9	0.769	0.057
188.6	0.894	0.065	232.0	0.887	0.065	150.2	0.789	0.058
239.7	0.928	0.068	281.9	0.914	0.067	163.7	0.801	0.061
			318.7	0.938	0.069	248.9	0.855	0.062

Table 3.11: Solubility of CO_2 in aqueous (0.15 mass fraction DEA + 0.15 mass fraction AMP) solutions in the temperature range of 303.1 – 323.1 K.

303.1 K			***313.1 K***			***323.1 K***		
CO_2 Partial pressure (kPa)	Loading (α_{CO_2})	x_{CO_2}	CO_2 Partial pressure (kPa)	Loading (α_{CO_2})	x_{CO_2}	CO_2 Partial pressure (kPa)	Loading (α_{CO_2})	x_{CO_2}
4.021	0.516	0.037	6.795	0.518	0.038	8.998	0.432	0.032
20.00	0.651	0.047	22.63	0.618	0.047	27.01	0.560	0.041
70.11	0.761	0.055	60.45	0.718	0.053	68.21	0.650	0.047
116.3	0.817	0.058	102.0	0.761	0.056	107.8	0.698	0.050
152.3	0.848	0.060	146.0	0.803	0.060	135.6	0.720	0.052
191.8	0.879	0.062	185.3	0.838	0.061	174.3	0.752	0.054
			241.8	0.868	0.063	225.2	0.789	0.055
						282.0	0.826	0.058

α_{CO_2} = loading of CO_2 = moles of CO_2 / moles of amine blend.

x_{CO_2} = mole fraction of CO_2 in liquid phase.

Table 3.12: Interaction parameters of (CO_2 – DEA–AMP- H_2O) system

Binary Interaction Parameters	***kg.mol^{-1}***	***AAD/% correlation***
$\beta\left(R\ R'\ R''\ N\ COO^{-} - R\ R'\ R''\ N\ H^{+}\right)$	-2.228221	**5.3**
$\beta\left(R\ R'\ R''\ N\ COO^{-} - R\ R'\ R''\ N\right)$	-0.948782	
$\beta\left(R\ R'\ R''\ N\ H^{+} - HCO_3^{-}\right)$	-2.044120	
$\beta\left(R\ R'\ R''\ N - R\ R'\ R''\ N\ H^{+}\right)$	-1.235838	
$\beta\left(R\ R'\ R''\ N - HCO_3^{-}\right)$	-0.793460	
$\beta\left(R\ R'\ R'\ N\ H^{+} - R\ R'\ R'\ N\right)$	-0.647058	
$\beta\left(R\ R'\ R'\ N\ H^{+} - HCO_3^{-}\right)$	0.117060	
$\beta\left(R\ R'\ R'\ N - HCO_3^{-}\right)$	0.451332	
$\beta\left(R\ R'\ R''\ N\ COO^{-} - R\ R'\ R'\ N\ H^{+}\right)$	-0.681037	
$\beta\left(R\ R'\ R''\ N\ COO^{-} - R\ R'\ R'\ N\right)$	-1.92113	
$\beta\left(R\ R'\ R''\ N\ H^{+} - R\ R'\ R'\ N\right)$	-0.336185	
$\beta\left(R\ R'\ R''\ N - R\ R'\ R'\ N\ H^{+}\right)$	0.274220	

Table 3.13: Interaction parameters of (CO_2 – DEA–MDEA- H_2O) system

Binary Interaction Parameters	***kg.mol^{-1}***	***AAD/% correlation***
$\beta\left(R\ R'\ R''\ N\ COO^{-} - R\ R'\ R'\ N\ H^{+}\right)$	-0.841042	**8.0**
$\beta\left(R\ R'\ R''\ N\ COO^{-} - R\ R'\ R'\ N\right)$	0.293588	
$\beta\left(R\ R'\ R'\ N\ H^{+} - HCO_3^{-}\right)$	1.764229	
$\beta\left(R\ R'\ R''\ N - R\ R'\ R'\ N\ H^{+}\right)$	-0.761452	
$\beta\left(R\ R'\ R'\ N - HCO_3^{-}\right)$	1.301074	
$\beta\left(R\ R'\ R'\ N\ H^{+} - R\ R'\ R'\ N\right)$	0.681454	
$\beta\left(R\ R'\ R''\ N\ H^{+} - HCO_3^{-}\right)$	-0.028994	
$\beta\left(R\ R'\ R''\ N - HCO_3^{-}\right)$	0.048992	
$\beta\left(R\ R'\ R''\ N\ COO^{-} - R\ R'\ R''\ N\ H^{+}\right)$	0.511067	
$\beta\left(R\ R'\ R''\ N\ COO^{-} - R\ R'\ R''\ N\right)$	0.464867	
$\beta\left(R\ R'\ R''\ N\ H^{+} - R\ R'\ R'\ N\right)$	0.512859	
$\beta\left(R\ R'\ R''\ N - R\ R'\ R''\ N\ H^{+}\right)$	-0.329676	

3.5 VLE OF CO_2 IN *N*-methyl-2-ethanolamine AND *N*- ethylaminoethanol SOLUTIONS

This section is devoted to the generation of systematic CO_2 solubility data in two recently proposed alkanolamine, namely; *N*-methyl-2-ethanolamine and *N*-ethylaminoethanol along with the generation of equilibrium constants (deprotonation and carbamate reversion) for EAE.

3.5.1 (MAE + CO_2 + H_2O) System

The CO_2 solubility in aqueous *N*-methyl-2-ethanolamine solutions (6.76, 10.52, 14.27, 18.78 and 30 by mass percentage) at temperatures 303.1, 313.1 and 323.1 K are presented in Tables 3.14-3.18, where the CO_2 loading has been expressed as the number of moles of CO_2 absorbed per mole of alkanolamine. It is evident from the tables that at a fixed temperature, an increase in total MAE concentration (mol. kg^{-1}) leads to a decrease in solution CO_2 loading capacity and even a moderate increase in CO_2 pressure results in CO_2 loading as high as 1.0. The tables also reveal that at a constant amine concentration and CO_2 pressure, an increase in temperature leads to a decrease in solution CO_2 loading capacity. Figure 3.12 shows the comparison in the CO_2 solubility among 30 mass percentage solutions of MAE, EAE, DEA, and MEA at 313.1 K. It has been a significant observation that MAE, in the total pressure range of 1 to 350 kPa possesses higher CO_2 loading capacity than alkanolamines like DEA and MEA. This significant improvement on the part of MAE can be explained, at least; qualitatively. MEA (primary alkanolamine), DEA, MAE, and EAE all forms carbamate, while reacting with CO_2. For MEA, the stoichiometric loading capacity is exactly 0.5. Apart from MEA, all (DEA, MAE, EAE) are secondary amines and it is their carbamate instability, which instigates their enhanced CO_2 loading. EAE resembling a moderately sterically hindered amine (methyl group attached to the alpha-C atom to the amine nitrogen) is expected to vehicle maximum CO_2 in the lot. One methyl group attached to the donor nitrogen is probably not sufficient for MAE to induce severe carbamate instability. It is not only the carbamate instability but also the basicity, plays an instrumental role in deciding the course of alkanolamine + CO_2 reaction. As stated earlier, that the amine basicity depends on the availability of the nitrogen lone pair, which can be influenced by the presence of steric effect offered by the bulky groups (alkyl group); the electron withdrawing effect of functional groups (hydroxyl

group); electron donating effect of functional groups (alkyl group) attached to the alkanolamine molecule and the possibility of intermolecular/intramolecular hydrogen bonding (in case of DEA). In MAE, the inductive effect of methyl group attached to the donor atom nitrogen increases the electron density of nitrogen lone pair, hence, enhanced the basicity in comparison to MEA, DEA and EAE. In DEA, the electron withdrawing effect of two ethanol groups reduces the electron density on the donor site (N atom) and results in weakening of N-H bond. However, this effect is mitigated by the extensive intramolecular hydrogen boding. Moreover, due to the H-bonded structure, carbamate reversion for DEA is more facile than in comparison to MEA and very often it's stoichiometric loading towards CO_2 reaches to 0.7. EAE is expected to be more basic in nature than unhindered-secondary and primary amines. Hence, the order of basicity is likely to follow the trend, MAE > EAE > MEA > DEA (later in this chapter, the EAE basicity will be discussed in detail). The order of carbamate stability is likely to follow the order MEA > DEA > MAE > EAE, which can well explain our experimental observations.

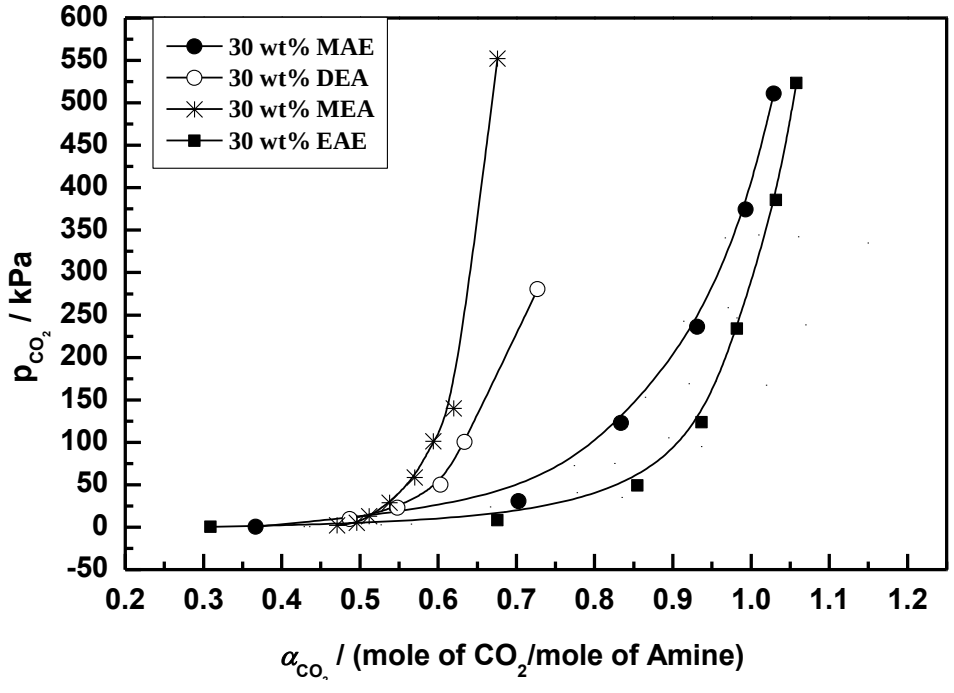

Figure 3.12: Comparison of the solubility of CO_2 in aqueous solutions of MEA, DEA, MAE, EAE of 0.3 mass fraction at 313.1 K; —, polynomial fit.

Table 3.14: Solubility of CO_2 in aqueous (0.068 mass fraction MAE) solutions in the temperature range of 303.1 – 323.1 K.

303.1 K			***313.1 K***			***323.1 K***		
CO_2 Partial pressure (kPa)	Loading (α_{CO_2})	x_{CO_2}	CO_2 Partial pressure (kPa)	Loading (α_{CO_2})	x_{CO_2}	CO_2 Partial pressure (kPa)	Loading (α_{CO_2})	x_{CO_2}
5.1	0.708	0.012	4.0	0.566	0.010	5.1	0.554	0.009
7.2	0.748	0.013	35.2	0.835	0.014	25.9	0.753	0.013
23.1	0.854	0.014	95.1	0.937	0.016	80.3	0.894	0.015
50.85	0.946	0.016	167.7	1.020	0.017	152.8	0.955	0.016
85.1	0.986	0.017	238.5	1.070	0.018	238.6	1.032	0.017
177.9	1.12	0.019	334.9	1.150	0.019			
242.7	1.144	0.019						
352.8	1.162	0.020						

Table 3.15: Solubility of CO_2 in aqueous (0.11 mass fraction MAE) solutions in the temperature range of 303.1 – 323.1 K.

303.1 K			***313.1 K***			***323.1 K***		
CO_2 Partial pressure (kPa)	Loading (α_{CO_2})	x_{CO_2}	CO_2 Partial pressure (kPa)	Loading (α_{CO_2})	x_{CO_2}	CO_2 Partial pressure (kPa)	Loading (α_{CO_2})	x_{CO_2}
0.9	0.345	0.009	3.0	0.527	0.014	2.0	0.416	0.011
5.1	0.647	0.018	41.1	0.778	0.021	24.1	0.687	0.019
44.3	0.857	0.023	105.3	0.895	0.024	86.3	0.848	0.023
93.75	0.935	0.025	171.8	0.955	0.025	167.5	0.924	0.025
181.9	1.018	0.027	246.9	0.982	0.026	276.8	0.992	0.027
322.5	1.10	0.029	342.2	1.061	0.029	353.3	1.043	0.028

Table 3.16: Solubility of CO_2 in aqueous (0.14 mass fraction MAE) solutions in the temperature range of 303.1 – 323.1 K.

303.1 K			***313.1 K***			***323.1 K***		
CO_2 Partial pressure (kPa)	Loading (α_{CO_2})	x_{CO_2}	CO_2 Partial pressure (kPa)	Loading (α_{CO_2})	x_{CO_2}	CO_2 Partial pressure (kPa)	Loading (α_{CO_2})	x_{CO_2}
3.2	0.534	0.020	1.0	0.436	0.017	4.0	0.474	0.019
35.1	0.778	0.029	18.1	0.685	0.026	48.1	0.722	0.027
85.45	0.879	0.033	75.3	0.826	0.031	132.3	0.818	0.031
161.3	0.934	0.035	169.1	0.921	0.035	203.8	0.891	0.033
249.8	0.989	0.037	258.7	0.971	0.036	264.5	0.930	0.035
351.9	1.023	0.038	344.6	1.01	0.038	355.9	0.956	0.036

Table 3.17: Solubility of CO_2 in aqueous (0.19 mass fraction MAE) solutions in the temperature range of 303.1 – 323.1 K.

303.1 K			***313.1 K***			***323.1 K***		
CO_2 Partial pressure (kPa)	Loading (α_{CO_2})	x_{CO_2}	CO_2 Partial pressure (kPa)	Loading (α_{CO_2})	x_{CO_2}	CO_2 Partial pressure (kPa)	Loading (α_{CO_2})	x_{CO_2}
1.0	0.366	0.019	1.0	0.429	0.022	3.0	0.422	0.022
17.1	0.678	0.035	24.1	0.667	0.034	27.1	0.637	0.033
87.4	0.846	0.043	72.6	0.774	0.040	94.8	0.753	0.039
159.2	0.902	0.046	153.1	0.865	0.044	148.5	0.806	0.041
247.7	0.963	0.049	242.8	0.914	0.047	239.7	0.865	0.044
341.3	0.988	0.050	341.1	0.967	0.049	332.8	0.915	0.047

Table 3.18: Solubility of CO_2 in aqueous (0.30 mass fraction MAE) solutions in the temperature range of 303.1 - 323.1 K.

303.15 K			***313.15 K***			***323.15 K***		
CO_2 Partial pressure (kPa)	Loading (α_{CO_2})	x_{CO_2}	CO_2 Partial pressure (kPa)	Loading (α_{CO_2})	x_{CO_2}	CO_2 Partial pressure (kPa)	Loading (α_{CO_2})	x_{CO_2}
0.101	0.282	0.014	0.299	0.367	0.019	0.598	0.292	0.015
3.094	0.592	0.030	30.60	0.703	0.035	8.401	0.568	0.028
46.31	0.789	0.039	122.9	0.834	0.041	68.01	0.731	0.036
119.8	0.897	0.044	236.0	0.931	0.046	145.4	0.817	0.040
238.2	0.995	0.049	374.3	0.993	0.049	237.4	0.887	0.044
378.5	1.072	0.052	510.7	1.029	0.052	378.9	0.959	0.047
510.3	1.120	0.055				508.7	1.018	0.050

α_{CO_2} = loading of CO_2 = moles of CO_2 / moles of MAE.

x_{CO_2} = mole fraction of CO_2 in liquid phase.

3.5.2 (EAE + CO_2 + H_2O) system

The solubility data of CO_2 in aqueous solution of the weight percentages (6, 12, 18, 24 and 30 mass % are presented at (303.1- 323.1K) are presented in Tables (3.19-3.23), where the CO_2 loading has been expressed in terms of (number of moles of CO_2 /number of moles of EAE). Form the tables; it is evident that at a fixed temperature, an increase in total EAE content leads to a decrease in solution CO_2 loading capacity. Those tables also reveal that at a constant EAE concentration and CO_2 partial pressure, an increase in temperature leads to decrease in solution CO_2 loading. Calculated liquid phase mole fraction of CO_2 is also presented in the aforesaid tables. Figure 3.13 compares the CO_2 solubility of aqueous EAE, MAE, AMP and MDEA, and EAE manifests a slightly better CO_2 loading capability than AMP, better than MAE and very better than MDEA. MAE alone; can be considered as marginally better solvent than MDEA towards CO_2 absorption.

This trend of CO_2 solubility certainly owes an explanation. The CO_2 absorption in alkanolamine depends on the carbamate stability/formation. The alkanolamines, which form unstable carbamate or do not form at all; should manifest a stoichiometric CO_2

loading of 1.0. The presence of bulky methyl group at alpha-carbon atom to the donor site (lone pair of electrons on N atom) offers a steric hindrance to the EAE carbamate and possibly categorizes it as moderately sterically hindered amine. AMP-carbamate species suffers steric interaction between the methyl group substituent and the carbon atom of CO_2, as evidenced in the (OH)C-NC(COO^-) angle tightens from 114.53^0 in MEA-carbamate to 111.38^0 in AMP-carbamate, suggesting that the N-atom, together with carbamate functionality, is forced away from one of the methyl groups (P Singh, 2011). Moderate sterically hindered amines are characterized by their high rates and high capacities of CO_2 absorption, making them very suitable for the removal of CO_2 and the bulk, non-selective removal of CO_2 and H_2S. Very often, the CO_2 loading for EAE and AMP reach more than 1.0 under low to moderate CO_2 pressure. A severely sterically hindered amine like MDEA has comparatively lower CO_2 absorption rate and capacity (lower tan EAE and AMP), making it more suitable for the kinetically selective removal of H_2S in the presence of CO_2. MDEA act as a base (as they lack a free proton) and catalyze the hydration of CO_2 to form bicarbonate. The instability of MAE carbamate might not be as pronounced as EAE and AMP carbamate, which supports the reduced CO_2 absorption capacity on the part of MAE.

It is not only the carbamate instability but basicity of the alkanolamines (out of their molecular structure and presence of electron donating and withdrawing groups, intra/inter molecular hydrogen bonding) also plays a major role in the reaction course. MDEA being a tertiary alkanolamine, is less basic than primary and secondary alkanolamines like AMP, MAE and EAE. In MDEA the two ethanol groups present create a strong electron withdrawing effect. In it's protonated form ($MDEAH^+$), there is, however, only one amine proton that these groups can bond with, limiting the stabilizing effect of the hydrogen bonding. The steric hindrance effect cannot improve the basicity for tertiary alkanolamines.

It is possibly a methyl group substitution at the alpha-carbon atom in EAE leads to subtle but significant changes in the electronic environment of the nitrogen atom donor site. At the donor site, the lone electron pair orbital of nitrogen interacts with the Π Me and Π Me* methyl group orbital. These interactions result in a lower charge at the donor site and a higher and more delocalized HOMO (highest occupied molecular orbital) i.e. making it a weaker base. The bond between the nitrogen and the hydrogen atom (N-H) weakens on the substitution of a methyl group at the alpha-carbon atom next to the

nitrogen group (P Singh, 2011). This phenomenon possibly; is much pronounced in AMP because of the presence of two methyl groups at alpha-carbon, hence, reduction of basicity to a further extent. In MAE, the inductive effect of methyl group attached to the donor atom nitrogen increases the electron density of nitrogen lone pair, hence enhanced the basicity in comparison to EAE and AMP. The order of basicity is the following: MAE > EAE > AMP > MDEA. The carbamate instability is likely to follow the order EAE > AM P> MAE > MDEA. A sheer conjecture is that the carbamate stability and basicity of the alkanolamines does not enjoy a linear relationship.

In view of the aforesaid discussions, one can possibly explain the CO_2 absorption pattern; EAE > AMP > MAE > MDEA. NMR studies of the equilibrated liquid phase of those alkanolamines (upon reaction with CO_2) and quantum mechanical ab initio calculations with cautious implementation may establish our presumptions. It might not be inappropriate here to mention the findings of Young et al. (2010), who calculated both nucleophilicities and accessibilities of three alkanolamines MEA, MAE, and AMP to predict their reactivities with CO_2. After DFT geometry-optimization calculations, they obtained different types of nucleophilicities (the global, group, and atomic nucleophilicities of each amine) using MP2 quantum mechanical calculations. Only global nucleophilicity matched an experimental pKa order (MAE > AMP > MEA). However, it failed to predict the slow rate of the sterically hindered AMP and the order of rate constants, MAE > MEA > AMP. They have calculated the accessibilities of amines to CO_2 by monitoring collisions at the reaction centers: N atoms in amines and C in CO_2 through Molecular dynamic simulations. The accessibility results indicate that global nucleophilicity needs quantitative correction for steric effects to predict better reactivities of amines with CO_2. Though, the rate studies are not in the purview of present dissertation, nonetheless the findings of Young et al. cannot be completely disintegrated from the larger context of the present work. Computational chemistry toolbox do not posses any tailor made explanation of all our findings, but it does have certainly when applied with judgment, painstaking detailing of facts and patience.

The appreciable CO_2 loading over low to moderately high range of CO_2 partial pressure seems to be encouraging. In comparison to DEA, both MAE and EAE is having higher loading capacity for CO_2, hence those alkanolamines hopefully can replace the DEA in blends of DEA with MDEA and AMP.

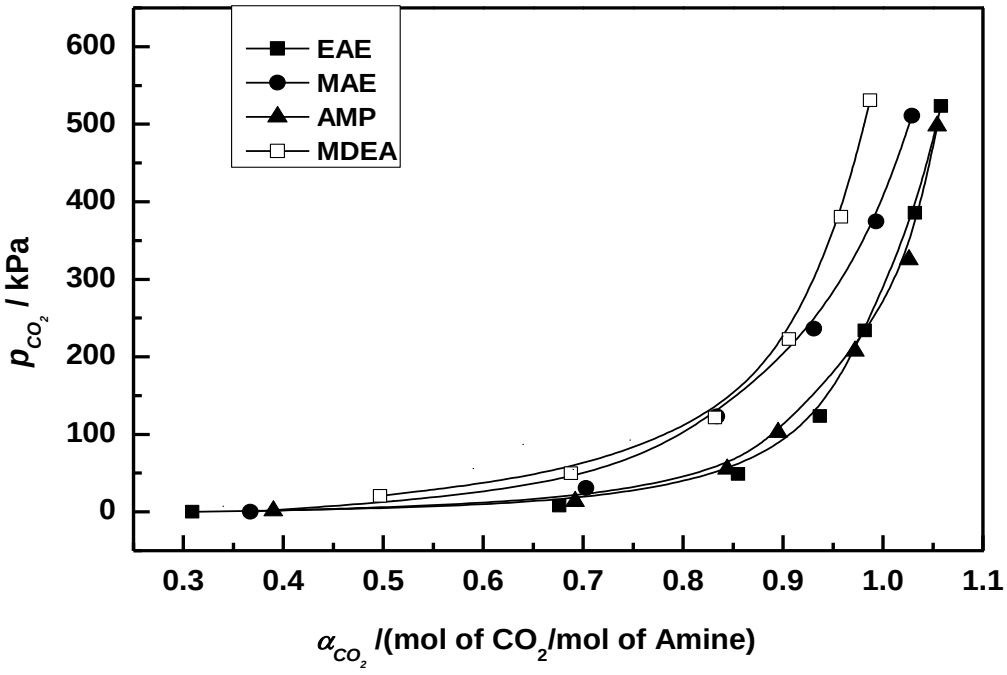

Figure 3.13: Comparison between solubility of CO_2 (1) in aqueous alkanolamine solutions of 0.30 mass fraction at 313.1 K; —, polynomial fit.

Table 3.19: Solubility of CO_2 in aqueous (0.06 mass fraction EAE) solutions in the temperature range of 303.1 – 323.1 K.

303.1 K			***313.1 K***			***323.1 K***		
CO_2 Partial pressure (kPa)	Loading (α_{CO_2})	x_{CO_2}	CO_2 Partial pressure (kPa)	Loading (α_{CO_2})	x_{CO_2}	CO_2 Partial pressure (kPa)	Loading (α_{CO_2})	x_{CO_2}
5.011	0.884	0.011	5.898	0.868	0.011	6.498	0.779	0.001
64.20	1.155	0.015	58.51	1.135	0.014	37.81	0.981	0.012
125.8	1.216	0.015	136.7	1.209	0.015	139.5	1.024	0.013
260.3	1.233	0.016	238.3	1.259	0.016	246.7	1.054	0.013
378.6	1.304	0.016	371.3	1.305	0.016	473.1	1.064	0.014
524.2	1.355	0.017	521.5	1.383	0.017			

Table 3.20: Solubility of CO_2 in aqueous (0.12 mass fraction EAE) solutions in the temperature range of 303.1 – 323.1 K.

303.1 K			***313.1 K***			***323.1 K***		
CO_2 Partial pressure (kPa)	Loading (α_{CO_2})	x_{CO_2}	CO_2 Partial pressure (kPa)	Loading (α_{CO_2})	x_{CO_2}	CO_2 Partial pressure (kPa)	Loading (α_{CO_2})	x_{CO_2}
7.498	0.829	0.022	7.401	0.764	0.020	6.397	0.691	0.018
68.70	1.036	0.027	72.11	0.985	0.026	49.51	0.917	0.024
154.8	1.071	0.028	166.1	1.043	0.027	127.6	0.984	0.026
267.1	1.119	0.029	244.4	1.072	0.028	234.1	1.011	0.027
381.6	1.125	0.030	378.3	1.083	0.029	375.5	1.018	0.027
523.3	1.171	0.031	520.2	1.143	0.030	516.1	1.067	0.028

Table 3.21: Solubility of CO_2 in aqueous (0.18 mass fraction EAE) solutions in the temperature range of 303.1 – 323.1 K.

303.1 K			***313.1 K***			***323.1 K***		
CO_2 Partial pressure (kPa)	Loading (α_{CO_2})	x_{CO_2}	CO_2 Partial pressure (kPa)	Loading (α_{CO_2})	x_{CO_2}	CO_2 Partial pressure (kPa)	Loading (α_{CO_2})	x_{CO_2}
0.701	0.479	0.020	0.803	0.453	0.019	0.802	0.355	0.015
13.41	0.833	0.035	16.51	0.838	0.035	9.491	0.684	0.029
85.78	1.001	0.042	84.49	1.006	0.042	55.42	0.882	0.037
179.7	1.039	0.043	157.6	1.044	0.043	123.9	0.954	0.040
285.8	1.075	0.044	266.1	1.054	0.044	255.8	1.031	0.043
397.7	1.111	0.046	386.5	1.093	0.045	377.6	1.066	0.044
522.6	1.159	0.048	508.3	1.122	0.046	514.7	1.109	0.046

Table 3.22: Solubility of CO_2 in aqueous (0.24 mass fraction EAE) solutions in the temperature range of 303.1 – 323.1 K.

303.1 K			***313.1 K***			***323.1 K***		
CO_2 Partial pressure (kPa)	Loading (α_{CO_2})	x_{CO_2}	CO_2 Partial pressure (kPa)	Loading (α_{CO_2})	x_{CO_2}	CO_2 Partial pressure (kPa)	Loading (α_{CO_2})	x_{CO_2}
0.801	0.501	0.030	0.498	0.374	0.046	1.299	0.296	0.018
31.69	0.868	0.051	11.50	0.708	0.023	8.301	0.588	0.030
100.0	0.965	0.056	62.70	0.875	0.042	46.80	0.769	0.045
207.3	1.006	0.058	125.6	0.923	0.051	118.8	0.847	0.050
387.7	1.045	0.061	237.6	0.980	0.054	237.3	0.899	0.052
526.5	1.079	0.062	404.6	1.006	0.057	370.7	0.954	0.055
			512.5	1.025	0.058	519.4	0.995	0.058

Table 3.23: Solubility of CO_2 in aqueous (0.30 mass fraction EAE) solutions in the temperature range of 303.1 – 323.1 K.

303.1 K			***313.1 K***			***323.1 K***		
CO_2 Partial pressure (kPa)	Loading (α_{CO_2})	x_{CO_2}	CO_2 Partial pressure (kPa)	Loading (α_{CO_2})	x_{CO_2}	CO_2 Partial pressure (kPa)	Loading (α_{CO_2})	x_{CO_2}
0.299	0.331	0.027	0.301	0.309	0.025	0.699	0.339	0.027
4.398	0.661	0.052	8.091	0.676	0.053	8.597	0.616	0.048
44.09	0.877	0.068	49.01	0.855	0.066	45.90	0.782	0.061
131.2	0.962	0.074	123.7	0.937	0.072	122.9	0.880	0.068
242.8	1.000	0.076	234.0	0.982	0.075	246.9	0.953	0.073
390.6	1.029	0.078	385.5	1.032	0.079	367.4	0.989	0.076
525.9	1.050	0.080	523.3	1.058	0.080	501.5	1.009	0.077

α_{CO_2} = loading of CO_2 = moles of CO_2 / moles of EAE

x_{CO_2}= mole fraction of CO_2 in liquid phase.

3.6 DETERMINATION OF DEPROTONATION AND CARBAMATE REVERSION CONSTANTS FOR EAE

The appreciable CO_2 loading in aqueous EAE solutions over low to moderately high range of CO_2 pressure has been the incentive in using the generated VLE data for regressing the deprotonation and carbamate reversion constants for EAE. For this purpose, an approximate thermodynamic model is used.

The Chemical reaction equilibria 3.1- 3.4 and 3.6 are used. From those reactions, the following relations can be written,

$$K_1 = [H^+][OH^-] \tag{3.39}$$

$$K_2 = \frac{[H^+][HCO_3^-]}{[CO_2]} \tag{3.40}$$

$$K_3 = \frac{[H^+][CO_3^{2-}]}{[HCO_3^-]} \tag{3.41}$$

$$K_4 = \frac{[H^+][R\,R'\,R''N]}{[R\,R'\,R''NH^+]} \tag{3.42}$$

$$K_5 = \frac{[HCO_3^-][R\,R'\,R''N]}{[R\,R'\,R''NCOO^-]} \tag{3.43}$$

Eqs. 3.39- 3.43 with the following balance equations are considered in the model building.

Total amine balance:

$$m = [RR'R''N] + [RR'R''NH^+] + [RR'R''NCOO^-] \tag{3.44}$$

Carbon dioxide balance:

$$m\alpha = [CO_2] + [HCO_3^-] + [CO_3^{2-}] + [RR'R''NCOO^-] \tag{3.45}$$

Equation of electroneutrality:

$$[H^+] + [RR'R''NH^+] = [OH^-] + [HCO_3^-] + 2[CO_3^{2-}] + [RR'R''NCOO^-] \tag{3.46}$$

In the low to moderate range of CO_2 pressure, the fugacity of CO_2 is assumed to be its partial pressure and solubility of CO_2 is identical to Henry's constant (H_{CO_2}). The vapour pressure of CO_2 is related to the free acid gas concentration in the liquid through Henry's

law. The vapour-liquid equilibrium of CO_2 over the aqueous alkanolamine solvent, assuming no solvent species in the vapour phase, is given as follows,

$$p_{CO_2} = H_{CO_2}[CO_2] \tag{3.47}$$

In this work, literature values (Li and Shen, 1993) of all equilibrium constants except

$K_4$and K_5 and Henry's constant are used and summarized in Table 3.24. The amine deprotonation constant (K_4) and carbamate reversion constant (K_5) are determined by forcing a fit with the experimental solubility data. Since the chemical reaction equilibria play an important role below 1.0 loading, hence, CO_2 solubility in aqueous EAE below 1.0 are used for regression. All the equilibrium constants considered here are apparent equilibrium constants based on molarity scale ($mol.L^{-1}\ solvent$).

In (CO_2 – EAE - H_2O) system, neutral species; pure alkanolamine (EAE) and H_2O, and ionic species; protonated EAE, HCO_3^- and carbamate ion ($EAECOO^-$) in the equilibrated liquid phase have been considered. The free molecular species CO_2 and the ionic species CO_3^{2-} and H^+ and OH^- in the liquid phase have been neglected on the basis of same reasoning mentioned in section 3.3.2. We can calculate molar concentrations ($mol.L^{-1}$ solvent) of species in liquid phase based on true molecular or ionic species.
The equilibrated liquid phase compositions and CO_2 pressure are as follows:

$$[RR'R''NCOO^-] = \frac{(K_5+m)-[(K_5+m)^2-4m^2\alpha(1-\alpha)]^{\frac{1}{2}}}{2} \tag{3.49}$$

$$[RR'R''N] = m - m\alpha - z \tag{3.49}$$

$$[HCO_3^-] = m\alpha - z \tag{3.50}$$

Where, $z = \frac{(K_5+m)-[(K_5+m)^2-4m^2\alpha(1-\alpha)]^{\frac{1}{2}}}{2}$

$$[CO_2] = \frac{K_4\,K_5\,[RR'R''NH^+]\,[RR'R''NCOO^-]}{K_2\,[RR'R''N]^2} \tag{3.51}$$

$$p_{CO_2} = H_{CO_2}\,\frac{K_4\,K_5}{K_2}\,\frac{m\alpha z}{(m-m\alpha-z)^2} \tag{3.52}$$

The equilibrium constants were determined by optimizing the objective function, which, in general, is the difference between the measured values of equilibrium CO_2

partial pressures and the values calculated from the developed model. However, simple minimization of the sum of differences between measured and calculated values would weigh the high partial pressure data and almost exclusion of the low partial pressure data. Hence, the objective function used in this work is the sum of the individual discrepancy functions:

$$F = \sum\left(p_i^{exp} - p_i^{cal}\right)^2 \tag{3.53}$$

The average absolute percentage deviations between the experimental and model correlated CO_2 pressure was 19 %. Table 3.25 presents the determined equilibrium constants at different temperatures.

Table 3.24: Temperature dependence of the equilibrium constants and Henry's constant (From Literature)

$$K_i/_{(kmol\ m^{-3})} = exp\left(C_1 + {C_2}/_{T} + {C_3}/_{T^2} + {C_4}/_{T^3} + {C_5}/_{T^4}\right) \text{ Where i=1, 2, 3}$$

$$H_{CO_2}/_{(kPa\ (kmol\ m^{-3})^{-1})} = exp\left(C_1 + {C_2}/_{T} + {C_3}/_{T^2} + {C_4}/_{T^3} + {C_5}/_{T^4}\right)$$

Equilibrium constant	C_1	$C_2 \times 10^{-4}$	$C_3 \times 10^{-8}$	$C_4 \times 10^{-11}$	$C_5 \times 10^{-13}$	Ref
K_1	39.5554	-9.879	0.568827	-0.146451	0.136145	[a]
K_2	-241.828	29.8253	-1.48528	0.332647	-0.282393	[a]
K_3	-294.74	36.4385	-1.84157	0.415792	-0.354291	[a]
H_{CO_2}	20.2629	-1.38306	0.06913	-0.015589	0.01200	[a]

[a] **Li and Shen, 1993**

Table 3.25: Derived equilibrium Constants for EAE in the temperature range of 303.1 – 323.1 K.

Equilibrium Constant/Temperature	K_4 / $kmol\ m^{-3}$ ***(Deprotonation)***	K_5 / $kmol\ m^{-3}$ ***(Carbamate Reversion)***
303.1 K	1.51040 e-010	1.1292
313.1 K	1.88981e-010	1.2160
323.1 K	2.93308e-010	1.6288

REFERENCES

Abharchaei, P.R. (**2010**). Kinetic study of carbon dioxide absorption by aqueous solutions of 2(methyl)-aminoethanol in stirred tank reactor 'Experimental and Numerical Study of Absorption Process and Mass Transfer Phenomena'. M.S. Dissertation, Chalmers University of Technology, Göteborg, Sweden.

Austgen, D.M., Rochelle, G.T., Peng, X. and Chen, C.C. (**1989**). Model of vapour liquid equilibria for aqueous acid gas- alkanolamine systems using the Electrolyte - NRTL equation. *Industrial and Engineering Chemistry Research*, 28, 1060 - 1073.

Edwards, T.J., Maurer, G., Newman, J., Prausnitz, J.M. (**1978**). Vapour-liquid equilibria in multicomponent aqueous solutions of volatile electrolytes. *AIChE Journal*, 24, 966-976.

Haji-Sulaiman, M.Z., Aroua, M.K. and Pervez, M.I. (**1996**). Equilibrium concentration profiles of species in CO_2-alkanolamine-water systems. *Gas Separation and Purification,* 10, 13-18.

Kumar, G. and Kundu, M. (**2012**). Vapour-liquid equilibrium of CO_2 in aqueous solutions of N-methyl-2-ethanolamine. *Canadian Journal of Chemical Engineering*, 90, 627-630.

Kumar, G. and Kundu, M. (**2013**). Vapor-Liquid Equilibrium of CO_2 in Aqueous Blends of (N-ethyl-ethanolamine + N-methyl-diethanolamine) and (N-ethyl-ethanolamine + 2-amino-2-methyl-1-propanol). *Journal of Chemical and Engineering Data,* (**Submitted**).

Kumar, G., Mondal, T.K. and Kundu, M. (**2012**). Solubility of CO_2 in aqueous blends of (Diethanolamine + 2-amino-2-methyl-1-propanol) and (Diethanolamine + N-methyldiethanolamine). *Journal of Chemical and Engineering Data,* 57, 670-680.

Kundu, M. (**2004**). Vapour-Liquid Equilibrium of Carbon Dioxide in Aqueous Alkanolamines. Ph. D. Dissertation, IIT Kharagpur, pp. 135.

Lee, J.I., Otto, F.D. and Mather, A.E. (**1974b**). The Solubility of H_2S and CO_2 in aqueous monoethanolamine solutions. *Canadian Journal of Chemical Engineering,* 52, 803-805.

Li, M.H., and Shen, K.P. (**1993**). Calculation of equilibrium solubility of carbon dioxide in aqueous mixtures of monoethanolamine with methyldiethanolamine. *Fluid Phase Equilibria,* 85, 129-140.

Mimura, T., Suda, T., Iwaki, I., Honda, A. and Kumazawa, H. (**1998**). Kinetics of Reaction between Carbon dioxide and Sterically Hindered Amines for Carbon dioxide

Recovery from Power Plant Flue Gases. *Chemical Engineering Communication*, 170, 245-260.

Park, M.K., and Sandall, O.C. (**2001**). Solubility of Carbon dioxide and Nitrous oxide in 50 mass % Methyldiethanolamine. *Journal of Chemical and Engineering Data*, 46, 166-168.

Posey, M.L. (**1996**). Thermodynamic model for acid gas loaded aqueous alkanolamine solutions. Ph.D. Thesis, University of Texas, Austin.

Seo, D.J., Hong, W.H. (**1996**). Solubilities of carbon dioxide in aqueous mixtures of diethanolamine and 2-amino-2-methyl-1-propanol. *Journal of Chemical and Engineering Data*, 41, 258 - 260.

Silkenbäumer, D., Rumpf, B., and Lichtenthaler, R.N. (**1998**). Solubility of carbon dioxide in aqueous solutions of 2-Amino-2-methyl-1-propanol and *N*-methyldiethanolamine and their mixtures in the temperature range from 313 to 353 K and pressure up to 2.7 MPa. *Industrial and Engineering Chemistry Research*, 37, 3133 - 3141.

Young, J.H., Shim, J.G., Kim, J.H., Lee, J.H., Jang, K.R. and Kim, J. (**2010**). Nucleophilicity and accessibility calculations of alkanolamines: Application to carbon dioxide absorption reactions. *Journal of physical Chemistry A*, 114, 12907-12913.

Chapter 4

VAPOUR – LIQUID EQUILIBRIUM OF CO_2 IN AQUEOUS BLENDS OF ALKANOLAMINES

Chapter 4

VAPOUR – LIQUID EQUILIBRIUM OF CO_2 IN AQUEOUS BLENDS OF ALKANOLAMINES

4.1 INTRODUCTION

Removal of carbon dioxide (CO_2) and hydrogen (H_2S) sulfide from natural gas and refinery off gases is a very important industrial operation, which necessitates the application as well as promotion of a new range of alkanolamines including MAE and EAE; the very recent interest. By varying the relative composition of amines in their aqueous blends; hence exploiting individual's merit; an optimum as well as energy efficient absorbent can be designed for a specific application. Specifically the use of sterically hindered amines in the aqueous blends of amines enhances the capacity and rate of absorption of acid gases with good stripping characteristics, reduced co-absorption capacity of hydrocarbons and degradation resistance of the formulated solvent. Because of the need to exploit poorer quality crude and natural gas twined with the enhanced environmental obligations, highly economical and selective acid gas treating processes are of dire need. As a result, there has been a rekindling of interest in new alkanolamine formulations and particularly in aqueous blends of those alkanolamines.

EAE resembling a moderately sterically hindered secondary amine (methyl group attached to the alpha-C atom to the amine nitrogen) is expected to vehicle maximum CO_2 in the lot. One methyl group attached to the donor nitrogen is probably not sufficient for MAE (secondary amine) to induce severe carbamate instability. Both EAE and MAE have

shown better CO_2 loading capability while compared to DEA and MEA (Chapter 3). In view of this, the present chapter emphasizes on reporting CO_2 solubility data in 22 blended aqueous alkanolamine solutions involving MAE + AMP/MDEA and EAE + AMP/MDEA at temperatures (303.1, 313.1 and 323.1) K in an effort to create a maiden database on the proposed blends, the relative amine compositions of the constituent alkanolamines were varied from 0.03 mass fraction to 0.27 mass fraction while keeping the total alkanolamine mass fraction in the blends constant at 0.30 (30 mass %). Whether MAE and EAE could replace DEA in aqueous (DEA+AMP/MDEA) blends was the motivation behind this chapter. The generated data were analyzed in the light of fluid phase equilibria as well as chemistry of aqueous alkanolamine systems. Later in this chapter most suitable blend for CO_2 absorption was identified and generated data on that particular type of blends were correlated with a thermodynamic frame work.

4.2 MATERIALS AND EXPERIMENTATION

N-methyl-diethanolamine (MDEA), *N*-methy-2-ethanolamine (MAE), *N*-ethyl ethanolamine (EAE) and 2-amino-2-methyl-1-propanol (AMP) were supplied by E. Merck, Germany, and had a mole % purity of > 98, > 98, > 97, and > 95 respectively. The process of preparing the solution and experimental procedure is same which already has been stated in ***chapter 3***.

4.3 VLE ON (CO_2 + MAE + AMP/MDEA + H_2O) SYSTEM

This section presents experimental data on CO_2 solubility in aqueous blends of *N*-methyl-2-ethanolamine (MAE) + *N*-methyl-diethanolamine (MDEA) and *N*-methyl-2-ethanolamine (MAE) +2-amino-2-methyl-1-propanol (AMP) at temperatures (303.1, 313.1 and 323.1) K and CO_2pressure in the range of (1 to 550) kPa. Aqueous ternary mixtures of (MAE + MDEA) and (MAE+AMP) with the following compositions(0.03 mass fraction/ 0.399 mol.L^{-1} MAE + 0.27 mass fraction/ 2.266 mol.L^{-1} MDEA), (0.06 mass fraction/ 0.799 mol.L^{-1} MAE + 0.24 mass fraction/ 2.014 mol.L^{-1} MDEA), (0.09 mass fraction/ 1.198 mol.L^{-1} MAE + 0.21 mass fraction/ 1.762 mol.L^{-1} MDEA), (0.12 mass fraction/ 1.598 mol.L^{-1} MAE + 0.18 mass fraction/ 1.511 mol.L^{-1} MDEA), (0.15mass fraction/ 1.997 mol.L^{-1} MAE + 0.15 mass fraction/ 1.259 mol.L^{-1} MDEA), (0.21mass fraction/ 2.796 mol.L^{-1} MAE + 0.09 mass fraction/ 0.755 mol.L^{-1} MDEA) and (0.24 mass fraction/ 3.195 mol.L^{-1} MAE + 0.06 mass fraction/ 0.503 mol.L^{-1} MDEA) and (0.03 mass fraction/

0.399 mol.L^{-1} MAE + 0.27 mass fraction/ 3.029 mol.L^{-1} AMP), (0.06 mass fraction/ 0.799 mol.L^{-1} MAE + 0.24 mass fraction/ 2.692 mol.L^{-1} AMP), (0.09 mass fraction/ 1.198 mol.L^{-1} MAE + 0.21 mass fraction/ 2.356 mol.L^{-1} AMP), (0.12 mass fraction/ 1.598 mol.L^{-1} MAE + 0.18 mass fraction/ 2.019 mol.L^{-1} AMP), (0.15 mass fraction/1.997 mol.L^{-1} MAE + 0.15 mass fraction/ 1.682 mol.L^{-1} AMP), (0.21 mass fraction/ 2.796 mol.L^{-1} MAE + 0.09 mass fraction/ 1.009 mol.L^{-1} AMP) and (0.24 mass fraction/ 3.195 mol.L^{-1} MAE + 0.06 mass fraction/ 0.673 mol.L^{-1} AMP) were considered to identify suitable blends having maximum CO_2 absorption capacity. The suitability of aqueous (MAE + MDEA/AMP) in comparison to aqueous (DEA + MDEA/AMP) blend was explored. The total alkanolamine mass fraction in the blends were held constant at 0.30 (30 mass %).

4.3.1 Results and Discussions

The solubility of CO_2 in (MAE + MDEA + H_2O) system is presented in Table 4.1-4.7. It is evident from the tables, that at a fixed temperature, for an increase in mass fraction of MAE in the alkanolamine blends, there is a decrease in solution CO_2 loading capacity, in general. For any constant relative compositions in (MAE + MDEA + H_2O) blend and CO_2 pressure, there is a decrease in solution CO_2 loading capacity with increasing temperature. Figure 4.1 reveals that above a certain CO_2 pressure (70 kPa), corresponding to a CO_2 loading of 0.73 mol of CO_2 / mol of amine, the CO_2 solubility in an aqueous (0.03 mass fraction MAE + 0. 27 mass fractions MDEA) solution is greater than any (MAE + MDEA) blend containing higher amount of MAE. As reported earlier by Li and Shen, (1993) for (MEA + MDEA) blend; Park *et al*. (2002) for (MEA + AMP) and (DEA + AMP) blends; Li and Chang (1994) for (MEA + AMP) blend; Seo and Hong (1996) for (DEA + AMP) and Kundu and Bandyopadhyay (2006 a, b) for (DEA + AMP) and (DEA + MDEA) blends, a similar cross-over occurs in the solubility curve in the Figure 4.1. This crossover may be primarily due to the fact that MDEA does not form carbamate with CO_2 and the stoichiometric loading of MDEA is 1.0 mole of CO_2 / mole of amine. However, MAE forms a comparatively stable carbamate with CO_2. MAE being a very closely resembling sterically hindered amine, it's stoichiometric CO_2 loading reaches up to 0.7-0.75 instead of 0.5 applicable for primary and secondary alkanolamines. Hence, for an aqueous solution of MAE, it is reasonable to assume that MAE completely gets converted to product at CO_2 loading greater than 0.73-0.75 mole of CO_2 / mole of amine. At low to moderate loadings MAE relinquishes before the tertiary alkanolamine MDEA.

However, as CO_2 loading increases, the un-reacted MAE decreases and results in an increased ratio of MDEA to MAE. Therefore, both MAE and MDEA affect the solubility of CO_2 at moderate to high loadings. If the CO_2 loading is considerably high, the equilibrium is closer to that of MDEA than to that of MAE, and the CO_2/ (MAE + MDEA) equilibrium curve containing higher than 0.03 mass fraction of MAE should cross the CO_2 / (MAE + MDEA) curve containing equal or lesser than 0.03 mass fraction of MAE. The addition of MAE to an aqueous MDEA solution reduces the equilibrium loadings. Moreover with increasing temperature the crossover point shifts towards a higher equilibrium CO_2 pressure. Figures 4.2-4.4 present the comparison between the CO_2 solubility in aqueous blends of (DEA + MDEA + H_2O) and (MAE + MDEA + H_2O) at 303.1, 313.1, and 323.1 K. From the Figures 4.2-4.4, it can be concluded that CO_2 loading capacity of (0.06 mass fraction DEA + 0.24 mass fraction MDEA) solvent is higher than any of the blends of (DEA + MDEA + H_2O) and (MAE + MDEA + H_2O). At temperatures 313.1 K and 323.1 K, (0.12 mass fraction MAE + 0.18 mass fraction MDEA) and (0.15 mass fraction MAE + 0.15 mass fraction MDEA) show better loading capability towards CO_2 than the (0.06 mass fraction DEA + 0.24 mass fraction MDEA) blend until about 0.7 mole of CO_2 / mole of amine. This observation owes an explanation, which is as follows. Being a carbamate active alkanolamine with a faster depletion than MDEA, MAE plays an critical role towards CO_2 absorption until moderate to moderately high loadings. At a stoichiometric loading of about 0.7 and above equilibrium loading will shift towards MDEA contribution. Hence, some specific (MAE + MDEA + H_2O) blends having comparable CO_2 loading capacity as that of (DEA + MDEA + H_2O) solvent possess the potential to replace the latter.

The solubility of CO_2 in (MAE + AMP + H_2O) system is presented in Tables 4.8-4.15. It is evident from the tables, that at a fixed temperature, for an increase in mass fraction of MAE in the alkanolamine blends, there is a decrease in solution CO_2 loading capacity, in general. For any constant relative compositions in (MAE + AMP + H_2O) blend and CO_2 pressure, there is a decrease in solution CO_2 loading capacity with increasing temperature. For (MAE + AMP + H_2O) blends above a certain CO_2 pressure (5 kPa), corresponding to a CO_2 loading of 0.55 mole of CO_2 / mole of amine, the CO_2 solubility in an aqueous (0.015 mass fraction MAE + 0.285 mass fraction AMP) solution

is greater than any (MAE + AMP) blend containing higher amount of MAE as shown in Figure 4.5. This kind of similar crossover was evident in (MAE + MDEA + H_2O) system.

AMP shows a similar behavior to that of MDEA, so far its equilibrium CO_2 loading capacity is concerned. At low to moderate loadings MAE relinquishes before the sterically hindered alkanolamine AMP. As CO_2 loading increases, the unreacted MAE diminishes and results in an increased ratio of AMP to MAE. Therefore, both MAE and AMP affect the solubility of CO_2 at moderate loadings. If the CO_2 loading is moderate to high, the equilibrium is closer to that of AMP than to that of MAE, and the CO_2/ (MAE + AMP) equilibrium curve containing higher than 0.015 mass fraction of MAE should cross the CO_2/ (MAE + AMP) curve containing equal or lesser than 0.015 mass fraction of MAE. The addition of MAE to an aqueous AMP solution reduces the equilibrium loadings.

Figures 4.6-4.8 presents the comparison between CO_2 solubility in aqueous blends of (MAE + AMP) and (DEA + AMP) of relative amine compositions 6/24, 9/21, 12/18 and 15/15 by mass % at 303.1, 313.1, and 323.1 K. CO_2 loading capacity of (0.06 mass fraction DEA + 0.24 mass fraction AMP) solvent seems higher than any of the blends of (DEA + AMP + H_2O) and (MAE + AMP + H_2O). For all the other blends considered, CO_2 loading capacity of aqueous (DEA + AMP) was better than (MAE + AMP) blends at all temperatures.

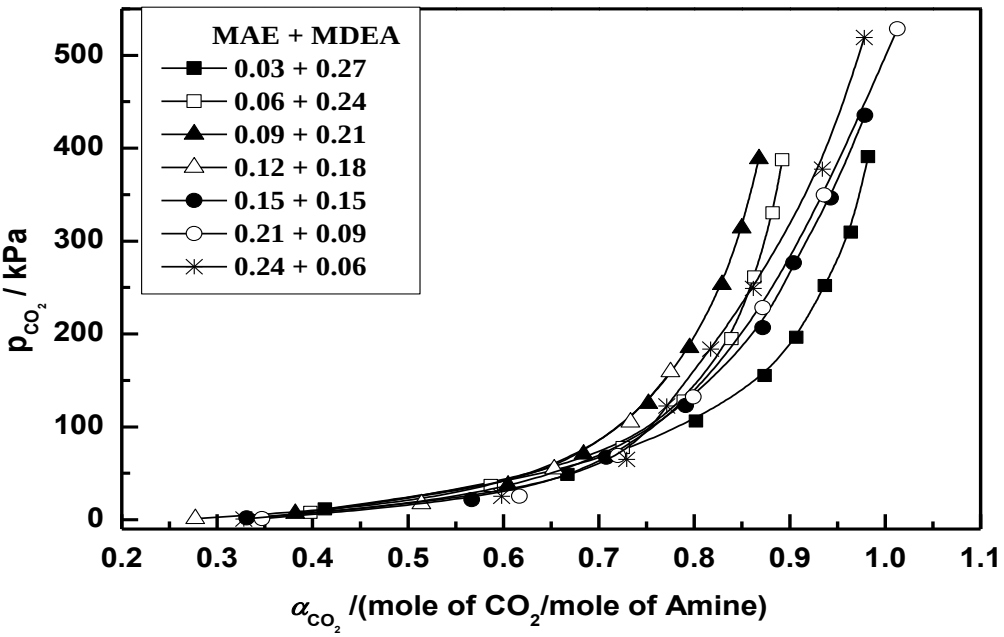

Figure 4.1: Solubility of CO_2 (1) in aqueous alkanolamine solution of different mass fraction of MAE (2) + MDEA (3) at T = 313.1 K; —, polynomial fit.

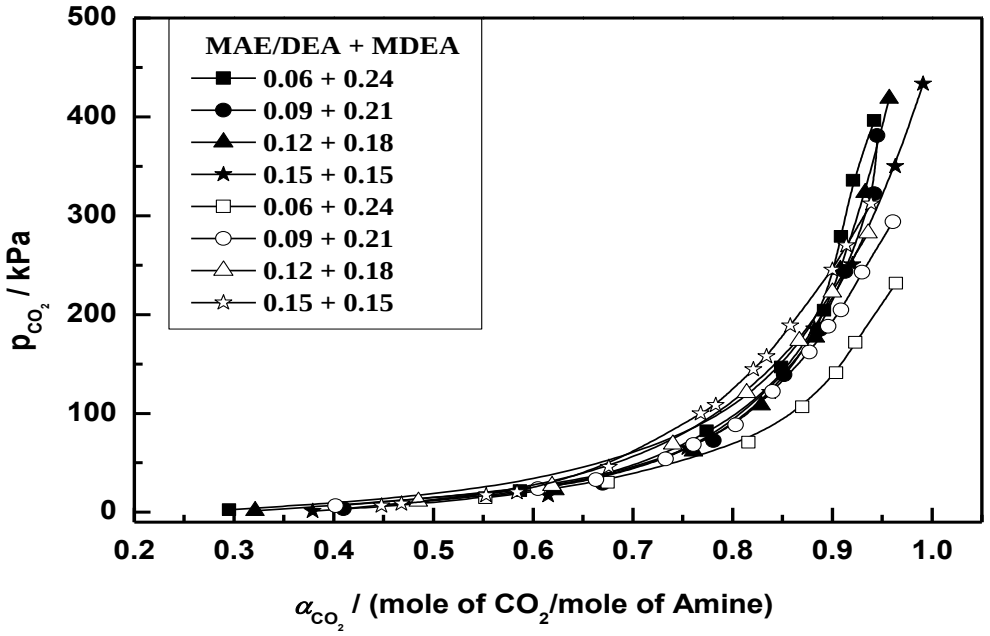

Figure 4.2: Comparison between solubility of CO_2 (1) in aqueous alkanolamine solution of different mass fractions of (solid symbol, MAE (2) + MDEA (3)) and (hollow symbol, DEA (2) + MDEA (3)) at T = 303.1 K; —, polynomial fit.

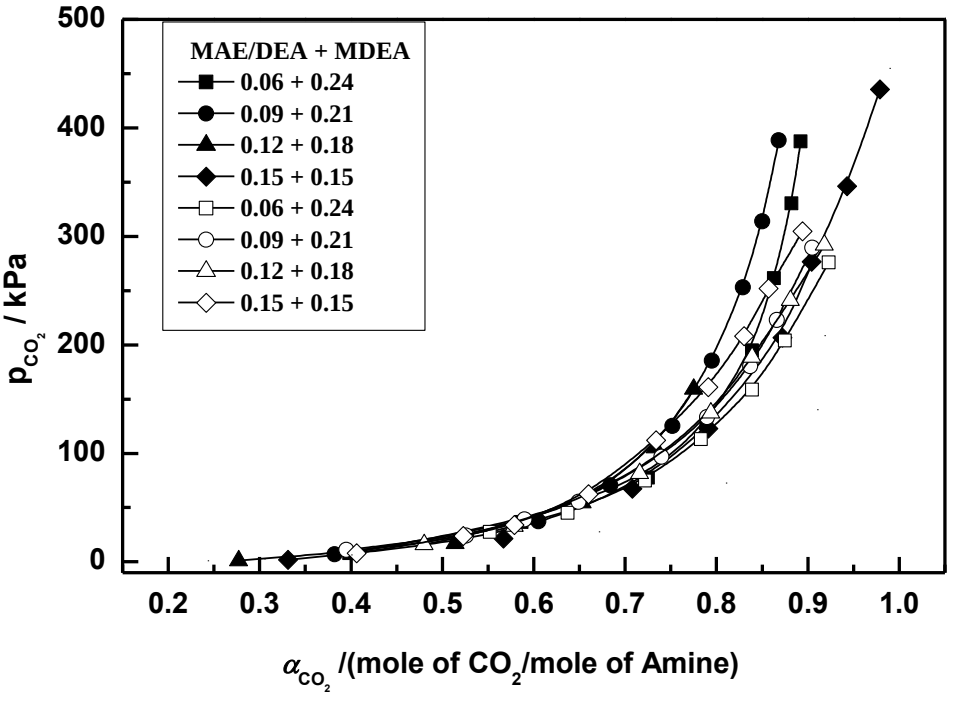

Figure 4.3: Comparison between solubility of CO_2 (1) in aqueous alkanolamine solution of different mass fractions of (solid symbol, MAE (2) + MDEA (3)) and (hollow symbol, DEA (2) + MDEA (3)) at T = 313.1 K; —, polynomial fit.

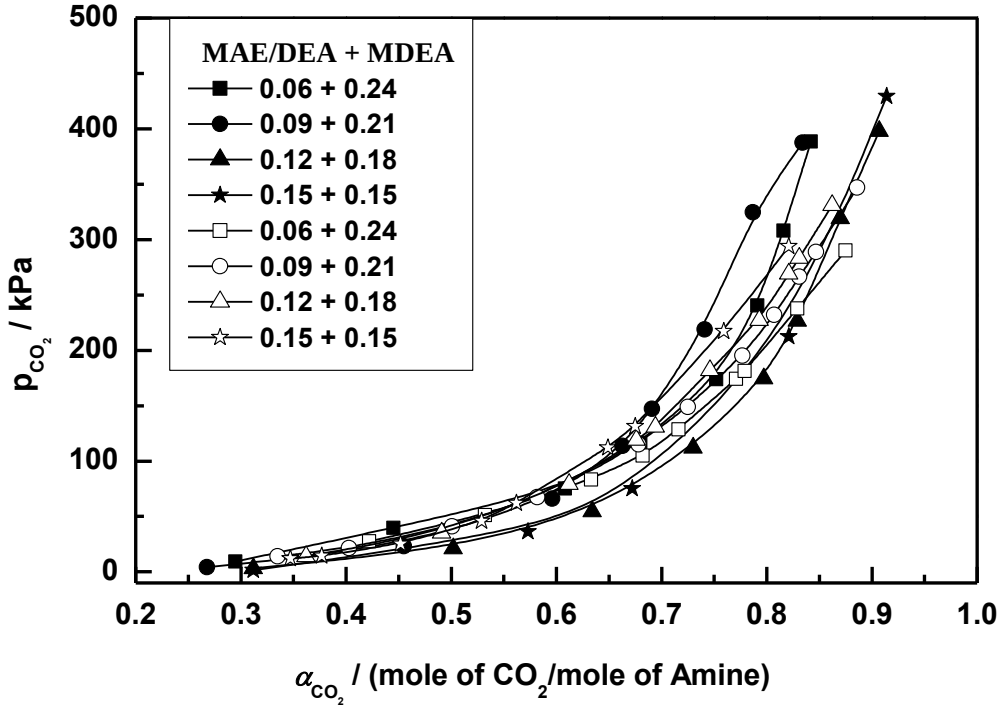

Figure 4.4: Comparison between solubility of CO_2 (1) in aqueous alkanolamine solution of different mass fractions of (solid symbol, MAE (2) + MDEA (3)) and (hollow symbol, DEA (2) + MDEA (3)) at T = 323.1 K; —, polynomial fit.

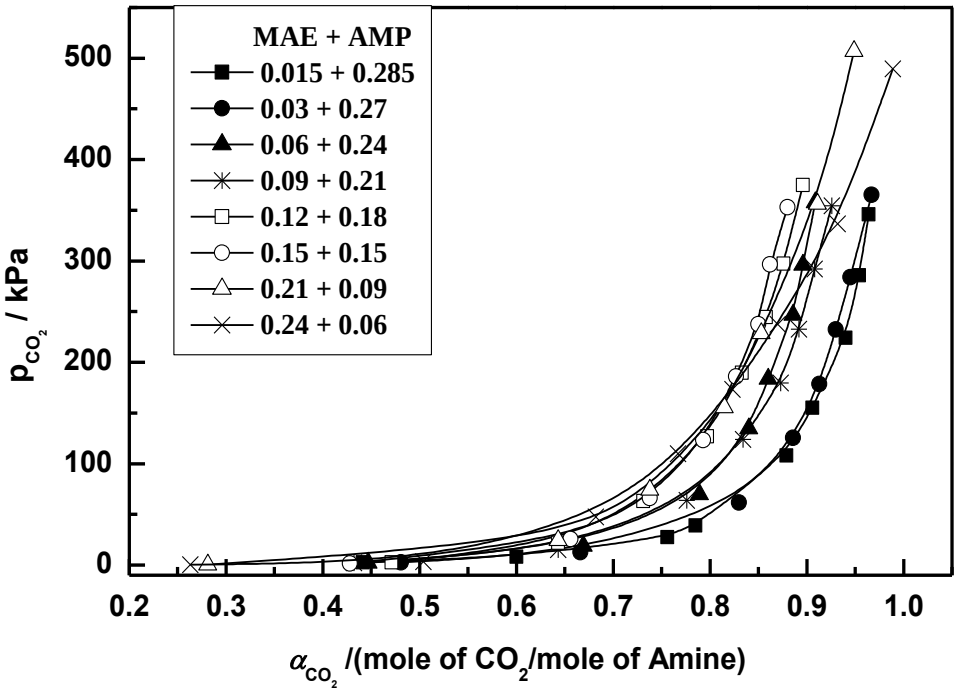

Figure 4.5: Solubility of CO_2 (1) in aqueous alkanolamine solutions of different mass fractions of MAE (2) + AMP (3) at T = 313.1 K; —, polynomial fit.

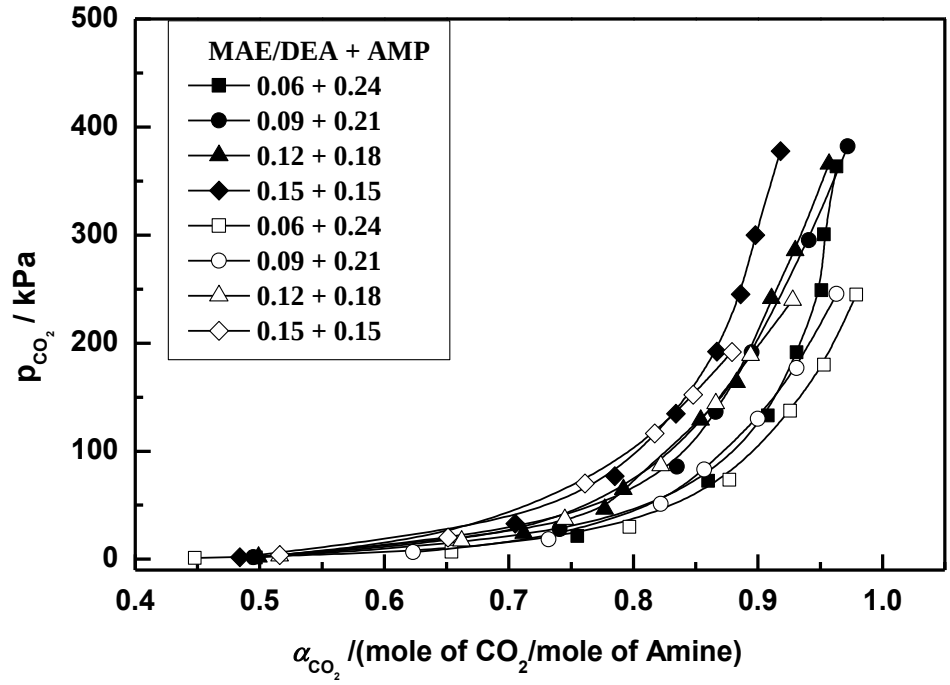

Figure 4.6: Comparison between solubility of CO_2 (1) in aqueous alkanolamine solution of different mass fractions of (solid symbol, MAE (2) + AMP (3)) and (hollow symbol, DEA (2) + AMP (3)) at T = 303.1 K; —, polynomial fit.

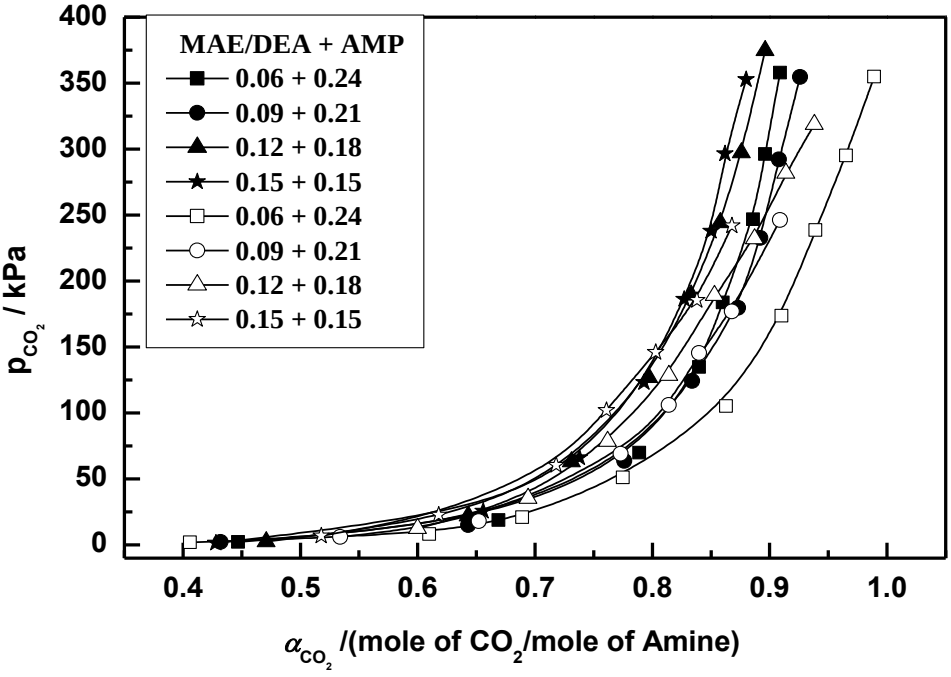

Figure 4.7: Comparison between solubility of CO_2 (1) in aqueous alkanolamine solution of different mass fractions of (solid symbol, MAE (2) + AMP (3)) and (hollow symbol, DEA (2) + AMP (3)) at T = 313.1 K; —, polynomial fit.

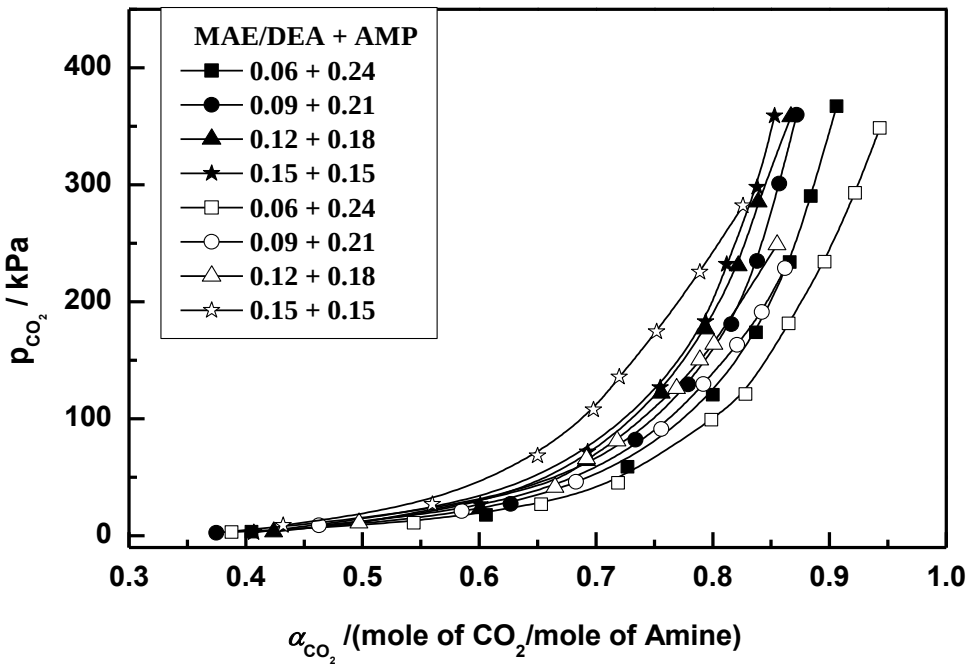

Figure 4.8: Comparison between solubility of CO_2 (1) in aqueous alkanolamine solutions of different mass fractions of (solid symbol, MAE (2) + AMP (3)) and (hollow symbol, DEA (2) + AMP (3)) at T = 323.1 K; —, polynomial fit.

Table 4.1: Solubility of CO_2 in aqueous (0.03 mass fraction MAE + 0.27 mass fraction MDEA) solutions in the temperature range of 303.1 – 323.1 K.

303.1 K			***313.1 K***			***323.1 K***		
CO_2 Partial pressure kPa	Loading (α_{CO_2})	x_{CO_2}	CO_2 Partial pressure kPa	Loading (α_{CO_2})	x_{CO_2}	CO_2 Partial pressure kPa	Loading (α_{CO_2})	x_{CO_2}
6.401	0.452	0.028	11.59	0.413	0.026	12.89	0.314	0.020
43.81	0.751	0.046	48.71	0.667	0.041	49.90	0.532	0.033
118.9	0.875	0.053	106.3	0.802	0.049	107.9	0.695	0.043
187.3	0.914	0.055	155.2	0.874	0.053	155.7	0.751	0.046
262.8	0.951	0.057	196.5	0.907	0.055	207.6	0.788	0.048
317.7	0.970	0.059	252.0	0.937	0.057	275.3	0.825	0.050
363.1	0.992	0.060	309.4	0.964	0.058	335.8	0.847	0.051
			390.7	0.982	0.059	401.5	0.861	0.052

Table 4.2: Solubility of CO_2 in aqueous (0.06 mass fraction MAE + 0.24 mass fraction MDEA) solutions in the temperature range of 303.1 – 323.1 K.

303.1 K			***313.1 K***			***323.1 K***		
CO_2 Partial pressure kPa	Loading (α_{CO_2})	x_{CO_2}	CO_2 Partial pressure kPa	Loading (α_{CO_2})	x_{CO_2}	CO_2 Partial pressure kPa	Loading (α_{CO_2})	x_{CO_2}
2.399	0.295	0.020	7.902	0.398	0.026	9.098	0.295	0.020
21.89	0.587	0.038	36.61	0.587	0.038	39.78	0.445	0.023
82.11	0.774	0.050	77.48	0.725	0.047	75.07	0.608	0.040
146.9	0.849	0.054	127.7	0.789	0.051	116.5	0.680	0.044
204.3	0.892	0.057	194.8	0.839	0.054	173.7	0.752	0.048
278.9	0.909	0.058	261.3	0.863	0.055	240.6	0.791	0.051
335.9	0.921	0.059	330.4	0.882	0.056	308.2	0.816	0.052
396.4	0.942	0.060	387.4	0.892	0.057	388.6	0.842	0.054

Table 4.3: Solubility of CO_2 in aqueous (0.09 mass fraction MAE + 0.21 mass fraction MDEA) solutions in the temperature range of 303.1 – 323.1 K.

303.1 K			***313.1 K***			***323.1 K***		
CO_2 Partial pressure kPa	Loading (α_{CO_2})	x_{CO_2}	CO_2 Partial pressure kPa	Loading (α_{CO_2})	x_{CO_2}	CO_2 Partial pressure kPa	Loading (α_{CO_2})	x_{CO_2}
3.602	0.410	0.028	6.811	0.382	0.027	4.110	0.268	0.019
29.22	0.670	0.046	37.20	0.605	0.041	23.03	0.455	0.031
72.28	0.781	0.053	70.58	0.684	0.047	66.19	0.596	0.041
138.9	0.852	0.057	125.2	0.752	0.051	113.8	0.663	0.045
185.1	0.888	0.060	185.2	0.795	0.054	147.1	0.691	0.047
243.6	0.913	0.061	253.1	0.829	0.056	218.7	0.741	0.050
322.3	0.942	0.063	313.9	0.850	0.057	324.5	0.787	0.053
380.9	0.945	0.063	388.4	0.868	0.058	387.5	0.834	0.056

Table 4.4: Solubility of CO_2 in aqueous (0.12 mass fraction MAE + 0.18 mass fraction MDEA) solutions in the temperature range of 303.1 – 323.1 K.

303.1 K			***313.1 K***			***323.1 K***		
CO_2 Partial pressure kPa	Loading (α_{CO_2})	x_{CO_2}	CO_2 Partial pressure kPa	Loading (α_{CO_2})	x_{CO_2}	CO_2 Partial pressure kPa	Loading (α_{CO_2})	x_{CO_2}
1.413	0.321	0.023	1.198	0.277	0.020	3.098	0.312	0.023
22.41	0.622	0.045	17.03	0.514	0.037	21.02	0.502	0.036
61.68	0.761	0.054	54.52	0.653	0.047	54.51	0.634	0.045
108.4	0.829	0.058	105.2	0.733	0.052	112.0	0.730	0.052
176.8	0.883	0.062	159.4	0.775	0.055	174.7	0.797	0.056
245.4	0.908	0.064				226.5	0.829	0.058
323.4	0.933	0.065				319.2	0.870	0.061
418.5	0.957	0.067				398.0	0.907	0.064

Table 4.5: Solubility of CO_2 in aqueous (0.15 mass fraction MAE + 0.15 mass fraction MDEA) solutions in the temperature range of 303.1 – 323.1 K.

303.1 K			***313.1 K***			***323.1 K***		
CO_2 Partial pressure kPa	Loading (α_{CO_2})	x_{CO_2}	CO_2 Partial pressure kPa	Loading (α_{CO_2})	x_{CO_2}	CO_2 Partial pressure kPa	Loading (α_{CO_2})	x_{CO_2}
1.004	0.379	0.029	1.701	0.331	0.034	1.614	0.312	0.024
17.02	0.615	0.046	21.58	0.567	0.043	36.27	0.573	0.043
64.89	0.755	0.056	67.33	0.708	0.053	75.22	0.672	0.050
121.5	0.838	0.062	122.8	0.791	0.059	212.3	0.821	0.066
185.6	0.882	0.065	206.7	0.872	0.064	429.5	0.914	0.067
250.7	0.920	0.067	276.6	0.904	0.067			
349.8	0.963	0.070	346.3	0.943	0.069			
433.5	0.991	0.072	435.4	0.979	0.072			

Table 4.6: Solubility of CO_2 in aqueous (0.21 mass fraction MAE + 0.09 mass fraction MDEA) solutions in the temperature range of 303.1 – 323.1 K.

303.1 K			***313.1 K***			***323.1 K***		
CO_2 Partial pressure kPa	Loading (α_{CO_2})	x_{CO_2}	CO_2 Partial pressure kPa	Loading (α_{CO_2})	x_{CO_2}	CO_2 Partial pressure kPa	Loading (α_{CO_2})	x_{CO_2}
0.503	0.391	0.032	1.002	0.347	0.029	0.902	0.310	0.026
22.12	0.681	0.055	25.18	0.617	0.050	21.81	0.542	0.044
64.48	0.803	0.064	69.03	0.720	0.058	66.30	0.659	0.054
133.6	0.899	0.072	132.2	0.799	0.064	129.7	0.740	0.060
213.4	0.956	0.076	228.1	0.872	0.070	218.5	0.795	0.064
317.4	1.026	0.081	349.5	0.936	0.074	326.5	0.855	0.068
542.9	1.101	0.086	528.4	1.013	0.080	428.0	0.898	0.072
						545.6	0.943	0.075

Table 4.7: Solubility of CO_2 in aqueous (0.24 mass fraction MAE + 0.06 mass fraction MDEA) solutions in the temperature range of 303.1 – 323.1 K.

303.1 K			***313.1 K***			***323.1 K***		
CO_2 Partial pressure kPa	Loading (α_{CO_2})	x_{CO_2}	CO_2 Partial pressure kPa	Loading (α_{CO_2})	x_{CO_2}	CO_2 Partial pressure kPa	Loading (α_{CO_2})	x_{CO_2}
2.003	0.474	0.041	0.601	0.328	0.028	0.891	0.323	0.028
20.08	0.635	0.054	25.23	0.598	0.051	17.93	0.539	0.046
72.89	0.754	0.063	64.78	0.729	0.061	60.78	0.650	0.055
146.9	0.834	0.069	122.3	0.771	0.065	120.3	0.734	0.062
230.2	0.881	0.073	183.9	0.817	0.068	188.1	0.797	0.067
352.2	0.951	0.078	249.2	0.862	0.072	217.3	0.805	0.068
528.3	0.991	0.081	377.3	0.934	0.077	328.2	0.871	0.072
			519.3	0.978	0.081	516.8	0.950	0.078

Table 4.8: Solubility of CO_2 in aqueous (0.015 mass fraction MAE + 0.285 mass fraction AMP) solutions in the temperature range of 303.1 – 323.1 K.

303.1 K			***313.1 K***			***323.1 K***		
CO_2 Partial pressure kPa	Loading (α_{CO_2})	x_{CO_2}	CO_2 Partial pressure kPa	Loading (α_{CO_2})	x_{CO_2}	CO_2 Partial pressure kPa	Loading (α_{CO_2})	x_{CO_2}
2.011	0.545	0.044	2.578	0.441	0.036	4.896	0.432	0.035
9.805	0.710	0.057	8.112	0.600	0.048	12.68	0.571	0.046
47.02	0.859	0.068	27.51	0.756	0.060	48.02	0.741	0.059
108.0	0.920	0.073	39.08	0.785	0.063	120.9	0.832	0.066
161.4	0.948	0.075	107.9	0.879	0.070	174.7	0.863	0.068
208.8	0.959	0.075	155.2	0.906	0.072	223.2	0.889	0.070
273.4	0.973	0.076	224.0	0.940	0.074	276.6	0.905	0.071
367.8	0.990	0.078	285.6	0.954	0.075	359.2	0.928	0.073
			345.8	0.964	0.076			

Table 4.9: Solubility of CO_2 in aqueous (0.03 mass fraction MAE + 0.27 mass fraction AMP) solutions in the temperature range of 303.1 – 323.1 K.

303.1 K			***313.1 K***			***323.1 K***		
CO_2 Partial pressure kPa	Loading (α_{CO_2})	x_{CO_2}	CO_2 Partial pressure kPa	Loading (α_{CO_2})	x_{CO_2}	CO_2 Partial pressure kPa	Loading (α_{CO_2})	x_{CO_2}
1.901	0.518	0.042	2.702	0.481	0.040	3.897	0.398	0.033
15.03	0.743	0.060	12.51	0.666	0.054	13.70	0.577	0.047
66.91	0.868	0.069	61.59	0.830	0.066	45.47	0.723	0.058
125.5	0.930	0.074	125.3	0.886	0.071	108.1	0.815	0.065
185.5	0.963	0.076	178.5	0.913	0.073	176.9	0.842	0.067
250.8	0.982	0.078	232.3	0.930	0.074	233.7	0.875	0.070
301.4	1.009	0.079	284.1	0.945	0.075	290.6	0.899	0.071
359.6	1.021	0.080	365.1	0.967	0.077	353.3	0.915	0.073

Table 4.10: Solubility of CO_2 in aqueous (0.06 mass fraction MAE + 0.24 mass fraction AMP) solutions in the temperature range of 303.1 – 323.1 K.

303.1 K			***313.1 K***			***323.1 K***		
CO_2 Partial pressure kPa	Loading (α_{CO_2})	x_{CO_2}	CO_2 Partial pressure kPa	Loading (α_{CO_2})	x_{CO_2}	CO_2 Partial pressure kPa	Loading (α_{CO_2})	x_{CO_2}
1.487	0.497	0.041	2.098	0.447	0.037	3.501	0.405	0.034
21.32	0.755	0.062	18.78	0.669	0.055	17.78	0.606	0.050
72.29	0.860	0.070	69.91	0.789	0.064	58.81	0.727	0.059
132.9	0.908	0.073	134.7	0.840	0.068	120.4	0.800	0.065
191.6	0.931	0.075	183.7	0.860	0.070	173.9	0.837	0.068
248.9	0.951	0.076	246.7	0.886	0.071	233.8	0.866	0.070
300.5	0.953	0.077	296.1	0.896	0.072	290.4	0.884	0.071
363.6	0.963	0.077	357.8	0.909	0.073	367.0	0.906	0.073

Table 4.11: Solubility of CO_2 in aqueous (0.09 mass fraction MAE + 0.21 mass fraction AMP) solutions in the temperature range of 303.1 – 323.1 K.

303.1 K			***313.1 K***			***323.1 K***		
CO_2 Partial pressure kPa	Loading (α_{CO_2})	x_{CO_2}	CO_2 Partial pressure kPa	Loading (α_{CO_2})	x_{CO_2}	CO_2 Partial pressure kPa	Loading (α_{CO_2})	x_{CO_2}
1.701	0.495	0.042	2.001	0.432	0.037	2.601	0.375	0.032
27.89	0.741	0.061	15.11	0.643	0.054	27.11	0.627	0.052
85.54	0.835	0.069	63.67	0.776	0.064	82.10	0.734	0.061
136.4	0.866	0.071	124.1	0.834	0.068	129.4	0.779	0.064
191.4	0.895	0.073	179.6	0.873	0.072	180.8	0.816	0.067
295.3	0.941	0.077	232.7	0.892	0.073	234.7	0.838	0.069
382.1	0.972	0.079	292.2	0.908	0.074	301.0	0.857	0.070
			354.6	0.926	0.076	359.9	0.872	0.071

Table 4.12: Solubility of CO_2 in aqueous (0.12 mass fraction MAE + 0.18 mass fraction AMP) solutions in the temperature range of 303.1 – 323.1 K.

303.1 K			***313.1 K***			***323.1 K***		
CO_2 Partial pressure kPa	Loading (α_{CO_2})	x_{CO_2}	CO_2 Partial pressure kPa	Loading (α_{CO_2})	x_{CO_2}	CO_2 Partial pressure kPa	Loading (α_{CO_2})	x_{CO_2}
2.001	0.499	0.043	2.597	0.471	0.040	3.489	0.424	0.037
24.12	0.712	0.060	22.01	0.643	0.054	23.32	0.601	0.051
46.58	0.77	0.065	63.22	0.731	0.061	64.40	0.692	0.058
129.0	0.854	0.071	189.5	0.833	0.069	176.8	0.794	0.066
163.7	0.883	0.073	244.4	0.858	0.071	230.7	0.822	0.068
241.6	0.911	0.075	297.2	0.876	0.073	285.3	0.839	0.070
285.7	0.930	0.077	374.7	0.896	0.074	358.2	0.867	0.072
365.7	0.957	0.079						

Table 4.13: Solubility of CO_2 in aqueous (0.15 mass fraction MAE + 0.15 mass fraction AMP) solutions in the temperature range of 303.1 – 323.1 K.

303.1 K			***313.1 K***			***323.1 K***		
CO_2 Partial pressure kPa	Loading (α_{CO_2})	x_{CO_2}	CO_2 Partial pressure kPa	Loading (α_{CO_2})	x_{CO_2}	CO_2 Partial pressure kPa	Loading (α_{CO_2})	x_{CO_2}
1.701	0.484	0.042	1.397	0.428	0.037	2.685	0.407	0.036
32.82	0.705	0.060	25.61	0.656	0.056	26.62	0.601	0.052
77.01	0.785	0.066	66.21	0.738	0.063	71.81	0.693	0.059
134.5	0.834	0.070	123.2	0.793	0.067	126.7	0.755	0.064
192.1	0.867	0.073	186.1	0.827	0.070	183.0	0.794	0.067
245.1	0.886	0.074	237.7	0.850	0.071	232.0	0.812	0.069
300.0	0.898	0.075	296.5	0.862	0.072	297.8	0.838	0.071
377.6	0.918	0.077	352.8	0.880	0.074	358.8	0.853	0.072

Table 4.14: Solubility of CO_2 in aqueous (0.21 mass fraction MAE + 0.09 mass fraction AMP) solutions in the temperature range of 303.1 – 323.1 K.

303.1 K			***313.1 K***			***323.1 K***		
CO_2 Partial pressure kPa	Loading (α_{CO_2})	x_{CO_2}	CO_2 Partial pressure kPa	Loading (α_{CO_2})	x_{CO_2}	CO_2 Partial pressure kPa	Loading (α_{CO_2})	x_{CO_2}
0.511	0.333	0.030	0.489	0.281	0.026	1.001	0.289	0.026
6.402	0.620	0.055	24.50	0.643	0.057	17.01	0.575	0.051
56.41	0.793	0.069	74.31	0.738	0.064	86.21	0.685	0.060
93.89	0.855	0.074	155.6	0.815	0.071	134.6	0.776	0.067
143.1	0.899	0.077	228.5	0.853	0.074	188.9	0.807	0.070
265.4	0.967	0.083	356.1	0.911	0.078	269.6	0.864	0.075
504.7	1.046	0.089	507.1	0.949	0.081	397.3	0.923	0.079
						515.8	0.945	0.081

Table 4.15: Solubility of CO_2 in aqueous (0.24 mass fraction MAE + 0.06 mass fraction AMP) solutions in the temperature range of 303.1 – 323.1 K.

303.1 K			***313.1 K***			***323.1 K***		
CO_2 Partial pressure kPa	Loading (α_{CO_2})	x_{CO_2}	CO_2 Partial pressure kPa	Loading (α_{CO_2})	x_{CO_2}	CO_2 Partial pressure kPa	Loading (α_{CO_2})	x_{CO_2}
0.301	0.274	0.025	0.301	0.263	0.024	0.901	0.208	0.019
3.312	0.552	0.049	3.511	0.504	0.045	2.312	0.414	0.038
44.30	0.735	0.065	47.70	0.682	0.060	34.01	0.620	0.055
98.31	0.813	0.071	109.8	0.767	0.067	86.09	0.694	0.061
165.8	0.872	0.076	173.3	0.823	0.072	147.2	0.752	0.066
301.4	0.955	0.083	237.6	0.870	0.076	215.9	0.786	0.069
			336.7	0.932	0.081	327.6	0.837	0.073
			489.6	0.989	0.085	491.3	0.917	0.080

α_{CO_2} = loading of CO_2 = moles of CO_2 / moles of amine blend.

4.4 VLE ON (CO_2 + EAE + AMP/MDEA + H_2O) SYSTEM

This section presents experimental vapor-liquid equilibrium data of CO_2 over aqueous blends of *N*-ethyl-ethanolamine (EAE) + *N*-methyl-diethanolamine (MDEA) and *N*-ethyl-ethanolamine (EAE) + 2-amino-2-methyl-1-propanol (AMP) at temperatures (303.1, 313.1 and 323.1) K and CO_2 pressure varying from 0.3 to 550 kPa. Different concentrations of (EAE + MDEA) blends, namely 0.06/0.24, 0.12/0.18, 0.18/0.12, 0.24/0.06 mass fractions (mole fraction ratio = 0.0163/0.0487, 0.0328/0.0368, 0.0494/0.0246, 0.0666/0.0125, respectively) were used to determine the vapor-liquid equilibrium of carbon dioxide. Blends of (EAE + AMP) were also studied (mass fraction ratio of 0.06/0.24, 0.12/0.18, 0.15/0.15, 0.24/0.06 or mole fraction ratio = 0.0168/0.0672, 0.0336/0.0504, 0.0420/0.0420, 0.0672/0.0168, respectively) to find out one appropriate composition having maximum CO_2 absorption capability. The aptness of aqueous (EAE + MDEA/AMP) blends with respect to their CO_2 absorption capability in contrast to aqueous (DEA + MDEA/AMP) and (MAE + MDEA/AMP) are also reported.

4.4.1 Results and Discussion

Equilibrium solubility of CO_2 in (EAE + MDEA + H_2O) system is presented in Tables 4.16-4.19. It has been found that for any specific blend of (EAE + MDEA + H_2O) and total pressure of CO_2, equilibrium solubility of carbon dioxide declines as the temperature rises.

CO_2 solubility in aqueous (EAE + MDEA) blends of varying relative amine compositions and total amine mass fraction of 0.30 are shown in Figures 4.9 - 4.11. The very figures reveal that the specific blend having mass fractions ratio of (0.12/0.18) or mole fraction ratio of (0.0328/0.0368) possess the highest CO_2 loading capacity at all the three temperatures studied. It is also evident that the blend having the mass fraction ratio of (0.06 / 0.24 or mole fraction ratio = 0.0163/0.0487) is having the least capacity among various blends. This is even lesser than 0.3 mass fraction aqueous EAE below a loading of 0.85-0.95 depending on the temperature studied. EAE as a secondary hindered alkanolamine pushes the stoichiometric loading of CO_2 in alkanolamine to an extent of 0.9 and until that point; blends having higher EAE shows better capacity, which is prevalent in all the Figures 4.9-4.11. After approximately a loading of 0.85-0.95 (depending on the temperatures) the blends which posses' higher amounts of MDEA that take the lead irrespective of the temperature, hence, a crossover occurs in the solubility curve. After

EAE is diminished at a faster rate than the tertiary alkanolamine component of the blend (MDEA), solution loading with respect to CO_2 is exclusively borne by MDEA present in the solution. From the Figures 4.9-4.11, it is well explicable that EAE enhances the CO_2 loading capacity of MDEA solutions when it is present in equal amounts to that of MDEA in the blend (As in the case of EAE/MDEA blend having mass fraction ratio of 0.12/0.18, where moles of EAE and MDEA present are 0.034 and 0.037, respectively out of 25 mL solution).

The VLE data of CO_2 in (EAE + AMP + H_2O) ternary system is reported in Tables 4.20-4.23. It has been found that for any specific blend of (EAE + AMP + H_2O) and total pressure of CO_2, equilibrium solubility of carbon dioxide declines as the temperature rises.

CO_2 solubility in aqueous (EAE + AMP) blends are shown in Figures 4.12-4.14 by varying relative amine compositions and keeping total amine mass fraction fixed at 0.30. The very figures reveal that EAE/AMP blend having mass fraction ratio of 0.12/0.18 is the most effective one towards CO_2 loading at all the three temperatures studied. Figures 4.12 - 4.14 unequivocally advocate that aqueous EAE by (0.0839 mole fraction (out of 25 mL solution) or 0.3 mass fraction) and EAE/AMP blend having mass fraction ratio of (0.24/0.06) are lesser effective than other EAE + AMP blends and marginally equals to AMP solution of 0.0972 mole fraction (out of 25 mL solution) or (0.3 mass fraction) so far their CO_2 absorption is concerned. CO_2 loading capacity among various EAE + AMP blend are having very narrow distinction since one of them is secondary and another is primary hindered alkanolamine unlike that of EAE + MDEA blend.

Figure 4.15 compares the CO_2 absorption capability of same mass fractions (0.06/0.24) of different blends namely, (0.0163 mole fraction of EAE + 0.0487 mole fraction of MDEA), (0.0192 mole fraction of MAE + 0.0484 mole fraction of MDEA), and (0.0136 mole fraction of DEA + 0.0481 mole fraction of MDEA) at 313.1 K. EAE + MDEA blend proved to be the best among all. DEA + MDEA blend is marginally better than MAE + MDEA blend towards CO_2 absorption. All the alkanolamine mole fractions are calculated on the basis of 25 mL solution.

Figure 4.16 compares the CO_2 absorption capability of same mass fractions (0.06/0.24) of different blends namely, (0.0168 mole fraction of EAE + 0.0672 mole fraction of AMP), (0.0194 mole fraction of MAE + 0.0776 mole fraction of AMP), and (0.0138 mole fraction of DEA + 0.0771 mole fraction of AMP) at 313.1 K. EAE + AMP

blend proved to be the best among all. DEA + AMP blend is more effective than MAE + AMP blend towards CO_2 absorption.

Blends like (0.03 mass fraction MAE + 0.27 mass fraction MDEA), (0.12 mass fraction MAE + 0.18 mass fraction MDEA) and (0.15 mass fraction MAE + 0.15 mass fraction MDEA) seemed to have comparable CO_2 loading capability as that of (DEA+MDEA) blends. Apart from (0.06 mass fraction DEA + 0.24 mass fraction AMP) solvent all other (DEA+AMP) blends have comparable CO_2 loading capacity to their respective (MAE +AMP) counterparts.

This chapter revealed that both for EAE + MDEA and EAE + AMP blends, presence of equal moles of corresponding alkanolamines make the blend most suitable towards CO_2 absorption. CO_2 solubility in (EAE/MAE/DEA + MDEA/AMP) solutions was compared at 313.1 K. (EAE + MDEA/AMP) blends proved to be most suitable solution in this regard. (DEA + MDEA/AMP) and (MAE + MDEA/AMP) solutions are hardly distinguishable of their CO_2 loading capability.

Kinetic studies, anti-corrosion properties, hydrocarbon solubility, VLE in the regeneration section, and dilapidation resistance etc. are the various characteristics need attention and evaluation to have a final affirmation in favor of (MAE + MDEA) / (MAE + AMP) / (EAE + MDEA) / (EAE + AMP) blends as potential solvents for CO_2 capture.

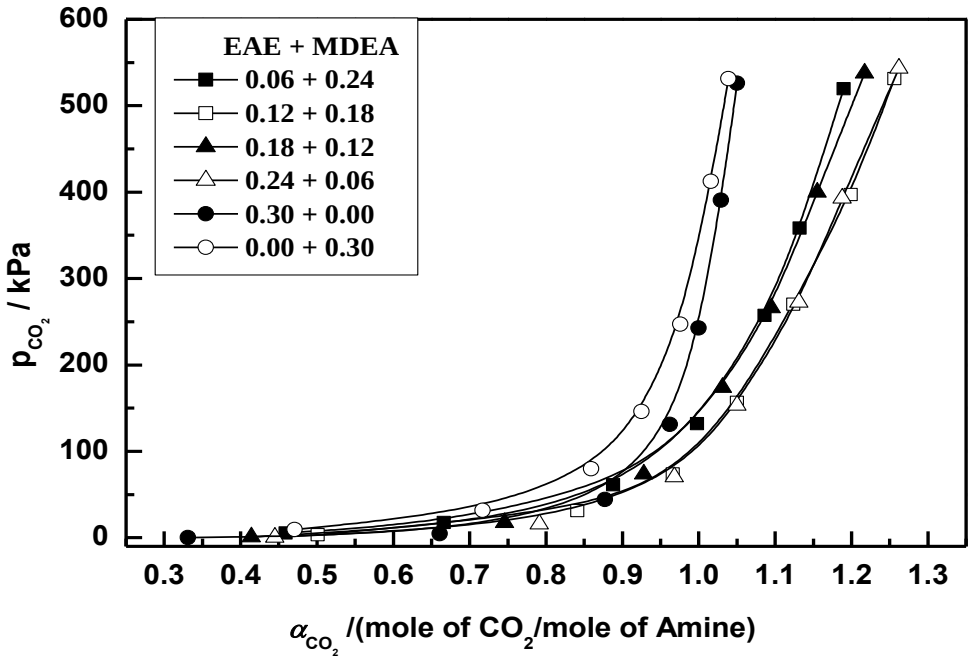

Figure 4.9: Solubility of CO_2 (1) in aqueous alkanolamine solutions of different mass fractions of EAE (2) + MDEA (3) at T = 303.1 K; —, polynomial fit.

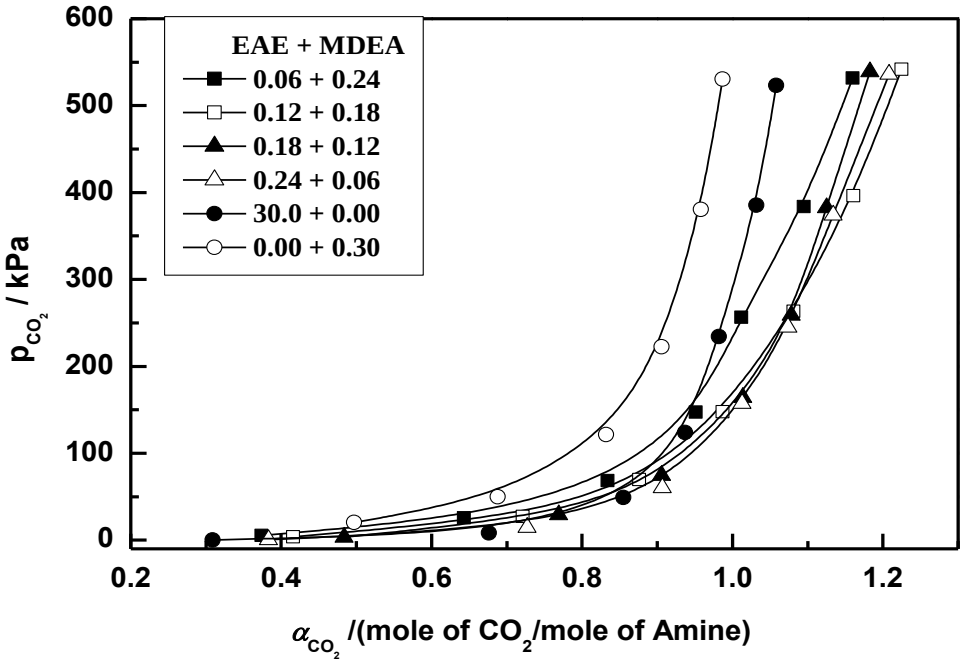

Figure 4.10: Solubility of CO_2 (1) in aqueous alkanolamine solutions of different mass fractions of EAE (2) + MDEA (3) at T = 313.1 K; —, polynomial fit.

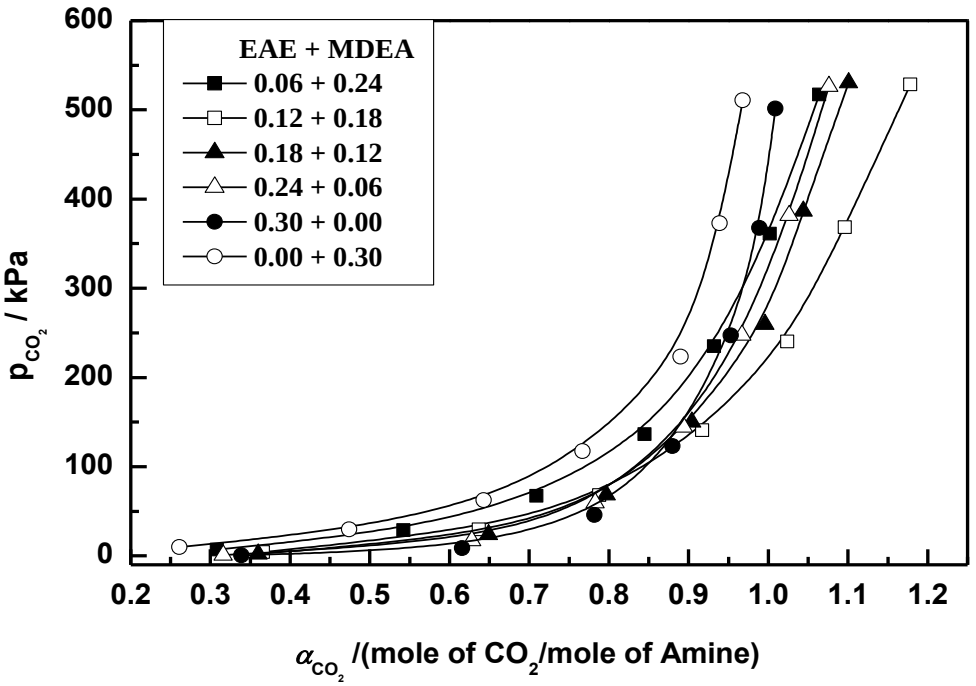

Figure 4.11: Solubility of CO_2 (1) in aqueous alkanolamine solutions of different mass fractions of EAE (2) + MDEA (3) at T = 323.1 K; —, polynomial fit.

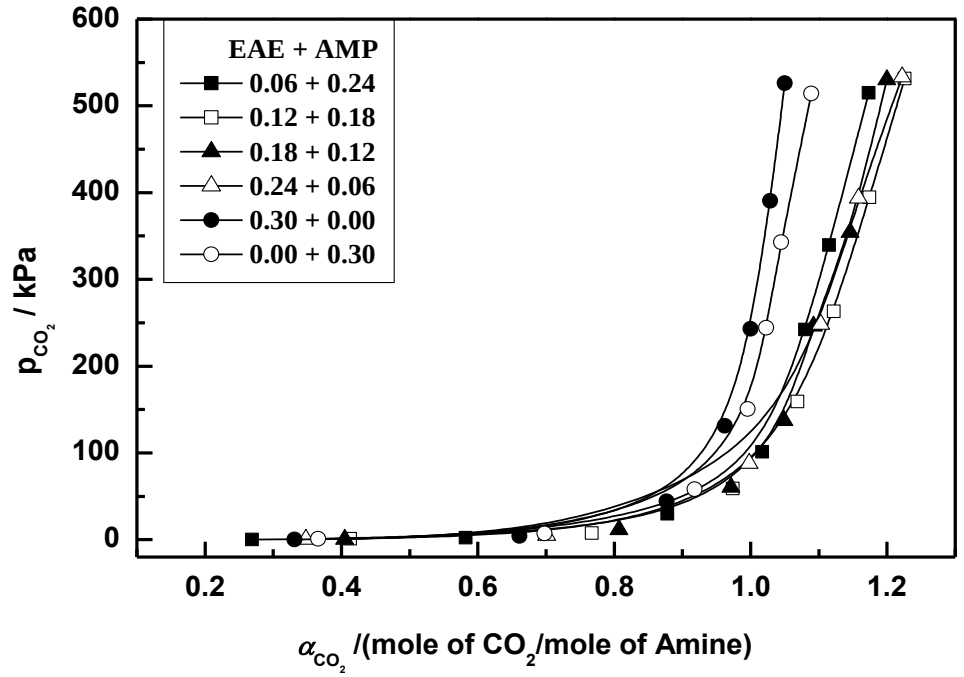

Figure 4.12: Solubility of CO_2 (1) in aqueous alkanolamine solutions of different mass fractions of EAE (2) + AMP (3) at T = 303.1 K; —, polynomial fit.

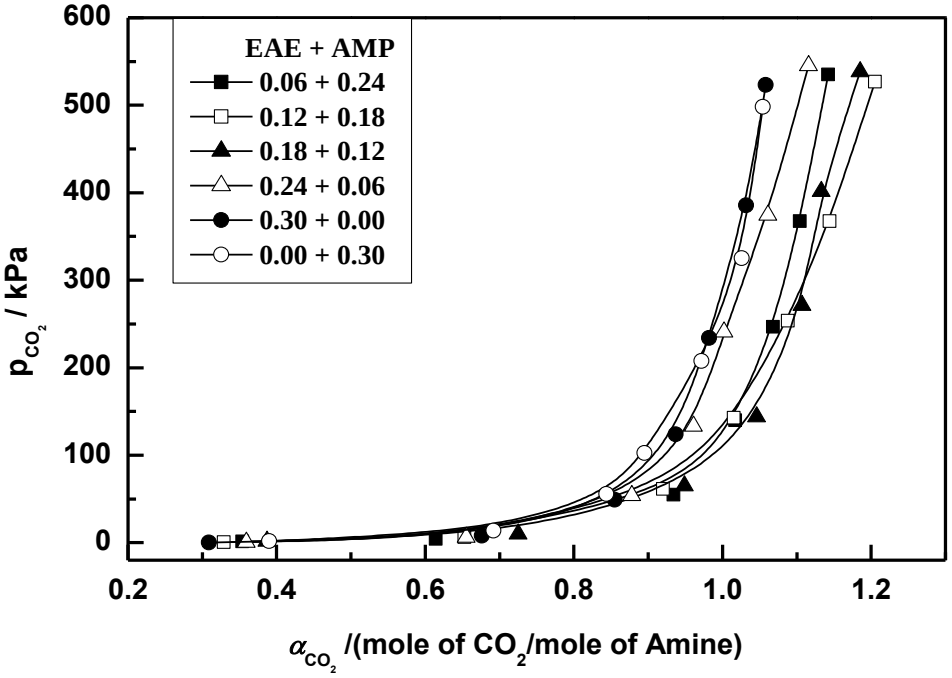

Figure 4.13: Solubility of CO_2 (1) in aqueous alkanolamine solutions of different mass fractions of EAE (2) + AMP (3) at T = 313.1 K; —, polynomial fit.

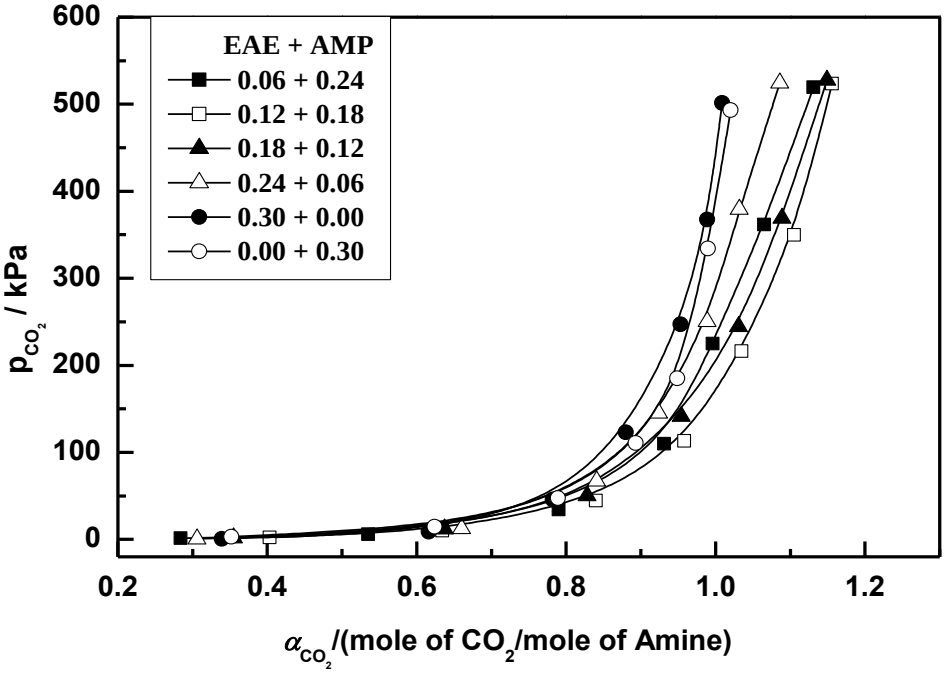

Figure 4.14: Solubility of CO_2 (1) in aqueous alkanolamine solutions of different mass fractions of EAE (2) + AMP (3) at T = 323.1 K; —, polynomial fit.

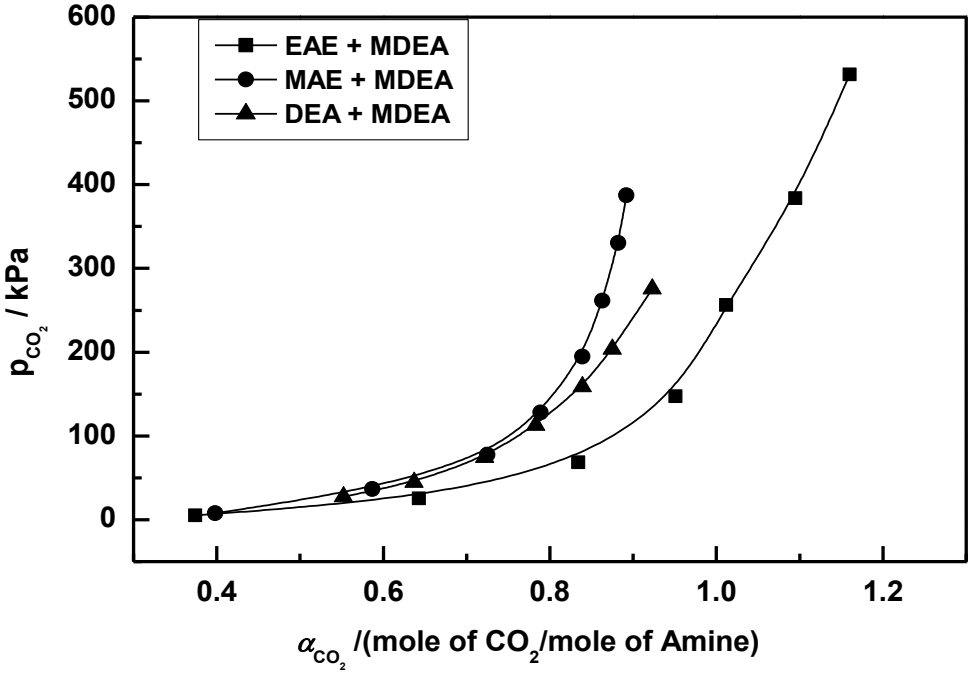

Figure 4.15: Comparison between solubility of CO_2 (1) in aqueous alkanolamine solution of (EAE/MAE/DEA (2) + MDEA (3)) of mass fraction 0.06 (2) + 0.24 (3) at T = 313.1 K; —, polynomial fit.

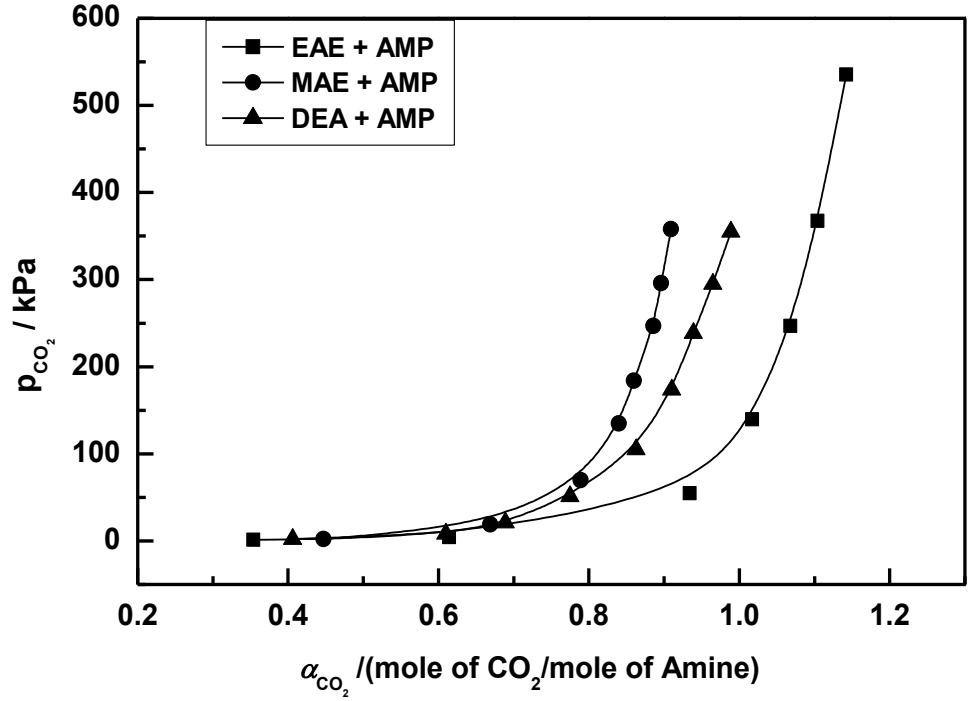

Figure 4.16: Comparison between solubility of CO_2 (1) in aqueous alkanolamine solution of (EAE/MAE/DEA (2) + AMP (3)) of mass fraction 0.06 (2) + 0.24 (3) at T = 313.1 K; —, polynomial fit.

Table 4.16: Solubility of CO_2 in aqueous (0.06 mass fraction EAE + 0.24 mass fraction MDEA) solutions in the temperature range of 303.1 – 323.1 K.

303.1 K			***313.1 K***			***323.1 K***		
CO_2 Partial pressure kPa	Loading (α_{CO_2})	x_{CO_2}	CO_2 Partial pressure kPa	Loading (α_{CO_2})	x_{CO_2}	CO_2 Partial pressure kPa	Loading (α_{CO_2})	x_{CO_2}
5.297	0.459	0.029	5.301	0.374	0.024	6.798	0.308	0.020
17.61	0.666	0.041	25.49	0.643	0.040	28.61	0.542	0.034
61.20	0.888	0.055	68.58	0.834	0.051	67.30	0.709	0.044
131.9	0.998	0.061	147.3	0.951	0.058	136.3	0.845	0.052
257.4	1.086	0.066	256.4	1.012	0.062	234.8	0.932	0.057
358.4	1.132	0.068	383.8	1.095	0.066	360.9	1.002	0.061
519.7	1.190	0.072	531.6	1.160	0.070	517.1	1.064	0.065

Table 4.17: Solubility of CO_2 in aqueous (0.12 mass fraction EAE + 0.18 mass fraction MDEA) solutions in the temperature range of 303.1 – 323.1 K.

303.1 K			***313.1 K***			***323.1 K***		
CO_2 Partial pressure kPa	Loading (α_{CO_2})	x_{CO_2}	CO_2 Partial pressure kPa	Loading (α_{CO_2})	x_{CO_2}	CO_2 Partial pressure kPa	Loading (α_{CO_2})	x_{CO_2}
3.389	0.501	0.034	3.601	0.416	0.028	4.301	0.366	0.025
31.31	0.841	0.055	27.29	0.721	0.048	29.61	0.637	0.042
73.80	0.966	0.063	69.70	0.876	0.057	67.90	0.788	0.052
156.5	1.050	0.068	147.5	0.987	0.064	140.6	0.917	0.060
270.0	1.124	0.072	263.4	1.081	0.070	240.4	1.024	0.066
396.9	1.199	0.077	396.2	1.161	0.075	368.3	1.096	0.071
531.2	1.256	0.080	541.9	1.225	0.079	528.4	1.178	0.076

Table 4.18: Solubility of CO_2 in aqueous (0.18 mass fraction EAE + 0.12 mass fraction MDEA) solutions in the temperature range of 303.1 – 323.1 K.

303.1 K			***313.1 K***			***323.1 K***		
CO_2 Partial pressure kPa	Loading (α_{CO_2})	x_{CO_2}	CO_2 Partial pressure kPa	Loading (α_{CO_2})	x_{CO_2}	CO_2 Partial pressure kPa	Loading (α_{CO_2})	x_{CO_2}
1.001	0.414	0.030	3.199	0.484	0.035	2.097	0.360	0.026
17.60	0.746	0.052	29.41	0.769	0.054	24.11	0.649	0.046
73.71	0.928	0.064	74.39	0.906	0.063	68.31	0.797	0.056
173.9	1.031	0.071	164.3	1.014	0.070	150.1	0.904	0.063
266.0	1.095	0.075	258.8	1.078	0.074	259.7	0.996	0.069
400.0	1.155	0.079	382.7	1.125	0.077	386.4	1.044	0.072
537.6	1.217	0.083	539.0	1.183	0.081	530.3	1.101	0.075

Table 4.19: Solubility of CO_2 in aqueous (0.24 mass fraction EAE + 0.06 mass fraction MDEA) solutions in the temperature range of 303.1 – 323.1 K.

303.1 K			***313.1 K***			***323.1 K***		
CO_2 Partial pressure kPa	Loading (α_{CO_2})	x_{CO_2}	CO_2 Partial pressure kPa	Loading (α_{CO_2})	x_{CO_2}	CO_2 Partial pressure kPa	Loading (α_{CO_2})	x_{CO_2}
0.601	0.445	0.034	0.499	0.383	0.029	1.097	0.316	0.024
16.01	0.791	0.059	14.81	0.727	0.054	17.01	0.628	0.047
70.31	0.968	0.071	60.19	0.907	0.067	59.48	0.783	0.058
153.3	1.050	0.077	157.5	1.013	0.074	144.6	0.894	0.066
272.6	1.131	0.082	244.9	1.074	0.078	247.4	0.967	0.071
393.2	1.188	0.086	374.1	1.134	0.082	381.8	1.026	0.075
543.5	1.262	0.091	536.2	1.208	0.087	526.3	1.076	0.078

Table 4.20: Solubility of CO_2 in aqueous (0.06 mass fraction EAE + 0.24 mass fraction AMP) solutions in the temperature range of 303.1 – 323.1 K.

303.1 K			***313.1 K***			***323.1 K***		
CO_2 Partial pressure kPa	Loading (α_{CO_2})	x_{CO_2}	CO_2 Partial pressure kPa	Loading (α_{CO_2})	x_{CO_2}	CO_2 Partial pressure kPa	Loading (α_{CO_2})	x_{CO_2}
0.199	0.269	0.022	1.201	0.354	0.029	1.198	0.284	0.023
2.097	0.582	0.047	4.098	0.614	0.049	6.002	0.535	0.043
29.81	0.878	0.069	54.61	0.934	0.073	34.41	0.790	0.062
101.1	1.017	0.079	139.7	1.017	0.079	110.0	0.931	0.072
242.3	1.080	0.083	246.7	1.068	0.082	224.7	0.996	0.077
339.7	1.115	0.086	367.5	1.104	0.085	361.7	1.065	0.082
515.1	1.173	0.090	535.2	1.142	0.088	519.5	1.131	0.087

Table 4.21: Solubility of CO_2 in aqueous (0.12 mass fraction EAE + 0.18 mass fraction AMP) solutions in the temperature range of 303.1 – 323.1 K.

303.1 K			***313.1 K***			***323.1 K***		
CO_2 Partial pressure kPa	Loading (α_{CO_2})	x_{CO_2}	CO_2 Partial pressure kPa	Loading (α_{CO_2})	x_{CO_2}	CO_2 Partial pressure kPa	Loading (α_{CO_2})	x_{CO_2}
1.001	0.413	0.034	0.402	0.329	0.027	2.301	0.403	0.033
7.697	0.767	0.060	6.299	0.653	0.052	10.19	0.633	0.050
59.02	0.974	0.076	61.22	0.920	0.072	44.31	0.840	0.066
159.2	1.069	0.082	142.9	1.015	0.078	113.2	0.958	0.074
263.0	1.122	0.086	253.7	1.088	0.084	216.2	1.035	0.080
394.5	1.174	0.090	367.3	1.144	0.088	349.8	1.105	0.085
531.5	1.226	0.093	527.0	1.205	0.092	523.4	1.156	0.088

Table 4.22: Solubility of CO_2 in aqueous (0.15 mass fraction EAE + 0.15 mass fraction AMP) solutions in the temperature range of 303.1 – 323.1 K.

303.1 K			***313.1 K***			***323.1 K***		
CO_2 Partial pressure kPa	Loading (α_{CO_2})	x_{CO_2}	CO_2 Partial pressure kPa	Loading (α_{CO_2})	x_{CO_2}	CO_2 Partial pressure kPa	Loading (α_{CO_2})	x_{CO_2}
0.701	0.405	0.033	1.598	0.387	0.031	1.801	0.355	0.029
11.79	0.807	0.063	10.01	0.725	0.057	11.91	0.637	0.051
60.62	0.971	0.075	65.01	0.949	0.074	50.09	0.828	0.065
137.4	1.049	0.081	144.1	1.046	0.081	141.3	0.954	0.074
246.1	1.092	0.084	271.3	1.107	0.085	244.5	1.031	0.080
354.2	1.146	0.088	401.6	1.133	0.087	368.9	1.089	0.084
530.3	1.200	0.092	538.3	1.185	0.090	527.8	1.149	0.088

Table 4.23: Solubility of CO_2 in aqueous (0.24 mass fraction EAE + 0.06 mass fraction AMP) solutions in the temperature range of 303.1 – 323.1 K.

303.1 K			***313.1 K***			***323.1 K***		
CO_2 Partial pressure kPa	Loading (α_{CO_2})	x_{CO_2}	CO_2 Partial pressure kPa	Loading (α_{CO_2})	x_{CO_2}	CO_2 Partial pressure kPa	Loading (α_{CO_2})	x_{CO_2}
0.399	0.348	0.028	0.601	0.359	0.029	0.497	0.306	0.025
5.002	0.701	0.056	6.299	0.655	0.052	12.61	0.660	0.053
88.21	0.998	0.077	53.80	0.878	0.069	67.20	0.841	0.066
248.1	1.103	0.085	133.4	0.961	0.075	145.2	0.924	0.072
393.9	1.158	0.089	240.8	1.002	0.078	250.3	0.989	0.077
533.4	1.222	0.093	374.4	1.061	0.082	379.3	1.032	0.080
			545.5	1.116	0.086	524.6	1.086	0.084

α_{CO_2} = loading of CO_2 = moles of CO_2 / moles of amine blend.

4.5 MODELLING

It is necessary to correlate the experimental data within a thermodynamic framework which provide a means to confidently interpolate between and extrapolate beyond the range of reported experimental data. As (EAE + MDEA + H_2O) evolved out as one of the most effective blends, hence, it was correlated with a thermodynamic framework. As the two equilibrium constants are found out as fit parameters by regressing my own experimental data, the non-ideality is lumped in the equilibrium constants and accurate speciation is far from impeccable.

I have used equations (3.1-3.6) to represent the chemical equilibria of (CO_2 + EAE + MDEA + H_2O) system. The equilibrium constants deprotonation (K_4) and carbamate reversion for EAE ($presently\ K_6,\ K_5\ in\ chapter\ 3$) are regressed from my own experimental data and presented in Table 3.25. The other temperature dependent equilibrium constants along with their literature sources are presented in Table 3.3. The equilibrium constants (converted in molality scale) are defined in terms of activity coefficients, γ, and molalities; m ($mol.kg^{-1}\ water$) of the species present in the equilibriated liquid phase.

For the (CO_2 + EAE + MDEA + H_2O) systems, the equilibrated liquid phase is assumed to contain four molecular species (free molecular CO_2, H_2O, EAE, and MDEA) and ionic species ($MDEAH^+$, $EAEH^+$, HCO_3^-, $EAECOO^-$, H_3O^+, OH^- and CO_3^{2-}. For developing the model, both MDEA and EAE are treated as solutes and only solvent considered is water. The standard state associated with solvent water is the pure liquid at the system temperature and pressure. The adopted standard state for ionic solutes is the ideal, infinitely dilute aqueous solution at the system temperature and pressure. The reference state chosen for molecular solute CO_2 is the ideal, infinitely dilute aqueous solution at the system temperature and pressure. Amine is assumed to be nonvolatile (relative to the other molecular species), an assumption that can be easily be relaxed if necessary. It is assumed a physical solubility (Henry's law) relation for the (non-condensable) acid gases. Vapor phase is assumed to be ideal because of the moderate pressure range of experimentation. The Henry's constant is taken from literature and presented in Table 3.3. The following vapor-liquid equilibrium relation is applicable.

$$P_{CO_2} = m_{CO_2} H_{CO_2} \tag{4.1}$$

I have assumed a zero interaction model by assuming activity coefficients as 1.0 in the equations (3.11-3.16). Equations (3.11-3.20) along with relation (4.1) were considered (non-linear equation set) to solve for the eleven species present in the equilibrated liquid phase. Then the activity coefficient model is used, which is based on extended *Debye-Hückel* theory of electrolytic solution to address the liquid phase non-ideality as discussed in chapter 3.0 (section 3.3.6). The interaction parameters of the activity coefficient model for (CO_2 + EAE + MDEA + H_2O) systems were obtained by regression analysis using the quaternary solubility data generated in this work. The EAE-MDEA and MDEA-EAE interaction parameters have been neglected because of the little influence on the uncertainty in the VLE prediction due to the relatively lower mole fractions of EAE and MDEA in comparison to that of water. Six solvent-ion pair interactions $H_2O - \mathrm{MDEAH^+EAECOO^-}$, $MDEA - \mathrm{MDEAH^+EAECOO^-}$, $EAE - \mathrm{MDEAH^+EAECOO^-}$, $MDEA - \mathrm{EAEH^+EAECOO^-}$, $MDEA - \mathrm{EAEH^+HCO_3^-}$, $EAE - \mathrm{MDEAH^+HCO_3^-}$ and one ion-ion interaction $\mathrm{MDEAH^+ - EAECOO^-}$ have been assumed to be zero. Kundu and Bandyopadhyay (2006a) made similar assumptions for DEA + AMP blend and supported that assumptions using parametric sensitivity analysis. No parameters involving interactions with CO_2, OH^-, and CO_3^{2-}.have been considered because of their comparatively low concentration and to reduce the model complexity. Twelve numbers of interaction parameters $\left(\beta_{ij}(kg.mol^{-1})\right)$ were regressed with overall average correlation deviations in CO_2 pressure (with respect to the experimentally generated CO_2 pressure) by 27 %. The interaction parameters are listed in Table 4.24

Table 4.24: Interaction parameters of (CO_2 – EAE–MDEA- H_2O) system.

Interaction parameters of (CO_2 + EAE + MDEA+H_2O) system	***kg.mol^{-1}***	***AAD% correlation***
$\beta(EAECOO^- - MDEAH^+)$	0.941042	27.0
$\beta(EAECOO^- - MDEA)$	-0.593588	
$\beta(EAECOO^- - EAEH^+)$	0.664229	
$\beta(EAECOO^- - EAE)$	-0.761452	
$\beta(EAE - MDEAH^+)$	0.901074	
$\beta(EAE - EAEH^+)$	-0.681454	
$\beta(EAE - HCO_3^-)$	-0.038994	
$\beta(MDEA - HCO_3^-)$	1.213432	
$\beta(MDEAH^+ - MDEA)$	0.511067	
$\beta(MDEAH^+ - HCO_3^-)$	1.680012	
$\beta(EAEH^+ - HCO_3^-)$	0.051285	
$\beta(EAEH^+ - MDEA)$	0.329676	

REFERENCES

Kundu, M., Bandyopadhyay, S.S. (**2006a**). Solubility of CO_2 in water + diethanolamine + 2-amino-2-methyl-1-propanol. *Journal of Chemical and Engineering Data,* 51, 398−405.

Kundu, M., Bandyopadhyay, S.S. (**2006b**). Solubility of CO_2 in water + diethanolamine + N-methyldiethanolamine. *Fluid Phase Equilibria***,** 248, 158−167.

Li, M.H. and Shen, K.P. (**1993**). Calculation of equilibrium solubility of carbon dioxide in aqueous mixtures of monoethanolamine with methyldiethanolamine. *Fluid Phase Equilibria*, 85, 129-140.

Li, M.H., Chang, B.C. (**1994**). Solubilities of carbon dioxide in water + monoethanolamine + 2-amino-2- methyl-1-propanol. *Journal of Chemical and Engineering Data*, 39, 448-452.

Park, S.H., Lee, K.B., Hyun, J.C., Kim, S.H. (**2002**). Correlation and prediction of the solubility of carbon dioxide in aqueous alkanolamine and mixed alkanolamine solutions. *Industrial Engineering and Chemistry Research***,** 41, 1658-1665.

Seo, D.J., Hong, W.H. (**1996**). Solubilities of carbon dioxide in aqueous mixtures of diethanolamine and 2-amino-2-methyl-1-propanol. *Journal of Chemical and Engineering Data***,** 41, 258-260.

Chapter 5

THERMODYNAMICS OF (ALKANOLAMINE + WATER) AND (CO_2 + ALKANOLAMINE + WATER) SYSTEM

Chapter 5

THERMODYNAMICS OF (ALKANOLAMINE + WATER) AND (CO_2 + ALKANOLAMINE + WATER) SYSTEM

5.1 INTRODUCTION

To model the thermodynamics of (acid gas + alkanolamine + water) systems, we have to understand the constituent binary systems and they are namely, (alkanolamine + water), (acid gas + water) and (acid gas + alkanolamine) systems. (Alkanolamine + water), (acid gas + water) systems are single weak electrolyte systems and the degree of dissociation of electrolyte in each is negligible except at high dilutions, chemical equilibrium can be ignored. As the acid gas approaches zero in the acid gas - alkanolamine solutions, a binary amine-water system results. The binary parameters associated with acid gas + alkanolamine interactions were found not to affect the representation of VLE in aqueous solutions. Because of chemical reactions these species are never simultaneously present in aqueous solution at significant concentrations. By improving our knowledge of the thermodynamics in the binary alkanolamine-water system, we can extrapolate the binary model to very low acid gas loading. At low acid gas loading, model predictions of acid gas solubility are sensitive to parameters

that quantify the interactions in the amine-water system. Kundu and Bandyopadhyay (2007) studied the thermodynamics and associated non-ideal behavior of binary MEA + H_2O, DEA + H_2O and MDEA + H_2O systems, which is required to predict the vapor-liquid equilibrium of acid gases such as CO_2 and H_2S over aqueous alkanolamine solutions. The binary interaction parameters, obtained from the regression analysis, using various thermodynamic data such as freezing point depression and heat of mixing beside the total pressure data, find their application in modeling the ternary and quaternary (acid gas + alkanolamine + water) systems without any further regression (Kundu and Bandyopadhyay, 2006; Kundu, 2004; Li and Mather, 1994, 1997). The relationship between each data type and the model parameters is different. Chang *et al.* (1993) measured freezing point depression of the most common alkanolamines using commercially available osmometer and a modified Beckmann apparatus (Skau and Aurther, 1971). They then used this data along with total pressure data to obtain a set of reliable NRTL parameters for several (alkanolamine + water) systems.

Molecular simulation using conductor like screening model is a useful alternative to those models based on activity coefficients of the compounds using the structural property information of pure components and binary interaction parameters between the components. Development of a COSMO-RS model for the (alkanolamine + water) systems are presented here with representation of excess Gibbs free energy, excess enthalpy and activity coefficient, chemical potential for binary (MAE/EAE + H_2O) system. The binary interaction parameters, obtained from the regression analysis of COSMO predicted activity coefficient, excess enthalpy, and excess Gibbs energy can be utilized in modeling ternary (acid gas + alkanolamine + water) systems, and their values need not to be regressed further. The ternary (CO_2 + MAE/EAE + H_2O) system interaction parameters may also be regresses out using the thermodynamic data obtained by COSMO prediction. The ternary system non-ideality as well is explained by molecular simulation.

5.2 MOLECULAR MODELLING

Molecular modelling encompasses all theoretical methods and computational techniques, which, are used to model the behavior of molecules. Molecular simulation based on quantum mechanics calculation is an attractive alternative to conventional engineering modeling techniques. Molecular simulation strategies give an intermediate layer between

direct experimental measurements and engineering models (as shown in Figure 1.1). Molecular simulation method can provide results applicable over wider ranges of process conditions because of the fewer approximations that are made during computation. The prediction of thermodynamic property of mixture and vapor-liquid equilibrium starts with quantum theory and solvation model.

5.2.1 Continuum Solvation Models

Quantum chemical methods originally have been developed for isolated molecules, i.e. for molecules in vacuum or, at best, in the gas phase. However, the practical impossibility of a rigorous representation of a molecular environment by quantum chemical tools, attempts have been made by many researchers to combine the quantum chemical description of a molecule with an approximate continuum description of the surrounding solvent. This kind of combination provides an alternative method to characterize molecular interactions and account for liquid-phase non-ideality. Models based on this method use results of computational quantum mechanics to predict thermo physical properties without the use of any experimental data. Present thesis owes to such a model, which has been originally developed by Klamt in 1995. The model, which views the surrounding of a molecule as continuum and a perfect electrical conductor, is known as Conductor-like Screening Model (COSMO). Klamt and coworkers later extended the model to include interactions between molecules in a condensed phase. They termed the extended model as COSMO-RS.

5.2.2 Conductor-like Screening Model –Real solvent (COSMO-RS)

The knowledge of thermodynamic properties of solutions or mixtures of liquids is a major requirement in chemical engineering, since it is essential for all kinds of separation processes such as absorption, adsorption, distillation, solubility of gases. 'With the advancement of molecular modeling theories, predictions of chemical, physical and transport properties are possible in near future using purely theoretical considerations' (Putnam *et al*., 2003).

COSMO-RS is a general and fast methodology for the a priori prediction of thermo-physical data of liquids. COSMO-RS is a method based on unimolecular quantum chemical calculations of the individual liquid in the system; not of the mixture and can be considered as an alternative to the structure-interpolating group contribution methods (GCMs). COSMO-RS

and GCMs are two different approaches for the prediction of activity coefficients of molecules in the liquid phase. In GCMs (using defined groups) the interaction energy of any system can be well approximated by the sum of group interaction energies. This means that a liquid is not a mixture of interacting molecules but a mixture of interacting structural groups (Eckert and Klamt, 2001). GCMs have a very restricted applicability because it depends on the availability of group interaction parameters and especially on experimental results. COSMO-RS instead is a method for predicting the thermodynamic properties of mixtures on the basis of unimolecular quantum chemical calculations of the individual molecules or, to be more precise, on the basis of molecular surface as computed by quantum chemical methods (QM) (Eckert and Klamt, 2001).

QM-COSMO calculations provide a discrete surface around a molecule embedded in a virtual conductor (Klamt and Schuurmann, 1993). Of this surface, each segment i is characterized by its area, a_i, and the screening charge density (SCD) σ_i on this segment, (which takes into account the electrostatic screening of the solute molecule by its surroundings) and the back polarization of the solute molecule. In addition, the total energy of the ideally screened molecule, E_{COSMO}, is provided. Within the COSMO-RS theory, a liquid is assumed as an ensemble of closely packed ideally screened molecules, as shown in Figure5.1.

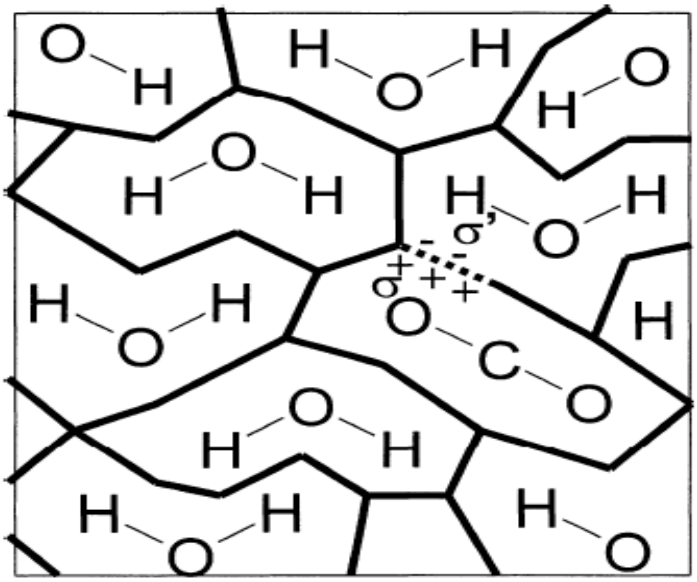

Figure 5.1: COSMO-RS view of surface-contact interactions of molecular cavities (Eckert and Klamt, 2005).

In order to achieve this close packing, the system has to be compressed, and thus the cavities of the molecules get slightly deformed (although the volume of the individual cavities does not change significantly). As is visible in Figure 5.1, each piece of the molecular surface is in close contact with another piece. Assuming that there still is a conducting surface between the molecules, that is, each molecule still is enclosed by a virtual conductor and in a contact area, the surface segments of both molecules have net SCDs σ and σ' (Figure 5.1). In reality, there is no conductor between the surface contact areas. Thus, an electrostatic interaction arises from the contact of two different SCDs. The specific interaction energy per unit area resulting from this ‘‘misfit’’ of SCDs is given by

$$E_{misfit}(\sigma, \sigma') = a_{eff} \frac{\alpha'}{2} (\sigma + \sigma')^2 \qquad (5.1)$$

Where, a_{eff} is the effective contact area between two surface segments, and α' is an adjustable parameter.

The basic assumption of Eq. (5.1) (which is the same as in other surface-pair models like UNIQUAC) is that the residual non-steric interactions can be described by pairs of geometrically independent surface segments. Thus, the size of the surface segments a_{eff} should be chosen in such a way that it effectively corresponds to a thermodynamically independent entity. There is no simple way to define a_{eff} from first principles, and it should be considered as an adjustable parameter (Klamt *et al.*, 2002). Obviously, if σ equals -σ' , the misfit energy of a surface contact will vanish. Hydrogen bonding (HB) can also be described by the two adjacent SCDs. HB donors have a strongly negative SCD, whereas HB acceptors have strongly positive SCDs. Generally, a HB interaction is expected if two pieces of surface of opposite polarity are in contact. Such a behavior is described by a functional of the form

$$E_{HB} = a_{eff} C_{HB} min\left[0; \min(0;\ \sigma_{donar} + \ \sigma_{HB})\ max\left(0;\ \sigma_{acceptor} - \sigma_{HB}\right)\right] \qquad (5.2)$$

Where C_{HB} and σ_{HB} are adjustable parameters. In addition to electrostatic misfit and HB interactions, COSMO-RS also takes into account van der Waals (vdW) interactions between surface segments via

$$E_{vdW} = \ a_{eff}(\tau_{vdW} \ + \ \tau'_{vdW}) \qquad (5.3)$$

Where, τ_{vdW} and τ'_{vdW} are element-specific adjustable parameters. The vdW energy is dependent only on the element type of the atoms that are involved in surface contact. It is spatially nonspecific. E_{vdW} is an additional term to the energy of the reference state in solution. Currently nine of the vdW parameters (for elements H, C, N, O, F, S, Cl, Br and I) have been optimized. For the majority of the remaining elements reasonable guesses are available (Klamt *et al.*, 1998).

The link between the microscopic surface-interaction energies and the macroscopic thermodynamic properties of a liquid is provided by statistical thermodynamics. Since in the COSMO-RS view, all molecular interactions consist of local pair wise interactions of surface segments, the statistical averaging can be done in the ensemble of interacting surface pieces. Such an ensemble averaging is computationally efficient, especially in comparison to the computationally demanding molecular dynamics or Monte Carlo approaches, which require averaging over an ensemble of all possible different arrangements of all molecules in the liquid. Asa result, the computational effort of a COSMO-RS calculation is not significantly higher than that of a UNIFAC calculation.

To describe the composition of the surface-segment ensemble with respect to the interactions (which depend on σ only), only the probability distribution of σ has to be known for all components, C_i. Such probability distributions, $p^{C_i}(\sigma)$, are called "σ -profiles''. The σ-profile of the whole system/mixture $p_s(\sigma)$ is just a sum of the σ -profiles of the components C_i weighted with their mol fraction (x_i) in the mixture C_i

$$p_s(\sigma) = \sum_{i=S} x_i \, p^{C_i}(\sigma) \qquad (5.4)$$

The chemical potential of a surface segment with SCD σ in an ensemble described by normalized distribution function $p_s(\sigma)$

$$\mu_S(\sigma) = -\frac{RT}{a_{eff}} \ln\left[\int p_S(\sigma') exp\left\{\frac{a_{eff}}{RT}\left[\mu_S(\sigma') - E_{misfit}(\sigma,\sigma') - E_{HB}(\sigma,\sigma')\right]\right\} d\sigma'\right] \quad (5.5)$$

Where $\mu_S(\sigma)$ is a measure for the affinity of the system S to a surface of polarity σ. It is a characteristic function of each system and is called ''σ-potential''. It should be noted that E_{vdW} is not included in Eq. (5.5) (not part of the statistical averaging) because it is not a function of individual surface contacts. Instead, E_{vdW} is added a posteriori to the reference energy in solution. Eq. (5.5) is an implicit equation. It is solved iteratively. This is done in

milliseconds on any PC. Thus, COSMO-RS computations of thermodynamic properties are very fast. Eq. (5.5) is exact, thus avoiding errors in the calculation of properties at very small concentrations. The chemical potential (the partial Gibbs free energy) of component C_i in system S is readily available from integration of the σ-potential over the surface of C_i

$$\mu_S^{C_i} = \mu_{C,S}^{C_i} + \int P^{C_i}(\sigma)\mu_S(\sigma)d\sigma \tag{5.6}$$

Where, $\mu_{C,S}^{C_i}$is a combinatorial contribution to the chemical potential. It contains one adjustable parameter, λ_C

$$\mu_{C,S}^{C_i} = \frac{\partial G_{C,S}}{\partial N_i} \tag{5.7}$$

Where

$$G_{C,S} = -NkT\,\lambda_C \left[\sum_i sin^2\left(\frac{X_i\pi}{2}\right) ln\left(\frac{A_i}{A_0}\right) + ln(A_0)\right] \tag{5.8}$$

It should be noted that the chemical potential of Eq. (5.6) is a ‘‘pseudo-chemical potential,’’ which is the standard chemical potential minus $RT\ ln\ (x_i)$ (Ben-Naim, 1987). The chemical potential μ_S of Eq. (5.6) allows for the prediction of almost all thermodynamic properties of compounds or mixtures, such as activity coefficients, excess properties, or partition coefficients and solubility.

COSMO-RS computes chemical potential of pure component in ideal gas (μ_{gas}^{Ci}):

$$\mu_{gas}^{Ci} = E_{gas}^{Ci} - E_{COSMO}^{Ci} - E_{vdW}^{Ci} + \omega_{ring} n_{ring}^{Ci} + n_{gas} RT \tag{5.9}$$

Where, E_{gas}^{Ci} is the total energy of the molecule in the gas phase computed by quantum mechanics, $E_{COSMO}^{Ci}$is the total COSMO energy of the molecule in solution computed by solvation model using quantum mechanics, $E_{vdW}^{Ci}$is the vdW energy of the molecule and the rest of the terms in Eq. (5.9) are correction parameters for molecules with ring shape geometry. Once the chemical potentials of pure compound are computed in solution and ideal gas phase, vapor pressure of pure compound can be calculated by Eq. (5.10):

$$P_{vap(T)}^{Ci} = exp\left(\frac{\mu_{Ci}^{Ci} - \mu_{gas}^{Ci}}{kT}\right) \tag{5.10}$$

Where, $P_{vap(T)}^{Ci}$ the vapor pressure of pure component (C_i), k is the Boltzmann constant, T is the temperature and μ_{Ci}^{Ci} is the pseudo-chemical potential of pure component C_i in a solution of C_i. After vapor pressure of pure compound has been calculated, COSMO-RS can predict vapor liquid equilibrium based on the following equations:

$$\gamma_S^{Ci} = exp\left(\frac{\mu_S^{Ci} - \mu_{Xi}^{Ci}}{RT}\right) \tag{5.11}$$

$$P^{tot} = \sum_i P_{vap}^{Ci} x_i \gamma_S^{Ci} \tag{5.12}$$

$$y_i = \frac{P_{vap}^{Ci} x_i \gamma_S^{Ci}}{P^{tot}} \tag{5.13}$$

In above equations, γ_S^{Ci} is the activity coefficient of pure compound C_i in solution, and the solution is considered as the continuum medium according to COSMO model. P^{tot} is total vapor pressure of the mixture that is used to predict the vapor liquid equilibrium diagram, x_i is the mole fraction of compounds in liquid phase and y_i is the mole fraction of compounds in gas phase. Hence, vapor liquid equilibrium in COMSO-RS is based on vapor pressure and activity coefficients of pure compounds.

5.2.3 COSMO-RS Application

Originally COSMO-RS was developed mainly for the prediction of various kinds of partition coefficients (Klamt *et al*., 2000). In 1998, it was applied to activity coefficients and complete vapor–liquid equilibria of binary mixtures by chemical engineers (Clausen and Arlt, 2000). Since then COSMO-RS has become very popular and is widely used in chemical engineering for all kinds of phase equilibrium predictions (vapor–liquid, liquid–liquid, and solid–liquid) and for the efficient screening of solvents and additives for chemical process optimization (Franke, 2002; Klamt *et al.,* 2010). The strength of COSMO-RS as compared with other conventional chemical engineering tools, such as group contribution methods, is its broad homogeneous applicability from simple compounds toward complicated, multifunctional, or novel chemical compounds. Although developed and parameterized exclusively on neutral compounds, in 2002 COSMO-RS was proven to be able to treat ionic liquids as mixtures of anions and cations (Marsh *et al.,* 2002; Diedenhofen *et al*., 2002). Since then ionic liquids have become an important application area of COSMO-RS in chemical engineering. Klamt *et al.*, 2004 implemented the COSMO-RS method for the prediction of vapor-liquid equilibria

for the mixtures of dimethylether (1) and propene (2) and of nitroethane (1) and propylene glycol monomethylether (1-methoxy-2-propanol) (2). Good quality predictions were achieved using experimental values for the pure compound vapor pressures and predicted activity coefficients for the mixture thermodynamics. The quantitative success combined with the relatively low computational and time requirements clearly demonstrated that COSMOtherm was an efficient and reliable tool for the prediction of VLE data for typical industrial relevant mixtures. Tamal Banarjee, 2006 predicted the phase equilibrium behavior and vapor pressure of ionic liquid system (phosphonium ionic liquids) using conductor like screening model. Ayman Gazawi, 2007 emphasized on the VLE and vapor pressure predictions using Turbo mole software package version 5.8 with DFT/TZVP ab initio method for; sigma profile, ideal gas heat capacity and ideal gas absolute entropy computation of 71 pure compounds. Yamada *et al.*, 2011 used density functional theory (DFT) calculations with the latest continuum solvation model (SMD/IEF-PCM) to determine the mechanism of CO_2 absorption into aqueous solutions of 2-amino-2-methyl-1-propanol (AMP). Possible mechanism of CO_2absorption process in the aqueous solvent was investigated by transition-state optimization and intrinsic reaction coordinates (IRC). They also predicted that the carbamate readily decomposed by a reverse reaction rather than by hydrolysis. Mustapha *et al.*, 2013 considered more than 2000 solvents comprising of four groups including the alkanolamine solvents (primary, secondary, tertiary, and sterically hindered alkanolamines and physical solvents), neutral solvents, mixed solvents and ionic liquids (ILs). They studied and predicted the thermodynamic properties, such as Henry's constant, partition coefficient, solubility in water and vapor pressure of all the solvents using COSMO-RS model. Because of its ability to treat complex molecules not only in water but in any solvent and mixture, COSMO-RS is widely used in pharmaceutical and general life science research for solvent screening and formulation research in drug development (Klamt and Smith, 2008; Wichmann *et al*., 2010). Although the σ-based COSMO-RS picture of molecular interactions surely opens interesting options for the description of drug activity in drug design, it has not yet been widely used in that area. The environmental distribution of compounds had been one of the starting points for the development of COSMO and COSMO-RS, and remains to be an interesting and challenging application area of COSMO-RS (Niederer and Goss, 2007; Goss and Arp 2009). Other application areas are fragrance, flavor, or other ingredient distribution in food,

perfumes, or personal care products, additives in polymers, and many more. Within the COSMOtherm software, a number of additional applications of COSMO-RS have been developed, including the prediction of dissociation constants in aqueous and non-aqueous solvents (Klamt *et al.,* 2003; Eckert *et al.,* 2009), the prediction of the free energy of molecules at liquid–liquid and liquid–vapor interfaces, and the prediction of the free energies and of the partitioning of solutes in polymers, micellar systems, and bio membranes (Klamt *et al*., 2008). Furthermore, a set of QSAR descriptors, the so-called σ-moments, have been derived from the COSMO-RS theory, which can be used to regress almost any kind of partition property even in complex cases as blood–brain partitioning, soil sorption, adsorption to activated carbon, and many more.

5.3 COMPUTATIONAL PROCEDURE

The calculation procedure of COSMO-RS is divided into two steps: quantum mechanical COSMO calculations for the molecular species involved and COSMO-RS statistical calculations performed within the COSMOtherm program (Eckert and Klamt, 2005) as shown in Figure 5.2.

In the first step QM COSMO calculations have to be done for the molecular species involved, where the information about solvents and solutes is extracted. In these calculations, the continuum solvation model COSMO is applied in order to simulate a virtual conductor environment for the molecule. Then the solute molecule induces a polarization charge density, Y, on the interface of the molecule and the conductor. These charges act back on the solute and produce a more polarized electron density than in vacuum.

Throughout the quantum chemical self-consistency algorithm cycle, the solute molecule is converged to its energetically optimal state in a conductor with respect to electron density. The molecular geometry can be optimized using conventional methods for calculation in vacuum (Diedenhofen *et al.,* 2003). The calculations end up with the self-consistency state of the solute in the presence of a virtual conductor that surrounds the solute outside the cavity. These quantum chemical calculations have to be performed only once for each molecule of interest and then can be stored in a database (Diedenhofen *et al.,* 2003).

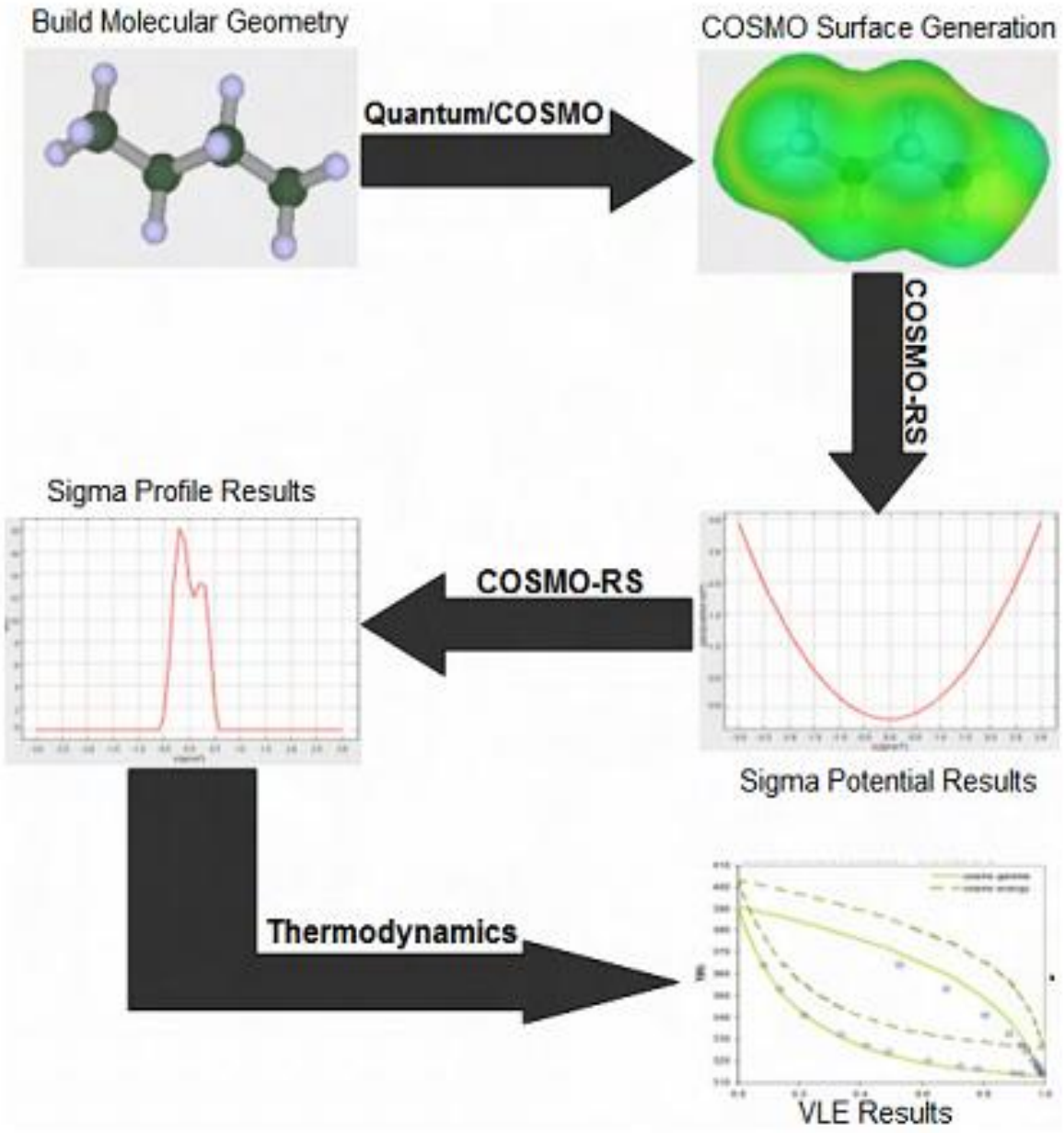

Figure 5.2: Overall summary of COSMO-RS computation. First, start the computation by building a molecule then perform a Quantum and COSMO calculations to generate COSMO surface. Second, generate sigma potential and sigma profile by COSMO-RS theory. Finally, perform thermodynamics calculation such as VLE by applying statistical thermodynamics (Eckert and Klamt, 2005).

The COSMO-RS calculation that predicts the thermodynamic properties such as chemical potentials, Henry constants, solubilities, vapour pressures, etc. are done in few seconds and then can be used in the task of screening a large number of compounds from a database. It depends on a small number of 16 adjustable parameters, some of which are physically predetermined (Putnam *et al.*, 2003) (from known properties of individual latoms) and that are not specific for functional groups or type of molecules. Moreover, it is the statistical thermodynamics that enables the determination of the chemical potential of all components in the mixture and, from these, thermodynamic properties are derived. The deviations of the real fluid behavior with respect to an ideal conductor are taken into account, the electrostatic energy differences and hydrogen-bonding energies are quantified as functions of the local COSMO polarization charge densities, σ and σ', of the interacting surface of the molecule divided into segments (Eckert and Klamt, 2005).The COSMO-RS parameters are to be optimized only for the QM method and that are used as a basis for the COSMO-RS calculations. Unlike the GCM method, the resulting parameterization is completely general and can be used to predict the properties of almost any mixture.

The COSMOtherm calculations have been performed the latest version of software that is COSMOtherm C30_1201. Performing COSMO-RS computation to predict thermodynamic properties for any type of molecule requires generating three types of files:

- **.Cosmo file,**
- **.Energy file**
- **.Vap file.**

The .cosmo and .energy files are generated by TURBOMOLE software while the .vap file is generated by COSMOtherm programme package. Once these files are generated the COSMOtherm programme can be used to perform thermodynamic calculations. COSMOtherm predicts the thermodynamic properties by using the chemical potential derived from the COSMO-RS theory.

The thermodynamic properties calculated in this work through COSMOtherm includes,

- Excess enthalpy
- Excess Gibbs free energy

- Activity coefficient
- Total pressure
- Activity coefficient at infinite dilution

The input for the alkanolamine-water system is given from the resulted .cosmo files through the quantum chemical COSMO calculations based on the density functional theory (DFT) level generated by TURBOMOLE software. Figure 5.3 shows main window of COSMOtherm representing different sections. COSMOtherm requires a special parameterization for each and every single method / basis set combination. Each of these parameterizations was derived from molecular structures quantum chemically optimized at the given method / basis set level. COSMO-RS calculations were done at the different parameterization levels, which are as follows:

- BP/TZVP (DFT/COSMO calculation with the BP functional and TZVT basis set using the optimized geometries at the same level of theory) parameter file: BP_TZVP_C30_1201.ctd.
- BP/SVP/AM1 (DFT/COSMO single-point calculation with the BP functional and SVT basis set upon geometries optimized at semi-empirical MOPAC-AM1/COSMO level) - parameter file: BP_SVP_AM1_C30_1201.ctd.
- B88-VWN/DNP (DFT/COSMO calculation with the B88-VWN functional and numerical DNP basis using the optimized geometries at the same level of theory) - parameter file: DMOL3_PBE_C30_1201.ctd.
- BP/TZVP/FINE (DFT/COSMO calculation with TZVP basis set followed by a single point BP-RI_DFT level calculation) – parameter file: BP_TZVP_FINE_HB2012_C30_1201.

Following are some glossaries used in MM calculations using COSMOtherm:

➔ BP/TZVP and DMOL3-PBE are production level, BP/SVP/AM1 is screening level, BP/TZVP/FINE is high level sets for COSMOtherm parameters.

➔ MOPAC is a computer program in computational chemistry implementing semi-empirical quantum chemistry algorithms.

➔ (Austin Model 1) AM1are semi-empirical quantum chemistry algorithms.

➔ TZVP, SVP, DMOL3 are basis sets.

➔ BP, and PBE (Perdew-Burke-Ernzerhof) are exchange functional correlations available in TURBOMOLE for DFT calculations.

This database levels are listed in the databases panel in general settings menu in the COSMOtherm program (Figure 5.4). The VLE and thermodynamic properties estimation of alkanolamine-water is done with BP_TZVP_C30_1201.ctd parameterization (parameterization through quantum chemical method which is a full Turbo mole BP-RI-DFT COSMO optimization of the molecular structure using the large TZVP basis set). First step for getting started the COSMOtherm program calculation involves the selection of alkanolamine and water molecule through the left section of the COSMOtherm main window:

- From one of the databases, using one of the buttons labeled SVP, TZVP, DMOL3, or TZVPD-FINE.

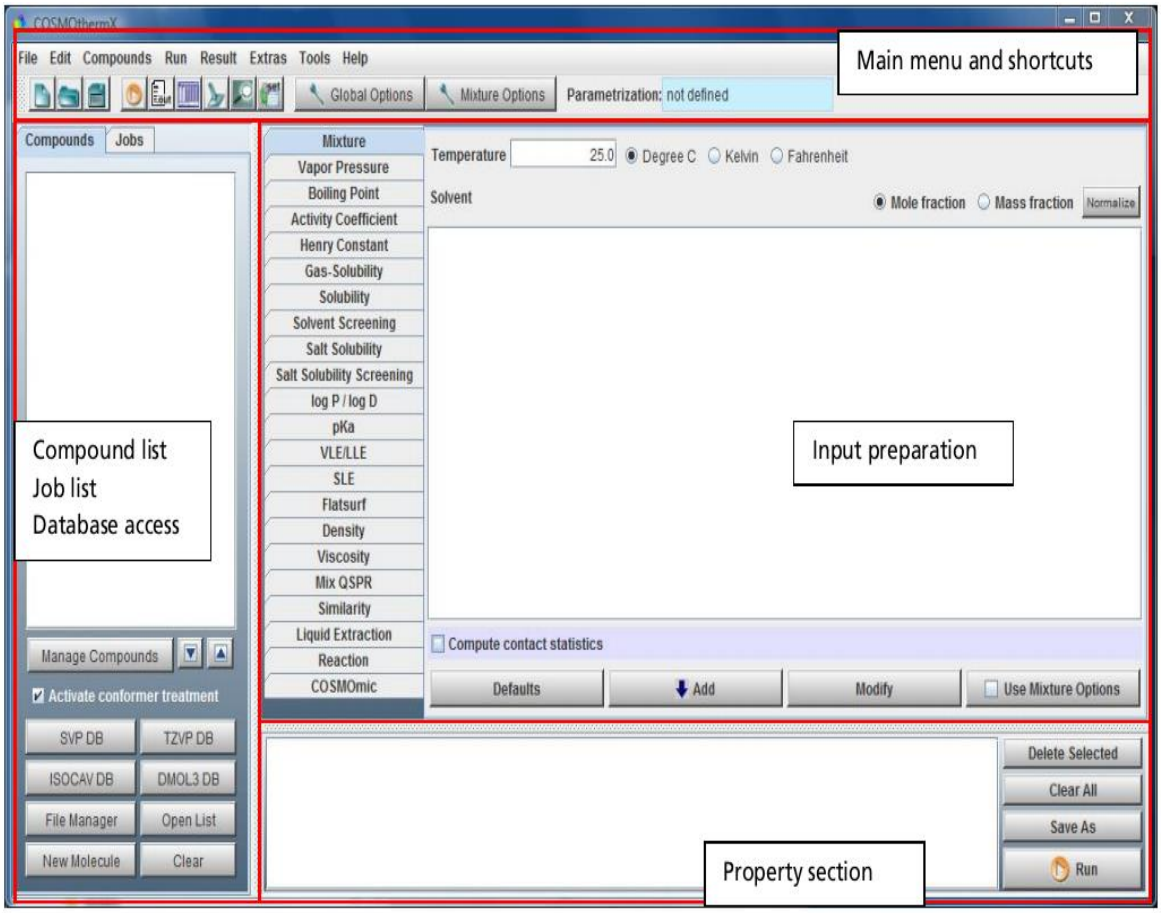

Figure 5.3: Main window of COSMOtherm representing different sections.

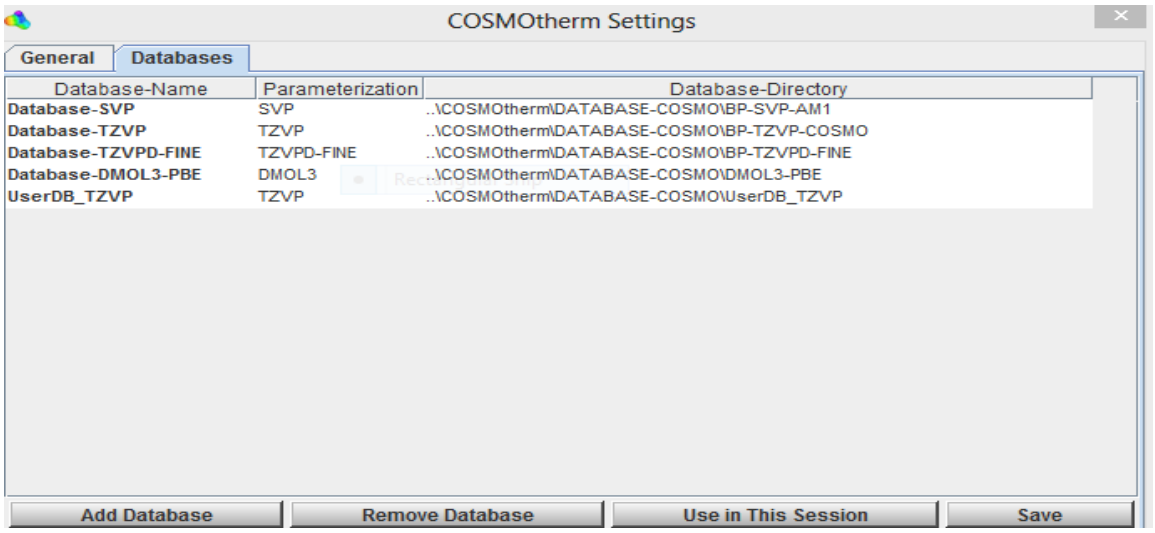

Figure 5.4: Window representing the different parameterizations.

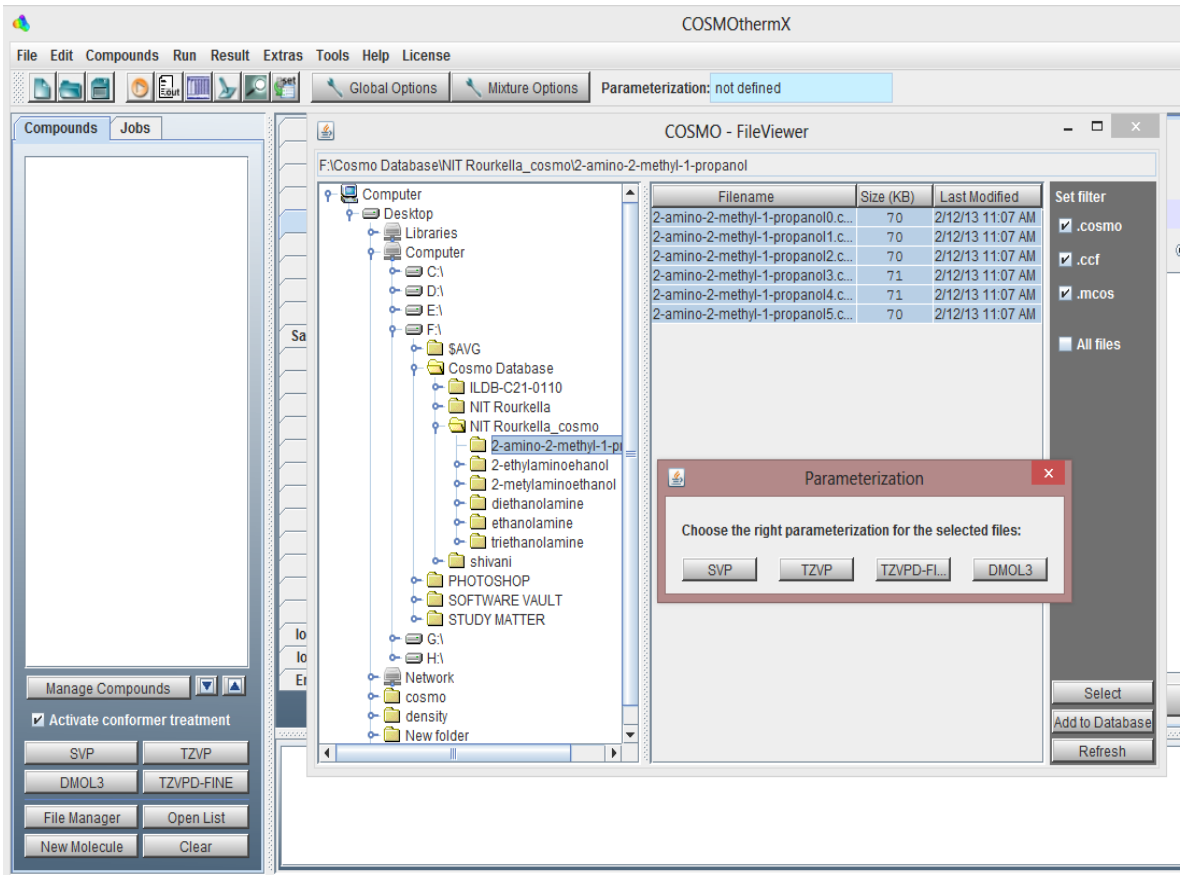

Figure 5.5: File manager window from where we select the .cosmo files for compounds and parameterization as BP-TZVP.

After selecting the alkanolamine and water molecule; we select **.vap** files to the input by right clicking on the compound name and selecting the compound properties and clicking the "USE IN INPUT" button (Figure 5.6). Other parameters such as unit of gas phase energy input and additional COSMOtherm output of the calculated properties can be selected from the global option in the main window. The largest section of the COSMOtherm software main window consists of the range of tabulated panels for the properties that can be calculated by using the flowchart (Figure 5.7). Through this panel we select the activity coefficient and fix the mole fraction of pure water for getting the activity coefficient at infinite dilution (Figure 5.8) whereas for calculating the other properties such as activity coefficient, excess enthalpy, excess Gibbs free energy, total pressure, chemical potential and activity coefficient model parameters we go through VLE properties Figure 5.9.

We choose the compounds, 2-ethylamino ethanoln (EAE) and water from the file manager and the TZVP database repectively for finding out infinite dilution activity coeffiecient of EAE in water. During compound selection by default, the conformers of 2-ethylamino ethanol are also selected and the conformer treatment is also activated. After the selection, we set the the water mole fraction to be 1.0 and temperature to the desired value of 303.1 K, and the activity coefficient is selected from the property panel (Figure 5.9). For the calculation of VLE properties for 2-ethylamino ethanol and water, the conditions are to be set here to "isothermal" calculation, by setting the temperature ranging from 303.1 – 323.1 K and then the selection of VLE property are done from the property panel (Figure 5.9). The output file resulting from the VLE calculation contains the activity coefficent, excess ethanlpy, excess Gibbs free energy, chemical potential, total pressure and parameters for different activity coefficient model.

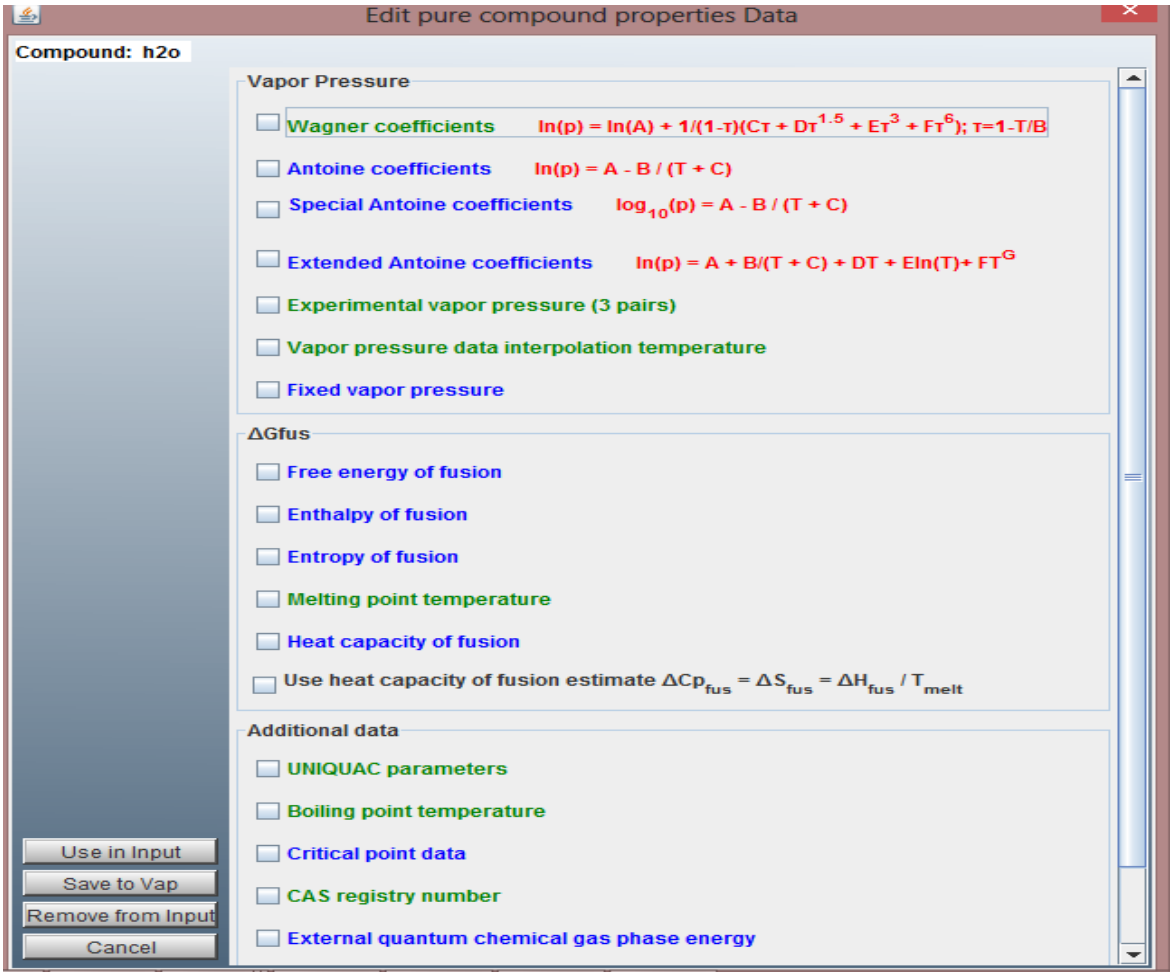

Figure 5.6: Showing the selection of compound properties.

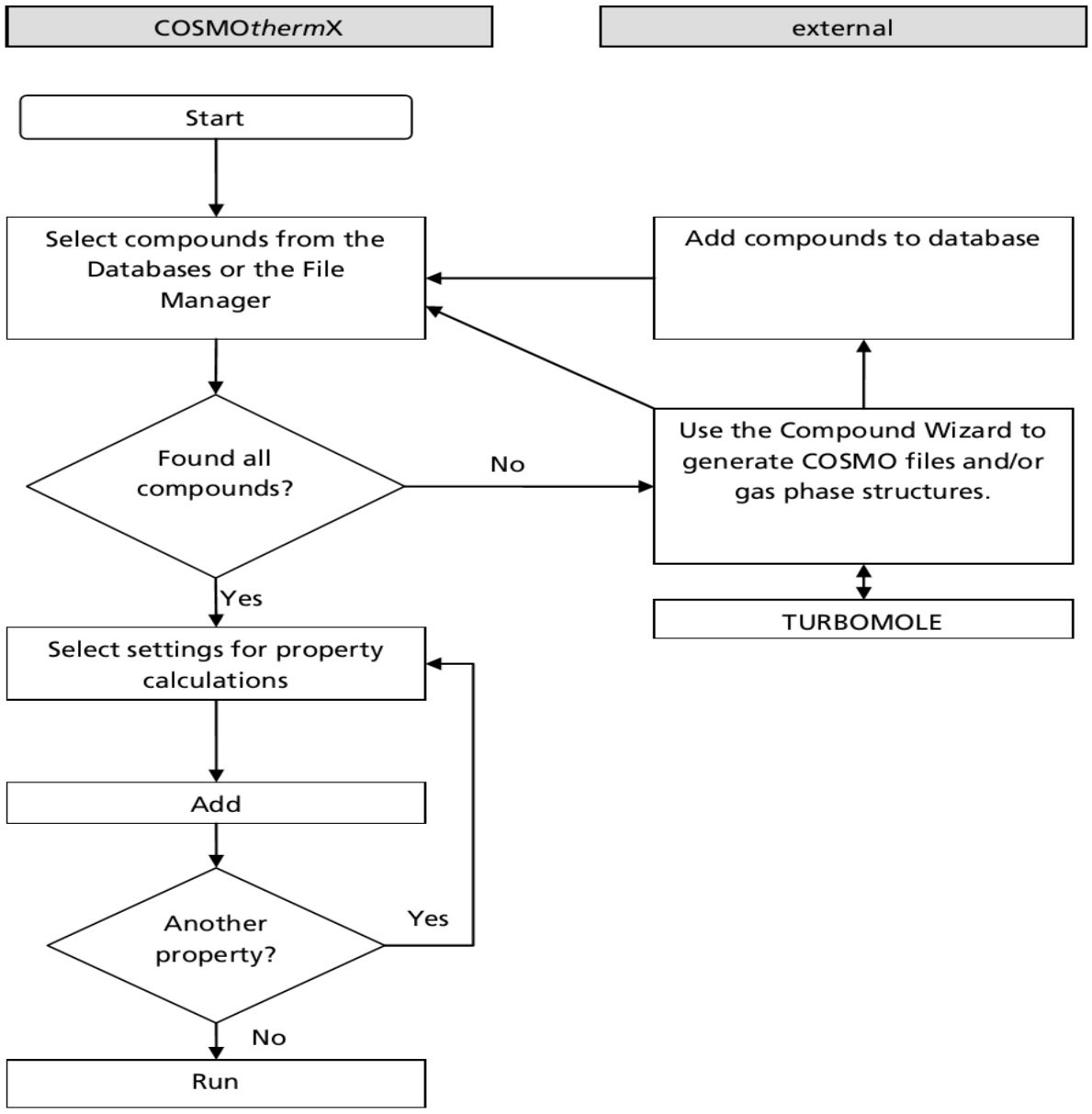

Figure 5.7: Flowchart for property calculation through COSMOtherm (reference COSMOtutorial).

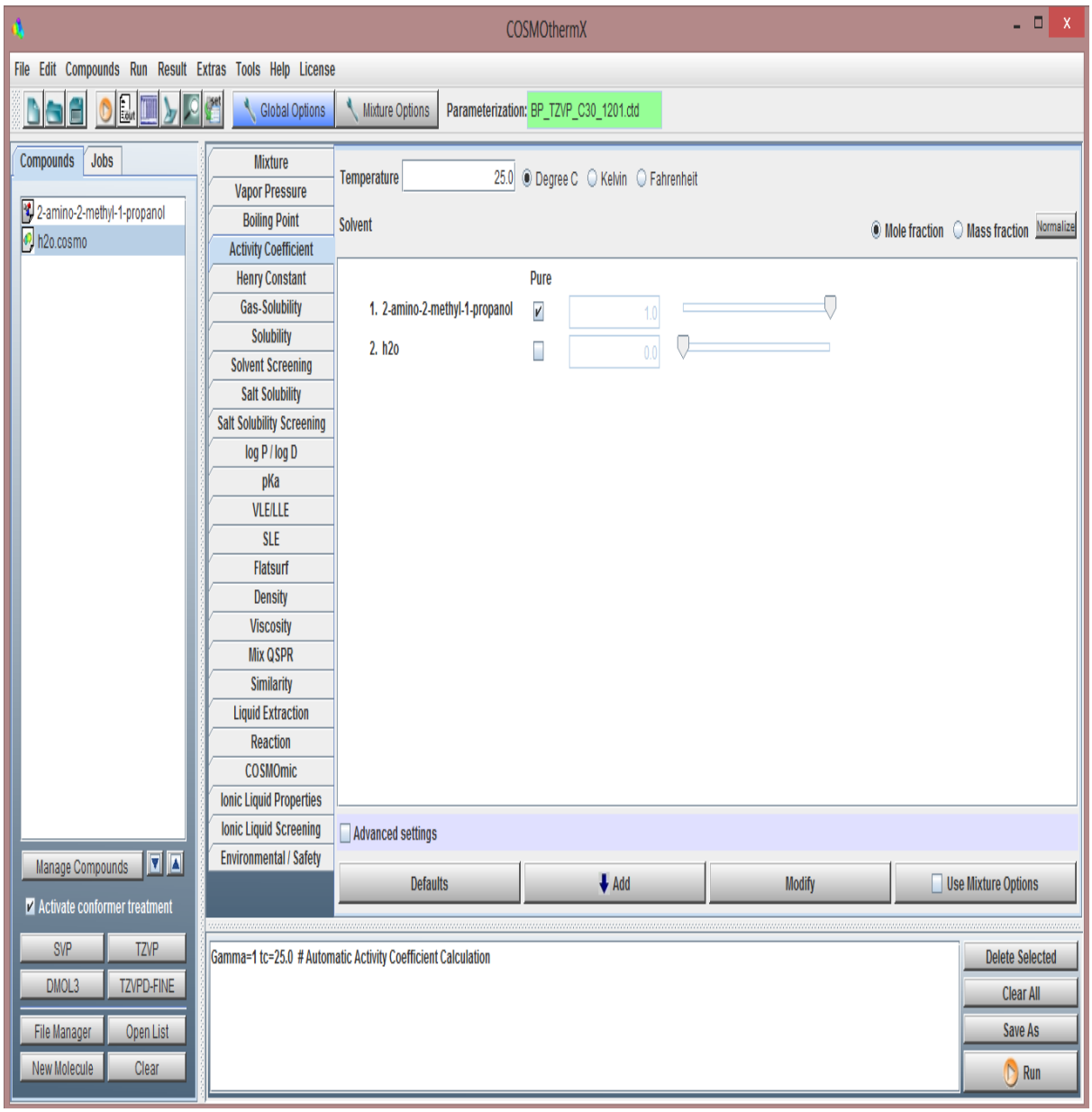

Figure 5.8: window showing the infinite dilution coefficient calcuation.

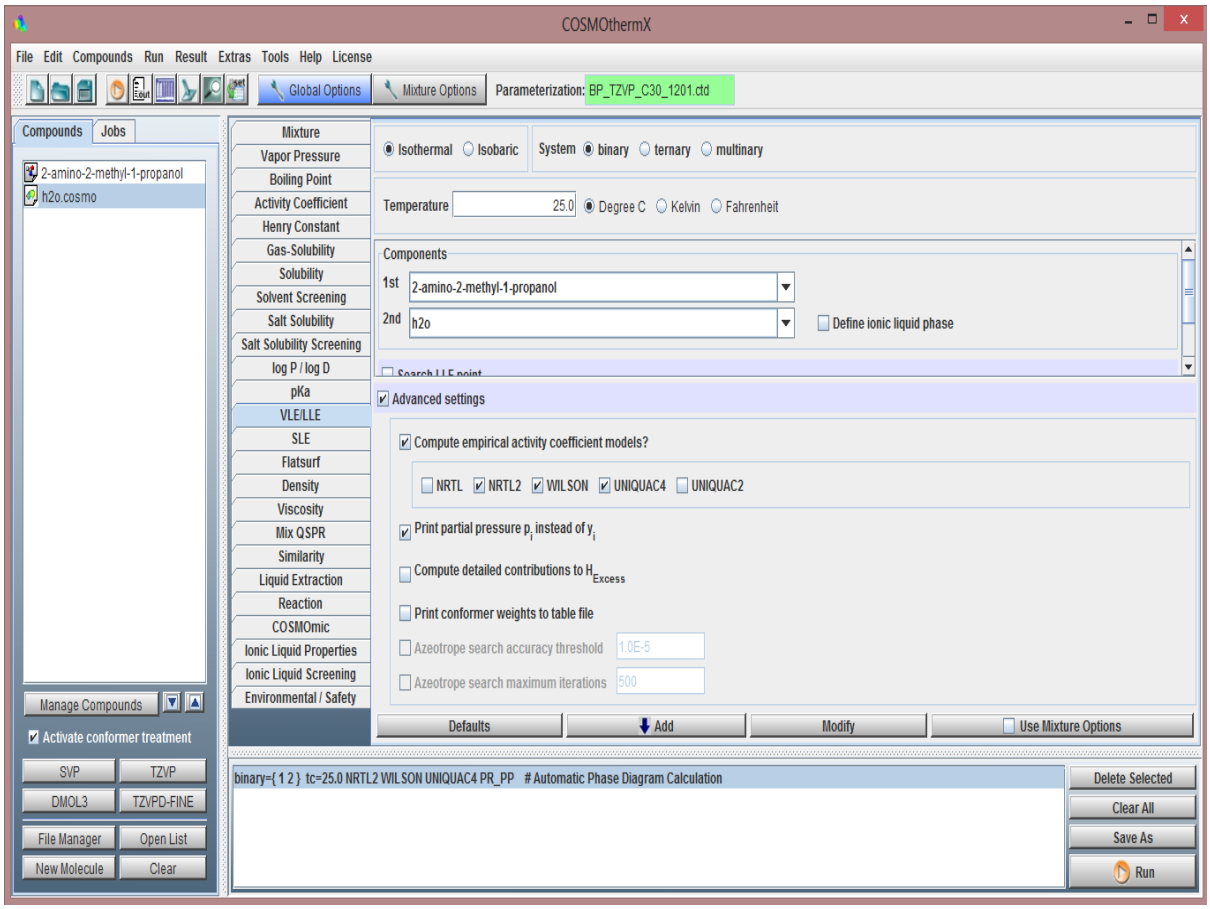

Figure 5.9: Window showing the VLE properties calculation.

5.4 RESULTS AND DISCUSSION

5.4.1 Binary Solution

COSMO-RS predicted excess enthalpy, excess Gibbs energy, chemical potential, and activity coefficients of (MAE + H_2O) and (EAE + H_2O) solutions are shown in Figures (5.10-5.17). The concept of chemical potential continues to be used in chemical literature, especially as it relates to chemically reactive systems including electrolyte systems. Indeed, because of its relation to Gibbs free energy, chemical potential is the thermodynamic variable generally manipulated to determine the equilibrium distribution of species in a chemically reacting system at constant temperature and pressure. Excess enthalpy data is useful for modeling because it is directly related to the temperature dependence of excess Gibbs energy. Therefore, in Gibbs energy model for activity coefficient, excess enthalpy measurements will

provide more accurate temperature dependence for the model. With the addition of methyl group to the amino group of alkanolamines, the value of molar excess Gibbs energy increases (it becomes less negative). Figure 5.15 for (EAE + H_2O) shows positive value for excess Gibbs energy, which is highest among all the alkanolamine + water system. Very high excess Gibbs energy value (0.7 KJ) of (EAE + H_2O) system is a signature of strong non-ideality, which may be due to the formation of hydrogen bonds between ethanol group and water. The concerned figures show that with the amine mole fraction tends to 1.0, $\ln \gamma_{alkanolamines}$ tends to zero or it can be stated as activity coefficient of pure alkanolamine tends to 1.0. The COSMO predicted values of, NRTL, WILSON, UNIQUAC parameter for activity coefficients for alkanolamine + water system, and infinite dilution activity coefficients of amines in water are tabulated in the Tables 5.1 to 5.8 for aqueous MAE and EAE systems over the range of temperature studied. The amine activity coefficient is important because it affects the acid gas solubility in the equilibrium. In the measurement of the dissociation constants of protonated alkanolamines, the amines are treated as solutes with asymmetrically normalized activity coefficients. Using this reference state the activity coefficient of alkanolamine goes to unity at infinite dilution. For pure liquid reference state at system temperature and pressure for each solvent (amine and water) species, the solvent activity coefficients are defined to approach unity as the solvents approach their pure liquid states. The symmetrically normalized activity coefficient of the alkanolamine tends to a value (γ^{∞}_{amine}) other than unity unless the alkanolamine and water form an ideal pair. The protonated amine dissociation constant needs to be corrected to the pure amine reference state according to the symmetric normalization convention of the equilibrium constant. The correction to the equilibrium constant is related to the symmetrically normalized activity coefficient of the corresponding alkanolamine (γ^{∞}_{amine}) at infinite dilution in water (as discussed in section 2.8). An infinite dilution, the activity coefficient value for MDEA is greater than 1.0 (Chang et al. (1993); Kundu and Bandyopadhyay (2007)) like MAE and EAE (Tables 5.4 & 5.8). COSMO predicted values of all the thermodynamic properties can be considered to be an important contribution so far as the acid gas-alkanolamine-water system is concerned.

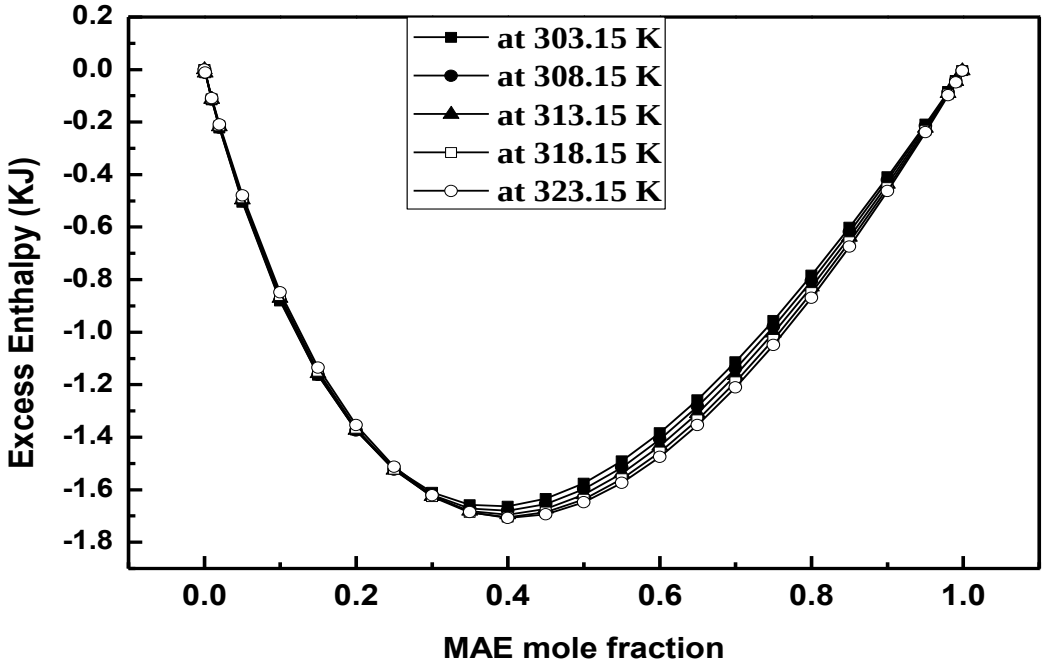

Figure 5.10: COMSO predicted Excess Enthalpy in (MAE + H_2O) system in the temperature range of 303.15 – 323.15 K.

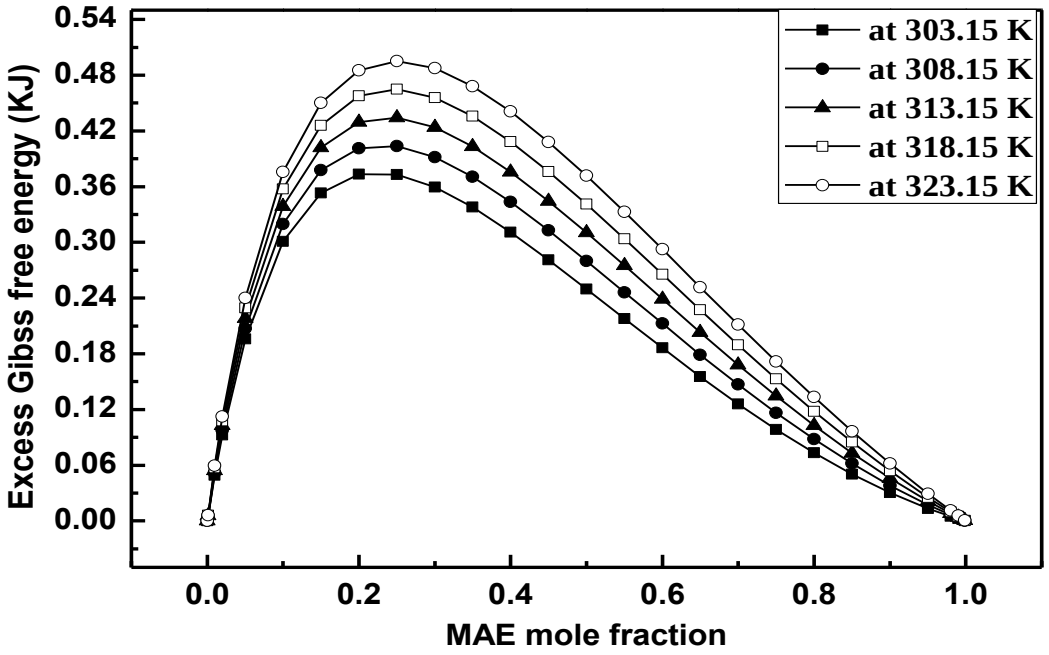

Figure 5.11: COMSO predicted Excess Gibbs free energy in (MAE + H_2O) system in the temperature range of 303.15 – 323.15 K.

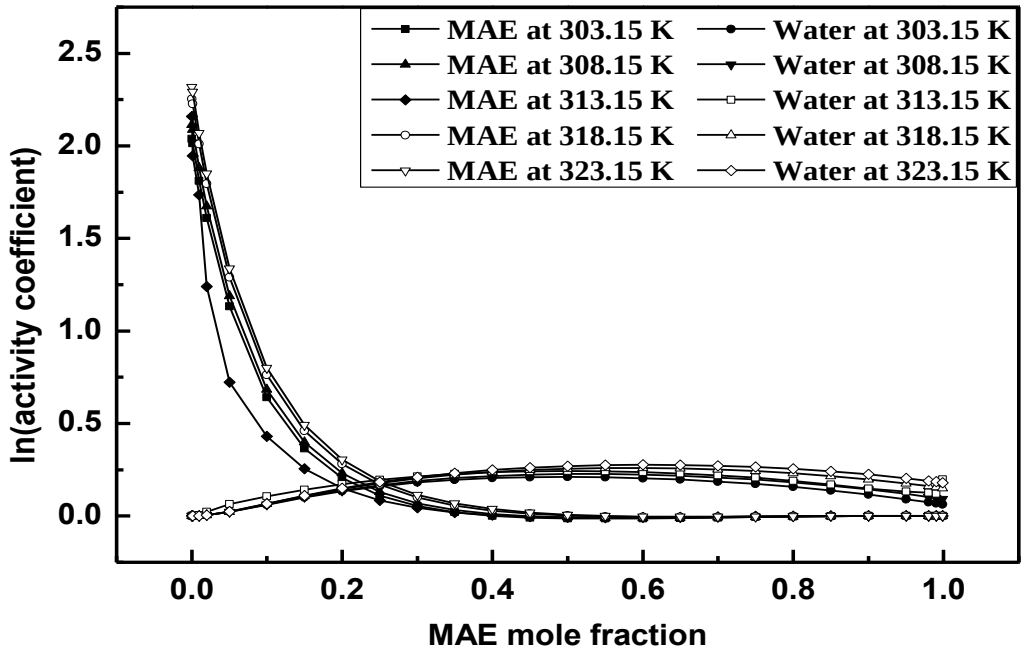

Figure 5.12: COMSO predicted MAE and water ln(activity coefficient) in (MAE + H_2O) system in the temperature range of 303.15 – 323.15 K.

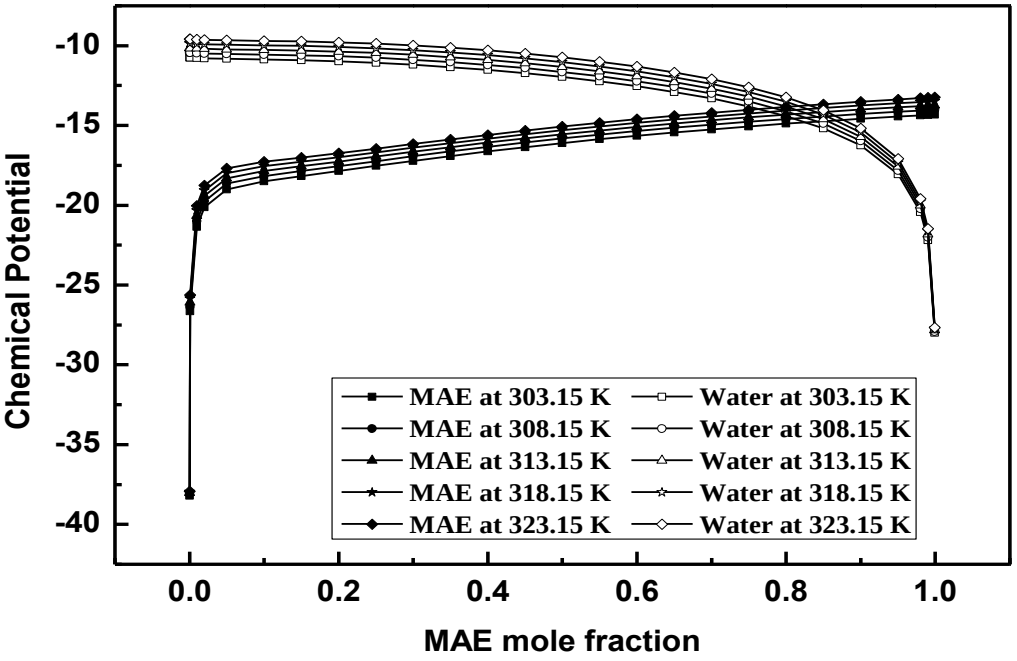

Figure 5.13: COMSO predicted MAE and water Chemical Potential in (MAE + H_2O) system in the temperature range of 303.15 – 323.15 K.

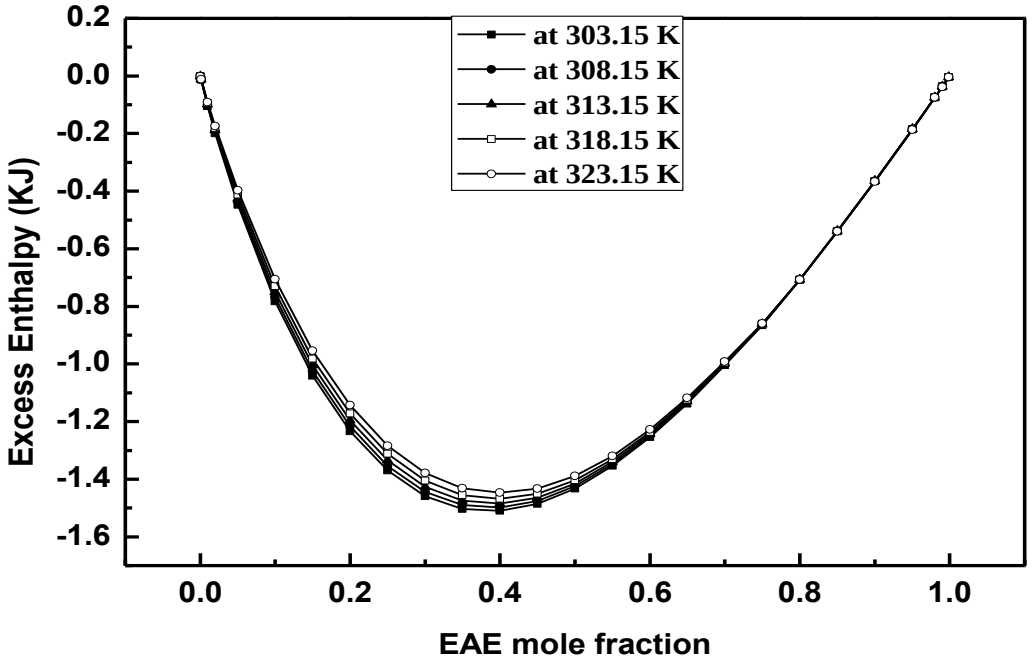

Figure 5.14: COMSO predicted Excess Enthalpy in (EAE + H_2O) system in the temperature range of 303.15 – 323.15 K.

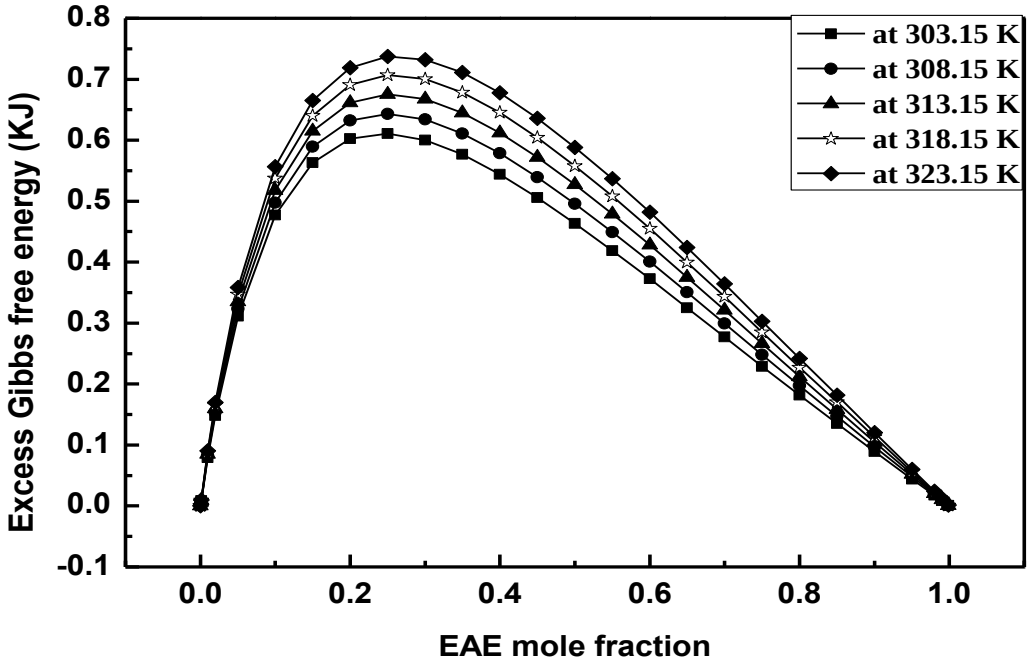

Figure 5.15: COMSO predicted Excess Gibbs free energy in (EAE + H_2O) system in the temperature range of 303.15 – 323.15 K.

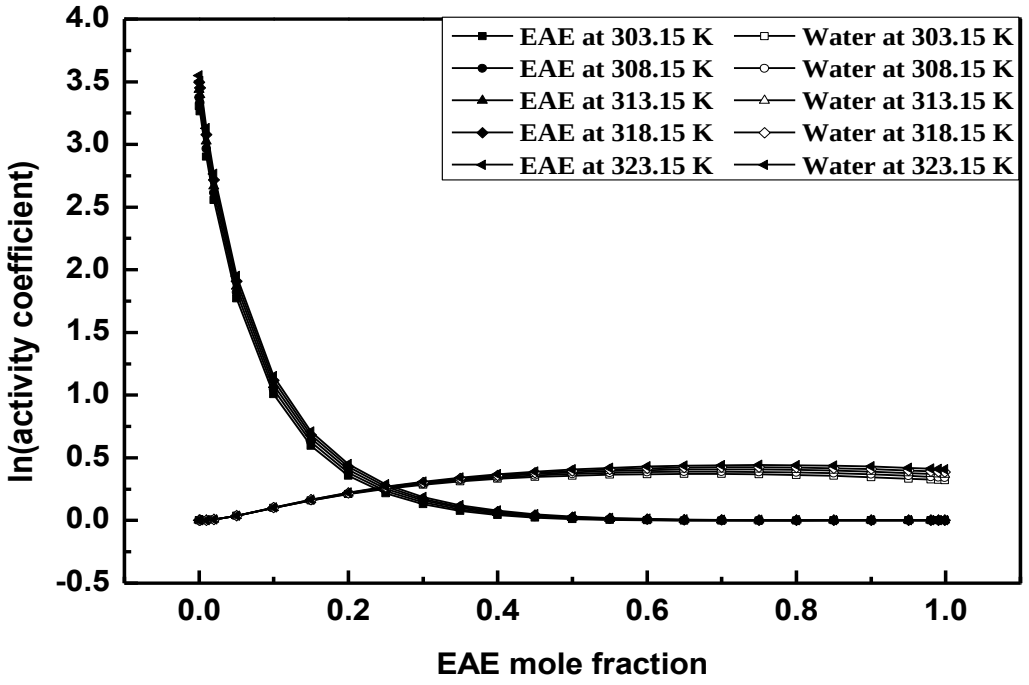

Figure 5.16: COMSO predicted EAE and water ln(activity coefficient) in (EAE + H_2O) system in the temperature range of 303.15 – 323.15 K.

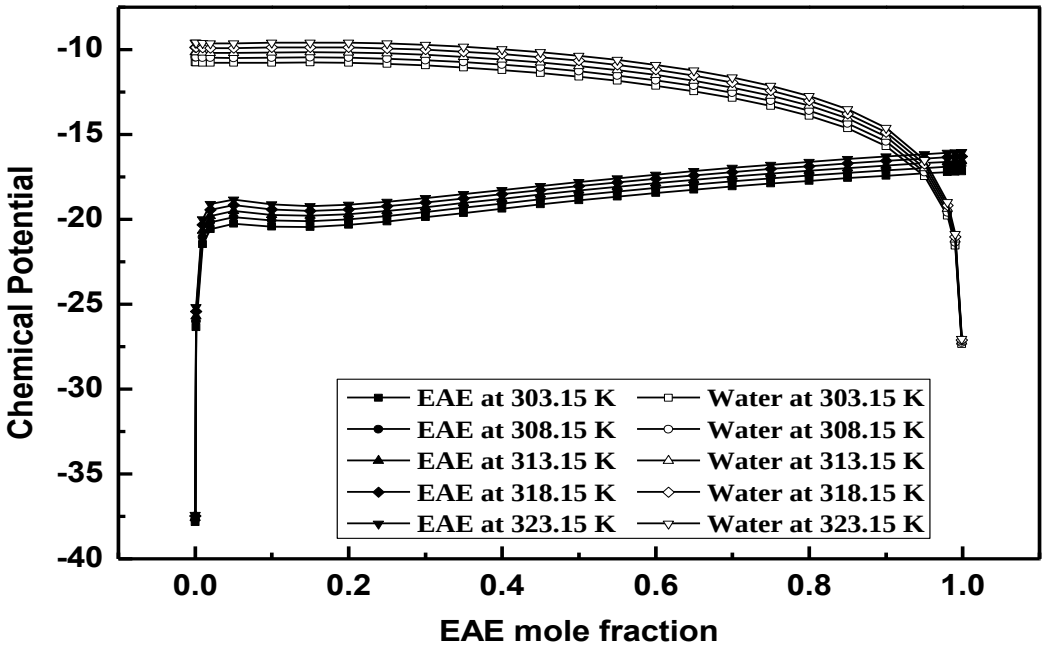

Figure 5.17: COMSO predicted EAE and water Chemical Potential in (EAE + H_2O) system in the temperature range of 303.15 – 323.15 K.

Table 5.1: COSMO predicted NRTL model parameters for the Activity Coefficients in (MAE + H_2O) system.

Temperature	***A***	$\tau_{12}{}^{a}$	$\tau_{21}{}^{b}$
303.15 K	0.3	-1.2266	3.75088
308.15 K	0.3	-1.19698	3.7676
313.15 K	0.3	-1.1792	3.78371
318.15 K	0.3	-1.3981	3.80121
323.15 K	0.3	-1.11038	3.80891

$\boldsymbol{a = \frac{g_{12} - g_{22}}{RT}}$, $\boldsymbol{b = \frac{g_{21} - g_{11}}{RT}}$

Table 5.2: COSMO predicted WILSON model parameters for the Activity Coefficients in (MAE + H_2O) system.

Temperature	$\lambda_{12}{}^{a}$	$\lambda_{21}{}^{a}$
303.15 K	0.22026	1.05118
308.15 K	0.0313	2.32767
313.15 K	0.07961	1.45416
318.15 K	0.15297	1.03381
323.15 K	0.1552	0.99812

$\boldsymbol{a = \lambda_{ij} = \frac{v_j}{v} i\, exp\left(-\frac{\lambda_{ij} - \lambda_{ii}}{RT}\right)}$

Table 5.3: COSMO predicted UNIQUAC model parameters for the Activity Coefficients in (MAE + H_2O) system.

Temperature	q_1	q_2	r_1	r_2	${\tau_{12}}^a$	${\tau_{21}}^b$
303.15 K	5.39484	2.05442	6.34185	1.35005	1.04531	1.24098
308.15 K	5.32084	2.02005	6.25656	1.32756	1.00362	1.263036
313.15 K	5.34557	2.00627	6.28733	1.31841	1.0095	1.23177
318.15 K	5.29686	1.875	6.23169	1.23214	1.02513	1.13809
323.15 K	5.34015	1.97407	6.28424	1.29725	1.00921	1.18964

$a = e^{-\Delta u_{12}/RT}$, $b = e^{-\Delta u_{21}/RT}$, r and q are structural parameters

Table 5.4: COSMO predicted Activity Coefficient of MAE at infinite dilution in water.

303.15 K	***308.15 K***	***313.15 K***	***318.15 K***	***323.15 K***
1.27555	2.03993	2.11784	2.19223	2.26301

Table 5.5: COSMO predicted NRTL model parameters for the Activity Coefficients in (EAE + H_2O) system.

Temperature	α	${\tau_{12}}^a$	${\tau_{21}}^b$
303.15 K	0.3	-0.97912	4.56439
308.15 K	0.3	-0.95219	4.59131
313.15 K	0.3	-0.92352	4.6041
318.15 K	0.3	-0.89703	4.62171
323.15 K	0.3	-0.87191	4.6395

$\boldsymbol{a = \frac{g_{12} - g_{22}}{RT}}$, $\boldsymbol{b = \frac{g_{21} - g_{11}}{RT}}$

Table 5.6: COSMO predicted WILSON model parameters for the Activity Coefficients in (EAE + H_2O) system.

Temperature	$\lambda_{12}{}^{a}$	$\lambda_{21}{}^{a}$
303.15 K	0.01402	1.95206
308.15 K	0.03241	1.11856
313.15 K	0.03038	1.10955
318.15 K	0.02837	1.09918
323.15 K	0.02739	1.08788

$$a = \lambda_{ij} = \frac{v_j}{v} i \, exp\left(-\frac{\lambda_{ij} - \lambda_{ii}}{RT}\right)$$

Table 5.7: COSMO predicted UNIQUAC model parameters for the Activity Coefficients in (EAE + H_2O) system.

Temperature	q_1	q_2	r_1	r_2	$\tau_{12}{}^{a}$	$\tau_{21}{}^{b}$
303.15 K	5.29206	1.43181	6.40967	0.94091	0.89129	0.91058
308.15 K	5.31132	1.44919	6.43491	0.95232	0.088632	0.91729
313.15 K	5.33515	1.48158	6.46571	0.97361	0.90992	0.90859
318.15 K	5.25906	1.44399	6.37537	0.9489	0.86853	0.90806
323.15 K	5.2619	1.42968	6.38067	0.9395	0.81794	0.93597

$a = e^{-\Delta u_{12}/RT}$, $b = e^{-\Delta u_{21}/RT}$, **r and q are structural parameters**

Table 5.8: COSMO predicted activity coefficient of EAE at infinite dilution in water.

303.1 5K	***308.15 K***	***313.15 K***	***318.15 K***	***323.15 K***
3.3259	3.39504	3.45989	3.52068	3.57686

5.4.2 Ternary Solution

COSMO predicted excess enthalpy, Gibbs free energy and activity coefficient of (CO_2 + MAE + H_2O) and (CO_2 + EAE + H_2O) systems against CO_2 mole fraction are shown in Figures 5.18-5.29 at fixed amine mole fractions of 0.05 and 0.1. With the addition of CO_2, the non-ideality of the system changes thus, the thermodynamic parameters are plotted against CO_2 mole fraction; an indication of changing solution CO_2 loading. COSMO simulated results corresponding to 0.05 and 0.1 mole fraction of MAE/EAE actually signifies alkanolamine solution concentrations relevant for CO_2 removal (containing less than 0.3 mass fractions of EAE in aqueous solutions). As the temperature increases, the excess Gibbs energy and enthalpy tends towards values that are more positive. As the CO_2 mole fractions tends to 0.5, excess enthalpy and Gibbs free energy of the ternary solutions tend to their maxima and minima for MAE/EAE activity coefficient, which are the signatures of non-ideality of the solution undergoing chemical reaction and vapor-liquid phase equilibrium.

Figures 5.30-5.31 show the COSMO predicted gas phase mole fractions of CO_2 versus liquid phase CO_2 mole fraction is depicted at fixed EAE mole fractions. Figure 5.30 shows three distinct segments. In the first segment liquid phase mole fraction increases with increasing gas phase CO_2 mole fractions; a signature of physical equilibrium. In the second segment, liquid phase CO_2 mole fraction increases without increment in gas phase CO_2 mole fractions; rather gas phase CO_2 mole fractions are decreasing, which signifies enhanced role of chemical reaction equilibria over physical equilibria. The last segment again emancipates physical equilibrium. As the alkanolamine mole fraction increases in the ternary solutions (Figure 5.31, where EAE mole fractions is 0.1), this distinct delineation among vapor-liquid phase equilibrium and chemical reaction equilibrium remains but the advantage of chemical reaction equilibria is becoming bleak. The observations from Figure 5.32 shows the gas phase mole fraction of CO_2 versus liquid phase CO_2 mole fractions depicted at fixed EAE mole fraction of 0.08 (using our own experimental data. Figures 5.30-5.32 affirm the fact, that at lower EAE concentration (say, EAE mole fraction is 0.05), we get maximum CO_2 loading in the liquid phase without a substantial increment in equilibrium CO_2 pressure. This benefit of chemical reaction equilibria is realizable for a solution containing less than 0.1 mole fraction of EAE. Hence, according to COSMO, aqueous MAE and EAE solutions containing 0.06-0.3 mass fractions of alkanolamine can be considered as potential solvents for effective CO_2

removal. The MAE and EAE solution thermodynamics change with the addition of CO_2 and that have been depicted here. The ternary solution activity coefficients obtained through COSMO calculations can be used to regress the binary/ternary interaction parameters of the concerned ternary system in developing activity coefficient based models. Total pressure data of (CO_2 + EAE + H_2O) system was simulated using COSMOtherm but it was always higher than my own; calculated based on my experimentation.

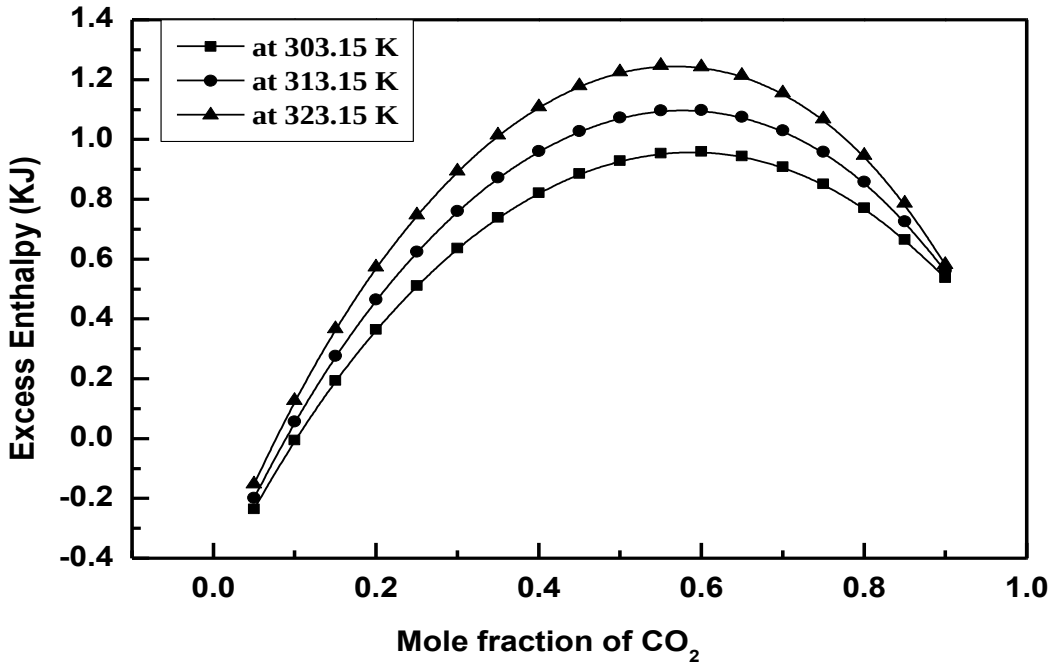

Figure 5.18: COMSO predicted Excess Enthalpy in (CO_2 + MAE + H_2O) system in the temperature range of 303.15 – 323.15 K at 0.05 MAE mole fractions.

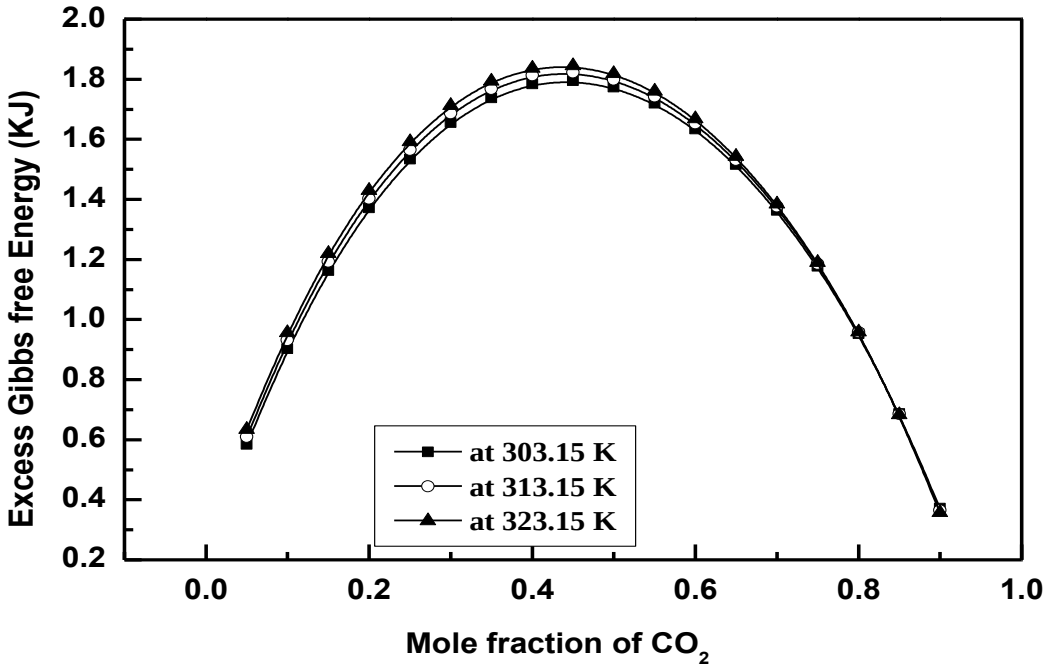

Figure 5.19: COMSO predicted Excess Gibbs free energy in (CO_2 + MAE + H_2O) system in the temperature range of 303.15 – 323.15 K at 0.05 MAE mole fractions.

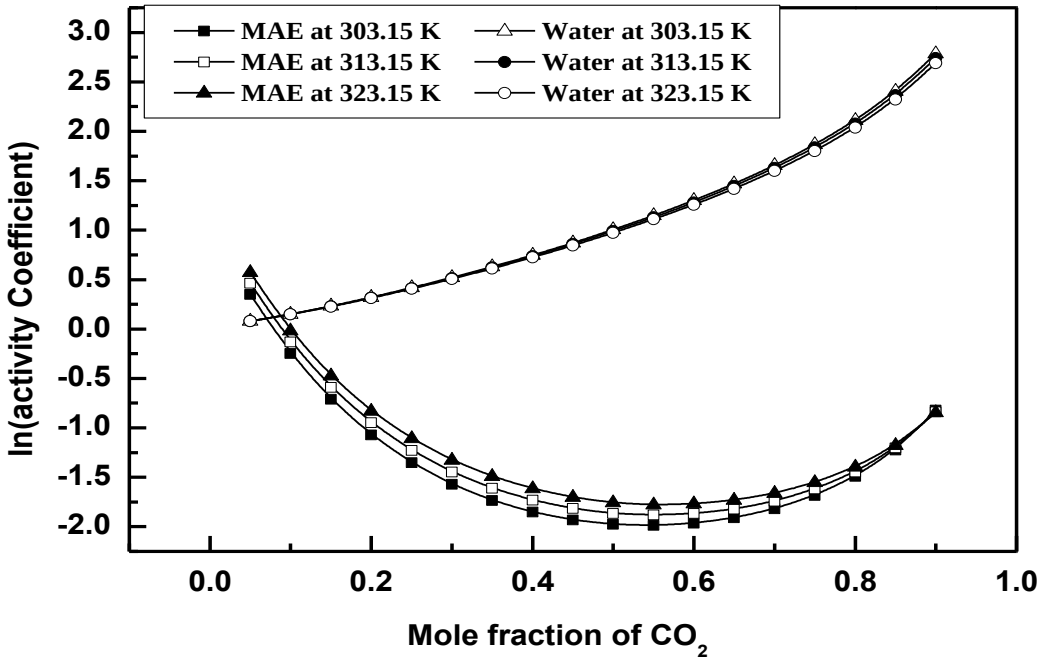

Figure 5.20: COMSO predicted MAE and water ln(activity coefficient) in (CO_2 + MAE + H_2O) system in the temperature range of 303.15 – 323.15 K at 0.05 MAE mole fractions.

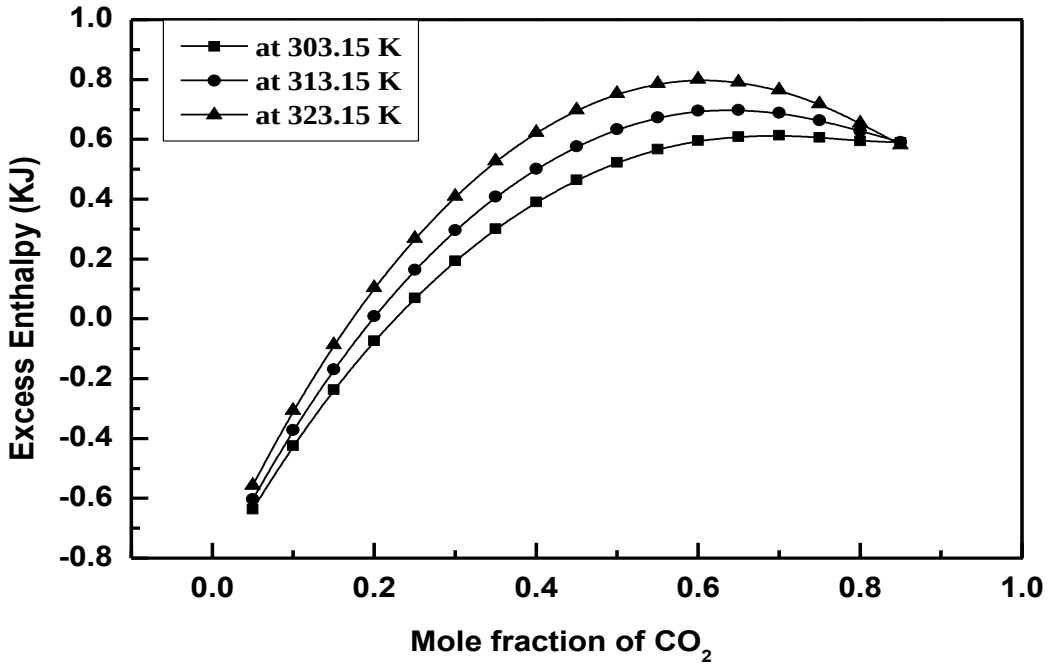

Figure 5.21: COMSO predicted Excess Enthalpy in (CO_2 + MAE + H_2O) system in the temperature range of 303.15 – 323.15 K at 0.1 MAE mole fractions.

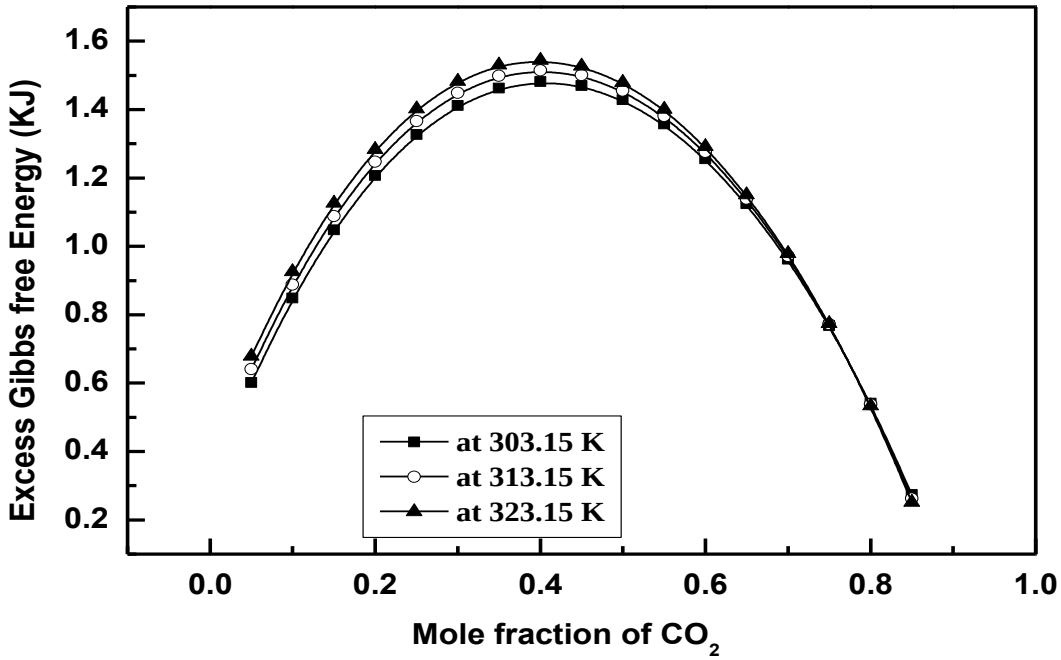

Figure 5.22: COMSO predicted Excess Gibbs free energy in (CO_2 + MAE + H_2O) system in the temperature range of 303.15 – 323.15 K at 0.1 MAE mole fractions.

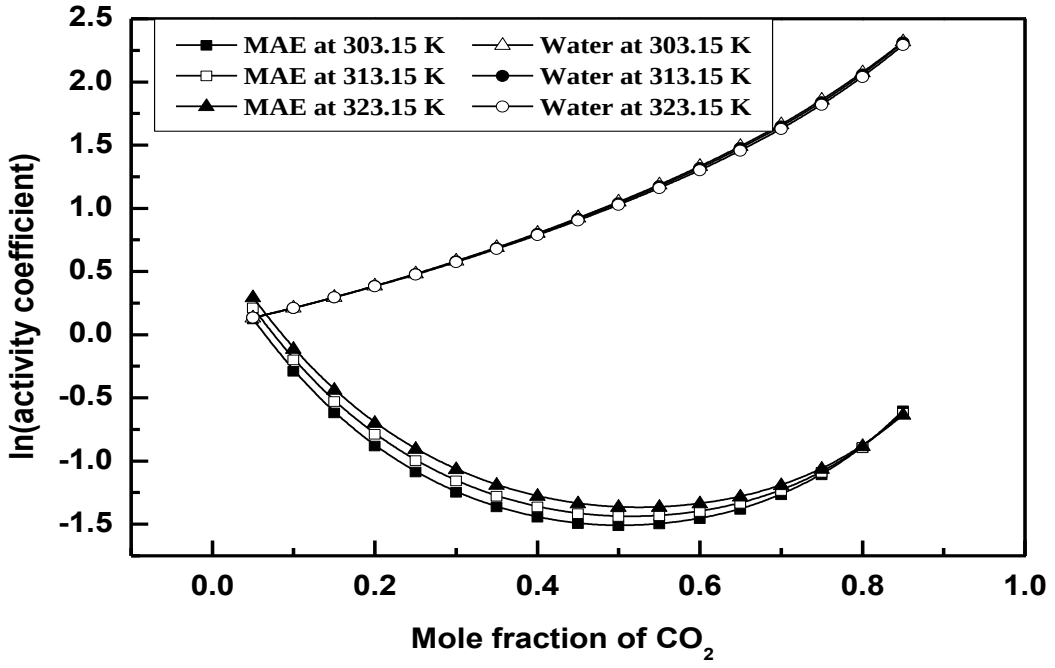

Figure 5.23: COMSO predicted MAE and water ln(activity coefficient) in (CO_2 + MAE + H_2O) system in the temperature range of 303.15 – 323.15 K at 0.1 MAE mole fractions.

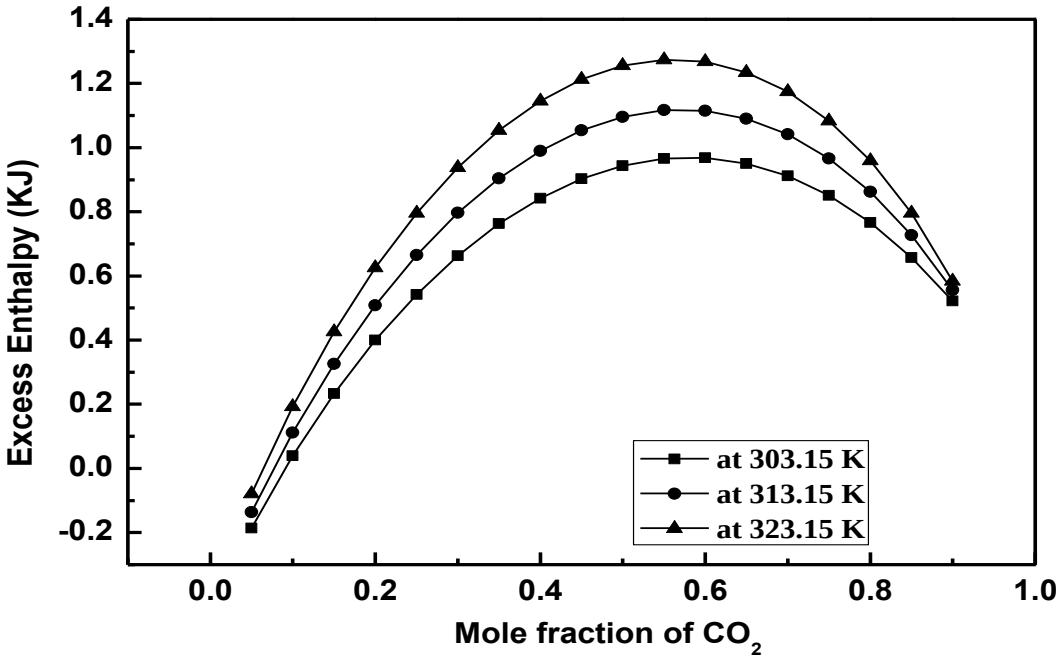

Figure 5.24: COMSO predicted Excess Enthalpy in (CO_2 + EAE + H_2O) system in the temperature range of 303.15 – 323.15 K at 0.05 EAE mole fractions.

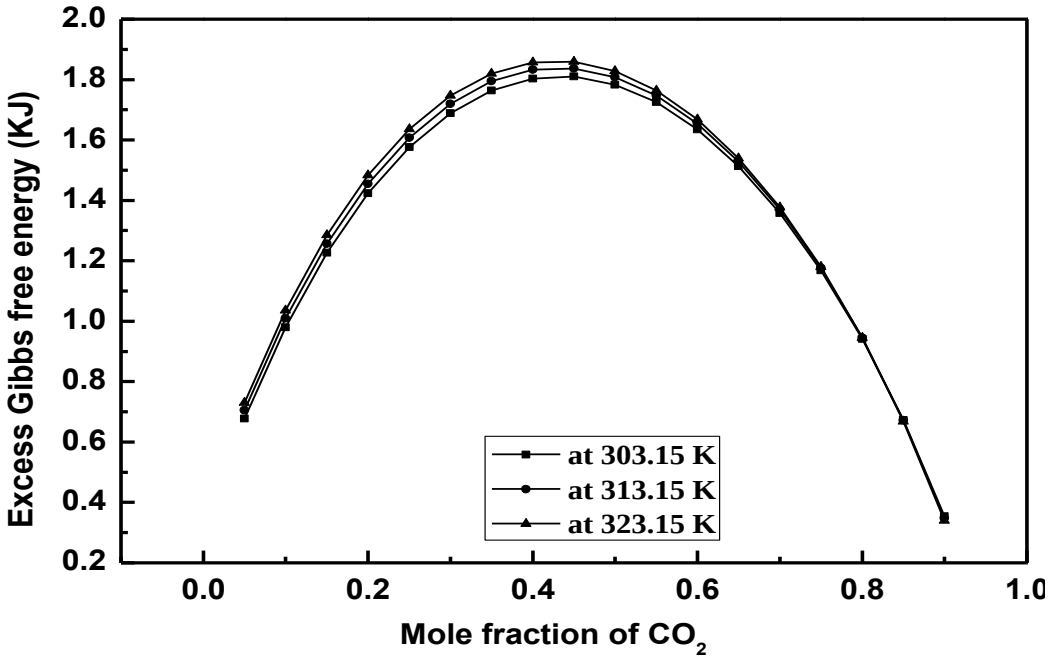

Figure 5.25: COMSO predicted Excess Gibbs free energy in (CO_2 + EAE + H_2O) system in the temperature range of 303.15 – 323.15 K at 0.05 EAE mole fractions.

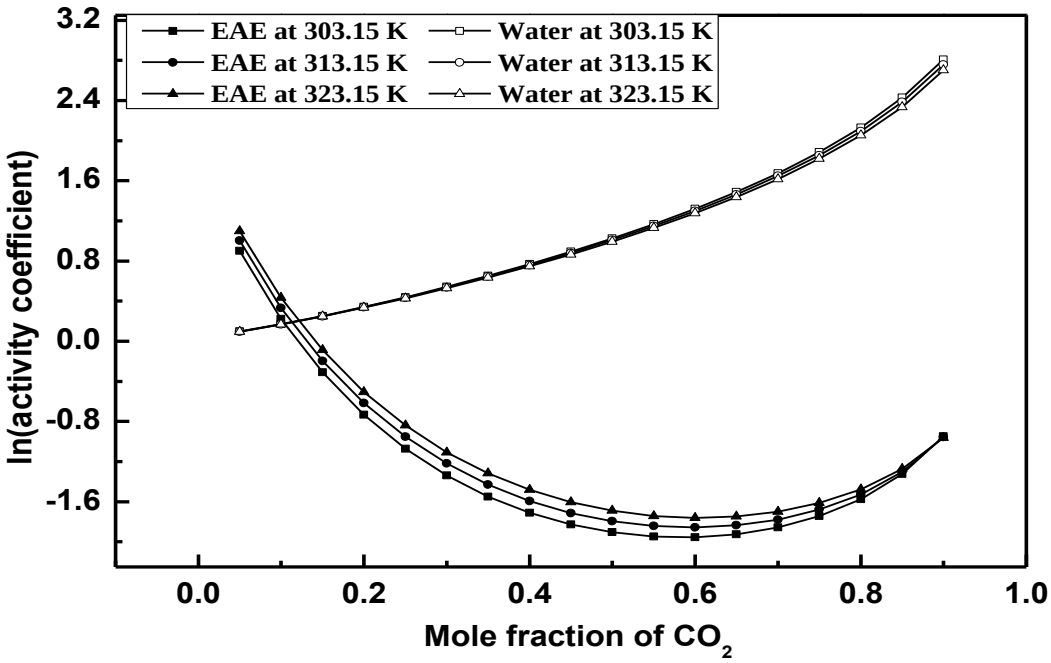

Figure 5.26: COMSO predicted EAE and water ln(activity coefficient) in (CO_2 + EAE + H_2O) system in the temperature range of 303.15 – 323.15 K at 0.05 EAE mole fractions.

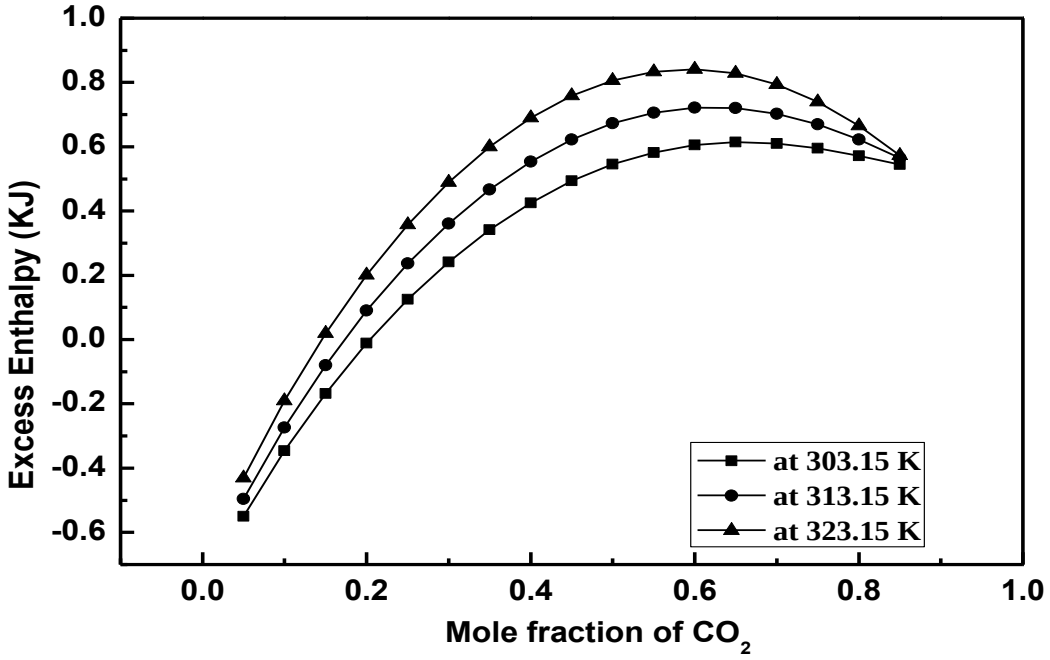

Figure 5.27: COMSO predicted Excess Enthalpy in (CO_2 + EAE + H_2O) system in the temperature range of 303.15 – 323.15 K at 0.1 EAE mole fractions.

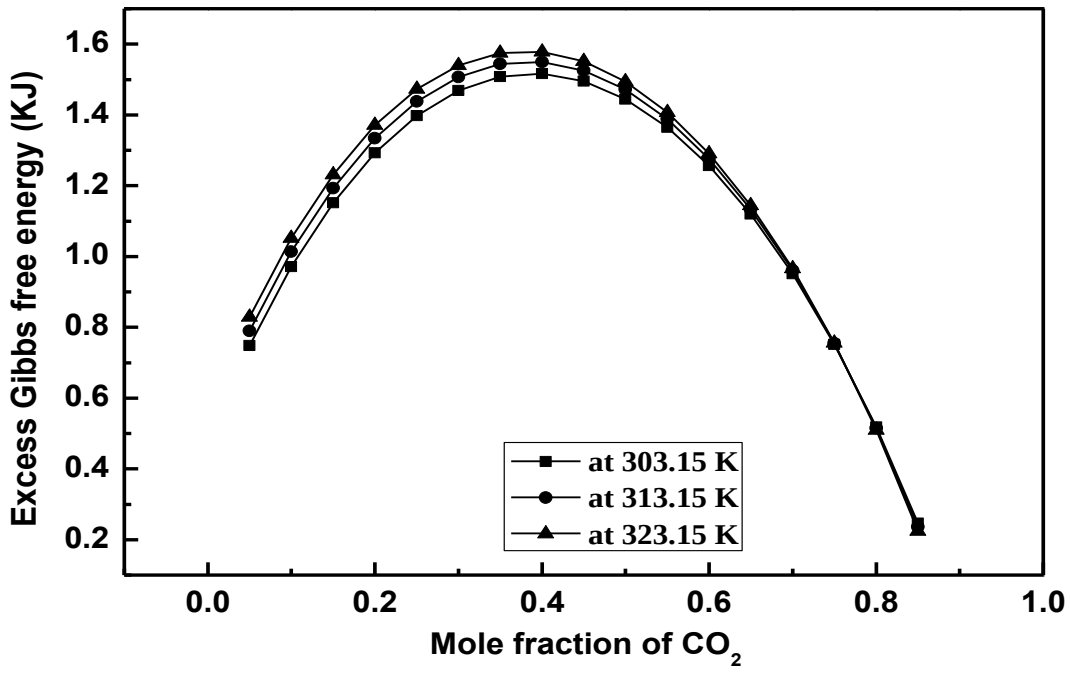

Figure 5.28: COMSO predicted Excess Gibbs free energy in (CO_2 + EAE + H_2O) system in the temperature range of 303.15 – 323.15 K at 0.1 EAE mole fractions.

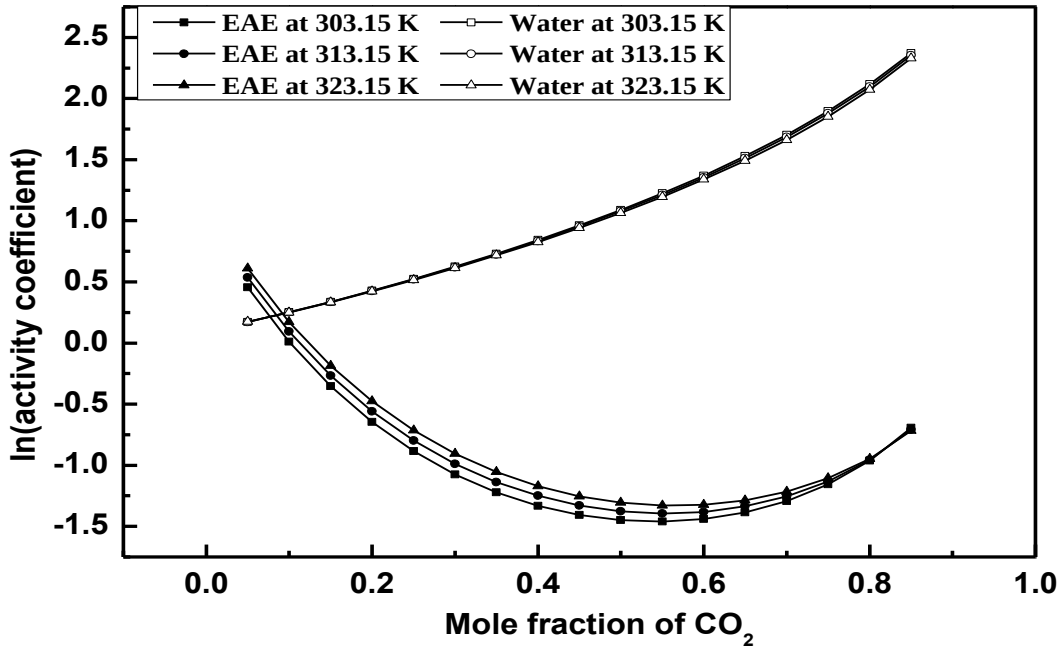

Figure 5.29: COMSO predicted EAE and water ln(activity coefficient) in (CO_2 + EAE + H_2O) system in the temperature range of 303.15 – 323.15 K at 0.1 EAE mole fractions.

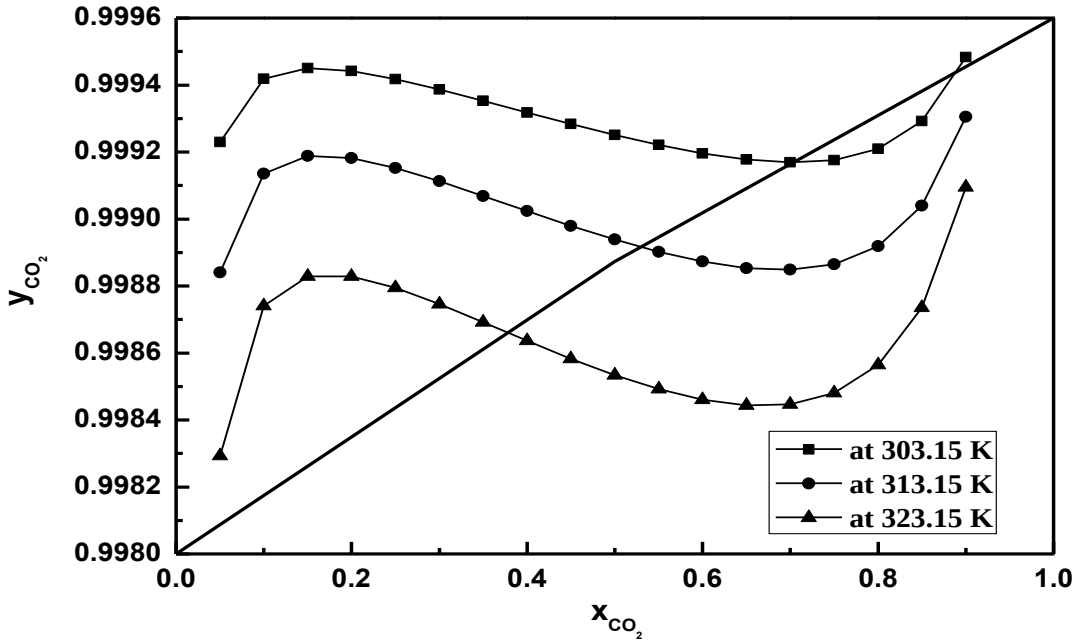

Figure 5.30: COSMO predicted Gas phase versus liquid phase mole fraction of CO_2 in (CO_2 + EAE + H_2O) system (0.05 EAE mole fractions) at temperature range of 303.15-323.15 K.

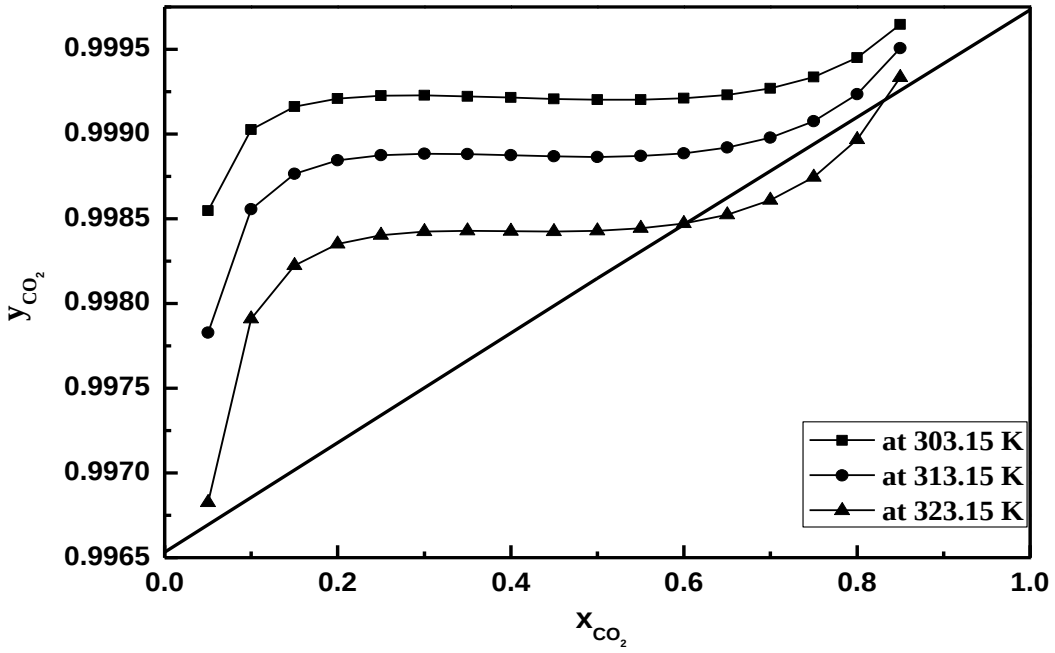

Figure 5.31: COSMO predicted Gas phase versus liquid phase mole fraction of CO_2 (CO_2 + EAE + H_2O) system (0.1 EAE mole fractions) at temperature range of 303.15-323.15 K.

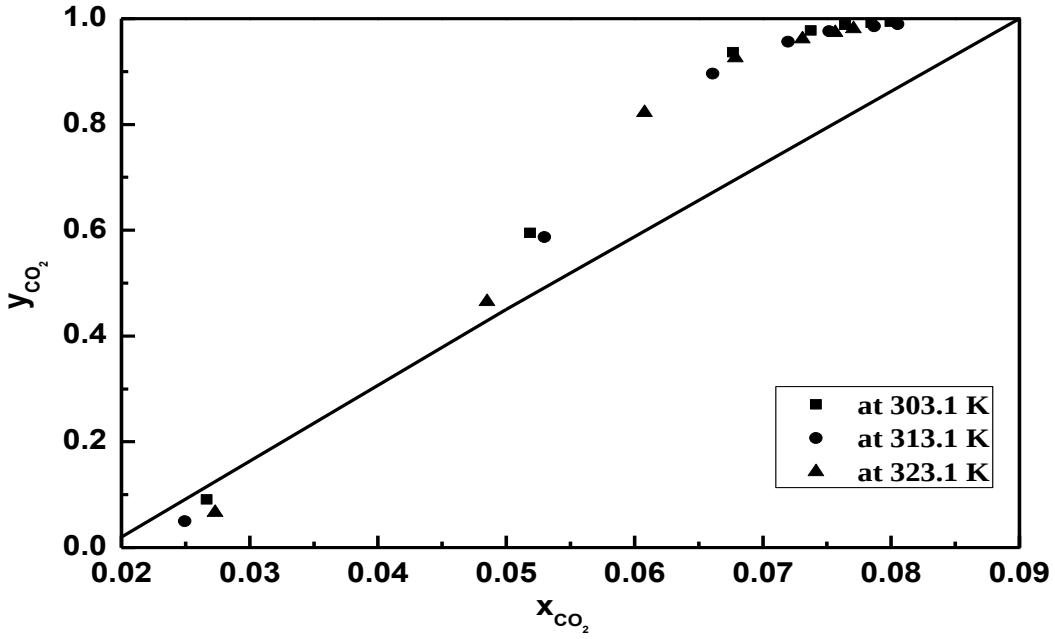

Figure 5.32: Experimentally calculated Gas phase versus liquid phase mole fraction of CO_2 (CO_2 + EAE + H_2O) system (0.08 EAE mole fraction= 30 wt% amine) at temperatures 303.1-323.1 K.

REFERENCES

Banerjee, T. (**2006**). Ionic liquids- Phase equilibria and thermodynamic property predictions using molecular modelling and dynamics, and their validations with experiments. Ph.D. Thesis. Indian Institute of Technology, Kanpur.

Ben-Naim, A. (**1987**). Solvation Thermodynamics, Plenum Press, New York.

Chang, H.T., Posey, M., and Rochelle, G.T. (**1993**). Thermodynamics of alkanolamine- water solutions from freezing point measurements. *Industrial and Engineering Chemistry Research*, 32, 2324- 2335.

Clausen, I. and Arlt, W. (**2000**). A priori calculation of phase equilibria for the thermal process technology with COSMO-RS. *Chemie Ingenieur Technik*, 72, 727-733.

Diedenhofen, M., Eckert, F. and Klamt, A. (**2002**). Prediction of infinite dilution activity coefficients of organic compounds in ionic liquids using COSMO-RS. *Journal of Chemical and Engineering Data*, 48, 475-479.

Diedenhofen, M., Eckert, F. and Klamt, A. **(2003).** Prediction of Infinite Dilution activityCoefficients of Organic Compounds in Ionic Liquids Using COSMO-RS. *Journal of Chemical and Engineering Data*, 48, 475-479.

Eckert, F. and Klamt, A. (**2005**). COSMOtherm. Version C2.1, Release 01.07, COSMOlogic GmbH & Co. Kg, Leverkusen, Germany.

Eckert, F., Leito, I., Kaljurand, I., KÜtt, A., Klamt, A. and Diedenhofen, M. (**2009**). Prediction of acidity in Acetonitrile solution with COSMO-RS. *Journal of Computational Chemistry*, 30, 799-810.

Eckert, F.; Klamt, A. (**2001**). Validation of the COSMO-RS Method: Six Binary Systems. *Industrial and Engineering Chemistry Research*, 40, 2371.

Eckert, F.; Klamt, A. (**2005**), COSMOtherm.Version C2.1, Release 01.07, COSMOlogic GmbH & Co. Kg, Leverkusen, Germany.

Franke, R., Krissmann, J. and Janowsky, R. (**2002**). What should the process engineer of COSMO-RS expect?. *Chemie Ingenieur Technik*, 74, 85-89.

Gazawi, A. (**2007**). Evaluating COSMO-RS for vapour liquid equilibrium and TURBOMOLE for ideal gas properties. M.Sc. Thesis. The graduate faculty of the university of Akron.

Goss, K.U. and Arp, H.P.H. (**2009**). Ambient gas / Particle partitioning. 3. Estimating partition coefficients of Apolar, Polar, and Ionizable organic compounds by their molecular structure. *Environmental Science and Technology*, 43, 1923-1929.

Klamt, A. (**1995**). Conductor-like Screening Model for Real Solvents: A New Approachto the Quantitative Calculation of Solvation Phenomena. *Journal of Physical Chemistry A*, 99, 2224.

Klamt, A. and Eckert, F. (**2000**). COSMO-RS: A novel and efficient method for the priori prediction of thermo physical data of liquids. *Fluid Phase Equilibria*, 172, 43-72.

Klamt, A. and Eckert, F. (**2004**). Prediction of vapor liquid equilibria using COSMOtherm. *Fluid Phase Equilibria*, 217, 53-57.

Klamt, A. and Smith, B.J. (**2008**). Challenge of drug solubility prediction. Mannhold Raimund (ed.)- Molecular Drug Properties Measurement and Prediction, Weinheim: John Wiley & Sons; 283-311.

Klamt, A., and Schüürmann, G. (**1993**). COSMO: A New Approach to Dielectric Screening in Solvents with Explicit Expressions for the Screening Energy and its Gradient. *Journal of Chemical Society*, Perkin Trans. II, 799-805.

Klamt, A., Arlt, W. and Eckert, F. (**2010**). COSMO-RS: An alternative to simulation for calculating thermodynamic properties of liquid mixtures. *Annual Reviews of Chemical and Biomolecular Engineering*, 1, 101-122.

Klamt, A., Eckert, F., Diedenhofen, M. and Beck, M.E. (**2003**). First principles calculations of aqueous pKa values for organic and inorganic acids using COSMO-RS reveal an inconsistency in the slope of the pKa. *The journal of Physical Chemistry A*, 107, 9380-9386.

Klamt, A., Jonas, V., Buerger, T. and Lohrenz, J. **(1998).** Refinement and Parameterization of COSMO-RS. *Journal of Physical Chemistry A*, 102, 5074.

Klamt, A., Krooshof, G. J. P. and Taylor, R. (**2002**), COSMOSPACE: alternative to conventional activity-coefficient models, *AIChE Journal*, 48(10), 2332.

Kundu, M. (**2004**). Vapour-Liquid Equilibrium of Carbon Dioxide in Aqueous Alkanolamines. Ph. D. Dissertation, IIT Kharagpur.

Kundu, M. and Bandyopadhyay, S.S. (**2006**). Solubility of CO_2 in water + diethanolamine + N-methyldiethanolamine. *Fluid Phase Equilibria*, 248, 158-167.

Kundu, M. and Bandyopadhyay, S.S. (**2006**). Solubility of CO_2 in water + diethanolamine + 2-Amino-2-methyl-1-Propanol. *Journal of Chemical and Engineering Data*. 51, 398-405.

Kundu, M. and Bandyopadhyay, S.S. (**2007**). Thermodynamics of alkanolamine and water system. *Chemical Engineering Communication*. 194, 1138-1159.

Li, Y.G., and Mather, A.E. (**1994**). The correlation and prediction of the solubility of carbon dioxide in a mixed alkanolamine solution. *Industrial and Engineering Chemistry Research*, 33, 2006-2015.

Li, Y.G., and Mather, A.E. (**1997**). Correlation and prediction of the solubility of CO_2 and H_2S in aqueous solutions of methyldiethanolamine. *Industrial and Engineering Chemistry Research*, 36, 2760-2765.

Marsh, K.N., Deev, A., Wu, A.C.T., Tran, E. and Klamt, A. (**2002**). Room temperature ionic liquids as replacements for conventional solvents -A review. *Korean Journal of Chemical Engineering*, 19, 357-362.

Mustapha, S.I., Okonkwo, P.C. and Waziri, S.M. (**2013**). Improvement of CO_2 absorption technology using conductor- like screening model for real solvents (COSMO-RS) method. *Journal of Environmental Chemistry and Ecotoxicology*, 5, 96-105.

Niederer, C. and Goss, K.U. (**2007**). Quantum chemical modeling of Humic acid / Air equilibrium partitioning of organic vapors. *Environmental Science and Technology*, 41, 3646-3652.

Putnam, R., Taylor, R., Klamt, A., Eckert, F. and Schiller, M. **(2003).** Prediction of infinite dilution activity coefficients using COSMO-RS. *Industrial and Engineering Chemistry Research*, 42, 3635-3641.

Skau, E.L., Aurther, J. C., Jr. (**1971**). Determination of melting and freezing temperatures. In techniques of chemistry, vol *I*. Physical methods of Chemistry; Weissberger, A., Rossiter, B. W., Eds.; Wiley-Interscience: New York, NY, 1971, Part V, Chapter 3.

Wichmann, K., David, J. am Ende, and Klamt, A. (**2010**). Drug solubility and reaction thermodynamics. Chemical Engineering in the Pharmaceutical Industry: R&D to Manufacturing, *John Wiley & Sons*; 457-476.

Yamada, H., Yoichi, M., Higashii, T. and Kazama, S. (**2011**). Density Functional Theory Study on Carbon Dioxide Absorption into Aqueous Solutions of 2-Amino-2-methyl-1-propanol Using a Continuum Solvation Model. *The journal of Physical Chemistry A*, 115, 3079-3086.

Chapter 6

Density of Aqueous Blended Alkanolamines

Chapter 6

DENSITY OF AQUEOUS BLENDED ALKANOLAMINE SOLUTIONS

6.1 INTRODUCTION

For effective removal of CO_2, some new alkanolamine blends like (MAE + AMP/MDEA + H_2O) and (EAE + AMP/MDEA + H_2O) have been proposed in the present dissertation. For the rational design of absorbers/strippers and its operation, knowledge of the physical properties of process solutions is necessary.

A few density data for (MAE + AMP/MDEA + H_2O) and (EAE + AMP/MDEA + H_2O) have been reported in the literature (Alvarez *et al*., 2006, 2008, Li *et al.*, 2007 and Venkat *et al.,* 2010). Alvarez *et al.,* 2006 presented the densities and kinematic viscosities of aqueous ternary solutions of 2-(methylamino) ethanol and 2-(ethylamino)-ethanol with diethanolamine, Triethanolamine, N-methyldiethanolamine and 1-amino-1-methyl-1-propanol at temperature range of 298.15-323.15 K. they varied the mass % ratio from 0/50 to 50/0, in 10 mass % steps and total amine concentration was 50 mass %.

In this chapter, densities of aqueous ternary mixtures of (MAE + AMP), (MAE + MDEA), (EAE + AMP) and (EAE + MDEA) at temperature (298.15, 303.15, 308.15, 313.15, 318.15, 323.15) K have been measured for (MAE)/ (AMP or MDEA) mass % ratios of 3/27, 6/24, 9/21 and 12/18 and for (EAE)/ (AMP or MDEA) mass % ratios of

6/24, 9/21, 12/18, 15/15, 18/12, 24/6 and 30/0. Density of the ternary mixtures were correlated as a function of temperature and amine composition.The total amine concentration was held constant at 30 mass %

6.2 EXPERIMENTAL SECTION

6.2.1 Materials

All amines have been supplied by Merck, with a purity of > 98 % for 2-(methylamino) ethanol (MAE), > 97 % for 2-(Ethylamino) ethanol (EAE), > 98 % for Methyldiethanolamine (MDEA) and > 95 % for 2-Amino-2-methyl-1-propanol (AMP). Distilled water degassed by boiling was used for making the amine solutions. The total amine contents of the solutions were determined by titration with standard HCl using methyl orange indicator. The uncertainty in the composition of the amine solution was estimated as ± 0.007 %.

6.2.2 Procedure

The densities of the amine solutions were measured using a 25.3 mL Gay-Lussac pycnometer. The pycnometer containing the amine solution was immersed in a constant temperature bath. The bath temperature was controlled within ± 0.05 K of the desired temperature using a circulator temperature controller (Polyscience, USA model No: 9712). The desired temperature of the amine solutions was checked with Pt 100 temperature sensor. Once the solution reached the desired temperature, it was weighed to within ± 0.001 g with an analytical balance. The uncertainty in the measurement of temperature was ± 0.04 K. Each reported density data was the average of three measurements. The average absolute deviations (AADs) for the density measurements with respect to the results reported in the literature are shown in Table 6.1. The uncertainty in the measured density was estimated to be 7.7×10^{-4} g.cm^{-3} (expanded uncertainty; for coverage factor k = 2).

To validate the pycnometer and the experimental procedure of the measurement, the densities of pure and aqueous MAE solutions of mass percentage (10, 25, 17.8, 40) were measured at (298.15 to 323.15) K and compared with the values reported by Alvarez *et al*. 2006 and Li *et.al*. 2007. The density values for aqueous MAE solutions are within a range of ± 0.003 to the interpolated values of Li *et.al.* and are presented in Table 6.1. The average absolute deviation in the density measurements of pure MAE and 17.8 % aqueous

MAE solutions in comparison to the data reported by Alvarez *et al.* and Li *et.al*. were found to be 0.15 % and 0.12 %, respectively.

6.3 MODELLING

The excess molar volumes were correlated by using the Redlich-Kister (R- K) equation:

$$V_{jk}^{E}\Big/_{(mL.\ mol^{-1})} = x_j x_k \sum_{i=0}^{n} A_i \left(x_j - x_k\right)^i \quad (6.1)$$

Where A_i are pair parameters and are assumed to be temperature dependent,

$$A_i = a + b(T/K) + c(T/K)^2 \quad (6.2)$$

The excess molar volume of liquid mixtures for a ternary system is given by

$$V^E = V_{12}^E + V_{13}^E + V_{23}^E \quad (6.3)$$

The excess volume of the liquid mixtures (binary/ternary) can be determined from the experimentally measured molar volume (or density) of binary/ternary liquid mixtures along with the pure component molar volume of the constituent liquids in the mixture as per Eq. (6.4)

$$V^E = V^m - \sum x_i \,.V_i^0 \quad (6.4)$$

Where V_m is the molar volume of the liquid mixture (binary/ternary) and V_i^o is the molar volume of the pure component liquid in the mixture at the system temperature.

The molar volume of the liquid mixture from experimentally measured density is calculated by

$$V_m = \frac{\sum x_i M_i}{\rho_m} \quad (6.5)$$

Where M_i is the molar mass of pure component i; ρ_m is the measured liquid density and x_i is the mole fraction of the pure component i. By Eq. 6.3 and Eq. 6.4, one can obtain the requisite binary interaction parameters (A_i).

A Nissan type of equation has been used here to correlate the ternary data of (MAE + AMP + H_2O) and (MAE + MDEA + H_2O) systems. The density of liquid mixtures can also be calculated by this alternative Eq. (6.6).

$$\rho_m = \sum_{i=1}^{n} x_i \rho_i + \sum_{i \neq j} A_{ij} x_i x_j \quad (6.6)$$

Where, A_{ij} are the binary interaction parameters and ρ_m is the density of the ternary mixture.

6.4 RESULTS AND DISCUSSIONS

6.3.1 (MAE (1) + AMP/MDEA (2) + H_2O (3)) System

The measured densities of the solutions of (MAE (1) + AMP (2) + H_2O (3)), and (MAE (1) + MDEA (2) + H_2O (3)) temperature range of (298.15 to 323.15) K are presented in the Tables 6.2 and 6.3, respectively, keeping the total amine mass percentage constant at 30 % with *w* is the mass fraction of each individual amine present in the solution.

A general set of temperature dependent R-K parameters for the (MAE + H_2O) binary system have been developed considering 62 number of data points including experimental data generated in this work in the temperature range of (298.15 to 323.15) K and the data of Li et al. over the entire composition range with a correlation deviation of 0.104 % and are presented in Table 6.4. A set of temperature dependent parameters for (AMP + H_2O) binary system have been developed with a correlation deviation of 0.033 % and are presented in Table 6.5 considering 66 number of data points from Henni *et al.* over the entire composition range and in the temperature range of (298.15 to 343.15) K. A general set of temperature dependent (MAE + AMP) binary interaction parameters have been developed considering (MAE + AMP + H_2O) ternary system data generated in this work in the temperature range of (298.15 to 323.15) K with a correlation deviation of 0.0046 % and are presented in Table 6.6 . The correlated ternary densities for the (MAE + AMP + H_2O) system are in reasonable agreement with respect to the measured densities as reflected in the AAD % of 0.1 between the measured and correlated data by R – K equation, where AAD % is the average absolute deviation percentage in

$$density = \left(\left[\sum_{n} \left(\rho_{m,cal} - \rho_{m,exp} \right) / \rho_{m,exp} \right] / n \times 100 \right)$$

n = number of data

A Nissan type of equation (Eq. 6.6) was used to correlate the ternary (MAE + AMP + H_2O) density data with a correlation deviation of 0.023 %. The resulting set of temperature-dependent fitting parameters is reported in Table 6.7.

A general set of temperature-dependent R-K parameters for (MDEA + H_2O) binary system have been developed with a correlation deviation of 0.082 % considering 33 data points taken from Al-Ghawas *et al*. in the temperature range (298.15 to 323.15) K and MDEA mass fraction range of 0.10 to 0.50, and these are presented in Table 6.8. The (MAE-MDEA) binary parameters have been developed considering (MAE + MDEA + H_2O) ternary system data generated in this work in the temperature range of (298.15 to 323.15) K keeping the total amine content as 30 % and with a correlation deviation of 0.019 % and are presented in Table 6.9. The correlated density by the R-K equation shows an AAD % of 0.46 with respect to the measured ternary density data. Equation 6.6 correlated the (MAE + MDEA + H_2O) density data in a more precise way than the R-K equation, showing a deviation of 0.016 % between the measured density and correlated density. The resulting set of temperature–dependent fitting parameters (Eq. 6.6) is reported in Table 6.10. For the (MAE + MDEA + H_2O) system. The density of the ternary mixture (MAE + MDEA + H_2O) decreases with increasing temperature and increasing mass fraction of MAE in the mixture.

Table 6.1: Comparison of the density data ($\rho_m(gm.cm^{-3})$) of pure MAE and MAE (1) + Water (2) from (298.15 - 323.15) K measured in this work with the literature values with $w_1 + w_2 = 1.0$.

Temperature /K	***Pure MAE***		***MAE+H_2O w_1=0.178***		***w_1=0.1***[a1]	***w_1=0.25***[a1]	***w_1=0.40***[a1]
	Ref [a1]	***This work***	***Ref*** [b1]	***This work***			
298.15	0.937683	0.93618	0.99645	0.99631	0.99604	0.99763	0.99000
303.15	0.933789	0.93226	0.99449	0.99438	0.99506	0.99639	0.98970
308.15	-	-	-	0.99312	0.99282	0.99297	0.98610
313.15	0.925948	0.92442	0.99011	0.99009	0.99126	0.99029	0.98406
318.15	-	-	-	0.98861	0.98917	0.98761	0.97950
323.15	0.918024	0.91648	0.98507	0.98489	0.98677	0.98101	0.97670
[c1] % AAD	= 0.15		= 0.12				

[a1] Li et.*al*., 2007

[b1] Alvarez et.*al*., 2006

[c1] $\text{AAD\%} = \left[\sum_n \left(Density_{presentwork} - Density_{lit}\right)/Density_{presentwork}\right]/n \times 100$

Table 6.2: Density, $(\rho_m(gm.cm^{-3}))$ for MAE (1) + AMP (2) + H_2O (3) from (298.15-323.15) K with $w_1 + w_2 = 0.3$.

w_1/w_2	***T/K = 298.15***	***303.15***	***308.15***	***313.15***	***318.15***	***323.15***
0.03/0.27	0.99498	0.99274	0.98990	0.98728	0.98438	0.98220
0.06/0.24	0.99656	0.99472	0.99221	0.98908	0.98584	0.98340
0.09/0.21	0.99741	0.99538	0.99229	0.98925	0.98640	0.98352
0.12/0.18	0.99834	0.99573	0.99288	0.98980	0.98688	0.98383

Table 6.3: Density, $(\rho_m(gm.cm^{-3}))$ for MAE (1) + MDEA (2) + H_2O (3) from (298.15 – 323.15) K with $w_1 + w_2 = 0.3$.

w_1/w_2	***T/K = 298.15***	***303.15***	***308.15***	***313.15***	***318.15***	***323.15***
3/27	1.02158	1.01897	1.01621	1.01336	1.01130	1.00901
6/24	1.02008	1.01791	1.01419	1.01182	1.00937	1.00743
9/21	1.01708	1.01455	1.01198	1.00949	1.00731	1.00509
12/18	1.01494	1.01253	1.00945	1.00680	1.00451	1.00205

Table 6.4: Redlich-Kister equation fitting coefficients of the excess volumes ($V_m^E(cm^3.mol^{-1})$) for **(**MAE (1) + H_2O (2)) system.

Estimated MAE-H_2O (R-K) Parameters		
Parameter		Value
A_0	a	-16.653710
	b	0.071870
	c	-0.000105
A_1	a	21.749515
	b	-0.114928
	c	0.000164
A_2	a	41.021672
	b	-0.257555
	c	0.000414
[a](AAD)% correlation		0.104%

Table 6.5: Redlich-Kister equation fitting coefficients of the excess volumes ($V_m^E(cm^3.mol^{-1})$) for **(**AMP (1) + H_2O (2)) system.

Estimated AMP-H_2O (R-K) Parameters		
Parameter		Value
A_0	a	-2.975265
	b	-0.014298
	c	0.000033
A_1	a	47.178166
	b	-0.266463
	c	0.000391
A_2	a	57.248373
	b	-0.361994
	c	0.000561
[a](AAD)% correlation		0.033 %

Table 6.6: Redlich-Kister equation fitting coefficients of the excess volumes ($V_m^E(cm^3.mol^{-1})$) for **(**MAE (1) + AMP (2) + H_2O (3)) system.

Estimated MAE-AMP (R-K) Parameters		
Parameter		Value
A_0	a	-816.722289
	b	6.208049
	c	-0.011006
A_1	a	-67009.754554
	b	442.374353
	c	-0.674821
A_2	a	-834911.311191
	b	5650.216157
	c	-8.663625
[a](AAD)% correlation		0.0046%

Table 6.7: Fitting parameters for density ($\rho_m(gm.cm^{-3})$) of (MAE (1) + AMP (2) + H_2O (3)) system by eq. (6.6).

Estimated Nissan (eq.(6.6)) Parameters		
Parameter		Value
A_{13}	a	67.154895
	b	-0.5083999
	c	0.000821
A_{23}	a	3.615593
	b	-0.108645
	c	0.000181
A_{12}	a	-1497.071440
	b	9.679702
	c	-0.015598
[b](AAD)% correlation		0.023 %

Table 6.8: Redlich-Kister equation fitting coefficients of the excess volumes ($(V_m^E(cm^3.mol^{-1})$) for (MDEA (1) + H_2O (2)) system.

Estimated MDEA-H_2O (R-K) Parameters		
Parameter		Value
A_0	a	1228.425354
	b	-4.973241
	c	0.002455
A_1	a	2456.537482
	b	-8.771605
	c	0.0003870
A_2	a	1150.258029
	b	-2.848991
	c	-0.0043031
[a](AAD)% correlation		0.082 %

Table 6.9: Redlich-Kister equation fitting coefficients of the excess volumes ($(V_m^E(cm^3.mol^{-1})$) for (MAE (1) + MDEA (2) + H_2O (3)) system.

Estimated MAE-MDEA (R-K) Parameters		
Parameter		Value
A_0	a	-1410.708503
	b	8.067376
	c	-0.014646
A_1	a	22693.917453
	b	-161.563185
	c	0.419448
A_2	a	-1205535.830713
	b	5000.899371
	c	-3.955480
[a](AAD)% correlation		0.019 %

Table 6.10: Fitting parameters for density ($\rho_m(gm.cm^{-3})$) of (MAE (1) + MDEA (2) + H_2O (3)) system by eq. (6.6).

Estimated Nissan (eq.(6.6)) Parameters		
Parameter		Value
A_{13}	a	-16.561841
	b	0.035510
	c	-0.000061
A_{23}	a	1.212662
	b	-0.118602
	c	0.000197
A_{12}	a	315.129579
	b	-2.166264
	c	0.003751
[b](AAD)% correlation		0.016%

[a] $AAD\% = \left[\sum_{n}\left(V^{E}_{m,cal} - V^{E}_{m,\exp}\right)/V^{E}_{m,\exp}\right]/n \times 100$

[b] $AAD\% = \left[\sum_{n}\left(Density_{presentwork} - Density_{lit}\right)/Density_{presentwork}\right]/n \times 100$

6.3.2 (EAE (1) +AMP/MDEA (2) +H_2O (3)) System

The measured densities of the solutions of (EAE (1) + AMP (2) + H_2O (3)) and (EAE (1) + MDEA (2) + H_2O (3)) at temperature range of (298.15 to 323.15) K are presented in the Tables 6.11 and 6.12, respectively, keeping the total amine mass percentage constant at 30 % with *w* is the mass fraction of each individual amine present in the solution.

From Tables 6.11 and 6.12, it is evident that the mixture density decreases with increasing temperature and with increasing content of EAE in the mixture for both the blends. For aqueous (EAE + MDEA), (EAE + AMP) mixtures, the density data were correlated with an average error of correlation of 0.012 %, 0.013% respectively. To correlate the density of liquid mixtures, a Redlich-Kister type equation for the excess molar volume was applied. The determined Redlich-Kister binary parameters for (EAE + MDEA), (EAE + AMP) system are listed below in Table 6.13 - 6.14, respectively.

The developed correlations for both the blends thus will be useful to generate the design database required for process design.

Table 6.11: Density, $(\rho_m(gm.cm^{-3}))$ for EAE (1) + AMP (2) + H_2O (3) from (298.15-323.15) K with $w_1 + w_2 = 0.3$.

w_1/w_2	*T/K = 298.15*	*303.15*	*308.15*	*313.15*	*318.15*	*323.15*
0.06/0.24	0.99495	0.99205	0.98915	0.98625	0.98335	0.98059
0.09/0.21	0.99464	0.99170	0.98876	0.98582	0.98288	0.98008
0.15/0.15	0.99339	0.99057	0.98775	0.98493	0.98212	0.97944
0.18/0.12	0.99336	0.99042	0.98748	0.98454	0.98160	0.97881
0.21/0.09	0.99285	0.98996	0.98707	0.98418	0.98129	0.97855
0.24/0.06	0.99281	0.98978	0.98676	0.98374	0.98071	0.97784
0.30/0.00	0.99158	0.98865	0.98572	0.98280	0.97987	0.97709

Table 6.12: Density, $(\rho_m(gm.cm^{-3}))$ for EAE (1) + MDEA (2) + H_2O (3) from (298.15-323.15) K with $w_1 + w_2 = 0.3$.

w_1/w_2	***T/K = 298.15***	***303.15***	***308.15***	***313.15***	***318.15***	***323.15***
0.06/0.24	1.01880	1.01641	1.01327	1.01060	1.00794	1.00484
0.09/0.21	1.01539	1.01284	1.01105	1.00785	1.00589	1.00224
0.12/0.18	1.01232	1.00942	1.00700	1.00436	0.99943	0.99821
0.15/0.15	1.00897	1.00671	1.00449	1.00218	0.99921	0.99594
0.18/0.12	1.00355	1.00255	0.99969	0.99687	0.99464	0.99116
0.21/0.09	1.00279	1.00065	0.99812	0.99535	0.99255	0.99024
0.24/0.06	1.00009	0.99725	0.99492	0.99141	0.98888	0.98521
0.30/0.00	0.99030	0.98927	0.98619	0.98303	0.98026	0.97681

Table 6.13: Redlich-Kister Binary parameters, A_0, A_1, A_2 for the excess volume for (EAE + MDEA + H_2O).

Estimated Correlation Parameters × 10^5		
A_0	a	0.008644405
	b	-7.94723E-05
	c	1.28889E-07
A_1	a	-0.381075752
	b	0.002588337
	c	-4.31562E-06
A_2	a	-2.56875848
	b	0.005282725
	c	-2.09658E-06

Table 6.14: Redlich-Kister Binary parameters, A_0, A_1, A_2 for the excess volume for (EAE + AMP + H_2O).

Estimated Correlation Parameters × 10^6		
A_0	a	-0.00428531
	b	2.55336E-05
	c	-4.07763E-08
A_1	a	-0.000539513
	b	-1.42435E-06
	c	7.67945E-09
A_2	a	-1.036525802
	b	0.005974003
	c	-9.21585E-06

REFERENCES

Al-Ghawas, H.A., Hagewiesche, D.P., Ruiz-Ibanez, G. and Sandall, O.C. (**1989**). Physicochemical properties important for carbon dioxide Absorption in aqueous Methyldiethanolamine. *Journal of chemical and Engineering Data*, 34. 385-391.

Alvarez, E., Gomez-Diaz, D., Rubina, M. D. L. and Navaza, J. M. (**2008**). Surface Tension of aqueous binary mixtures of 2-(Methylamino)ethanol and 2-(Ethylamino)ethanol and Aqueous ternary mixtures of these amines with triethanolamine or *N*-Methyldiethanolamine from (298.15 to 323.15) K. *Journal of chemical and Engineering Data*, 53. 318-321.

Alvarez, E., Gomez-Diaz, D., Rubina, M.D.L. and Navaza, J.M. (**2006**). Densities and viscosities of aqueous ternary mixtures of 2-(methylamino)ethanol and 2-(Ethylamino)ethanol with Diethanolamine, Triethanolamine, N-methyldiethanolamine, or 2-Amino-1-methyl-1-propanol from 298.15 to 323.15 K. *Journal of chemical and Engineering Data*, 51, 955-962.

Henni, A., Hromek, J.J., Tontiwachuthikul, P. and Chakma, A. (**2003**). Volumetric properties and viscosities for aqueous AMP solutions from 25 ^{0}C to 70 ^{0}C. *Journal of chemical and Engineering Data*, 48. 551-556.

Li, J., Mundhwa, M., Tontiwachuthikul, P. and Henni, A. (**2007**). Volumetric properties, viscosities, and refractive indices for aqueous 2-(Methylamino)ethanol solutions from (298.15 to 343.15) K. *Journal of chemical and Engineering Data*, 52,560-565.

Rebolledo-Libreros, M. E. and Trejo, A. (**2004**). Gas solubility of H_2S in aqueous solutions of *N*-methyldiethanolamine and diethanolamine with 2-amino-2-methyl-1-propanol at 313, 343 and 393 K in the range 2.5-1036 kPa. *Fluid Phase Equilibria*, 224, 83-88.

Sartori, G. and Savage, D. W. (**1983**). Sterically hindered amines for CO_2 removal from gases. *Industrial and Engineering Chemistry Fundamentals*, 22, 239-249.

Venkat, A., Kumar, G. and Kundu, M. (**2010**). Density and surface tension of aqueous solutions of (2-(Methylamino)-ethanol + 2-amino-2-methyl-1-propanol) and (2-(Methylamino)-ethanol + N-methyl-diethanolamine) from (298.15 to 323.15) K. *Journal of chemical and Engineering Data*, 55, 4580-4585.

Chapter 7

CONCLUSIONS AND FUTURE RECOMMENDATION

Chapter 7

CONCLUSIONS AND FUTURE RECOMMENDATION

7.1 CONCLUSIONS

In this chapter, the salient accomplishments and major conclusions of this work are summarized and recommendations on future directions are made.

- Recently, room temperature *ionic liquids* (ILs'), tertiary amino acid salts apart from alkanolamines are emerging as promising candidates to capture CO_2 but those are far from commercialization. In the present context, the role of alkanolamine solvents in sour gas treating research cannot be denied. In view of this, MAE and EAE has been proposed and their potency as solvent for CO_2 removal has been explored here.
- In this work, a precise experimental facility to measure the VLE of acid gases in alkanolamine solvents up to an acid gas partial pressure of 1000 kPa has been developed. The experimental set-up and procedure has been validated with the systematic VLE data generated on CO_2 solubility in (DEA + AMP/MDEA + H_2O) systems. The generated data were correlated with 5.3 % and 8.0 % deviations, respectively for (CO_2 + DEA + AMP + H_2O) and (CO_2+ DEA + MDEA + H_2O) systems using extended *Debye-Hückel* theory of electrolytic solution and the *Virial*

Equation of State. CO_2 solubility in aqueous MAE and EAE were determined at 303.1, 313.1 and 323.1 K. Deprotonation and carbamate reversion constants were determined for EAE regressing the VLE data of (CO_2+ EAE + H_2O) system. This experimental facility developed can also be used to measure the VLE of various other gas – liquid systems.

- A systematic VLE data on twenty two aqueous MAE and EAE blends; (MAE + MDEA/AMP) and (EAE + MDEA/AMP) and eight aqueous blends of (DEA + MDEA/AMP) were generated at 303.1, 313.1 and 323.1 K. It is expected that the generated CO_2 solubility data of this work will be useful as VLE database needed for process design of gas treating units. (EAE + MDEA) has been evolved as most effective blend for CO_2 capture and has been correlated with a thermodynamic framework.
- Among aqueous solvents of DEA, MAE and EAE, the CO_2 solubility was highest in EAE followed by MAE solution at comparable conditions of alkanolamine concentration, temperature and CO_2 pressure. The CO_2 solubility trends of the solvents were explained on the basis of carbamate instability, electronic structure, presence of electron donating and withdrawing groups, and intra/inter molecular hydrogen bonding pertaining to those solvents.
- A comprehensive study revealed that both for EAE + MDEA and EAE + AMP blends, presence of equal moles of corresponding alkanolamines make the blend most suitable towards CO_2 absorption.
- CO_2 solubility in (EAE/MAE/DEA + MDEA/AMP) solutions was compared at 313.1 K. (EAE + MDEA/AMP) blends proved to be most suitable solution in this regard. (DEA + MDEA/AMP) and (MAE + MDEA/AMP) solutions are hardly distinguishable of their CO_2 loading capability.
- Molecular simulation using conductor like screening model is a useful alternative to those models based on activity coefficients of the compounds using the structural property information of pure components and binary interaction parameters between the components. Development of a COSMO-RS model for the (MAE/EAE + water) systems are presented here with representation of excess Gibbs free energy, excess enthalpy and activity coefficient, chemical potential for binary (MAE/EAE + H_2O) systems.

- The COSMO predicted values of, NRTL, WILSON, UNIQUAC parameter for activity coefficients MAE/EAE + water system, and infinite dilution activity coefficients of MAE/EAE in water were determined.
- The ternary solution, thermodynamic properties like activity coefficients; excess Gibbs energy and excess enthalpy obtained through COSMO calculations may be used to regress the binary/ternary interaction parameters of the concerned ternary system in developing activity coefficient based models.
- The benefit of chemical reaction equilibria is realizable for a solution containing less than 0.1 mole fraction of MAE/EAE. Hence, aqueous MAE and EAE solutions containing 0.06-0.3 mass fractions of alkanolamine can be considered as potential solvent for effective CO_2 removal and this was confirmed in this study using COSMO-RS molecular modelling software. Though on commercial scale use of these dilute solutions would require a high volumetric flow rate of aqueous alkanolamine solution and huge absorption column. In industry concentrated solutions are used, thus the most effective solution loading is compromised.
- More number of thermodynamic property predictions by COSMOtherm software in the MAE and EAE mole fraction range of 0.05-0.1 in the ternary solution would have been much effective.
- In the present dissertation, densities of aqueous ternary mixtures of (MAE+AMP), (MAE+MDEA), (EAE+AMP) and (EAE+MDEA) at wide range of temperatures and relative amine compositions have been measured. Densities of the ternary mixtures were correlated as a function of temperature and amine composition. The total amine concentration was held constant at 30 mass %. The developed correlations thus will be useful to generate the design database required for process design.
- CO_2 solubility in (EAE/MAE/DEA + MDEA/AMP) solutions can acclaim them as a potential solvent for CO_2 removal provided the claim is being supported by the studies on kinetic studies, anti-corrosion properties, hydrocarbon solubility, VLE in the regeneration section, and dilapidation resistance etc.

7.2 RECOMMENDATIONS ON FUTURE DIRECTIONS

- In this work, an equilibrium cell-based VLE measurement setup has been used to measure CO_2 solubility up to 600 kPa CO_2 partial pressure. An essential next step should be the generation of VLE measurement up to 1000 kPa.
- Structural activity relationships (the effect of the solvent structure on the CO_2 absorption characteristics) of the proposed alkanolamines and reaction mechanism are to be established either by NMR studies or by molecular modelling.
- Accurate speciation; that is depiction and variation of all molecular and ionic species present in the equilibrated liquid phase and their variation with CO_2 loading is an essential step in future direction.
- Determination of equilibrium dissociation constant of MAE and EAE in water followed by matching them with molecular modeling prediction (through calculated pKa values).
- It is desirable to correlate the experimental VLE data on (MAE + CO_2 + H_2O), (EAE + CO_2 + H_2O), (MAE + AMP + CO_2 + H_2O), (MAE + MDEA + CO_2 + H_2O), (EAE + AMP + CO_2 + H_2O) and (EAE + MDEA + CO_2 + H_2O) with other standard models like NRTL, UNIQUAC, electrolyte equation of state models and comparison of the predictions of those models to that of molecular solvation models.
- The physical solubility of CO_2, (Henry's constant of CO_2) in the aqueous MAE/EAE solvents, is one of the most important parameters required to describe the vapour - liquid equilibrium of CO_2 in aqueous alkanolamine solvents. The determination of physical solubility of CO_2 in aqueous MAE/EAE solution is an essential future step.
- Kinetic studies, anti-corrosion properties, hydrocarbon solubility, VLE in the regeneration section, and dilapidation resistance etc. are the various characteristics need attention and evaluation to have a final affirmation in favour of (MAE + MDEA), (MAE + AMP), (EAE + MDEA) and (EAE + AMP) blends as potential solvents for CO_2 capture.

Appendix

1. EXPERIMENTAL CO_2 LOADING (α_{CO_2}) CALCULATION IN THE LIQUID PHASE

The method of calculation adopted regarding the number of moles of CO_2 absorbed in the liquid phase; was that of described by Park and Sandall (2001).

Quantity of CO_2 (n_{CO_2}) is transferred to the VLE cell is calculated by

$$n_{CO_2} = \frac{V_T}{R\,T_a}\left(\frac{P_1}{z_1} - \frac{P_2}{z_2}\right) \quad \text{(A.1)}$$

Where, V_T = volume of the buffer vessel.

z_1 and z_2 = compressibility factors corresponding to the initial pressure P_1 and the final pressure P_2 of buffer vessel.

Compressibility factors are calculated using Peng–Robinson equation of state.

T_a = Temperature of water-bath.

R = Universal gas Constant.

The moles of CO_2 remaining in the gas phase in VLE cell:

$$n_{CO_2}{}^{g} = \frac{V_g}{z_{CO_2}}\frac{P_{CO_2}}{RT_a} \quad \text{(A.2)}$$

Where, V_g = Volume of the VLE cell.

P_{CO_2} = Equilibrium pressure (total measured pressure – vapour pressure of liquid).

z_{CO_2} = compressibility factor corresponding to the corresponding to the VLE cell pressure.

The moles of CO_2 in the liquid phase is determined from

$$n_{CO_2}{}^{l} = n_{CO_2} - n_{CO_2}{}^{g} \quad \text{(A.3)}$$

The CO_2 loading in the liquid phase is defined as

$$L_{CO_2} = \frac{n_{CO_2}{}^{l}}{n_{Am}} = \alpha_{CO_2} \quad \text{(A.4)}$$

Where, n_{Am} are the moles of alkanolamine in the liquid phase.

2. STANDARD UNCERTAINTY FOR DENSITY MEASUREMENT

a) Standard uncertainty for temperature measurement:-

The temperature was controlled within ± 0.05 K using a circulator temperature controller. And maximum temperature that can be maintained by circulator is 72 ^{0}C.

$$u_B = \sigma = \frac{\Delta Z_{max}}{\sqrt{3}} = \frac{AC/100}{\sqrt{3}} M$$

Where AC (Accuracy class or minimum possible measurement) = 0.05; M = 72 ^{0}C.

$$u_B = 0.02$$

Then expanded uncertainty for coverage factor k=2.

$$u_B = 2*0.02 = \mathbf{0.04\ K}$$

b) Standard uncertainty for density measurement:-

Uncertainty in measured density is calculated by this partial derivative formula at different-different temperatures.

$$= \sqrt{\left[\frac{\partial}{\partial m}\left(\frac{m}{v}\right) dm\right]^2 + \left[\frac{\partial}{\partial T}\left\{\frac{m}{\frac{v * (T + 273.15)}{273.15}}\right\} dT\right]^2}$$

Where dm (deviation in mass) = 0.001 and dT (deviation in temperature) = 0.04.

So, the calculated uncertainty is 3.88×10^{-4}gm/cm^3.

Then expanded uncertainty for coverage factor k=2.

$$u_B = 2 \times (3.88 \times 10^{-4}) = \mathbf{7.76 \times 10^{-4}}$$

3. UNCERTAINTY CALCULATION FOR VLE EXPERIMENTATION

a) Standard uncertainty for pressure measurement

i) For transducer 1(Max. Limit-689 kPa)

Measurement range = 689 kPa, Accuracy = ±0.25 %, non-repeatability = ±0.1 % of reading ±2 counts, 4-position display

$$u_B = \frac{1 + \frac{0.25}{100} \times 689}{\sqrt{3}} = 1.57$$

Then expanded uncertainty for coverage factor k=2.

$u_B = 2 \times 1.57 = 3.14$

So for maximum pressure reading, P = 689 ± 3.14 kPa = 689 ± 0.46 % ≅ 689 ± 0.5 %.

ii) For transducer 2 (Max. Limit-1724 kPa)

Measurement range = 1724 kPa, Accuracy = ±0.25 %, non-repeatability = ±0.1 % ±2 counts, 4-position display

$u_B = \frac{1+\frac{0.25}{100}\times 1724}{\sqrt{3}}$ = 3.06

Then expanded uncertainty for coverage factor k=2.

u_B = 2× 3.06= 6.13

So for maximum pressure reading, P = 1724 ± 6.13 kPa = 689 ± 0.3556 % ≅ 689 ± 0.4 %.

b) For temperature measurement

Working temperature range = 70 ^{0}C, readout accuracy = ±0.25 ^{0}C.

$u_B = \frac{\frac{0.25}{100}\times 50+\frac{0.1}{100}\times 70}{\sqrt{3}}$ = 0.076

Then expanded uncertainty for coverage factor k=2.

u_B = 2× 0.076= 0.152

So for maximum temperature reading, T = 50 ± 0.15 ^{0}C ≅ 50 ± 0.1 K.

c) For volume measurement

volume range = 50 ml, readout accuracy = ±0.1 ml.

$u_B = \sigma = \frac{\Delta Z_{max}}{\sqrt{3}} = \frac{AC/_{100}}{\sqrt{3}} M$ = 2.88×10^{-2} ml.

Then expanded uncertainty for coverage factor k=2.

u_B = 2× 2.88×10^{-2} = 0.057 ml.

So for maximum volume, V = 50 ± 0.057 ml.

d) Uncertainty in loading calculation.

The CO_2 loading in the liquid phase is defined as

$L_{CO_2} = \frac{{n_{CO_2}}^l}{n_{Am}} = \alpha_{CO_2}$

The moles of CO_2 in the liquid phase is determined from

${n_{CO_2}}^l = n_{CO_2} - {n_{CO_2}}^g = \frac{V_T}{R\,T_a}\left(\frac{P_1}{z_1} - \frac{P_2}{z_2}\right) - \frac{V_g}{z_{CO_2}}\frac{P_{CO_2}}{RT_a}$

The above equation should be differentiated with respect to all contributing parameters, $P_1,\ P_2\ , P_{CO_2}, T_a$.

$n_{Am} = {v_{sol}}/{v_{molar}}$, where v_{sol}= volume of the alkanolamine solution taken

v_{molar}= molar volume of the concerned alkanolamine (considered constant).

Hence the parameter v_{sol}; with respect to which, n_{Am} and ${n_{CO_2}}^{l}$ should be differentiated.

$$\alpha_{CO_2}=\left[\left(\frac{V_T}{R\,T_a}\left(\frac{P_1}{z_1}-\frac{P_2}{z_2}\right)-\frac{V_g}{z_{CO_2}}\frac{P_{CO_2}}{RT_a}\right)\times {v_{molar}}/{v_{sol}}\right]$$

Error in calculating α_{CO_2}

$$= \left[\left[\left\{\left(\frac{-V_T}{{RT_a}^2}\left(\frac{P_1}{Z_1}-\frac{P_2}{Z_2}\right)+\left(\frac{V_g}{RT_a^2}\frac{P_{CO_2}}{Z_{CO_2}}\right)\right)\times {v_{molar}}/{v_{sol}}\right\}dT_a\right]^2 + \left[\left\{\left(\frac{V_T}{RT_aZ_1}\right)\times {v_{molar}}/{v_{sol}}\right\}dP_1\right]^2 + \left[\left\{\left(\frac{-V_T}{RT_aZ_2}\right)\times {v_{molar}}/{v_{sol}}\right\}dP_2\right]^2 + \left[\left\{\left(\frac{-V_g}{RT_aZ_{CO_2}}\right)\times {v_{molar}}/{v_{sol}}\right\}dP_{CO_2}\right]^2 - \left[\left\{\left(\frac{V_T}{R\,T_a}\left(\frac{P_1}{z_1}-\frac{P_2}{z_2}\right)-\frac{V_g}{z_{CO_2}}\frac{P_{CO_2}}{RT_a}\right)\times\left({v_{molar}}/{v_{sol}^2}\right)\right\}dv_{sol}\right]^2\right]^{\frac{1}{2}}$$

= uncertainty in loading of CO_2 in liquid phase after equilibrium.

For several experimental runs, the calculated uncertainty in loading ranged from ±0.027 to ±0.038. On an average, it was reported as ≅ 3 %.

Table A1: Fugacity Coefficient for (DEA + CO_2 + H_2O) system

Tempr. (T = K)	Molality of DEA	Loading (α_{CO_2})	Partial pressure	Fugacity co-eff
373.15	4.2	0.299	93.0	0.9979
373.15	4.2	0.469	486.0	0.9890
373.15	4.2	0.595	1110	0.9751
373.15	4.2	0.660	2019	0.9552
373.15	4.2	0.684	2660	0.9414
373.15	4.2	0.725	3742	0.9185

Table A2: Fugacity Coefficient for (DEA + MDEA + CO_2 + H_2O) system.

Tempr. (T = K)	DEA Molality	MDEA Molality	Loading (α_{CO_2})	Partial pressure	Fugacity co-eff
323.15	0.604	2.617	0.422	34.6	0.9987
323.15	0.604	2.617	0.532	58.1	0.9978
323.15	0.604	2.617	0.633	90.3	0.9965
323.15	0.604	2.617	0.682	111.9	0.9957
323.15	0.604	2.617	0.716	135.7	0.9948
323.15	0.604	2.617	0.771	181.3	0.9931
323.15	0.604	2.617	0.779	188.2	0.9928
323.15	0.604	2.617	0.829	244.6	0.9907
323.15	0.604	2.617	0.875	297.1	0.9887

Gaurav Kumar

Date of Birth : 16 January 1982

Email : patel.gauravpatel@gmail.com

Education :

- Ph.D. student
  Department of Chemical Engineering
  National Institute of Technology Rourkela
  India
  2009 – 2013

- M. Tech in Chemical Engineering
  Department of Chemical Engineering
  National Institute of Technology Rourkela
  India
  2007 – 2009

- B. Tech in Chemical Engineering
  IET Mahatma Jyotiba Phule Rohilkhand University, Bareilly
  Utter Pradesh
  India
  2007

Publications Based on the Work in Referred Journals

1. **G. Kumar** and M. Kundu. Vapor-Liquid Equilibrium of CO_2 in Aqueous Blends of (*N*-ethyl-ethanolamine + *N*-methyl-diethanolamine) and (*N*-ethyl-ethanolamine + 2-amino-

2-methyl-1-propanol). *Journal of Chemical & Engineering Data* (ACS), 58, 2959-2965, 2013.

2. **G. Kumar** and M. Kundu. Solubility of CO_2 in Aqueous Blends of (N-Methyl-2-ethanolamine + N-Methyl-diethanolamine) and (N-Methyl-2-ethanolamine + 2-Amino-2-methyl-1-propanol). *Journal of Chemical & Engineering Data* (ACS), 57, 3203–3209, 2012.

3. **G. Kumar,** T. K. Mondal and M. Kundu. Solubility of CO_2 in blends of (Diethanolamine + 2-amino-2-methyl-1-propanol) and (Diethanolamine + N-methyldiethanolamine). *Journal of Chemical & Engineering Data* (ACS), 57, 670–680, 2012.

4. **G. Kumar** and M. Kundu. Vapor-liquid equilibrium of CO_2 in aqueous solutions of N-methyl-2- ethanolamine. *Canadian journal of Chemical Engineering* (Wiley), 90, 627-630, 2012.

5. A.Venkat, **G. Kumar** and M. Kundu. Density and Surface Tension of Aqueous Solutions of (2-(Methylamino) ethanol + 2-Amino-2-methyl-1-propanol) and (2-(Methylamino) ethanol + N-methyl-diethanolamine) from (298 to 323) K. *Journal of chemical & Engineering Data* (ACS), 55, 4580-4585, 2010.

6. **G. Kumar,** Shivani, M. Kundu. Vapour Liquid Equilibria of (CO_2 +*N*-ethyl-ethanolamine + H_2O) System and Prediction of Solution Thermodynamics using Molecular Modeling. *Korean Journal of Chemical Engineering* (Springer). November 2013 (**Communicated**).

7. **G. Kumar**, Shivani, M. Kundu. Solubility of Carbon Dioxide in Aqueous 2-Amino-Methyl-1-Propanol Solutions. **National conference** on Recent Advances in Chemical and Environmental Engineering (RACEE-2012), NIT Rourkela, Jan 20-21, 2012 India.